Characterisation and determination of rosin compositions using analytical approaches

Louise McKeon B.Sc.

Thesis submitted for the Degree of Doctor of Philosophy

Supervisor: Fiona Regan

School of Chemical Sciences, Dublin City University

September 2014

Declaration

I hereby certify that this material, which I now submit for assessment on the programme of study leading to the award of Doctor of Philosophy is entirely my own work, and that I have exercised reasonable care to ensure that the work is original, and does not to the best of my knowledge breach any law of copyright, and has not been taken from the work of others save and to the extent that such work has been cited and acknowledged within the text of my work.

Signed: _____

ID No.: 56503870

Date:

Acknowledgements

A lot of people have helped me over the course of the last four years, both with science and life in general.

I would like to thank the IRCSET Enterprise Scheme and Henkel Ireland Ltd. for funding my PhD, and all the technicians, staff and other students in DCU who helped me over the years.

Thanks to my supervisor Prof. Fiona Regan and industrial supervisors Prof. Ray Leonard and Dr. Barry Burns in Henkel who were always a source of knowledge and encouragement.

A big thanks to everyone in my lab, especially Lisa, Ciprian, James, Tim, Rachel, Brendan, Aoife and Steve the CE for all the advice and fun.

Family are great for reminding you that sometimes other things are more important, so thanks mam, dad, Michelle and Joy for being awesome.

Friends have been some of the best bits of the last few years. Lisa, Ian, Celine and especially Pete, you guys helped me get through some rough times and I will always be grateful for that.

Now on to something new!

Table of Contents

Abstract

In this work, the composition of rosin and resin samples was studied using novel capillary electrophoretic methods. Rosins are complex natural products which can have a tendency to crystallise when used in the soldering industry, causing problems in certain applications. The current tests for tendency to crystallise are not always accurate and there is no existing rapid screening method for the identification of a suitable batch of rosin. Thus far the resin acids present in rosins are generally analysed by GC-MS requiring derivatisation which is unable to separate all of the acids in question. In this work capillary electrophoresis methods for the analysis of the acid and neutral fractions of rosin samples were developed and applied to natural and modified rosin samples to investigate possible links between the presence and concentration of any compound and the rosin's tendency to crystallise. A CE method was developed for the separation of nine resin acids for the first time. The simultaneous determination of nine neutral compounds present in rosin samples including terpenes and alcohols was also reported. The presence of neoabietic acid and elevated concentrations of abietic acid in rosin samples was found to indicate crystallisation of the rosin sample. The association constants of the inclusion complexes formed between the terpenes present in rosin samples and the cyclodextrins used for their analysis were investigated by affinity capillary electrophoresis. The surfactant-cyclodextrin interactions were found to be more significant than initially hypothesised. A rapid screening method for rosin samples was developed which could be used by industries to determine the suitability of a rosin batch for a particular use prior to purchasing.

Abbreviations

α-CD: α-cyclodextrin

ABA: Abietic acid

ACN: Acetonitrile

AWS: American welding society

BGE: Background electrolyte

CAPS: *N*-cyclohexyl-3-aminopropanesulfonic acid

CD: Cyclodextrin

CE: Capillary electrophoresis

CEC: Capillary electrochromatography

CGE: Capillary gel electrophoresis

CIEF: capillary isoelectric focusing

CITP: capillary isotachophoresis

CMC: Critical micelle concentration

CTAB: Cetyltrimethylammonium bromide

CZE: Capillary zone electrophoresis

DAD: Diode array detector

DHA: Dehydroabietic acid

EOF: electroosmotic flow

FID: flame ionisation detector

GC: Gas chromatography

HETP: height equivalent of a theoretical plate

HPγCD: (2-hydroxypropyl)-γ-cyclodextrin

HPLC: high-performance liquid chromatography

IPA: Isopropanol

ISO: Isopimaric acid

LOD: Limit of detection

LVO: Levopimaric acid

MeOH: Methanol

ME: Microemulsion

MECD: methyl- β-cyclodextrin

MEEKC: Microemulsion electrokinetic chromatography

MEKC: Micellar electrokinetic chromatography

MES: 2-(*N*-morpholino)ethanesulfonic acid

MS: Mass spectrometry

NEO: Neoabietic acid

NMR: Nuclear magnetic resonance

PAL: Palustric acid

PBS: phosphate buffered saline solution

PIM: Pimaric acid

RP: Reversed phase

RSD: Relative standard deviation

SAN: Sandaracopimaric acid

SBCD: Sulfobutylether -β-cyclodextrin

sβ-CD: sulphated β-cyclodextrin

SD: standard deviation

SDS: Sodium dodecyl sulphate

TFA: trifluoroacetic acid

Tris: Tris(hydroxymethyl)aminomethane

7OXO: 7-oxo-dehydroabietic

Chapter 1

Introduction

1.1 Background

In industry, rosins are used in a variety of products including paints, varnishes and solder flux. They have been known to randomly crystallise which causes problems in the products they are used in. This crystallisation tendency has not yet been linked to a specific part of their composition. Rosins are composed of around 90% acidic material and 10% neutral components. In this work, capillary electrophoresis (CE) and high-performance liquid chromatography (HPLC) were used to characterise the acidic and non-acidic part of rosins and to investigate any relationship between the composition of different rosins and their tendency to crystallise.

1.2 Rosins

Rosins, also known as colophony, are natural compounds. Pine oleoresin is a mixture of oils and non-volatiles secreted from trees. When the volatile resin components have been distilled off, rosin is the remaining solid material [1]. There are several types of rosin, depending on the part of the tree it is sourced from. Gum rosin is tapped from live pine trees, tall oil rosin is a by-product from paper pulp and wood rosin is extracted from tree stumps [2, 3]. Rosins have a variety of uses in industry, including paints, varnishes, adhesives, cosmetics and drug coating [4]. Gum and wood rosin are also used in solder flux [5]. Rosins are extracted from pine trees in many locations geographically, including China, France, America, Indonesia, Russia, Scandinavia and Portugal [2]. Their composition depends on their geographical location and the type of rosin. Joye and Lawrence observed that tall oil and wood rosins contained more abietic and dehydroabietic acid than gum rosins. They also note that rosins from America contain half the amount of pimaric acid as rosins from France [6]. Rosins samples are insoluble in water while some of their components are water soluble at higher pH values. Rosins are soluble in alcohol, benzene, ether, glacial acetic acid, oils, alkali hydroxides and turpentine [7].

There are many papers reporting health issues related to working with and around rosins as they are a known sensitizer when oxidised [2, 8-11], and related to conditions such as asthma [2, 8, 12] and contact dermatitis [3]

1.2.1 Rosin composition

Rosin consists mainly of resin acids (90%) which are diterpene monocarboxylic acids. The other 10% consists of neutral compounds which are mainly terpenic and can include alcohols, esters, aldehydes and hydrocarbons [1, 7, 13]. The first literature on the composition of rosins was reported by Baupe *et al.* in 1826 [14]. In 1926 it was confirmed that the resin acids were not in the form of acid anhydride as had been previously reported [14]. Their structures compose of a hydrophobic skeleton with hydrophilic carboxyl groups attached [15].

1.2.1.1 Acidic compounds

Of the acidic compounds, 90% are isomeric abietic acids and 10% are dihydroabietic acid and dehydroabietic acid [7]. The isomeric abietic acids form two groups; abietic acids with conjugated double bonds (40-60%) and pimaric acids with non-conjugated double bonds (9-27%) [3, 16] (see Table 1-1). The abietic acids contain an isopropyl group while the pimaric acids have a methyl and vinyl group. Their pK_a values range from 5.7-7.25 [1, 31, 84].

Table 1-1 Some of the components reported to be present in rosins [6, 11, 17]

Abietic-type acids	**Pimaric-type acids**	**Neutral compounds**
Abietic acid (ABA)	$\Delta^{(8,9)}$ Isopimaric acid	Isolongifolene
Dehydroabietic acid (DHA)	Pimaric acid (PIM)	3-Carene
Dihydroabietic acid	Elliotinoic acid	Aromadendrene
Palustric acid (PAL)	Sandaracopimaric acid (SAN)	α-Terpineol
Neoabietic acid (NEO)	Isopimaric acid (ISO)	Camphene
Levopimaric acid (LVO)	Dihydropimaric acid	Longifolene
Dihydropalustric acid	Tetrahydropimaric acid	α-Pinene
Tetrahydroabietic acid		β-Pinene
7-oxo-dehydroabietic acid (7-OXO)		4-Allylanisole

1.2.1.2 Neutral compounds

Compared to reports on the acidic composition of rosins, there are less reports on the composition of the neutral component of rosins. Zinkel *et al.* list α-terpineol, 4-allylanisole and longifolene as the main neutral components [1], however, the majority of reports on the neutral components of rosins deal with the aldehydes present. At soldering temperatures (over 200°C), the fumes produced when rosins break down contain aldehydes. GC-FID and GC-MS were used to analyse these aldehydes and ketones [18-20]. Aldehydes including formaldehyde, hexanal, acetaldehyde and cyclohexane carboxaldehyde were observed. Using a 2-hydroxymethylpiperidine derivatizing agent, Smith *et al.* saw increased sensitivity over Guenier's method (2,4-dinitrophenylhydrazine was the derivatizing agent), allowing the identification of more aldehydes and their derivatives. Formaldehyde and acetaldehyde were identified as being the predominant aldehydes present using TLC [21]. Genge *et al*. used MS with a heated inlet system and showed the presence of compounds of mass 314 to 320 that were not acids. They reported 6 to 13% of the rosin to be neutral, agreeing with the papers primarily reporting on the acidic compounds [17].

More recently, analysis of Indonesian pine trees by GC-MS reported the main terpenoids present to be α-pinene, β-pinene and 3-carene [22]. Some of the neutral compounds found to be present in rosins are listed in Table 1-1.

1.2.2 Rosin crystallisation

Rosins are mainly composed of resin acids, and can have a tendency to crystallise in the form of material seeding/precipitating out of solution [1, 23]. For the purpose of this thesis, the terms 'crystallisation' and 'crystals' refer to this precipitate. The crystals are water insoluble and alkali. This crystallisation causes problems in the production of soaps and varnishes, and by affecting the viscosity of solder pastes which are used in circuits [24]. Crystallisation generally occurs at random and has not yet been linked to a specific part of the composition of rosins, however, several papers and patents note that a high acidic content leads to a higher tendency to

crystallise [25, 26]. Stinson and Lawrence claim that higher abietic acid (ABA) content leads to a higher tendency to crystallise [27]. Fiebach and Grimm note that a higher tendency to crystallise is linked to fewer isomers present [28]. Zinkel notes that ABA contents above 30% leads to higher tendencies to crystallise. The species of pine and processing conditions the rosins were prepared under affects this tendency [1].

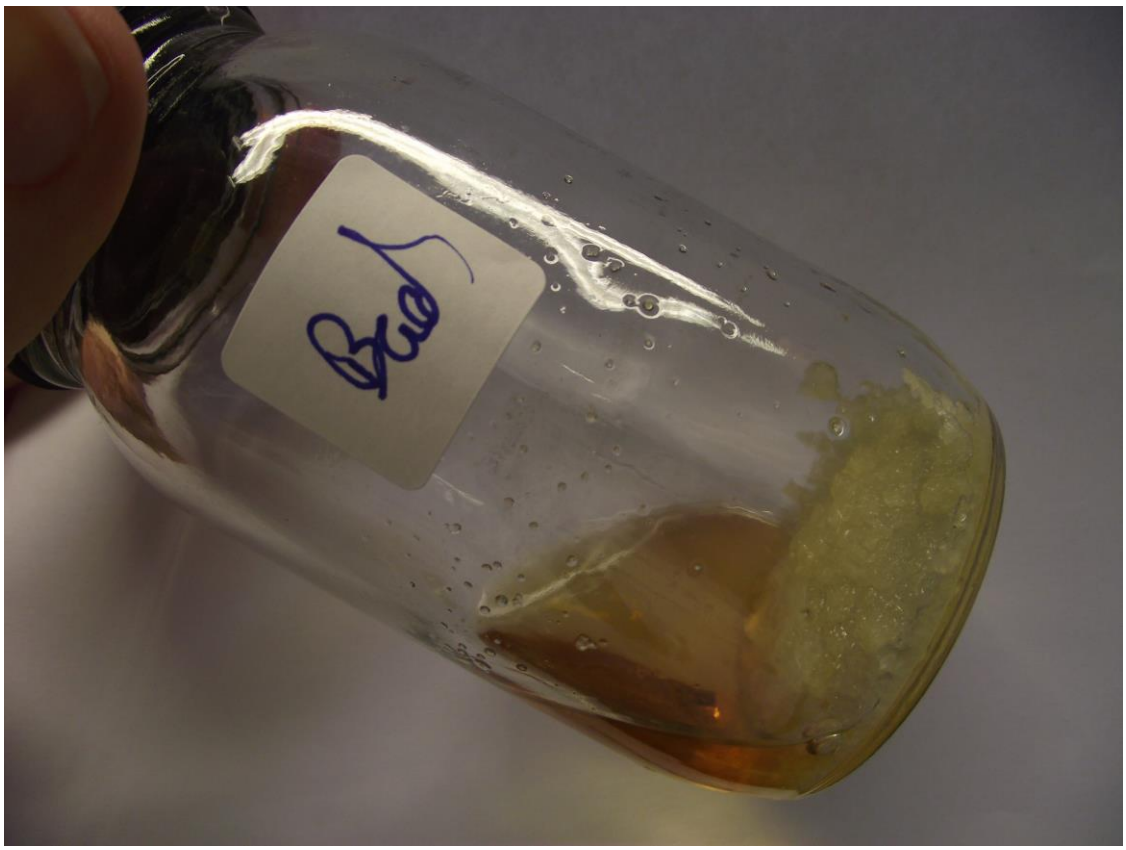

Figure 1-1 A rosin sample which crystallised.

Studies have been carried out attempting to understand why some rosin tends to crystallise more readily than others [24]. There are also several US patents for non-crystallising rosins and methods for inhibiting this crystallisation [26, 29]. Methods used in patents to try and make non-crystallising rosin are modifying the rosin by treating it with heat, chemicals or both [24].

There is no standardised method for determining the crystallisation of rosins. The “acetone test” is generally used by companies, where some rosin sample is simply

placed in a beaker of acetone and left unagitated for a period of time. Whether or not crystals form, how long they take to form and the amount of crystals that form all indicate tendency to crystallise [1]. The resin acid balance (RAB) test is also used (see section 4.3.3), but is only suitable for gum rosin samples, and is not always accurate.

Some of the work in this thesis was carried out in collaboration with an industrial partner, Henkel Ireland Operations and Research Ltd., Tallaght Business Park, Whitestown, Tallaght, Dublin 24, Ireland. Adhesive technologies make 50% of Henkel sales, including the solder material they produce which contains rosin. Their estimated global market for solder paste in 2012 was 46 million euros, and rosin batches returned or scrapped due to crystallisation issues was ~1%, costing roughly 460 thousand euro each year. There are also additional associated costs in sales and technical support for customers affected by the issues, and in the R & D department in trying to resolve the issues and identify suitable rosin batches.

1.2.3 Rosin reactions and modification

In industry, rosins are often modified for use in consumer products to improve a certain desired property, such as colour, solubility or oxidation resistance. This avoids some problems caused by gum rosin, such as discolouration when its double bonds are oxidised, and crystallisation. Modification shifts the resin acid ratio by causing ABA to be converted, primarily to dehydroabietic acid (DHA) and dihydro- and tetrahydroabietic acids [1]. This improves the resistance of the rosin to oxidation as DHA is aromatic and much harder to oxidise.

1.2.3.1 Oxidation

While pimaric type acids are not easily oxidised, abietic type acids oxidise easily in air due to the conjugated double bond [30]. This can be avoided by disproportionation, polymerisation, hydrogenating the bond to saturate it, or dehydrogenating it to increase unstauration which makes a stable aromatic ring,

1.2.3.2 Isomerisation.

Many of the components in rosins are isomers of each other. Pimaric acid (PIM) is an optical isomer of sandaracopimaric acid (SAN) (see Figure 1-2) [31].

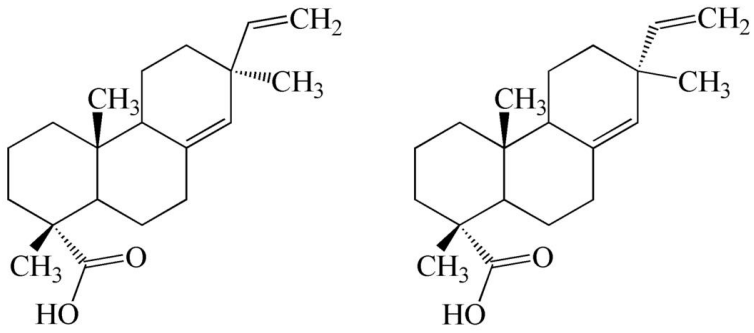

Pimaric acid Sandaracopimaric acid

Figure 1-2 Structures of pimaric and sandaracopimaric acid

A reported 23-40% of the acid part of commercial oleoresins is levopimaric acid, which when converted to gum rosin is almost completely isomerised to ABA, PAL and Neoabietic acid (NEO) [32]. Palustric acid (PAL) was first isolated from gum rosin by Loeblich *et al.* in 1954. It is an intermediate product when levopimaric acid is isomerised to abietic acid (ABA) (see Figure 1-3). Quicker modification can result in less isomerisation and so more levopimaric acid (LVO) present. NEO and PAL also isomerise to LVO but at a slower rate [1].

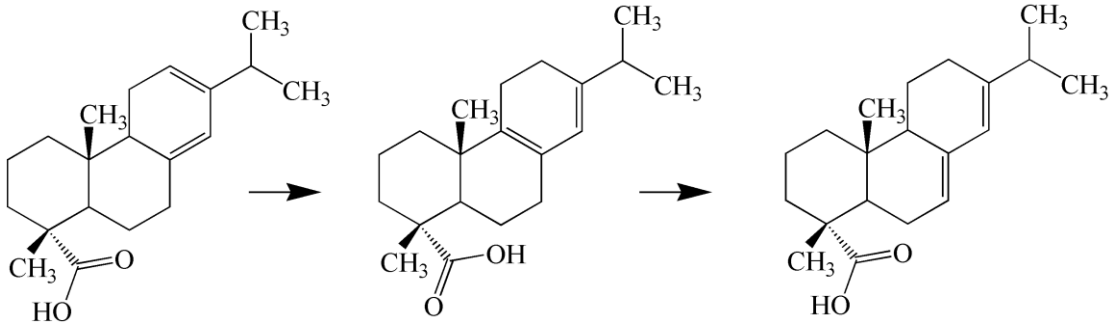

Levopimaric acid Palustric acid Abietic acid

Figure 1-3 Structures of levopimaric, palustric and abietic acid

NEO is another isomer of levopimaric acid [33, 34].

1.2.3.3 Dimerisation.

A method of rosin modification used to improve stability is dimerisation, as the number of double bonds is decreased. Abietic acid, the main constituent of rosin, can be dimerised (see Figure 1-4). This is in order to produce polymerised rosin which is more resistant to oxidisation than unmodified rosin [35].

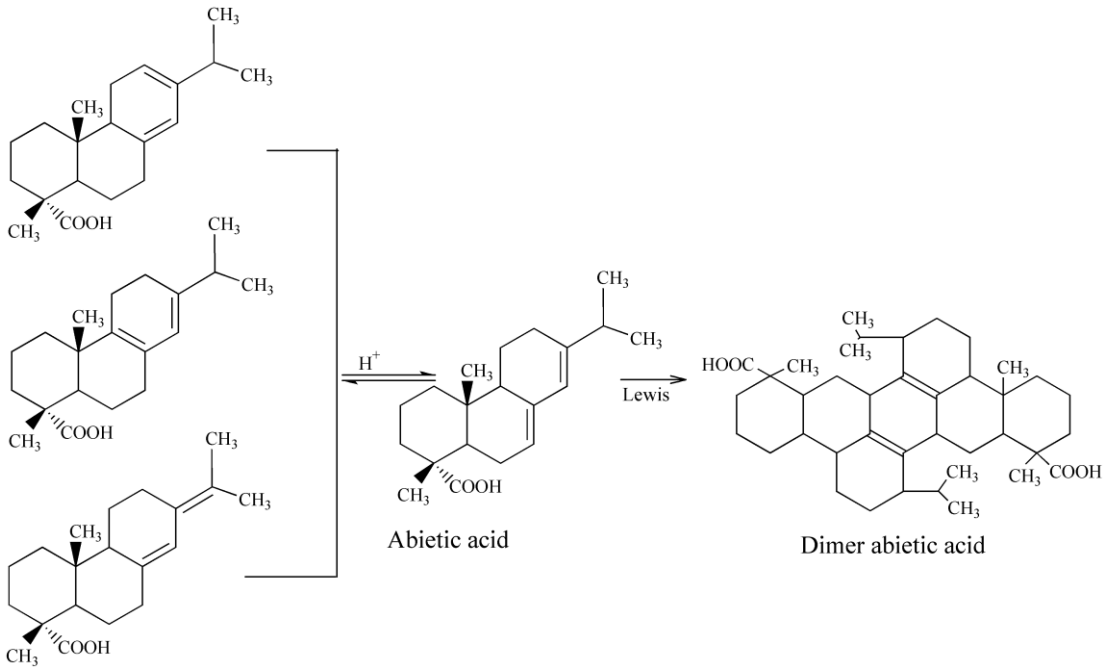

Figure 1-4 Dimerisation of abietic acid, adapted from [35]

The dimerisation reaction can be controlled so the extent of dimerisation is controlled, allowing for the production of partially-dimerised rosins.

1.2.3.4 Disproportionation.

Abietic acid is disproportionated to dehydroabietic acid (DHA) and dihydroabietic acid (Figure 1-5), which are more stable towards oxidation and result in a high softening point [1, 13, 30, 34]. Uses for disproportionated rosins include adhesives, paper sizing (the addition of a water-repellent layer to paper) and tackifiers (they give ‘stickiness’ to adhesives) [1, 36].

1.2.3.5 Hydrogenation.

ABA is also hydrogenated to dihydroabietic acid or tetrahydroabietic acid [30]. This improves resistance to discolouration and oxidation [1]. Hydrogenated rosin uses include cosmetics, tackifiers and plasticizers [36].

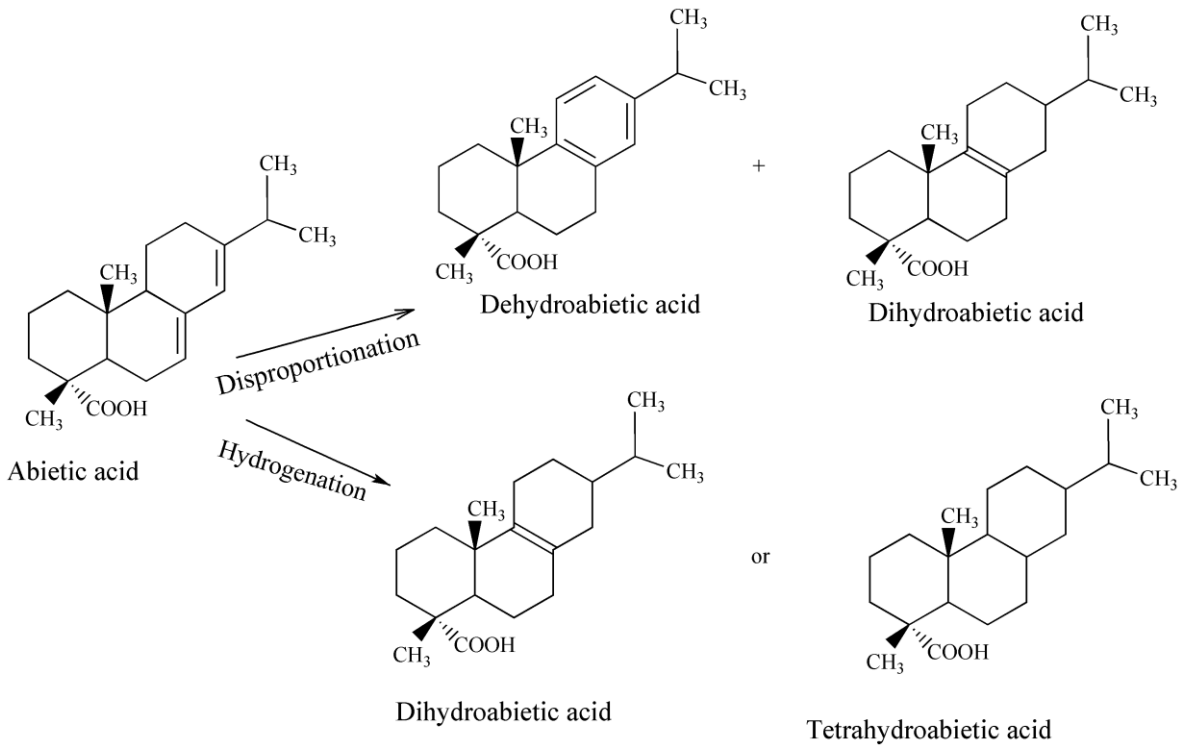

Figure 1-5 Disproportionation and hydrogenation of abietic acid

1.2.3.6 Other modifications.

Rosins can also be modified by esterification of the carboxylic acid to form different rosin esters depending on the colour, odour and viscosity requirements. Rosin esters are used in chewing gum [1]. Fumaric and maleic acids anhydrides are also used to modify rosins [37]. These acidified rosins are often used in inks and varnishes.

1.3 Soldering

Soldering is one of the areas affected by rosin crystallisation, as it causes the solder paste to become 'crumbly' in texture and unsuitable for use.

1.3.1 Definition

Soldering is defined by the American Welding Society as "a group of welding processes which produces coalescence of materials by heating them to a suitable temperature and by using a filler metal having a liquidus not exceeding 450° and below the solidus of the base materials." Simply speaking, it is the joining of materials together by heating them and a solder material which can be in liquid, paste or wire form. The solder joins the materials by wetting action. Wu describes wetting as "the behaviour of a liquid towards a solid surface with a contact" [38]. The joints are said to be wet when the solder leaves an unbroken, permanent film on them. Wetting occurs due to interactions between the solder atoms and the metal atoms which are stronger than the interactions between the solder atoms themselves. The solder forms an alloy with the metal it is joining. Wetting is affected by the solder material and the ease at which it forms alloys with the materials to be joined. The fluidity of the solder when heated and its ability to flow into narrow spaces by capillary action is also important. A good soldering material has good wetting action, flowability/spread, and capillary action [39].

Paste is about 90% of Henkel's solder business. The solder weight comprises of 88% metal and 12% flux, but because of their densities it is 50:50 metal:flux by volume. Of the 12% flux, 40-50% is a polar solvent with a high boiling point, 40-50% is rosin, ~6% is an activator and ~3% gelling agent.

1.3.2 Process

The basic steps of soldering are 1) fitting of the joints together, 2) the precleaning stage, 3) application of the flux, 4) application of heat and 5) application of the solder. The solder is first allowed to wet the surfaces. Then the space between the materials is filled with solder. The joint is then cooled and the flux residue is removed if necessary. As some fluxes contain a corrosive acid used to remove

oxides, their residue needs to be removed so it does not cause damage. Some examples of solders include tin alloys and zinc alloys e.g. tin-antimony solders [39].

1.3.3 Solder flux

Flux has several purposes; it removes oxides and other surface impurities from the metals surface and a small amount of the flux remains at the joint to prevent the metal from reforming oxides [39-41]. It is displaced by the solder so the solder forms an alloy with the base metal, and it mixes with the solder, lowering surface tension in order to further aide wetting [42]. Oxides are removed from the surface through chemical reactions between the flux and the oxide e.g. the oxide can be reduced to a soluble product.

Depending on the classification i.e. military, industry etc. fluxes are grouped in several ways. US federal specification QQ-S-571 E 1986 named four groups of flux, rosin flux (R), mildly activated rosin flux (RMA), activated rosin/resin flux (RA) and non-rosin flux (AC) [43]. Since then, standards J-STD-004 and 004B have become the standards rosins must follow [44]. Developed by the Assembly and Joining Processes Committee of the IPC (previously the Institute for Interconnecting and Packaging Electronic Circuits), J-STD-004 separates fluxes into 4 groups; rosins, resins (i.e. synthetic resins), organic and inorganic fluxes. It also notes the flux's activity level and whether or not they contain a halide. The European standard, ISO 9454-1 groups fluxes into resins, organic and inorganic [45].

1.3.3.1 Rosin flux

Rosin quality is graded by its colour, with the palest, water-white (WW), being the purest quality. This rosin is inactivated (R) and is a very weak acid. It is non-corrosive [1]. At soldering temperatures it liquefies and the acids present become chemically active. A liquid solution of it is normally prepared in an organic solvent which evaporates off [18].

Activators, such as polar organic compounds or halides, can be added to rosins to increase their efficiencies as fluxes at removing oxides [43]. Activated rosins leave

corrosive residues behind after soldering which need to be removed. Non-activated rosins are non-corrosive and their residue does not need to be removed unless required for appearance [39, 40]. Properties which make rosins good fluxes include their non-conductivity, non-corrosiveness and good heat conduction. Rosins can absorb leftover activator residue. The alloys formed by the solder and base material can affect the viscosity of rosins [46].

Non-activated rosin fluxes can be used for electrical components on copper as what little residue they leave can easily be removed by organic or semi- aqueous solvents if necessary. They are considered in the no-clean flux category. Mildly activated rosin flux is used on surfaces with more oxides as it has greater activity. Residue removal is not always required, unless a halide activator is involved. If cleaning is required an organic solvent first removes the non-polar rosin then a polar solvent removes the activator residue. Activated rosin/resin fluxes contain higher concentrations of activators. Because of this they are more corrosive and can be used on nickel and iron-based alloys too. Their residue must always be removed by the same method as for RMA [18].

1.4 Current rosin analysis methods

The focus of this work is the analysis of rosin samples. Resin acids are the main components of rosin and are also present in other natural samples. There have been reports of many different analytical techniques used for the characterisation of rosins, however, the analysis of the resin acids are generally applied to materials other than rosin e.g. paint varnish, including GC [3, 47-54], pyrolysis-GC-MS [55, 56], CE [31, 57-59], HPLC [3, 31] and TLC [48]. The first application of CE to the analysis of resin acids investigated pulp mill effluents [31]. Various binding media known to contain resin acids were analysed by CE and GC [57].

1.4.1 Gas Chromatographic methods of rosin analysis

GC is one of the most common methods of analysing the resin acids, generally in the form of their methyl esters [49, 51-53]. In 1959 Hudy was the first to report the use of GC for resin acid methyl ester analysis [47]. While separation of the resin acid methyl esters was achieved, Hudy reported problems with the thermal isomerisation of the LVO and PAL methyl esters on the column due to the high temperatures required (260-300°C). There was also a report of analysis using just MS for rosin analysis [17]. Genge analysed the resin acid methyl esters using a mass spectrometer over a 2 h run time. Some isomerisation was observed in the mass spectra but did not cause problems with analysis. Joye and Lawrence published several papers on the use of GC for the analysis of the acid fraction of rosins from various pine species using a thermal conductivity detector [49, 50, 60]. In a 35 min analysis time they separated the methyl esters of ISO, DHA, ABA and NEO, with LVO and PAL coeluting while also experiencing some isomerisation of LVO as described in section 1.2.3.2 (acid full names in Table 1-1). They quantified what percentage of the acidic fraction each acid methyl ester corresponded to. In separate papers, Nestler and Zinkel also used GC with a thermal conductivity detector for resin acid methyl ester analysis [52]. Nestler and Zinkel identified the methyl esters of NEO, DHA, ABA, ISO, PIM and those of LVO and PAL which did not separate. Selectivities reported for the acid methyl esters ranged from 0.75-1.86 [52].

Open-tubular column GC with an FID was used to separate and identify the methyl esters of PIM, SAN, PAL, ISO, DHA, ABA, and NEO in suitable and unsuitable

samples of rosin flux. A higher percentage of DHA was the only noticeable difference in the bad flux. As seen in Figure 1-6, resolution (R_s) values of R_s>2 were achieved, however, the analysis time is over 120 min [51].

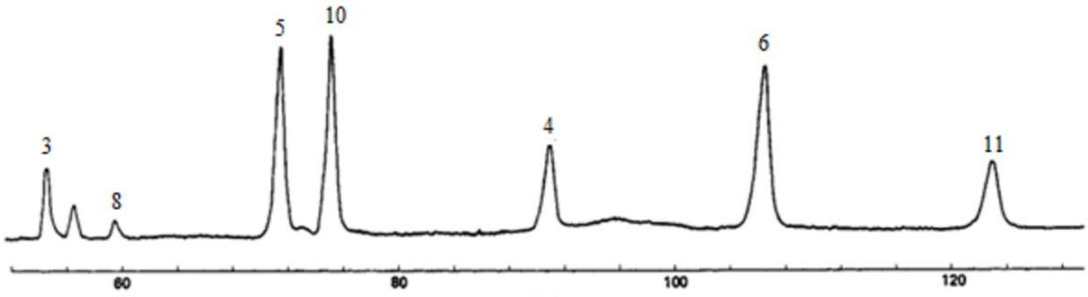

Figure 1-6 Chromatogram of a rosin flux sample analysed by open-tube-column GC-FID. Numbers indicate acids as follows; PIM (3), DHA (4), PAL (5), ABA (6), SAN (8) ISO (10), NEO (11), adapted from [51].

Since then GC has been used for the analysis of resin acids in many compounds, including rosin samples, varnishes and old binding media. A derivatisation method combining ethyl esters from the carboxylic groups and trimethylsilyl ethers from the hydroxyl groups of resin acids was used for their analysis by GC-MS [53]. The ethyl esters of PIM, SAN, ISO, DHA, NEO, 7OXO and ABA were identified. LVO and PAL were not separated, and secondary derivatisation products were found to form which is not desirable in an analytical technique. In a paper analysing the resin acids present in various resins used in paintings they improved on the sensitivity in a pyrolysis-GC-MS method using trimethylsilylation derivatisation, and while some pyrolysis products were observed, this derivatisation greatly reduced the number of secondary products [55].

GC-MS and LC-MS were investigated as comparative techniques for the analysis of resin and fatty acids in paper mill water [61]. LODs for the GC method were found to be 0.004-0.1 µg L^{-1} while the LODs for the LC method were 0.9-3 µg L^{-1}. The lower LODs and better selectivity achieved with GC-MS was not unexpected as the derivatization of a sample can result in less baseline noise as any possible contaminants are no longer seen. On the other hand, the required sample derivatization can be seen as a disadvantage as Latorre found the derivatives to be unstable with short lives which led to less reproducible results. The GC method had long analysis times (~40 min) but saw the separation of the trimethylsilyl esters of PIM, SAN, ISO, PAL, DHA, and ABA. While LC-MS showed good sensitivity and

a slightly shorter run time (27 min), it did not achieve separation of the resin acid peaks except for DHA in agreement with Luong's findings [31]

1.4.2 Capillary electrophoresis

Luong *et al.* developed what they believe to be the first application of CE to the analysis of resin acids [31]. Using a 30 mM sulfobutylether -β-cyclodextrin (SBCD) 20 mM methyl- β-cyclodextrin (MECD) in 20 mM borate buffer pH 9.25, they analysed a standard mix of ABA, DHA, ISO, LVO, NEO, PAL, PIM and SAN, along with three chlorinated congeners (see Figure 1-7). PAL and LVO were successfully separated which had not previously been achieved by GC-MS. PIM and SAN could not be baseline separated, and 7OXO was not studied.

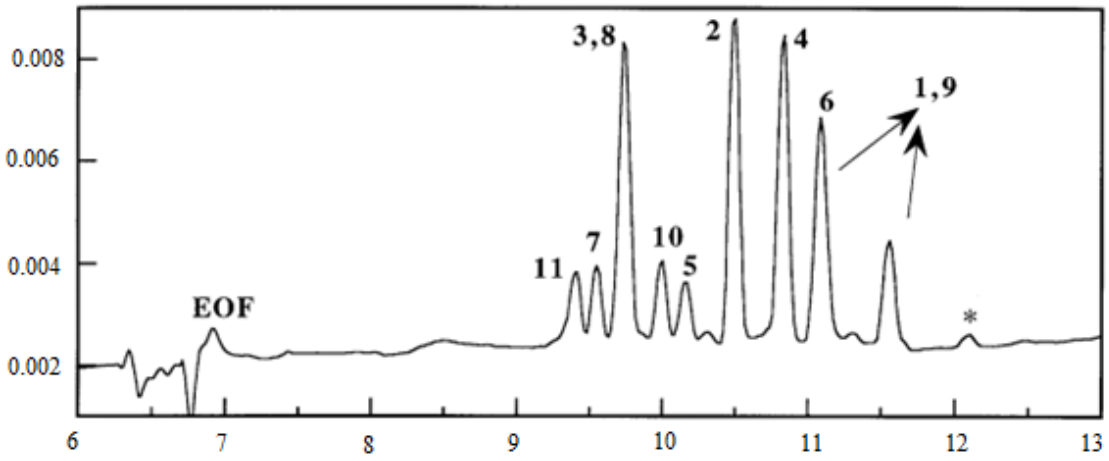

Figure 1-7 Electropherogram of resin acids analysed by CE. Numbers indicate acids as follows; 12-Chlorodehydroabietic acid (1 or 9), 14-Chlorodehydroabietic acid (1 or 9), 12,14-Chlorodehydroabietic acid (2), PIM (3), DHA (4), PAL (5), ABA (6), LVO (7), SAN (8) ISO (10), NEO (11), adapted from [31]. Buffer consisted of 20 mM MECD 20 mM SBCD in 20 mM sodium borate at pH 9.25, bubble cell capillary length was 47 cm (40 cm effective length) 50 µm I.D., 250 µm I.D. at detection window, UV detection at 214 nm, voltage at 15 kV.

No resolution values were published; however Figure 1-7 shows that baseline resolution values was not achieved for all of the acids. The LOD reported was 5 ppm or higher for the acids. They theorised that the cyclodextrins form inclusion

complexes between the hydrophobic CD cavity and the isopropyl part of the abietic type acids and the vinyl/methyl part of the pimaric type acids [31].

Rosins were previously used in binding and varnishes for paintings. Analysis of resin acids present in old paintings has been carried out using methods including GC-MS and CE [31, 54, 62]. Findeisen *et al*. further developed the work of Luong *et al.* to analyse resin acids in old painting samples [59]. A standard mix of ABA, DHA, ISO, LVO, NEO, PAL, PIM and larixol acetate was separated, with SAN still coeluting with PIM. Reducing the CD concentration to 10 mM SBCD 6.6 mM MECD and adjusting various CE conditions reduced the analysis time by almost 7 min. Six acid peaks were identified on a rosin electropherogram but not quantified (Figure 1-8).

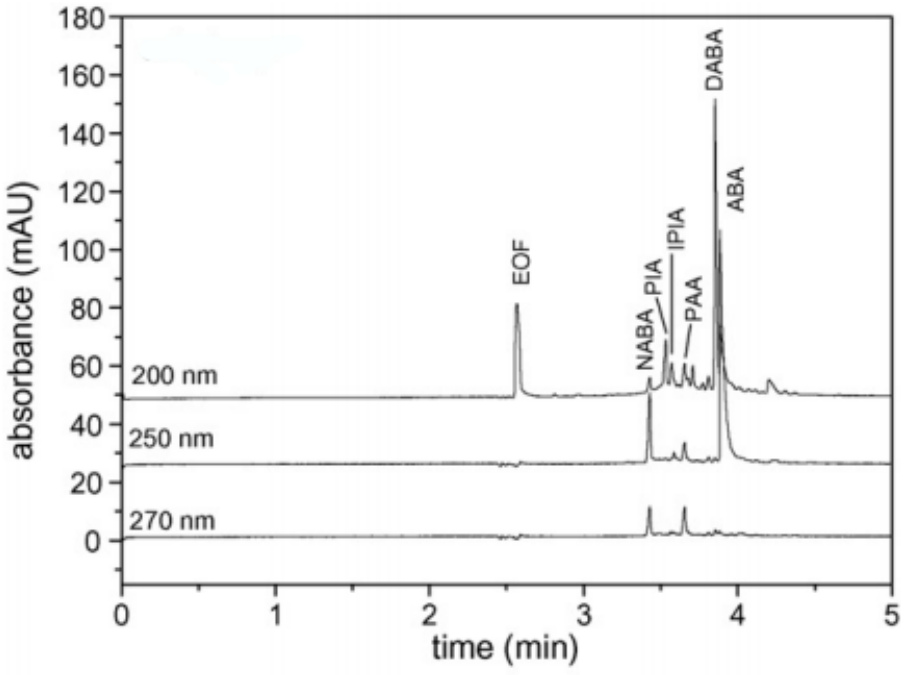

Figure 1-8 Electropherogram of a rosin sample analysed by CE. Buffer consisted of 6.6 mM MECD 10 mM SBCD 20 mM borate buffer at pH 9.25, Capillary 48.5 cm (40 cm to detector), 50 µm I.D., injections at 100 mbar s^{-1}, 25 kV, temperature at 20°C, detection at 200, 250 and 270 nm. Labels indicate acids as follows; Neoabietic acid (NABA), Pimaric acid (PIA), Dehydroabietic acid (DABA), Palustric acid (PAA), Abietic acid (ABA), Isopimaric acid (IPIA) [59].

Findeisen contributed to a second paper where Dell'Mour *et al*. compared CE and GC for the analysis of resin acids present in binders in museum objects [57]. A rosin

sample was analysed using 20 mM MECD 30 mM SBCD in 20 mM borate buffer pH 9.25 (see Figure 1-9). Capillary was 48.5 cm (40 cm effective length), separation at 15 kV after 100 mbar s^{-1} injections. UV detection was at 200, 250 and 270 nm. None of the six acids identified were quantified.

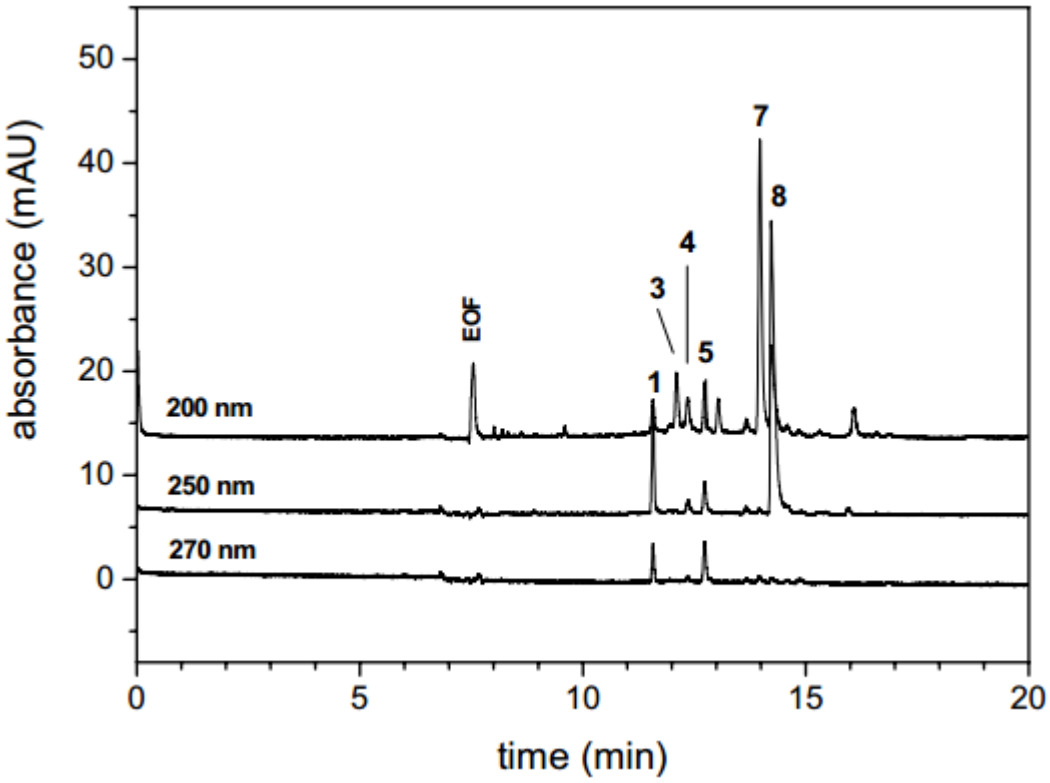

Figure 1-9 Electropherogram of a rosin sample analysed by CE. Buffer consisted of 20 mM MECD 30 mM SBCD 20 mM borate buffer at pH 9.25, Capillary 48.5 cm (40 cm to detector), 50 µm I.D., injections at 100 mbar s^{-1} , 15 kV, temperature at 20°C, detection at 200, 250 and 270 nm. Numbers indicate acids as follows; NEO (1), LVO (2), PIM (3), ISO (4), PAL (5), larixol acetate (6), DHA (7), ABA (8) [57]

In the work by Dell'Mour *et al.*, 7-oxo-dehydroabietic acid (7OXO) and sandaracopimaric acid (SAN) were not analysed. NEO, PIM, ISO, PAL, DHA and ABA peaks were identified in the electropherogram of a rosin sample. They found CE to give comparable resolution values and analysis times to those of GC. As expected due to the limited detection path lengths of the capillaries, the detection limits of the acids in CE were found to be higher. The CE detection limit of DHA (400 pg μL^{-1}) is higher than that of the GC (250 pg μL^{-1}) however, sample preparation procedures for the CE method were much simpler, with samples being dissolved in methanol as opposed to the derivatization required in GC.

1.4.3 Liquid Chromatography

There have been very few attempts at the analysis of rosin samples by HPLC. Sadhra *et al*. first reported the use of gradient HPLC for the separation of resin acids from a 0.42% w/v rosin sample in methanol using a C_{18} column and a methanol-water mobile phase (see Figure 1-10).

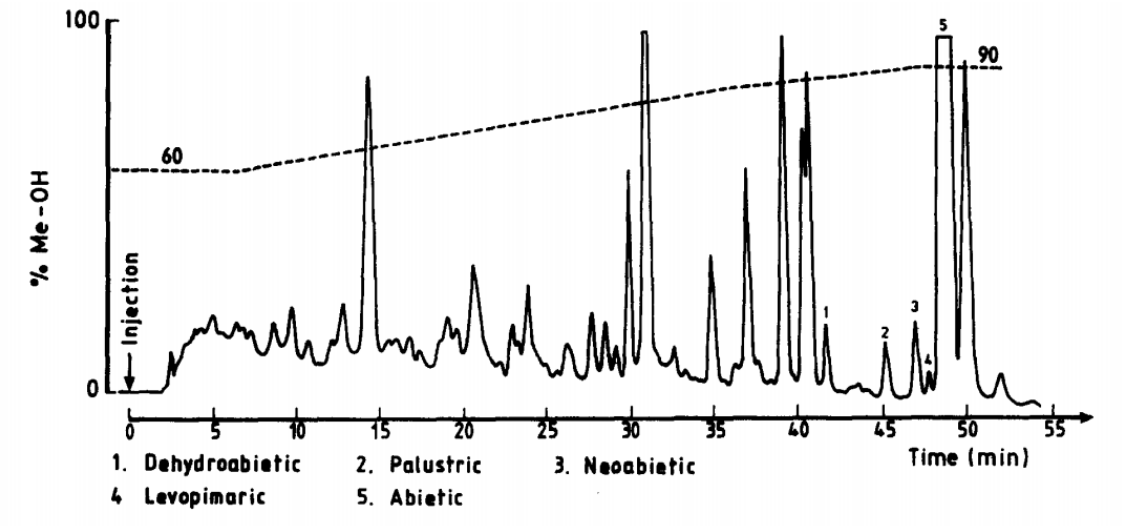

Figure 1-10 Chromatogram of a rosin sample analysed by HPLC [3].

A combination of 3 HPLC methods, MS, IR and NMR were used to identify 5 acid peaks in a rosin sample electropherogram although they were not baseline-separated. The LVO and ABA peaks could not be separated [3].

Luong *et al*. compared their CE method and HPLC method for resin acid analysis. A C_{18} column with a 90:10 ACN:water mobile phase was used but resulted in the separation of just DHA, with the other acids coeluting in two peaks (see Figure 1-11). In comparison, seven peaks were resolved by their CE method, those of DHA, PAL, ABA, NEO, LVO and ISO. More optimisation was carried out on the CE method so it is possible that further optimisation of the HPLC method could improve this separation [31].

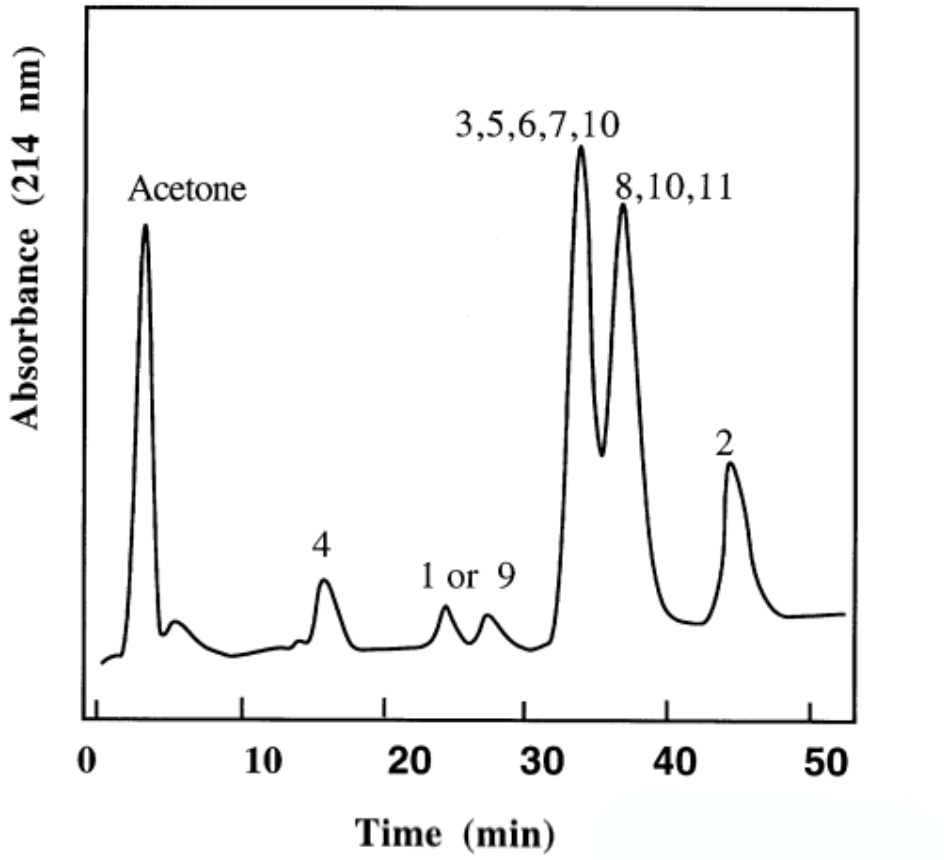

Figure 1-11 Chromatogram of a resin acid mix analysed by HPLC. The column was an LC-PAH column (4.6 mm x 5 cm, 3 μm), mobile phase consisted of 65:35 MeOH:1% acetic acid, detection at 214 nm, Numbers indicate acids as follows; 12-Chlorodehydroabietic acid (1 or 9), 14-Chlorodehydroabietic acid (1 or 9), 12,14-Chlorodehydroabietic acid (2), PIM (3), DHA (4), PAL (5), ABA (6), LVO (7), SAN (8), ISO (10), NEO (11) [31].

Reversed phase HPLC was used to determine a mixture of ABA, NEO, PAL, LVO, and DHA (Figure 1-12). A C_{18} column was used with a 5% acetic acid 85:10 methanol (MeOH):water mobile phase. DHA was found to elute much earlier than the other 4 acids which coeluted from 23-26 min [63].

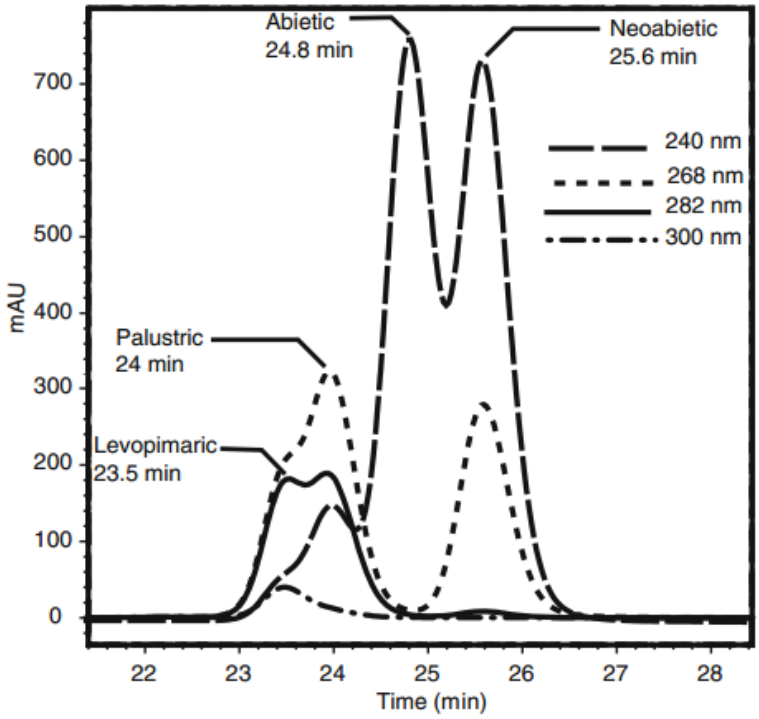

Figure 1-12 Chromatogram of 4 resin acids analysed by HPLC, C_{18} column (4.6 cm x 25 cm, 5 µm), mobile phase consisted of 5% acetic acid 85:10 MeOH:water, detection at 240, 268, 282 and 300 nm [63].

Multiwavelength analysis was used by a diode-array detector (DAD) in order to identify the resin acids as again LC was not successful at separating them at a single wavelength. The use of LC-MS was also reported for resin acid analysis in river water. While individual LODs of 0.25-0.4 µg L^{-1} were achieved for ABA, DHA, ISO, and PIM with good reproducibility, only DHA was sufficiently separated within the 15 min run time [64].

DHA, ABA and 7OXO were analysed in various cosmetic products containing rosin by HPLC-UV with an SPE sample clean-up [65]. They reported LODs of 7-19 µg g^{-1}. Using a urea-embedded column, PIM was detected but not baseline resolved from ABA and so not quantified.

1.4.4 Summary of analytical methods

From a review of the literature it was found that the majority of papers on rosin analysis use GC. While good separation, sensitivity and selectivity are achieved using GC, a derivatization step is required for the non-volatile resin acids which is time consuming and renders the samples unusable for further use. It can also result in the formation of other unwanted derivatisation products which interfere with analysis. LC has the advantage of allowing the sample to be injected directly onto the column without the need for derivatization. HPLC analysis times have been shown to be shorter than GC times (30-55 min compared to 35-120 min) and sensitivity is comparable. Better resolution has been seen using GC but the potential for HPLC method optimisation has not been fully explored as there has not yet been much analysis of rosin samples using HPLC. In the few investigations carried out so far, CE has shown better resolution than LC at shorter analysis times than both GC and LC (rosin and resin analysis so far ranging from 5-17 min). While GC and LC tend to have better precision, CE is also advantageous in its low sample and buffer volume requirements. The buffer is generally aqueous and so does not consume high amounts of organic solvents, and separations take place in a simple open tube in place of an expensive column. These all contribute to inexpensive analysis, and the cost of a CE system is comparable to that of a GC instrument (without MS) [57]. Like LC, sample derivatization is not necessary and the sample is injected straight to the capillary. In addition to this, as it is not a chromatographic separation technique, it will provide different separations and thus different information that can be used in conjunction with LC. The LODs reported for the resin acids by GC-MS and LC-MS methods were in the ng L^{-1} and μg L^{-1} range while the CE-UV and HPLC-UV LODs ranged from 0.4-19 mg L^{-1}. This highlights the greater sensitivity achieved using MS compared to a UV detector. Low sensitivity is also a disadvantage of CE analysis. This is due to the low sample amount injected, and the small detector path length. Changing the detector type is an obvious way to improve on this sensitivity e.g. CE-MS, other options include increasing the path length e.g. by using a bubble cell capillary, or by incorporating a preconcentration technique such as sample stacking or sweeping into the method.

LC has not been successful in the separation of most of the resin acids. GC-MS has been proven to be an effective technique for separating most of the resin acids but with a derivatisation step required. CE has also proved effective at separating most of the resin acids but with room for more optimisation.

1.5 Capillary Electrophoresis

1.5.1 Theory of Electrophoresis

Electrophoresis is used to separate different species according to their velocities under an external electric field. This electrophoretic velocity is described in Equation 1;

$$v = \mu_e E \qquad \text{Equation 1}$$

Where v is the velocity of the ion (ms^{-1}), μ_e is the electrophoretic mobility ($m^2V^{-1}s^{-1}$) and E is the electric field strength (Vm^{-1}). Each ion has this characteristic property known as electrophoretic mobility which means it moves when in an electric field. It is proportional to its charge and inversely proportional to its friction coefficient and described in Equation 2 [66];

$$\mu_e = \frac{q}{6\pi\eta r} \qquad \text{Equation 2}$$

Where q is the charge on fully dissociated ions, η is the viscosity of the solution and *r* is the Stokes' radius (hydrodynamic radius) of the ion [66]. Both size and charge affect analytes mobility; smaller and more highly charged ions travel faster. The movement of analytes is also affected by the electroosmotic flow (EOF) which is described in Equation 3;

$$\mu_{EO} = \frac{\varepsilon\zeta}{4\pi\eta} \qquad \text{Equation 3}$$

Where μ_{EO} is the electroosmotic mobility, ε is the dielectric constant of the medium, ζ is the zeta potential and η is the viscosity. The apparent mobility (μ_{app}) of an

analyte is the vector sum of the electrophoretic mobility and electroosmotic mobility (see Equation 4);

$$\mu_{app} = \mu_e + \mu_{EO} \qquad \text{Equation 4}$$

Separations are generally characterised by resolution and efficiency. Resolution (R_s) measures the separation between two peaks. It is calculated using Equation 5 [67]:

$$R_S = \frac{(2.35/2)(t_2 - t_1)}{(w_1 + w_2)} \qquad \text{Equation 5}$$

Where t_1 and t_2 are the retention times of the two peaks and w_1 and w_2 are the peak widths of the peaks at half peak height.

The efficiency of a column describes its ability to give sharp peaks. It is measured by the number of theoretical plates (N). A higher N value means higher efficiency. Capillary efficiency can be calculated using Equation 6 [68]:

$$N = 5.54\left(\frac{t_R}{W_{1/2}}\right)^2 \qquad \text{Equation 6}$$

Where t_R is the retention time and $W_{1/2}$ is the peak width at half peak height. It is also described as the height equivalent of a theoretical plate (HETP) in Equation 7 [66].

$$HETP = L/N \qquad \text{Equation 7}$$

Where L is the capillary length and N is the number of theoretical plates.

The theory of capillary zone electrophoresis (CZE) and its instrumentation has been described extensively in many reviews and books [66, 68-73]. The focus of the theory covered in this thesis refers to relevant methods of CE used, MEKC, MEEKC and cyclodextrin modified CE.

1.5.2 Micellar electrokinetic chromatography

In CZE, analytes are separated by their electrophoretic mobilities. Neutral analytes have no charge and therefore no electrophoretic mobility and so cannot be separated by conventional CZE. In order to separate neutral compounds by CE, techniques such as micellar electrokinetic chromatography (MEKC) are used [66, 74, 75].

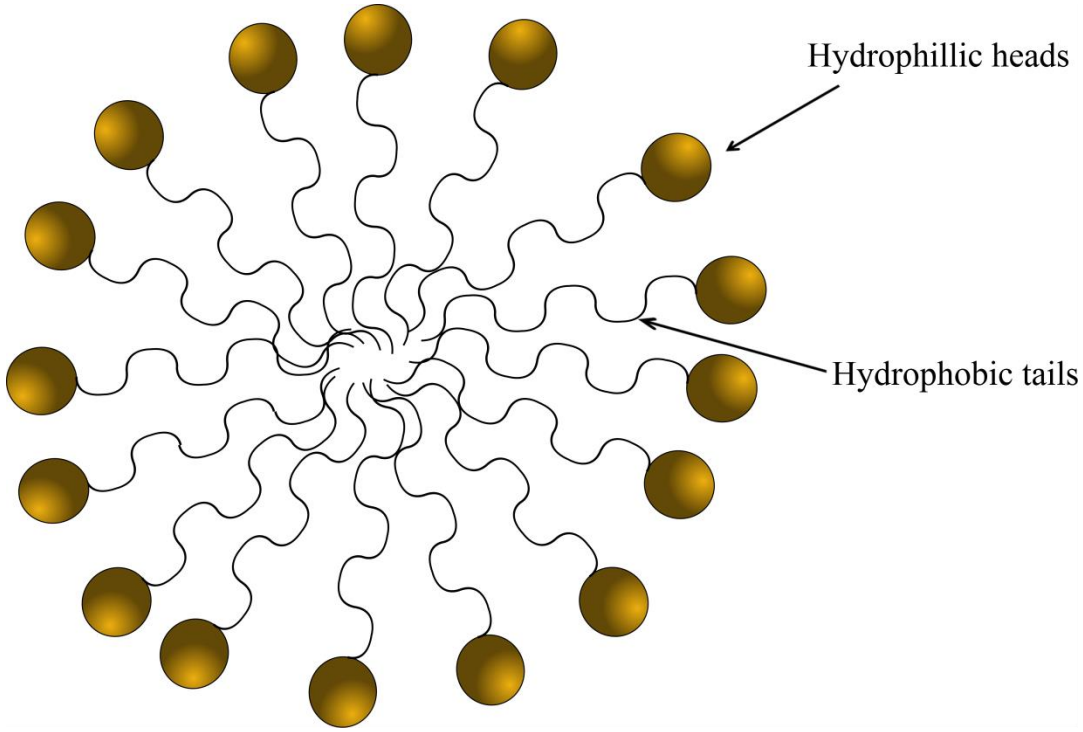

Figure 1-13 Illustration of a micelle.

In MEKC, charged surfactant molecules are added to the buffer. When they reach their 'critical micelle concentration' (CMC) the surfactants form aggregates in roughly sphere shapes with diameters of 3-6 nm called micelles which act as a pseudo-stationary phase for the neutral analytes to partition in and out of. The surfactants hydrophilic heads are on the outside of the micelle and their hydrophobic tails point inwards (see Figure 1-13).

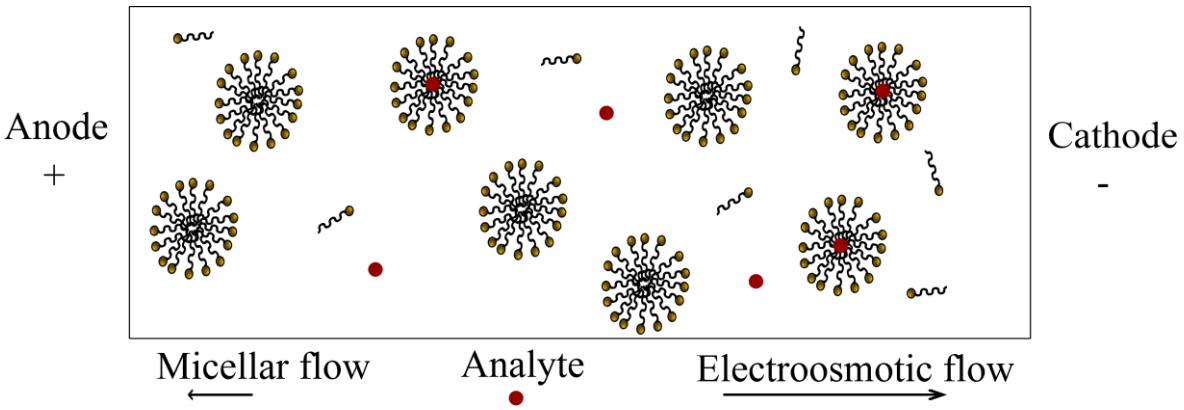

Figure 1-14 Diagram showing the mechanism of MEKC.

Terabe *et al*. first used micellar separation in capillary electrophoresis and named it MEKC [76]. Sodium dodecyl sulphate (SDS), an anionic surfactant, is the most commonly used, is widely available and is inexpensive. The anionic micelles have a negative charge and move against the electroosmotic flow (EOF) towards the anode. However, the EOF has a higher velocity so they have a net movement towards the cathode (see Figure 1-14). Analytes in the sample partition between the hydrophobic centre of the micelles and the aqueous solution. The extent to which analytes partition into the micelle depends on the analytes hydrophobicity, hydrogen bonding and ionic attractions.

1.5.3 Microemulsion electrokinetic chromatography

Microemulsion electrokinetic chromatography (MEEKC) was first reported by Watari *et al*. in 1991 [77]. It is similar to MEKC in that it uses a pseudo stationary phase but in this case the additive is a mixture of nano-sized oil droplets in an aqueous buffer (O/W) which is stabilized by the addition of a surfactant and a co-surfactant (see Figure 1-15). The surfactants also reduce the surface tension of the droplet. Other forms of MEEKC include water in oil (W/O), bicontinuous (B.C.) and ionic liquids in water (IL/W) [78]. Analytes are separated based on their mobilities and their level of partitioning into the microemulsions (MEs). The ME droplets diameters are less than 10 nm so they are optically transparent and slightly bigger than micelles [79].

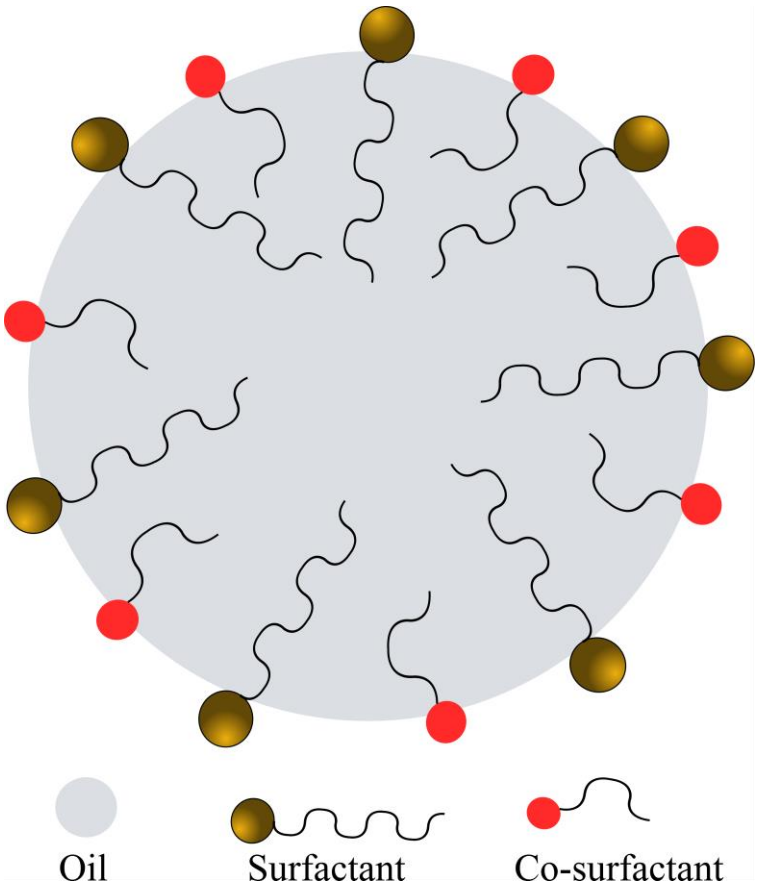

Figure 1-15 Illustration of a microemulsion, adapted from [78].

The SDS molecules coat the surface of the droplet. Because of the charge repulsion of the SDS surfactants, a co-surfactant, usually a short-chain alcohol such as 1-butanol, is necessary to reduce the surface tension and allow the droplets to hold their structure. The combination of the surfactant and co-surfactant reduce the surface tension between the oil and water to zero and allows the emulsion to form. Although the microemulsions are negatively charged and travel towards the anode, the EOF is stronger and carries them towards the cathode. Separation can be affected by the choice and concentration of the oil and surfactant, and other optional additives including organic solvents and cyclodextrins. Cetyltrimethylammonium bromide (CTAB) is a cationic surfactant that has been used in MEEKC. It can be particularly useful if the analyte is cationic and ion-pair reactions are occurring with negatively charged microemulsions. The use of CTAB results in a reversal of the EOF. Neutral surfactants can also be used but are generally more useful in separating charged analytes [79]. Combinations of surfactants have also been reported several times [78].

1.6 Cyclodextrins in CE separations

Cyclodextrins (CD) are often used as an additive in CE buffers for chiral separations. However, cyclodextrins can also be used to be separate cis- and trans- isomers (their electrophoretic mobilities are the same but they interact differently with the cyclodextrins) and compounds based on their hydrophobicity. The addition of charged cyclodextrins means longer elution times and higher currents. CDs are sometimes used in addition to micelles in MEKC to further optimise separation.

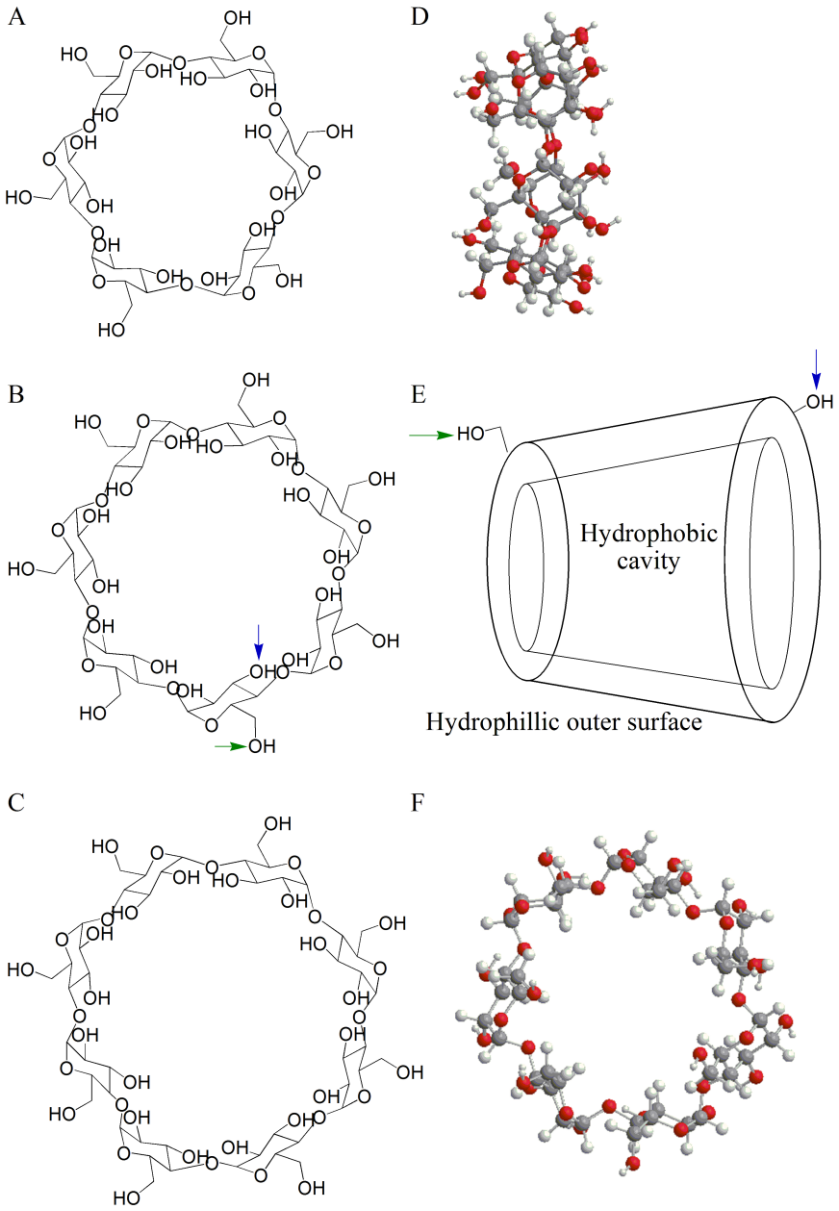

Figure 1-16 Structures of (A) α-cyclodextrin, (B) β-cyclodextrin and (C) γ-cyclodextrin. (D) and (F) show β-CD in 3D viewed from the side and top, (E) highlights the position of the primary and secondary hydroxyl groups in β-CD.

1.6.1 Cyclodextrins

Cyclodextrins (CDs) are cyclic oligosaccharides consisting of 6 (α), 7 (β) or 8 (γ) α 1, 4-linked glucopyranose units [80] (see Figure 1-16). They are crystalline, homogenous and non-hydroscopic. The glucose units orientate themselves in a chair conformation and the cyclodextrin molecule forms a truncated cone shape with a hydrophobic inner cavity. The outer surface is hydrophilic due to the presence of hydroxyl groups. The three native CDs have the same cavity depth but different widths (properties shown in Table 4-1). Due to their shape and surface chemistries, they easily form dynamic inclusion complexes with a wide range of compounds. They have a range of uses in analytical chemistry, from additives to background electrolytes in CE, to chemically bonded stationary phases in HPLC. As well as inclusion complexes, CDs can also form water soluble micelle-like aggregates that interact with compounds [81].

Natural CDs are insoluble in water so there are many synthetic derivatives including methyl, hydroxyl and ether CDs which are more water soluble. Commercially available CDs can be neutral, e.g. methyl-β-cyclodextrin; positively charged, e.g. 2-hydroxy-3-trimethylammoniopropyl β-cyclodextrin; or negatively charged, e.g. sulfobutylether-β-cyclodextrin. The primary hydroxyl groups are on carbon 6 on the narrow rim of the CD while the secondary hydroxyls are on the larger rim on carbons 2 and 3. These hydroxyl groups are chemically modified to form derivatized CDs. Neutral cyclodextrins elute with the EOF [80]. CDs are UV transparent; however, they can cause a small shift in UV lambda max due to electron and chromophore shielding. They also increase the fluorescent intensity of the guest molecule due to the apolar cavity [80].

1.6.2 Cyclodextrin inclusion complexes

Inclusion complexes are not formed by covalent bonds, but by physical forces such as hydrophobic interactions, hydrogen bonding and van der Waals forces between the ‘host’ and the ‘guest’ molecules. The guest molecule must be sterically compatible with the cavity of the CD (the host molecule in this case) and the thermodynamic interaction between the analyte, CD and solvent must favour the complex forming [82]. The guest molecule must also have greater affinity for the CD

cavity than for the background electrolyte. When the cyclodextrins form inclusion complexes, water molecules are displaced by the more non-polar guest molecule. Interactions occur by; 1) Van der Waal forces, 2) H-bonding can occur (not always) between guest and cyclodextrin cavity, 3) strain on the cyclodextrin ring is relaxed after inclusion complexes are formed (only applies to α-CD and is not the most important) and 4) interactions between (a) the guest molecule and the cyclodextrin cavity and (b) the displaced water and the rest of the water are more energetically favoured than interactions between (c) the water and the cyclodextrin cavity and (d) the guest molecule and water [80]. These dynamic inclusion complexes form and break slower as the size of the guest molecule increases, and quicker if the guest molecule is ionised [80].

The association constant of inclusion complexes is a means of quantifying the strength and stability of the complex formed. This information could potentially be used to predict behaviour of the complexes and aid in the optimisation of CD-modified buffers. Affinity capillary electrophoresis is a quick and simple method used for the determination of association constants.

1.7 Electrophoresis versus chromatography

In chromatography, analytes separate based on their partitioning between stationary and mobile phases. In electrophoresis, charged analytes separate based on differences in their mobilities in an electric field. As the two techniques separate analytes based on different properties, the resulting chromatograms and electropherograms will appear different even when analysing the same sample as the migration order, analysis time and peak shapes may all differ.

One of the advantages of CE over HPLC is its greater efficiencies, which results in better resolution of peaks. The reason CE separation results in better efficiencies is that it experiences less band broadening than peaks in LC separations. The Van Deemter equation illustrates the different causes of band broadening experienced in chromatographic separations (see Equation 8).

$$H = A + \frac{B}{\mu} + C\mu \qquad \text{Equation 8}$$

H is the height equivalent of a theoretical plate. Two of the three terms which contribute to band broadening in chromatography which affects theoretical plate height and therefore efficiency are not present in CE. The A term is the contribution of Eddy diffusion to band broadening. This is not an issue in CE as there is a single path while in HPLC the packed particles allow for different paths to be taken. The B term is the contribution of longitudinal diffusion to band broadening and is observed in CE and HPLC. The C term is the mass- transfer contribution to band broadening. It does not occur in CZE as the separation happens in a single moving phase as opposed to partitioning between a stationary and mobile phase as seen in LC [68]. μ indicates the linear flow rate of the mobile phase, showing that longitudinal diffusion decreases as the flow rate in increased while the opposite is true for mass transfer and eddy diffusion is unaffected by it.

There are several contributing factors to the diffusion which can lead to band broadening in CE. At low voltages, molecular diffusion is the main cause of band broadening, and causes peak dispersion (also known as peak variance). The main sources of peak dispersion are temperature, sample plug volume and analyte-wall interactions. The sample plug length can contribute to band broadening if above 3%

of the capillary. At high voltages, Joule heating can cause the flow profile to become parabolic. Joule heating results from the resistance of the solution to the current flow. Temperature increases, causing higher current which increases the temperature, so a cooling system removes the heat. The cooling system is at the capillary surface so the middle of capillary is at a slightly higher temperature. However, this is not a problem with capillary diameters under 100 μm [66].

Another reason for the higher efficiencies achieved with CE relative to HPLC is the flow profiles. In HPLC a mechanical pump pushes the mobile phase through the system causing a parabolic flow profile where resistance occurs at the column walls and there is a 'drag' where the analytes at the centre are traveling slightly faster. In CE the EOF pulls the buffer through the capillary with a flat flow profile which results in narrower peaks. The EOF is caused by an overall negative charge on the walls of fused silica capillaries due to the ionised silanol groups (SiO^-) that begin to exist when the pH rises above pH 3. Cations in the solution are attracted to the capillary wall and form a double layer. One is tightly bound by electrostatic forces and called the stern layer, the second, called the diffuse layer, is loosely bound. The diffuse layer of cations moves towards the cathode when an electric field is applied and drags the buffer and analytes with it. This almost uniform velocity of liquid across is due to the small diameter of the capillary. HPLC column diameters are 2.1-4.6 mm compared to 20-100 μm capillary diameter. The small diameter also means joule heating is dealt with efficiently so high voltages can be used.

Although HPLC has been more exhaustively developed with many mobile and stationary phases available, due to the nature of its separation higher efficiencies are achieved with CE separation. CE is an orthogonal technique to HPLC and can be used to extract different information.

1.8 Conclusion

The components of rosin samples which cause their crystallisation have not yet been confidently identified. GC analyses of resin acid methyl esters have identified the majority of the acid components while little research has been carried out on the neutral groups present in rosins. As HPLC and CE do not require a sample derivatization step, they have proven to be a quicker and simpler method for rosin analysis. The two complementary techniques use different separation mechanisms and will both be investigated for the analysis of the composition of both the acidic and neutral fractions of rosin samples. Different modes of CE are easily interchangeable and provide a range of separation mechanisms for analyte analysis. Rosin composition varies depending on their source. The developed separation methods will be applied to different rosin and resin samples to investigate any differences in the presence and concentration of analytes.

1.9 Aims and objectives

The aim of this work is to further the understanding of the composition of rosin samples using analytical techniques. The objectives are to develop a CE and/or HPLC method for the separation of some of the acidic components found in rosin and to develop another CE and/or HPLC method for the separation of some of the neutral components found in rosin. Different rosin and resin samples will be analysed using these methods. Other objectives include investigating any relationship between the composition of different rosins and their tendency to crystallise, and investigating the association constants of the inclusion complexes formed between cyclodextrins and some of the compounds present in rosins.

Chapter 2

Development of a cyclodextrin-based capillary electrophoresis method for the separation of nine resin acids

2.1 Introduction

Rosin consists mainly of resin acids (90%) which are tricyclic diterpene monocarboxylic acids. Of the acids, 90% are isomeric abietic acids and 10% are dihydroabietic acid and dehydroabietic acid [7, 83]. The isomeric abietic acids form two groups: abietic acids with conjugated double bonds (40-60%) and pimaric acids with non-conjugated double bonds (9-27%) [3, 16]. The abietic acids have an isopropyl group on carbon 7 while the pimaric acids instead contain a methyl and vinyl group. Their pK_a values range from 5.7-7.25, therefore at high pH they will be predominately ionised [1, 31, 84]. While an exact reason for rosin crystallisation has not yet been shown, it has been reported that higher acid concentrations- abietic acid in particular- result in a higher tendency to crystallise [26, 27].

The majority of reports on the resin acids present in rosins analyse the methyl ester derivatives of the acids using GC-MS and generally do not apply the method to rosin samples [6, 17, 47]. In this chapter, both HPLC and CE were investigated as alternative separation methods for the acids present in rosin samples.

2.1.1 HPLC

HPLC has been investigated for the analysis of resin acids but thus far only four have been successfully separated. As discussed in section 1.4.3, the use of gradient HPLC was reported for the separation of resin acids from rosin sample using a C_{18} column and a gradient methanol-water mobile phase. Five acid peaks were identified; however, LVO and ABA were not baseline-separated [3]. HPLC with an SPE sample clean-up and UV detection was used to analyse DHA, ABA and 7-oxodehydroabietic acid (7OXO) in various cosmetic products containing rosin [65]. In this study a reverse-phase amide column was used for rosin separation, as it is particularly suited for the separation of polar compounds. Several solvents were investigated as an optimum mobile phase and the solvent: water ratio was optimised. The addition of an acid and a base to the mobile phase to improve efficiencies was investigated. The addition of cyclodextrins to the mobile phase to improve separation was also explored.

2.1.2 Capillary electrophoresis (CE)

Few studies described in the literature apply CE methods to rosin sample analysis. While comparing CE and GC for the separation of binders in museum objects, Dell'Mour *et al*. analysed a rosin sample using a cyclodextrin-modified buffer [57]. Six acid peaks were identified in the rosin electropherogram, however, none were quantified. A standard mixture of abietic-, dehydroabietic- (DHA), neoabietic- (NEO), levopimaric, pimaric- (PIM), isopimaric- (ISO), and palustric acid (PAL) was separated with a 15 min run-time. The analysis of rosin was not the principle aim of that study so the method was not optimised. CE was reported to give comparable resolution values and analysis times to those achieved using GC. While the reported CE detection limit is higher than that of the GC, sample preparation procedures are simpler and no derivatisation is required.

In this chapter, the development of a new CE method is reported for the separation of nine resin acids in modified and unmodified rosin samples, where previously they could not be separated. The use of various buffers, cyclodextrin types and concentrations were investigated. Calibration curves were created to determine the concentrations of abietic-, dehydroabietic-, neoabietic-, pimaric-, isopimaric-, levopimaric-, sandaracopimaric- (SAN), palustric- and 7-oxo-dehydroabietic acid (7OXO) (structures shown in Figure 2-1) in the rosin samples.

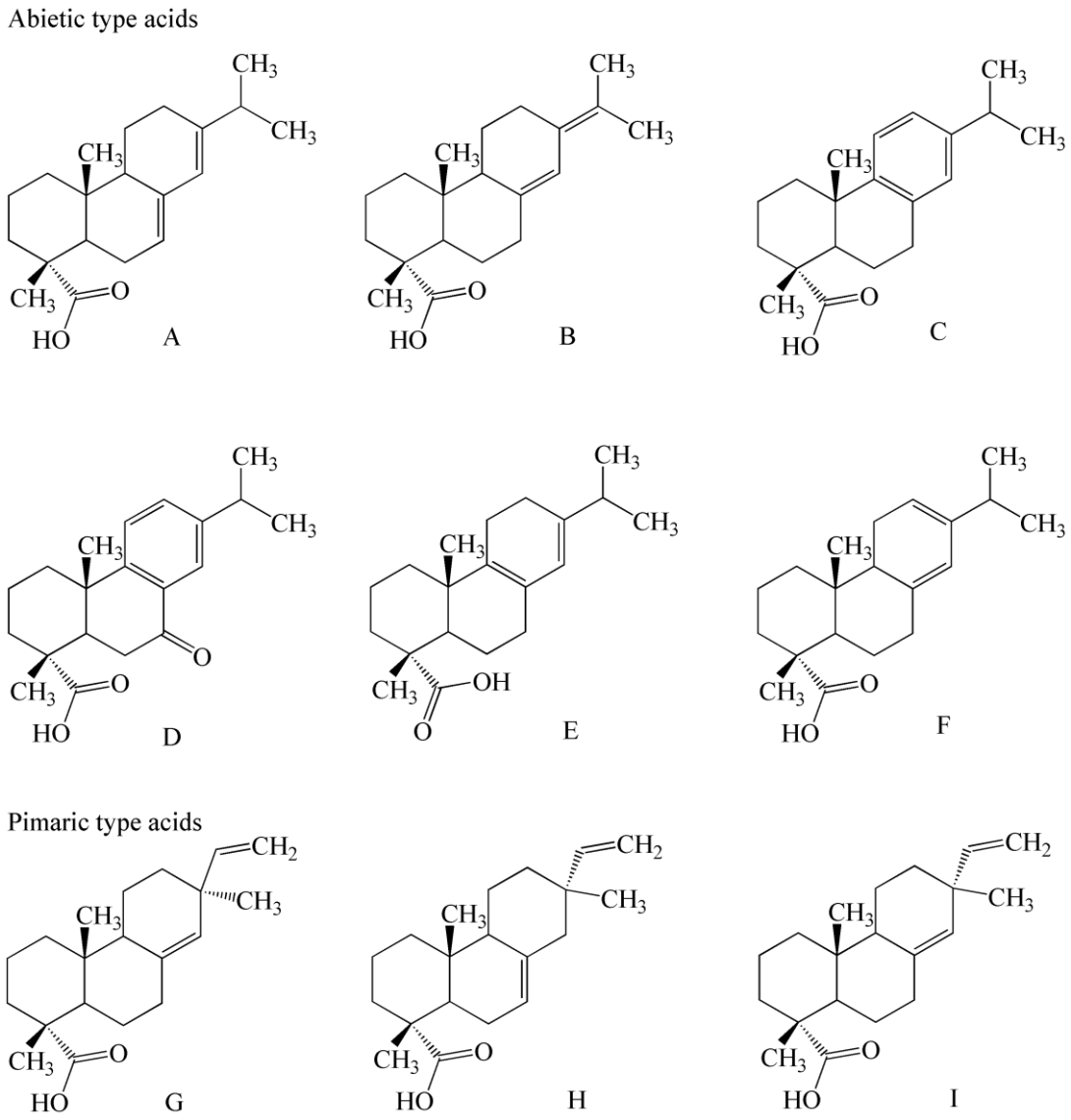

Figure 2-1 Chemical structures of the resin acids

Table 2-1 Acids as denoted in Figure 2-1

Letter in Figure 2-1	**Acid**	**LogD at pH 7.4[a]**	**Molecular weight (g mol^{-1})**
A	Abietic acid (ABA)	3.79	302.45
B	Neoabietic acid (NEO)	3.99	302.45
C	Dehydroabietic acid (DHA)	3.65	300.44
D	7-Oxodehydroabietic acid (7OXO)	3.75	314.17
E	Palustric acid (PAL)	3.93	302.45
F	Levopimaric acid (LVO)	3.87	302.45
G	Pimaric acid (PIM)	3.92	302.45
H	Isopimaric acid (ISO)	3.89	302.45
I	Sandaracopimaric acid	3.92	302.45

[a]LogD values calculated by ACD Labs

In CE separations, the pH of the buffer is important as it affects the EOF and so the technique itself. It is also important as it affects the charge of ionisable analytes. The Brønsted-Lowry definition of an acid names it as a substance with a tendency to lose a proton. In basic pH conditions, the resin acids lose a proton and so are charged. This gives them an electrophoretic mobility (see Equation 2) so they do not depend on the EOF for mobility and can separate according to their mass-to-charge ratios. Basic compounds would be in their charged states at acidic pH. pK_a is the negative logarithm of the acid dissociation constant, K_a. When the pH of the buffer is equal to the pK_a of the analyte, 50% of the analyte will be charged and 50% uncharged. When the pH of the buffer is more than 2 units higher than the analytes pK_a they will be predominantly charged.

2.1.3 Aims

The aim of this research is to investigate analytical techniques for the separation of nine resin acids found in rosin samples. The objectives are to investigate the use of both HPLC and CE as potential separation methods for the analysis of modified and unmodified rosin samples, and to optimise a method for the separation of a mixture of nine resin acids for future application to modified and unmodified rosin samples.

2.2 Experimental

2.2.1 Instrumentation

HPLC analysis was carried out on an Agilent 1100 HPLC system (Agilent Technologies Ireland Ltd., Unit 3, Euro House, Euro Business Park, Little Island, Cork, Ireland). The system uses a DAD (range 190-600 nm) and a fluorescent detector (excitation range is 200-700 nm and emission range is 280-900 nm). The software used was Agilent Chemstation. The column used was a Supelco Ascentis RP-Amide column (15 cm x 4.6 mm, 3 μm particles). CE analysis was carried out on an Agilent Capillary Electrophoresis System G1601A (Agilent Technologies Ireland Ltd., Euro Business Park, Little Island, Cork, Ireland). The CE system uses a DAD which has a range of 191-599 nm. Peaks were integrated using the Agilent 3D-CE Chemstation software. Capillaries used were 58 cm (49.5 cm effective length) fused silica capillaries, 50 μm inner diameter (CMScientific, Silsden, BD20 0DL, UK). The pH meter used was a HI2211 pH/ORP meter (Hanna Instruments, Rhode Island, USA) with a Calomel reference electrode (Metrohm AG, Switzerland).

2.2.2 Reagents

All reagents used were of analytical grade, including anhydrous sodium phosphate monobasic, sodium tetraborate, disodium tetraborate, phosphate buffered saline solution (PBS), Tris(hydroxymethyl)aminomethane, trizma® hydrochloride, 2-(*N*-morpholino)ethanesulfonic acid (MES), sodium acetate, *N*-cyclohexyl-3-aminopropanesulfonic acid (CAPS), acetic acid, N-[Tris(hydroxymethyl)methyl]-3-aminopropanesulfonic acid (TAPS), (2-hydroxypropyl)- γ-cyclodextrin (HPγCD), methyl- β-cyclodextrin (MECD), boric acid, acetonitrile (ACN), acetic acid, sodium dodecyl sulphate, sodium hydroxide (NaOH), methanol (MeOH) and hydrochloric acid (HCl) and were purchased from Sigma Aldrich Ireland Ltd. (Vale Road, Arklow, Wicklow, Ireland). Sulfobutylether -β-cyclodextrin (SBCD) was donated by CyDex Pharmaceuticals, Inc. (Ligand Pharmaceuticals, Inc. 11119 North Torrey Pines Road, Suite 200 La Jolla, CA 92037). Rosin samples were donated by Henkel Ireland Ltd., Dublin, Ireland. Abietic acid, dehydroabietic acid, 7-oxo-dehydroabeitic acid, palustric acid, neoabietic acid, levopimaric acid, pimaric acid,

sandaracopimaric acid and isopimaric acid were purchased from Dynacare-Gamma Medical laboratory Partnership (previously Orchid Cellmark), Canada. Buffers were prepared using deionised water (18.2 MΩ cm^{-1}).

2.2.3 HPLC separation conditions

Unless stated otherwise, separations were carried out at a flow rate of 1 mL min^{-1} with 20 µL injections. UV detection was at 254 nm and fluorescence excitation was at 250 nm with emission at 410 nm. The mobile phase consisted of 0.1% acetic acid 97:3 ACN: water. The mobile phase was filtered through a 0.45 µm nylon membrane and sonicated before use. Methanol blanks were run between each sample. The column was stored in ACN overnight at room temperature.

2.2.4 CE separation conditions

CE separations, were carried out at 20 kV with hydrodynamic injections of 4 s at 50 mbar and the temperature was 25°C. Measurement wavelengths were 240 nm for ABA and NEO, 265 nm for PAL and 200 nm for the rest of the resin acids. Separations were all repeated 3 times. New capillaries were conditioned with 0.1 M NaOH (30 min), water (30 min) and buffer (30 min). A pre-injection rinse consisted of 2 min MeOH, 3 min 0.1 M NaOH and 3 min buffer.

2.2.5 Sample and buffer preparation

Resin acid standards were prepared by dissolving the acids in methanol. The resin acid calibration standards were prepared by diluting the highest concentration sample. Gum rosin samples (sample RA in Table 5-2) were prepared fresh every day at 0.1% w/v by dissolving them in methanol.

Tris buffers were prepared to the required concentration and pH by mixing appropriate amounts of tris HCl and tris base in distilled water following the Sigma-Aldrich tris buffer mixing table e.g. a 20 mM tris buffer at pH 8 was prepared by mixing 1.776 g L^{-1} tris HCl and 1.06 g L^{-1} tris base. All buffers were filtered through a 0.2 µm nylon membrane filter. Buffers containing cyclodextrins were sonicated for 15 min.

2.3 Results and discussion

2.3.1 HPLC method development

The only paper found to report the HPLC analysis of rosin samples used a C_{18} column with a methanol-water mobile phase [3]. Since little separation of resin acids has been achieved using a C_{18} column, and the majority of compounds present in rosins are either polar or neutral, a reversed phase amide column was selected as it contains polar amide groups which allow the polar compounds to be retained on the column longer and so gives improved separation.

An initial analysis with an acetonitrile (ACN):water mobile phase resulted in a mass of peaks, then three more distinct peaks coeluting (see Figure 2-2). ACN was chosen for use in the mobile phase as the column must be stored in ACN.

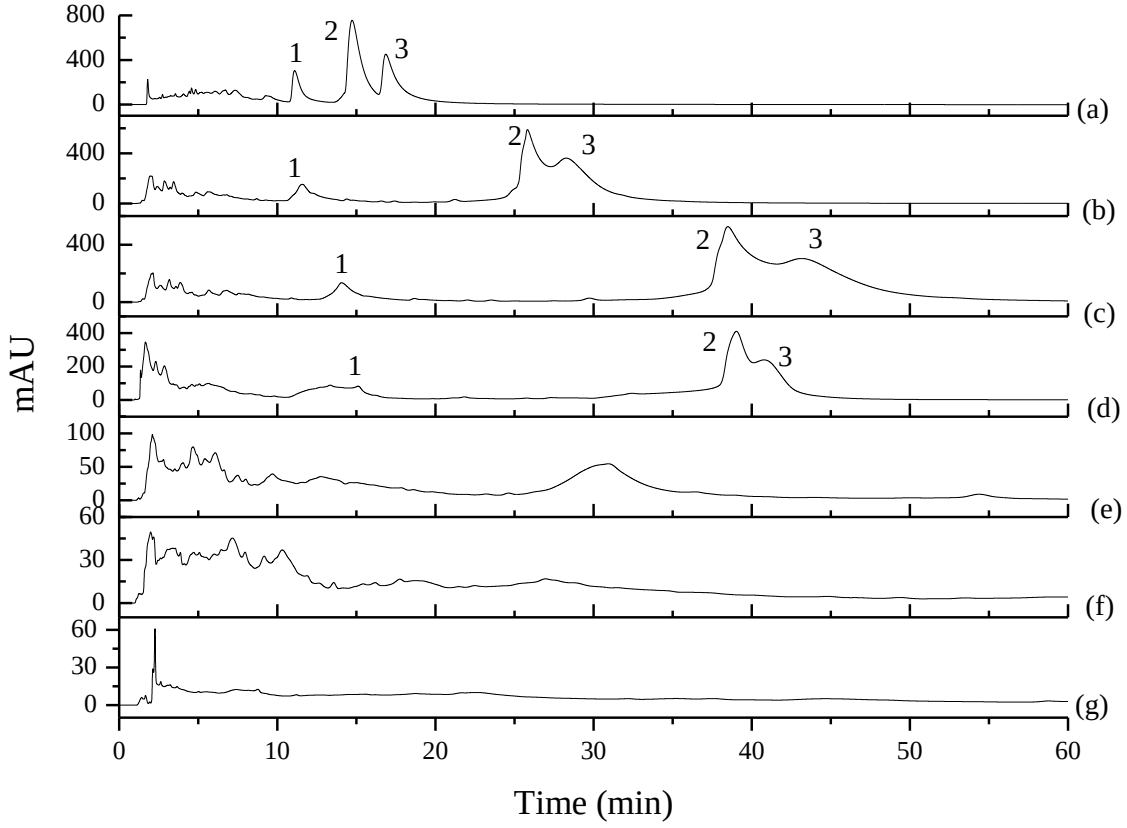

Figure 2-2 Chromatograms of 1.1% w/v rosin in MeOH samples, mobile phase consists of ACN:water at (a) 100:0, (b) 90:10, (c) 80:20, (d) 70:30, (e) 60:40, (f) 50:50 and (g) 40:60, pH 7.2, 20 µL injections at 1 mL min^{-1}, detection at 254 nm.

As the ratio of ACN decreased, peak 2 was found to elute later (80 min in a 50:50 ACN: water mobile phase compared to 30 min in a 90:10 ACN: water mobile phase). While the elution time of peak one remained relatively constant, its efficiency greatly decreased as ACN decreased (see Table 2-2) An ACN percentage greater than 80% gave shorter analysis times. This was expected as the hydrophobic analytes present will interact more with the mobile phase as the aqueous percentage is reduced. The resolution between the last two peaks improved with increasing concentration, while the resolution between peaks 1 and 2 decreased (see Table 2-2). Resolution and efficiency values were calculated using equations 5 and 6.

Table 2-2 Calculated resolution and efficiency values for Figure 2-2

Mobile phase	**Peak 1**		**Peak 2**		**Peak 3**
ACN: water	N[a]	R_s	N	R_s	N
100:0	1866	2.6	1131	1.1	1204
90:10	471	6.0	1584	0.7	561
80:20	475	6.4	944	0.7	398
70:30	78	5.1	1629	0.5	2399

[a]) N is the number of theoretical plates per column

While the 70:30 ACN: water mobile phase resulted in the highest efficiency values for peaks 2 and 3, the resolution value between them was the lowest achieved.

As methanol (MeOH) has a different elution strength than ACN, an investigation was carried out using a MeOH:water mobile phase with the RP-Amide column. When the percentage of methanol in the mobile phase was less than 80%, the pressure rose above the system limit.

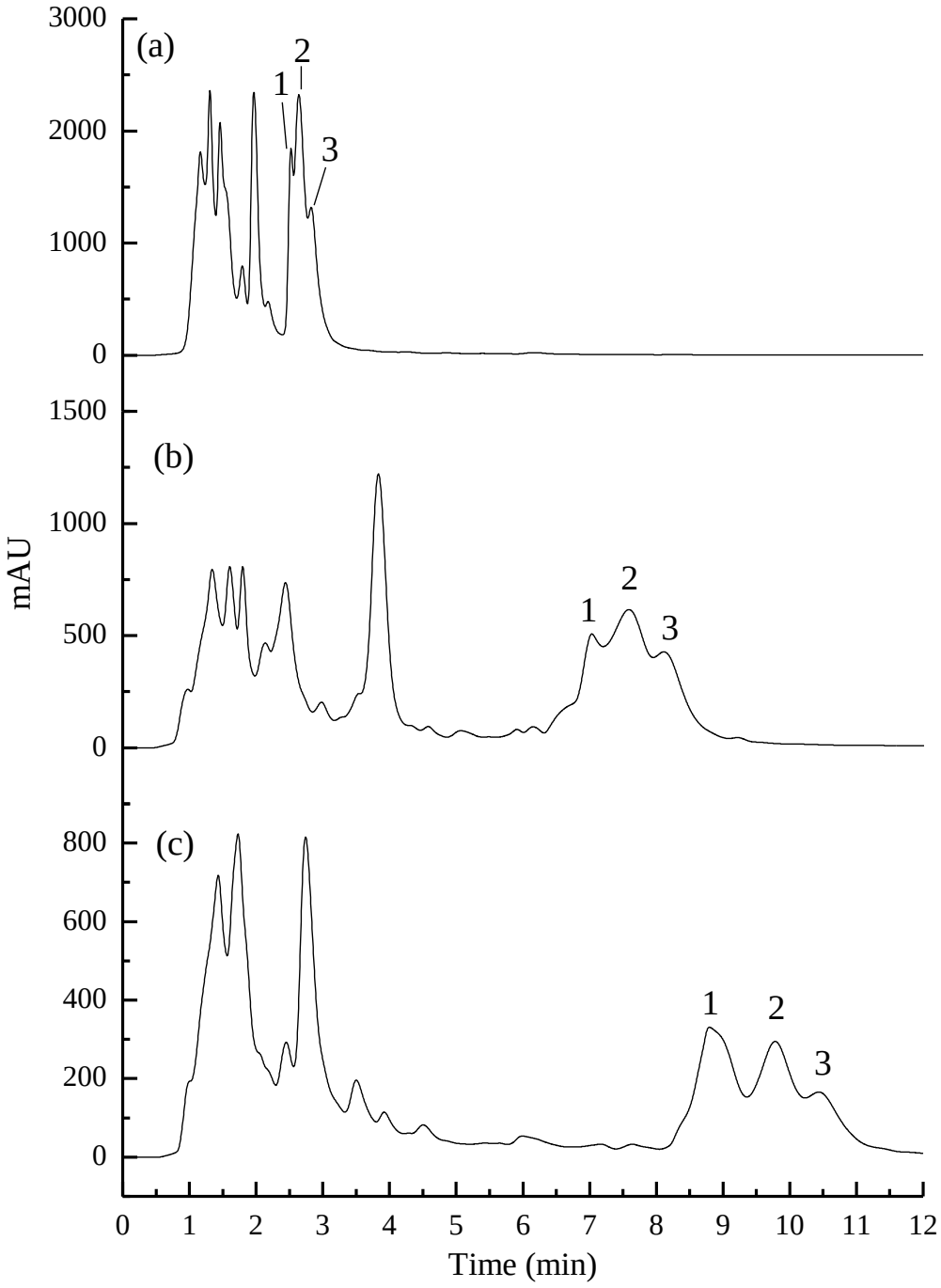

Figure 2-3 Chromatograms of 1.1% w/v rosin in MeOH samples, mobile phase (a) 100% MeOH, (b) 90:10 MeOH:water and (c) 80:20 MeOH:water, 20 µL injections at 1 mL min^{-1}, UV detection at 254 nm.

Higher percentages of methanol in the mobile phase resulted in the partial resolution of a higher number of peaks. The three chromatograms in Figure 2-3 show three coeluting peaks towards the end of the run time. The resolution between these peaks increased slightly with decreasing methanol concentration and while the N values for one of the peaks also improved with decreasing concentration, the opposite is true for the first peak (see Table 2-3).

Table 2-3 Calculated resolution and efficiency values for Figure 2-3

	Peak 1		**Peak 2**		**Peak 3**
Mobile phase (ACN: water)	N	R_s	N	R_s	N
100:0	4970	0.5	1467	0.7	1724
90:10	1263	0.7	943	0.6	1596
80:20	878	0.8	1420	0.7	2167

The resolution values achieved were less than those found when using ACN: water mobile phases with the RP-Amide column while the N values were similar so this was not considered for further optimisation.

As mobile phases containing upwards of 90% ACN gave higher resolution and efficiency values, further investigations were carried out using mobile phases with ACN concentration varying from 91-100%. As can be seen in Figure 2-4, the peak seen at 6.5 min when the mobile phase is 91:9 ACN: water split into two peaks when the percentage of ACN increased as the strength of the mobile phase increased. The resolution between these peaks increased with increasing ACN. This increase in mobile phase strength was also seen in the decrease in the resolution between these and peak 3, although it remains above 1.5. The efficiency of the 1st peak decreased with increasing ACN. The mobile phase used in further analysis was 97:3 ACN: water. The resolution and efficiency values in Table 2-4 refer to the peaks labelled 1 through 4 in Figure 2-4.

Table 2-4 Resolution and efficiency values for the chromatograms in Figure 2-4

Mobile phase	**Peak 1**		**Peak 2**		**Peak 3**		**Peak 4**
ACN: water	N	R_s	N	R_s	N	R_s	N
99:1	835	1.3	2264	3.6	1870	1.5	3365
98:2	1111	1.2	1194	2.5	938	1.1	1175
97:3	1344	1.1	1330	2.9	1039	1.1	1328
96:4	2735	1.2	1592	3.4	1314	1.2	1487
95:5	4480	1.1	1830	3.9	1452	1.3	1782
94:6	4101	0.9	2161	4.5	1699	1.5	3184
93:7	4484	0.6	1796	4.7	1752	1.5	2888
92:8			1796	5.0	1814	1.3	2252
91:9			1868	5.0	1495	1.2	1869

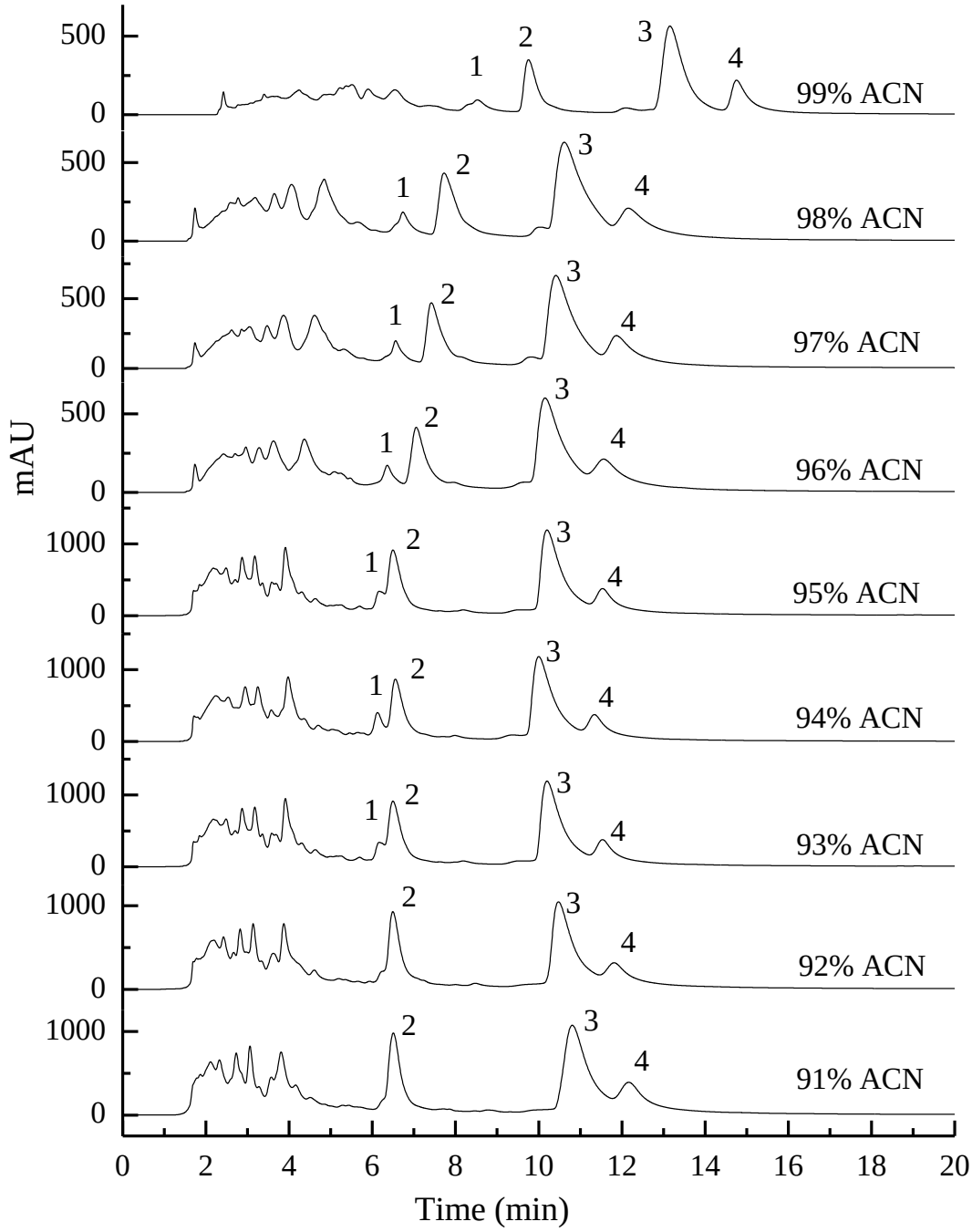

Figure 2-4 Chromatograms of 1.1% w/v rosin in MeOH samples analysed at different % ACN mobile phases, 20 µL injections at 1 mL min^{-1}, UV detection at 254 nm.

2.3.1.1 Optimisation of mobile phase pH

Further investigations were carried out to determine the optimal mobile phase composition (see Figure 2-5). The addition of 0.1% acetic acid was also investigated as the addition of acid to a mobile phase can improve sensitivity by improving peak shape and retention by suppressing silanol activity. They also reduce unwanted interactions between polar compounds and the stationary phase [85]

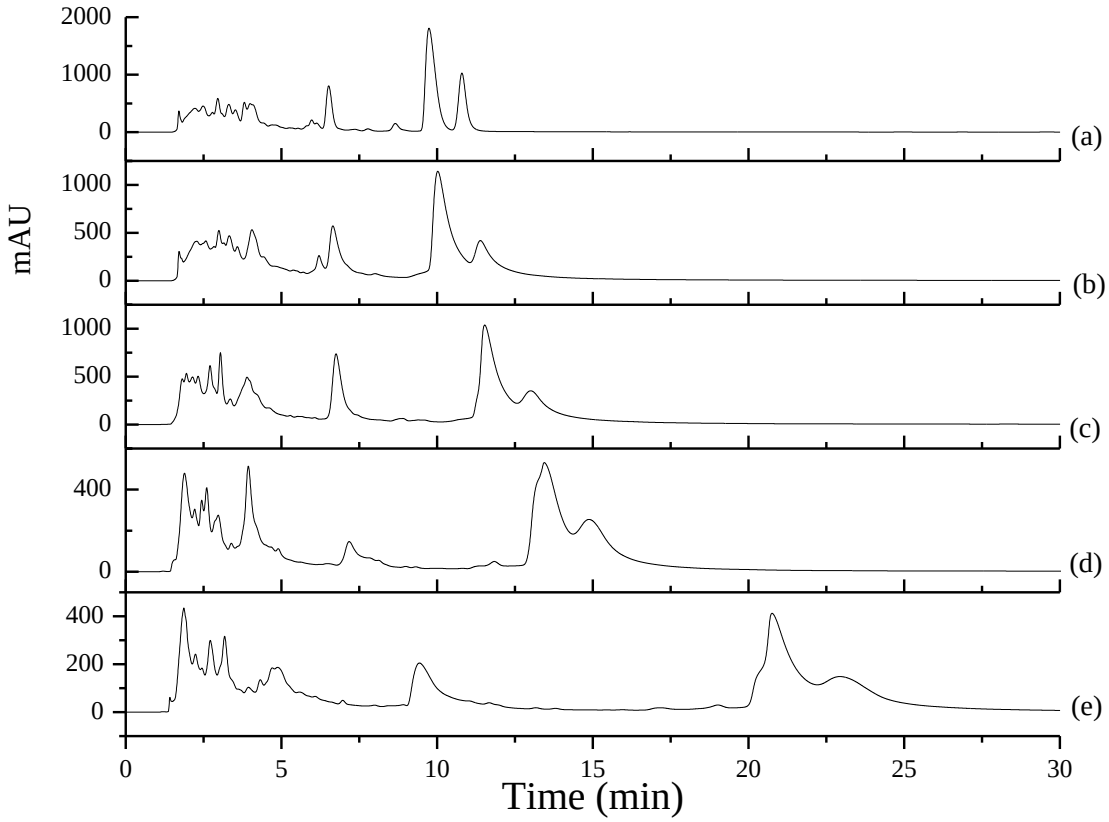

Figure 2-5 Chromatograms of 1.1% w/v rosin in MeOH samples, mobile phase consists of (a) 0.1% acetic acid 95:5 ACN:water, (b) 95:5, (c) 90:10, (d) 85:15, (e) 80:20 ACN:water, 20 µL injections at 1 mL min^{-1}, UV detection at 254 nm.

If the pH of the mobile phase is equivalent to the pK_a of the analytes, then half of the analytes will be protonated and the other half unprotonated which can result in broad or multiple peaks. Adjusting the pH to approximately two units below the pK_a of an acid ensures that the acids are 99% protonated. A 95:5 ACN:water mobile phase containing 0.1% acetic acid was prepared and rosin sample analysed. The resolution and efficiency values compared with those of 95:5 ACN:water were noticeably

higher (see Table 2-5), and the peaks were much sharper. The pK_a's of the resin acids present in rosins range from 5.7-7.25 [1, 31, 84]. The pH of the 97:3 ACN:water mobile phase was found to be pH 7.2 while the addition of 0.1% acetic acid lowered it to pH 3.6. The addition of acetic acid to the mobile phase caused the protonation of the acids where before some may still have been charged. This resulted in sharper peaks, as shown in Figure 2-5.

Table 2-5 Resolution and efficiency values for Figure 2-5

Mobile phase	**Peak 1**		**Peak 2**		**Peak 3**
ACN: water	N	R_s	N	R_s	N
80:20	551	6.6	2049	0.9	807
85:15	703	4.7	1178	0.8	814
90:10	1752	5.2	1531	1.0	801
95:5	1612	3.8	1348	1.1	1194
95:5 acetic acid	4621	6.3	3719	1.8	7363

As the addition of 0.1% acetic acid to the mobile phase resulted in better efficiencies, several other acids were investigated to see if they could improve the separation of the rosin samples.

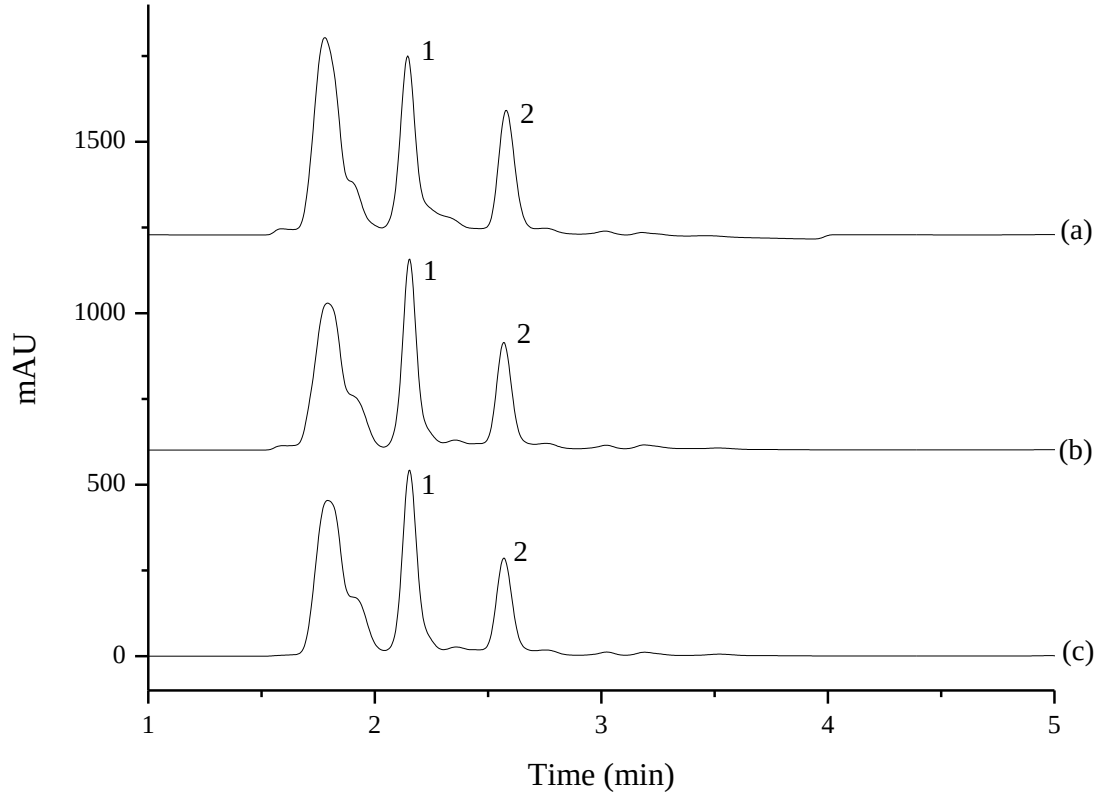

Figure 2-6 Chromatograms of a resin acid mixture analysed at 97:3 ACN:water mobile phase containing 0.1% (a) trifluoroacetic acid, (b) formic acid or (c) acetic acid, pH 3.6, 20 µL injections at 1 mL min-1, UV detection at 254 nm.

Although slightly higher resolution and efficiency values were achieved for the last two peaks in the acid mixture chromatogram, no further separation of the acids coeluting in these peaks was accomplished.

Table 2-6 Resolution and efficiency values for last two peaks in the chromatograms in Figure 2-6

	N	**Resolution**	**N**
Acetic acid	3449	1.6	5727
Formic acid	5124	1.9	8586
TFA	6434	2	10119

2.3.1.2 Fluorescence detection

The HPLC system also has a fluorescence detector running simultaneously to the UV detector which can be used in the identification of certain fluorescent compounds.

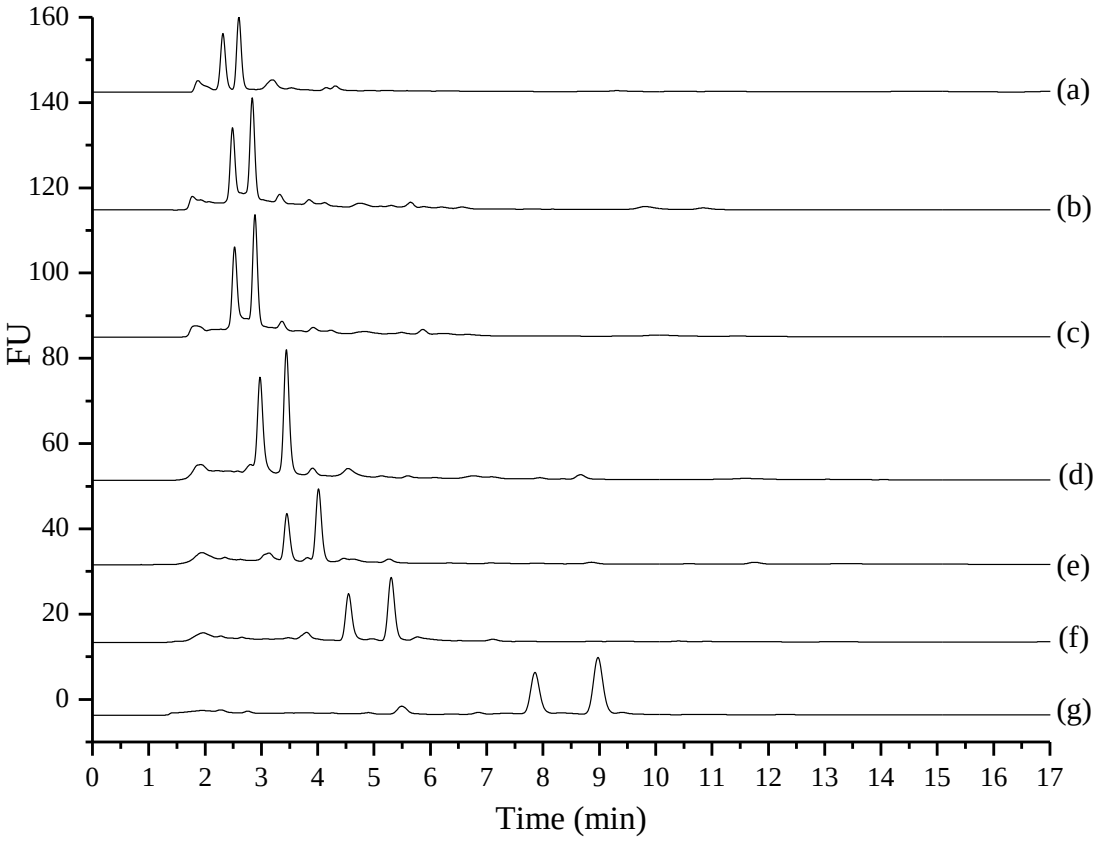

Figure 2-7 Chromatograms of 1.1% w/v rosin in MeOH samples, mobile phase consists of ACN:water at (a) 100:0, (c) 95:5, (d) 90:10, (e) 85:15, (f) 80:20, (g) 70:30 and (b) 0.1% acetic acid ACN:water 95:5, 20 µL injections at 1 mL min^{-1}, fluorescence excitation was at 250 nm and emission at 410 nm.

Increased ACN concentration decreased the elution time of the two peaks as the elution strength of the mobile phase was increased. This resulted in decreasing resolution values; however, the resolution values remained above 1.5. The efficiency values also decreased with increasing ACN concentration. The peaks in Figure 2-7 may be the peaks of dehydroabietic acid and 7-oxo- dehydroabietic acids which are both noted as fluorescent in literature [86]. A mobile phase with a lower ratio of ACN would be optimal for the separation using fluorescence detection, but as more

of the sample analytes are detected by UV, a 97:3 ACN: water mobile phase was used in further studies.

Table 2-7 Resolution and efficiency values for chromatograms in Figure 2-7

Mobile phase	**Peak 1**		**Peak 2**
ACN: water	N	R_s	N
70:30	9433	3.3	11003
80:20	5869	3.2	7845
85:15	4678	2.7	5687
90:10	2866	2.2	5045
95:5	2314	1.8	3891
95:5 0.1% acetic acid	2525	1.8	3551
100:0	2626	1.6	3810

2.3.1.3 Rosin types

Analysis so far was carried out on a sample of natural gum rosin. Rosins are sometimes modified for use in industry so samples of modified rosins, acid-modified hydrogenated rosin and disproportionated rosin (as seen in Figure 1-5), were analysed. A batch of natural gum rosin known to crystallise was also analysed to investigate how its chromatogram varied from that of gum rosin used in industry. As can be seen in Figure 2-8, the chromatograms of the modified rosins are very different from those of the gum rosins indicating a different composition. In both the disproportionated and acid-modified rosin, the peak of highest area is seen at around 6.6 min which was identified by peak spiking as DHA. In the disproportionated rosin sample, the peak area of this peak is more than twice the area of the same peak when seen in gum rosin samples. This is expected as ABA is disproportionated to DHA and dihydroabietic [34, 87]. The peak seen at 4 min in the disproportionated rosin chromatogram could correspond to dihydroabietic, or it may be the presence of 7OXO. The acid modified rosin also shows a peak at the same migration time as the 7OXO standard (standards in Figure 2-9). Abietic acid becomes a mix of dihydroabietic acid and tetrahydroabietic acid when hydrogenated [87]. Unfortunately, standards for these two acids were unattainable.

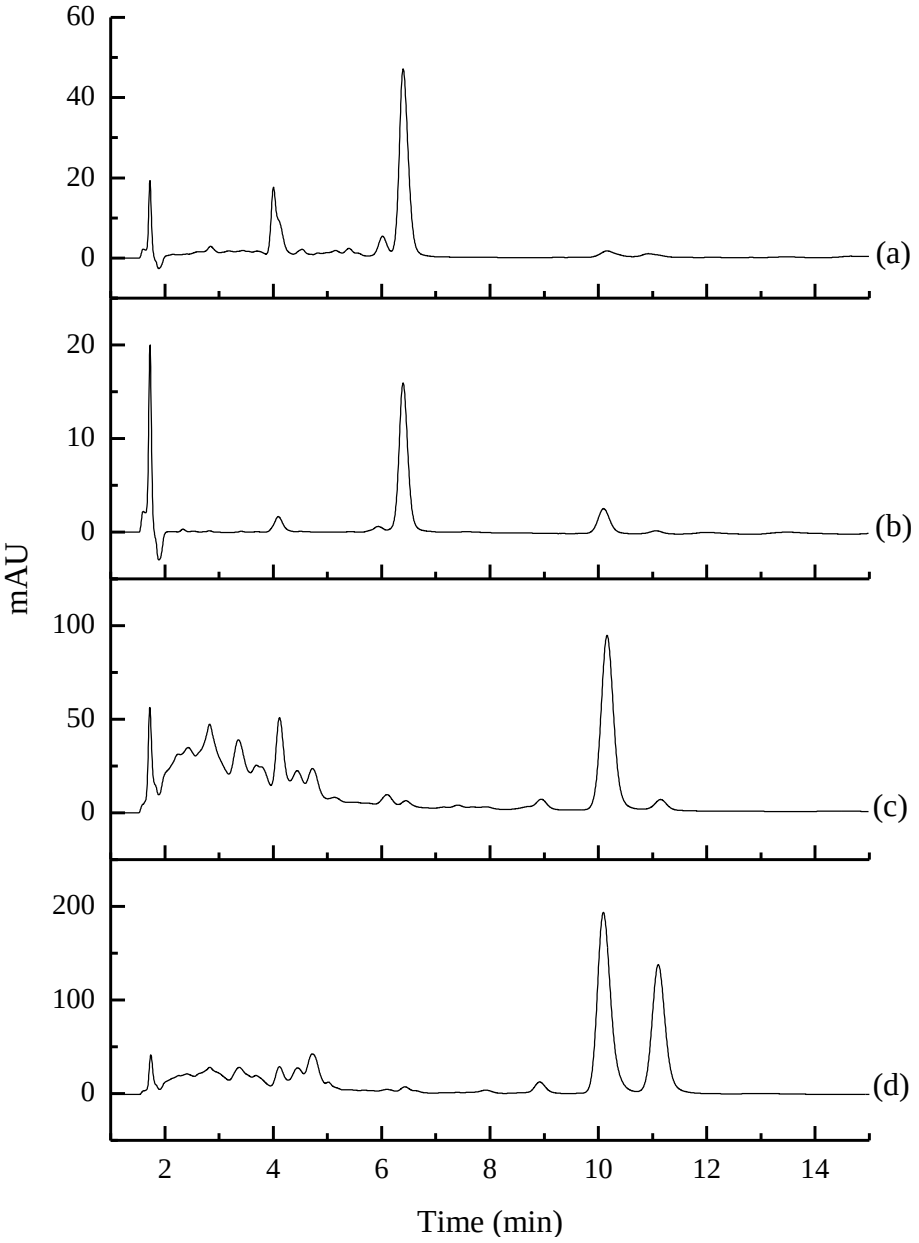

Figure 2-8 Chromatograms of 0.1% w/v rosin samples analysed using a 0.1% acetic acid 97:3 ACN: water mobile phase, 20 µL injections at 1 mL min^{-1}, UV detection at 254 nm. (a) Disproportionated rosin, (b) acid-modified hydrogenated rosin, (c) 'crystallising' gum rosin and (d) gum rosin.

While the gum rosin chromatograms are relatively similar, in the 'crystallising' rosin – a rosin which forms a precipitate - the last two peaks have lower signal intensities than in the good gum rosin chromatogram, in particular the last peak

Rosin gum samples were spiked with acids in order to identify the peaks currently being separated. Standards of the compounds were prepared and rosin samples were spiked to identify the compound groups, and the compounds themselves. Acid standards were analysed individually in order to identify which acids are eluting in which peak in the rosin electropherograms.

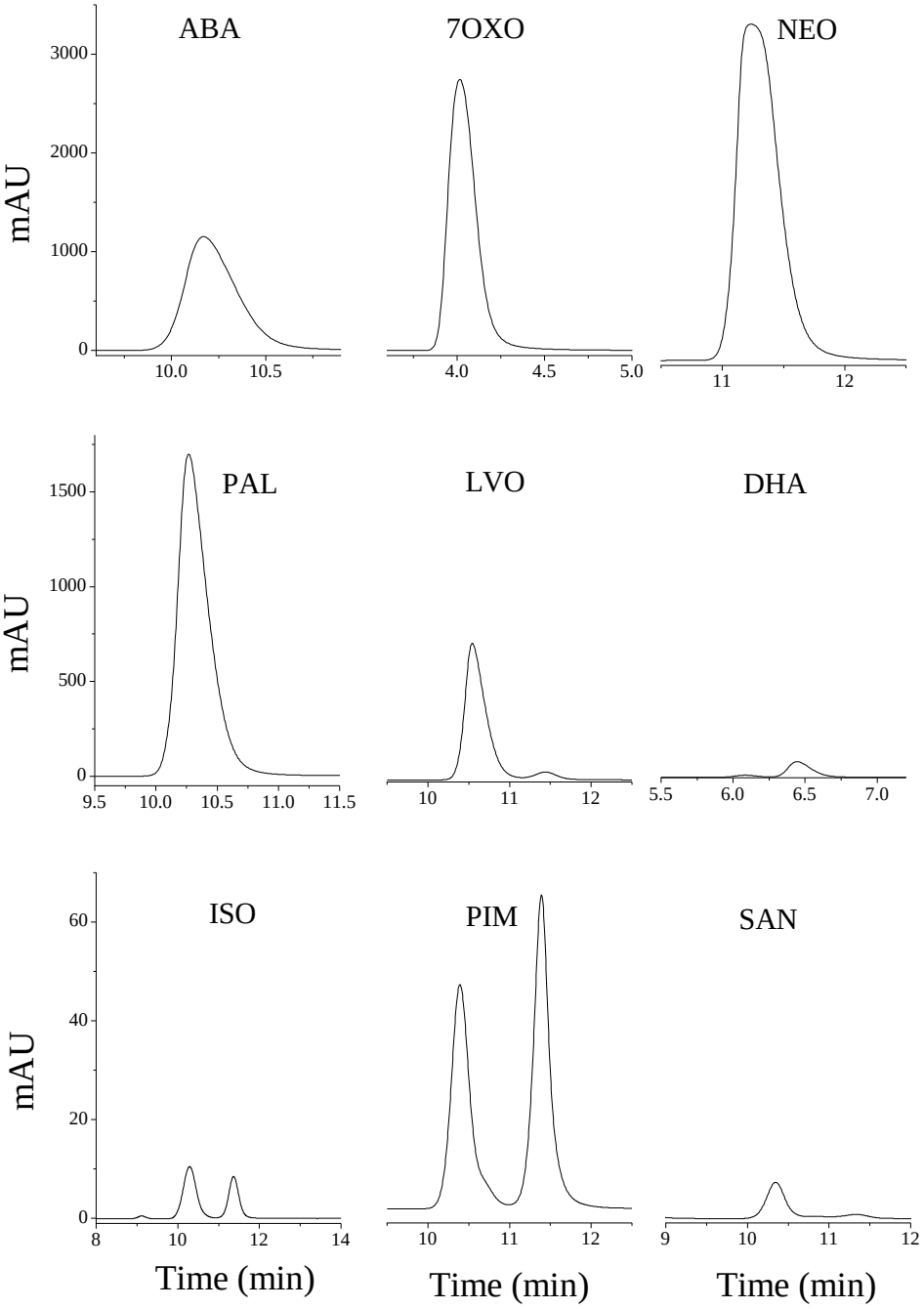

Figure 2-9 Chromatograms of 0.1% w/v resin acid standards in methanol analysed at 0.1% acetic acid 97:3 ACN:water mobile phase, 20 µL injection at 1 mL min^{-1}, UV detection at 254 nm.

Figure 2-9 shows chromatograms for the separation of the acid standards. They were found to vary greatly in migration time and peak intensity. While 7OXO and DHA elute at 4.2 and 6.5 min respectively, the other acids all elute from 10.2-11.7 min. There are small impurities seen in some chromatograms e.g. LVO, but this could be the presence of some of the other isomeric acids as isomers. PIM and ISO chromatograms both show two peaks of almost equal intensity. As the acid group contains a carbonyl, it is possible that the acids undergo tautomerization. Luong *et al.* also reported ISO displaying two peaks when analysed by HPLC [31]. The two peaks elute at the same migration times but both peaks are at a much higher intensity for pimaric acid, and the second peak is greater while the first one is in isopimaric acid. Isopimaric, dehydroabietic, pimaric and sandaracopimaric acid all have intensities of less than 100 mAU while all the other acids have intensities of 700-3500 mAU.

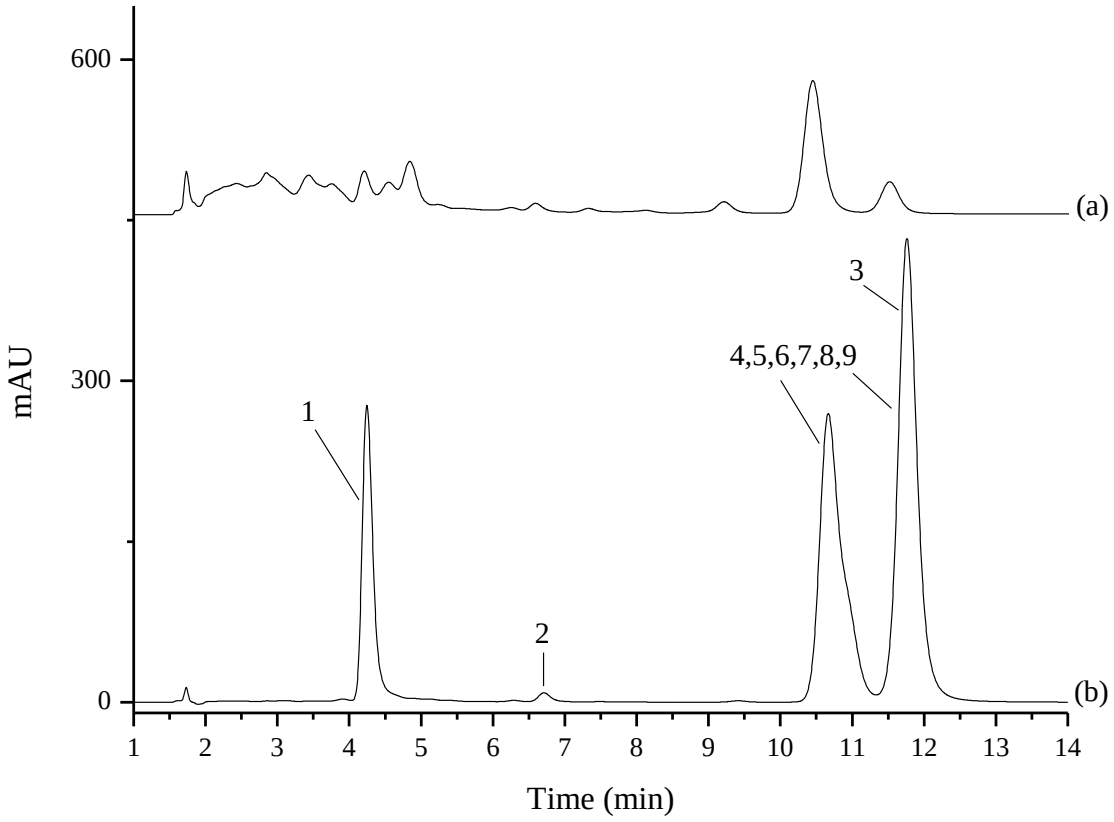

Figure 2-10 Chromatograms of (a) 0.1% w/v rosin in methanol sample and (b) a 0.01% w/v resin acid mixture analysed at 0.1% acetic acid 97:3 ACN:water mobile phase, 20 µL injection at 1 mL min^{-1}, UV detection at 254 nm. Numbers indicate acids as follows, (1) 7-oxodehydroabietic acid, (2) dehydroabietic acid, (3) neoabietic acid, (4) abietic acid, (5) palustric acid, (6) levopimaric acid, (7) sandaracopimaric acid, (8) isopimaric acid and (9) pimaric acid.

An acid mixture standard was prepared containing the nine resin acids in MeOH at 0.01% w/v. This was analysed by HPLC and the chromatogram overlayed with that of a gum rosin sample (see Figure 2-10 b). The acid standard mixture showed four peaks at 4.2, 6.8, 10.8 and 11.9 min. As there are nine acids present in the mixture, clearly several are coeluting. The last two peaks in the mixtures are similar to those seen in the rosin chromatograms although in the acid mixture the last peak has a greater absorbance than the second last. 7OXO elutes first at 4.2 min followed by DHA at 6.6 min. These two are the only of the acids to contain an aromatic ring, leaving them less polar than the other acids. They would be expected to elute before the others as the RP-Amide column retains more polar compounds longer. The rest of the acids then coelute in two peaks at 10.4 and 11.5 min. While the presence of an aromatic ring was sufficient to separate 7OXO and DHA, the interactions of the other acids with the stationary and mobile phase was not suitably differential enough to result in different retention times. The structures of these acids are very similar, varying only in the position of a double bond, and in the presence of either an isopropyl group or a methyl and vinyl group. SAN and PIM are optical isomers and so would not be expected to be separated without the use of chiral HPLC.

Spiking the rosin samples with the acids confirmed that all except DHA and 7OXO were coeluting as the two peaks seen at the end of the chromatogram. 7OXO and DHA spiked rosins corresponded to peaks in the rosin chromatogram seen at 4.2 and 6.6 min (see Figure 2-11).

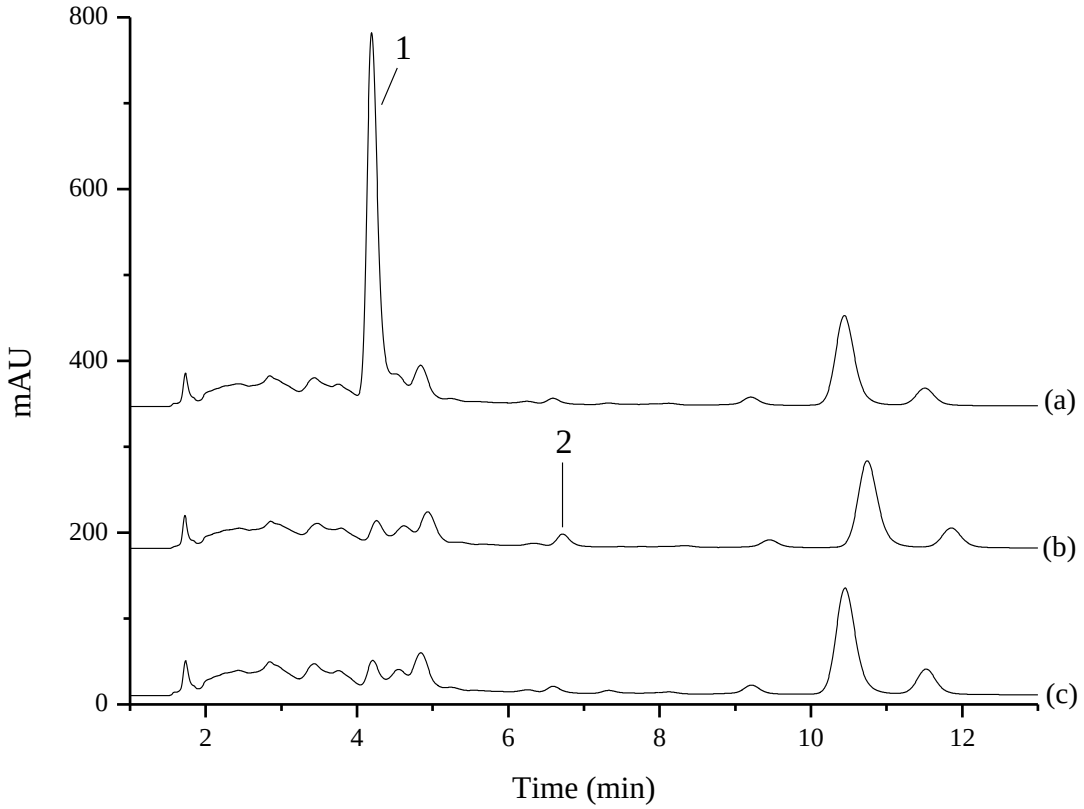

Figure 2-11 Chromatograms of 0.1% w/v rosin in methanol samples (a) spiked with 7OXO (1), (b) spiked with DHA(2) and (c) an unspiked rosin sample analysed at 0.1% acetic acid 97:3 ACN:water mobile phase, 20 µL injection at 1 mL min^{-1}, UV detection at 254 nm.

As expected due to the separation, when spiked with the rest of the acids, the last two peaks in the chromatogram increased.

While HPLC separates analytes based on how they partition between a mobile and a stationary phase, CE separates analytes based on their electrophoretic mobilities and so it can separate mixtures that HPLC cannot. Some modes of CE such as MEKC allow the use of both electrophoretic and chromatographic separation mechanisms through the use of a pseudo-stationary phase. As a successful separation of the mixture of nine resin acids has not been achieved using HPLC, the use of CE was investigated.

2.3.2 CE method development

Due to the reported capacity of CE to separate analytes unable to be separated using LC by using different separation mechanisms, CE was then investigated for the analysis of rosin samples. Unmodified gum rosin samples prepared in 0.1% w/v in methanol were analysed using a range of common CE buffers at concentrations from 10-50 mM as listed in Table 2-8.

Table 2-8 Buffers used in initial CE study

Buffer	**pH**
Phosphate	2, 3.3, 7, 10, 12
Acetate	3, 4, 6
Tetraborate	9.2
PBS	7.4
Tris	8
MES	6
Caps	10

Buffers at each pH were also prepared with and without cyclodextrins (CDs) (concentrations ranging from 5-30 mM). The addition of α-cyclodextrin (α-CD) and sulphated β-cyclodextrin (sβ-CD) provided little separation. As many of the compounds present in rosins such as some of the isomeric resin acids have very little structural difference, the use of more derivatized CDs were investigated. The functional groups available on their outside can allow for more interaction. When more than one CD is present, the main processes in competition are those between the two different complexes rather than between the free and complexed analyte [88].

Several papers showing the determination of some of the acids present in rosins report achieving superior separation using methyl β-cyclodextrin (MECD) and sulfobutylether β-cyclodextrin (SBCD), structures shown in Figure 2-12) [31, 59].

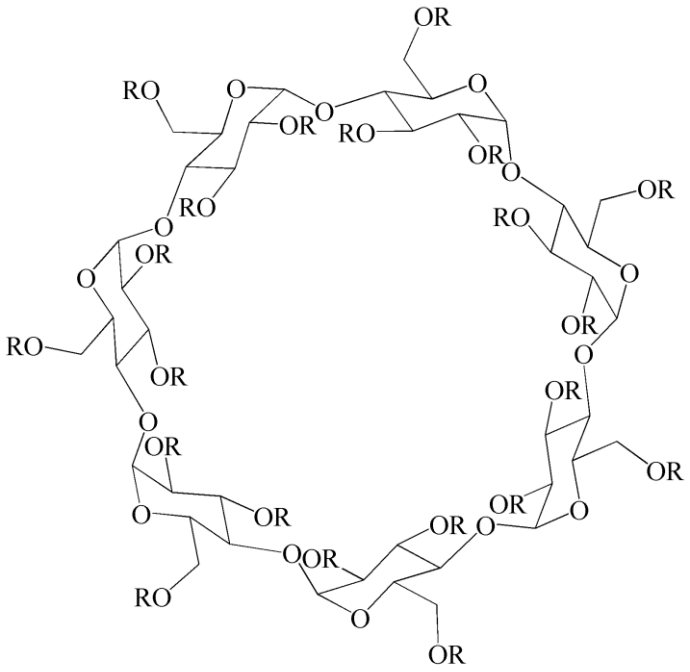

Figure 2-12 Structures of methyl β-cyclodextrin (MECD) and sulfobutylether β-cyclodextrin (SBCD).

SBCD is an anionic CD and MECD is neutral (Figure 2-13). Gum rosin samples were analysed by the CE buffers described in Table 2-8 containing MECD and SBCD. CD concentrations ranged from 1-10 mM. Each buffer was prepared with MECD and SBCD on their own to observe any separation effects. With all the buffers, the presence of methyl-β-cyclodextrin, a neutral CD, did not achieve separation of the components of the rosin sample. The use of SBCD alone in the buffer results in the sample eluting later, also with little separation. This was expected as SBCD is a negatively charged cyclodextrin [89] which would migrate against the EOF. This study supports observations in literature that on their own, neutral and charged cyclodextrin have weaker separation strengths than when present in a buffer in combination [90]. When there is a charged and a neutral CD present, sometimes the charged CD does not contribute to the separation of the analytes, but rather allows the selectivity of the neutral CD to be shown [88].

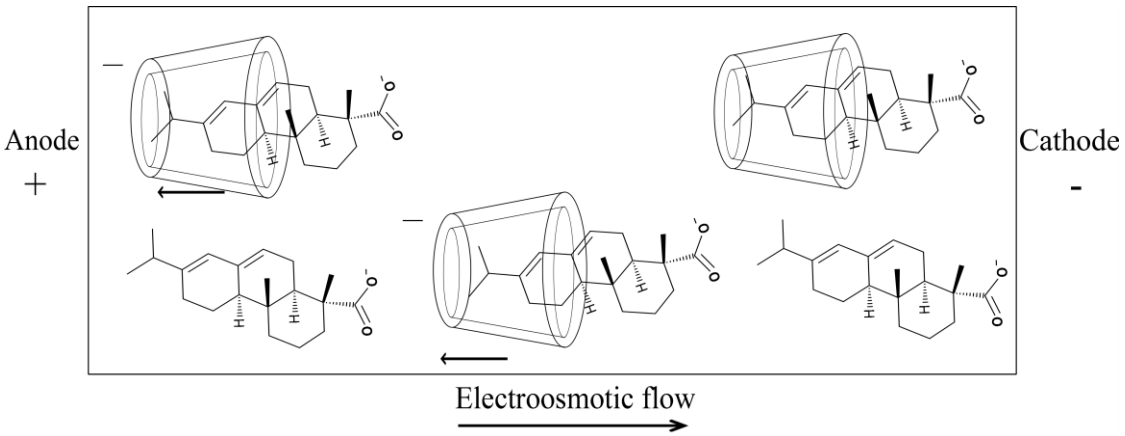

Figure 2-13 Schematic of a capillary containing neutral and charged cyclodextrins

The CE system can record at up to 5 different wavelengths simultaneously so detection in this study was carried out at 200, 214, 240, 265 and 310 nm. These wavelengths were chosen from various papers noting these as the maximum absorbance wavelengths for several of the compounds found in rosin [31, 59, 63, 91-93]. The separation parameters were 20 mM buffer concentration, 4 s injections at 50 mbar, 20 kV at 25°C.

A 20 mM phosphate buffer was prepared at pH 2.8. At this low pH the EOF is negligible so the components in the sample elute due to their electrophoretic mobility alone. The sample elutes with no separation at 25 min. The addition of cyclodextrins to a buffer increases elution time as the sample spends time interacting with the negatively charged cyclodextrin which travels against the EOF. Therefore, there were no further studies carried out using phosphate buffer at pH 2.8. Phosphate buffers at pH 7 and pH 12 were then prepared.

Figure 2-14 demonstrates the use of different detection wavelengths for identification purposes as different compounds absorb at different maximum wavelengths. When the rosin sample was analysed with 10 mM MECD 10 mM SBCD in 20 mM phosphate buffer pH 7 the maximum peak was at 7 min at 200 and 214 nm, while at 240 and 265 nm the maximum peak was at 7.1 min. Some peaks were found at all wavelengths, such as those at 7.1 and 7.7 min. Many other peaks did not appear at all wavelengths. 200 and 214 nm electropherograms shared more peaks, while 240 and 265 nm electropherograms had some peaks in common that the

other wavelengths did not. There were peaks at 6.8 and 7.2 min which appear at 200 and 214 nm but not at 240 and 265 nm. These could belong to compounds with double bonds which have UV absorbance at shorter wavelengths, such as terpenes (214 nm) [90].

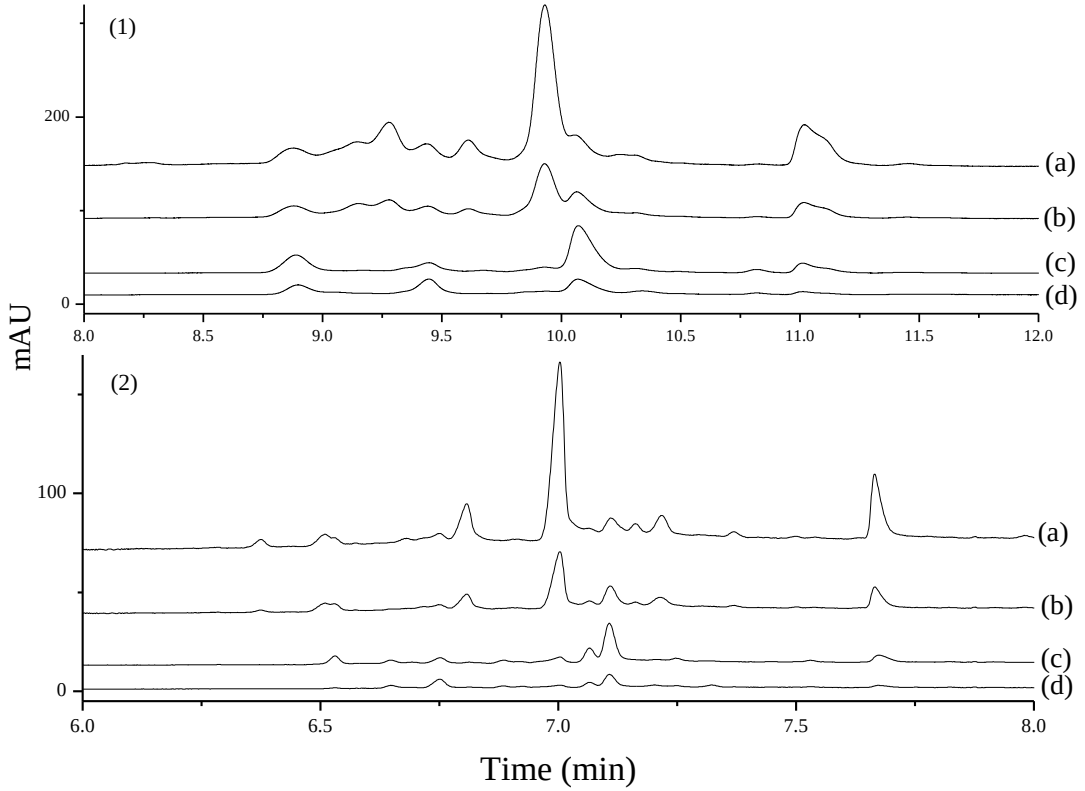

Figure 2-14 Electropherograms of 0.1% w/v rosin sample in methanol analysed in positive polarity, 20 kV, capillary 58 cm (49.5 cm to detector), 50 µm i.d., 25°C and 50 mbar 4 s injection times. Detection at (a) 200 nm, (b) 214 nm, (c) 240 nm and (d) 265 nm. Buffer consists of 10 mM MECD 10 mM SBCD in 20 mM phosphate buffer (1) pH 12 and (2) pH 7.

The peak at 7.1 min has stronger absorbance at 240 nm. There are many reports in literature of abietic acid having a maximum UV absorbance at around 240 nm [59, 63, 92, 93]. This was confirmed by running an abietic acid standard. Other resin acids are reported to have maximum wavelengths around this region too, such as neoabietic acid (252 nm) [63], palustric acid (266 nm) [63, 92], levopimaric acid (270 nm) [19, 25, 59, 63] and dehydroabietic acid (268 and 276 nm) [63, 92]. These were confirmed by running acids standards in a UV spectrometer.

When the rosin sample was analysed with 10 mM MECD, 10 mM SBCD in 20 mM phosphate buffer pH 12, there were more than 9 partially resolved peaks seen in the electropherogram. Several peaks were visible at all wavelengths, such as those at 8.8, 10.1 and 11 min. The peak with highest intensity was seen at 9.9 min at 200 nm. Analysis using a 10mM MECD 10 mM SBCD at both pH 7 and pH 12 showed more peaks in the electropherogram than analysis with a 5 mM MECD 5 mM SBCD and gave comparable resolution values and slightly better efficiency values. Increasing buffer concentration increases the buffering capacity and can impede unwanted capillary wall interactions.

Figure 2-15 shows the electropherogram of the rosin sample analysed using an acetate buffer.

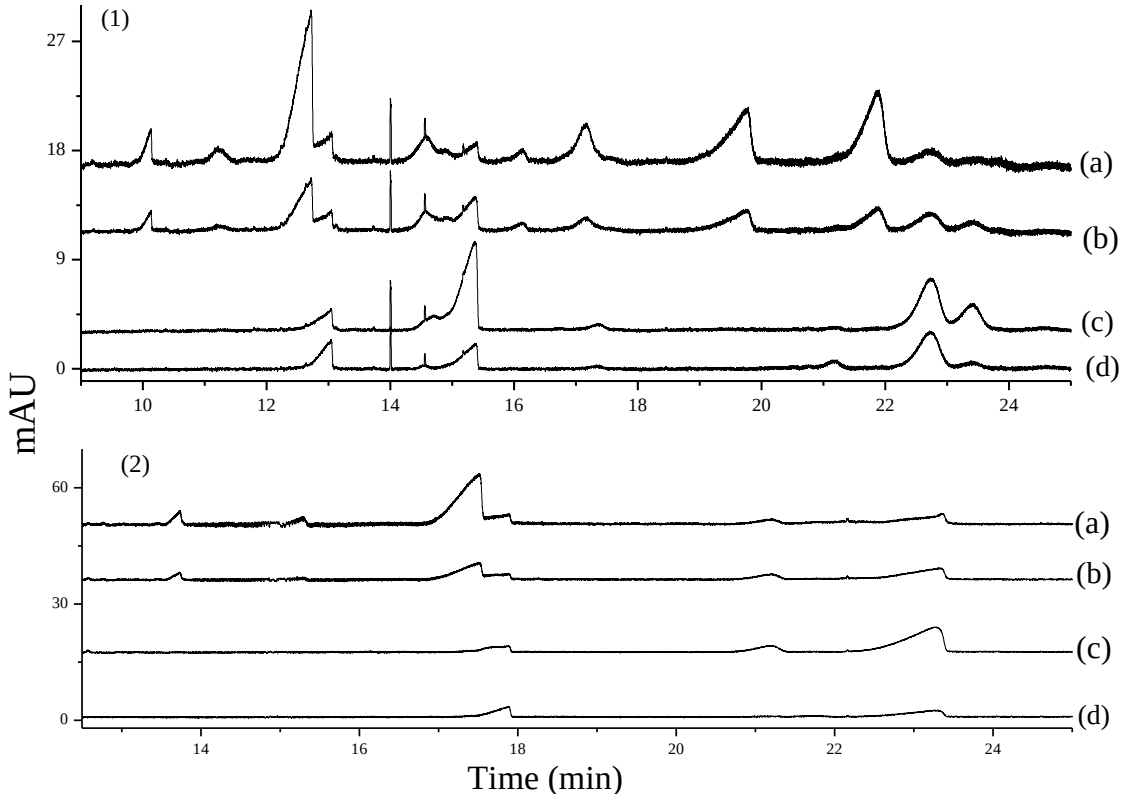

Figure 2-15 Electropherograms of 0.1% w/v rosin sample in methanol analysed in positive polarity, 20 kV, capillary 58 cm (49.5 cm to detector), 50 µm i.d., 25°C and 50 mbar 4 s injection times. Buffer consists of (1) 5 mM MECD 5 mM SBCD in 20 mM acetate buffer pH 4 and (2) 10 mM MECD 10 mM SBCD in 20 mM acetate buffer pH 4. Detection at (a) 200 nm, (b) 214 nm, (c) 240 nm and (d) 265 nm.

From this investigation peak fronting was visible at all wavelengths. Fronting can occur when the motilities of the analyte ions are faster than those of the buffer [94, 95]. At 310 nm there were no peaks observed. This suggests that the compounds detected around 310 nm are present in the rosin sample in very low concentrations. When the 0.1% rosin sample was analysed by 10 mM MECD 10 mM SBCD in 20 mM acetate buffer pH 4 only five peaks were resolved, despite there being upwards of 35 known compounds present in rosin.

As CAPS ([3-(cyclohexylamino)-1-propane sulfonic acid]) buffer is a zwitterionic buffer [96], a much higher buffer concentration can be used compared to more common buffers without creating excessive Joule heating which increases current. Since the 20 mM CAPS buffer was producing practically no current compared to the other buffers of equal concentration, a 50 mM CAPS buffer was also investigated for rosin analysis.

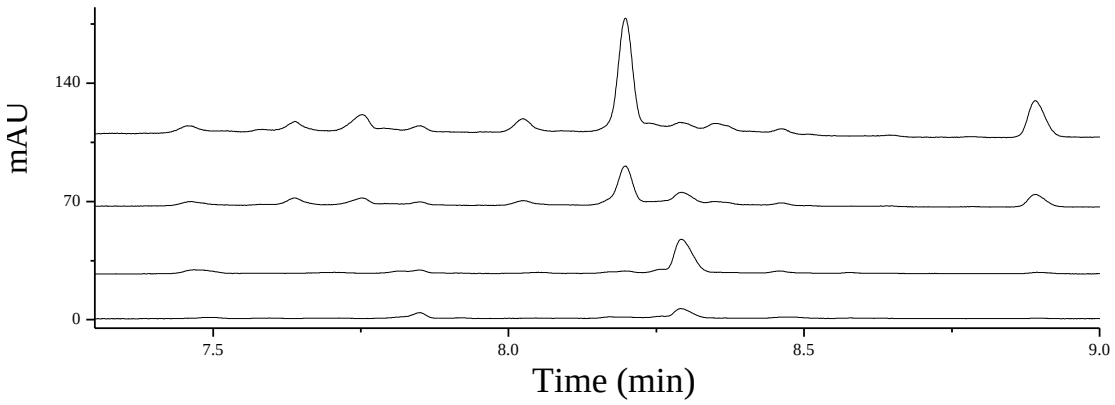

Figure 2-16 Electropherograms of 0.1% w/v rosin sample in methanol analysed in positive polarity, 20 kV, capillary 58 cm (49.5 cm to detector), 50 µm i.d., 25°C and 50 mbar 4 s injection times. Buffer consists of 10 mM MECD 10 mM SBCD 50 mM CAPS buffer pH 10. Detection at (a) 200 nm, (b) 214 nm, (c) 240 nm and (d) 265 nm.

From this study (Figure 2-16) approximately 11 peaks were seen when a rosin sample was analysed with 10 mM MECD 10 mM SBCD in 50 mM CAPS pH 10. The peak at 8.3 min was seen in all electropherograms but was at its highest intensity at 240 nm. This corresponds to abietic acid, whose max wavelength is around 240

nm [92]. When the CD concentrations were decreased to 5 mM, resolution and efficiencies decreased.

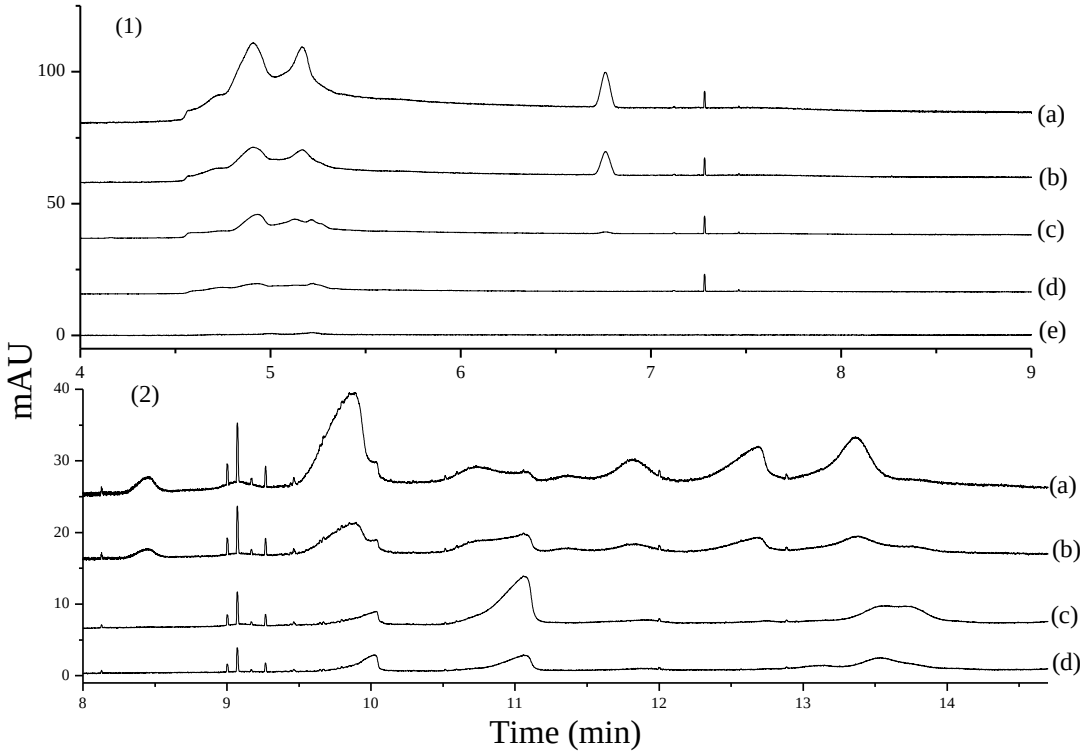

Figure 2-17 Electropherograms of 0.1% w/v rosin sample in methanol analysed in positive polarity, 20 kV, capillary 58 cm (49.5 cm to detector), 50 µm i.d., 25°C and 50 mbar 4 s injection times. Buffer consists of (1) 1 mM MECD 1 mM SBCD in 20 mM borate buffer pH 9 and (2) 5 mM MECD 5 mM SBCD in 20 mM borate buffer pH 9. Detection at (a) 200 nm, (b) 214 nm, (c) 240 nm, (d) 265 nm and (e) 310 nm.

Using 1 mM MECD 1 mM SBCD in 20 mM borate buffer pH 9 for rosin separation results in little separation as seen in Figure 2-17. When using a 5 mM MECD 5 mM SBCD in 20 mM borate buffer, the rosin sample had improved separation, resolution and efficiency values. The peak at 11 min was at its highest intensity at 240 nm, which corresponds to abietic acid [92].

The pK_a of MES buffer is 6.1 so a MES buffer was prepared at pH 6 to investigate its use as a suitable buffer (Figure 2-18).

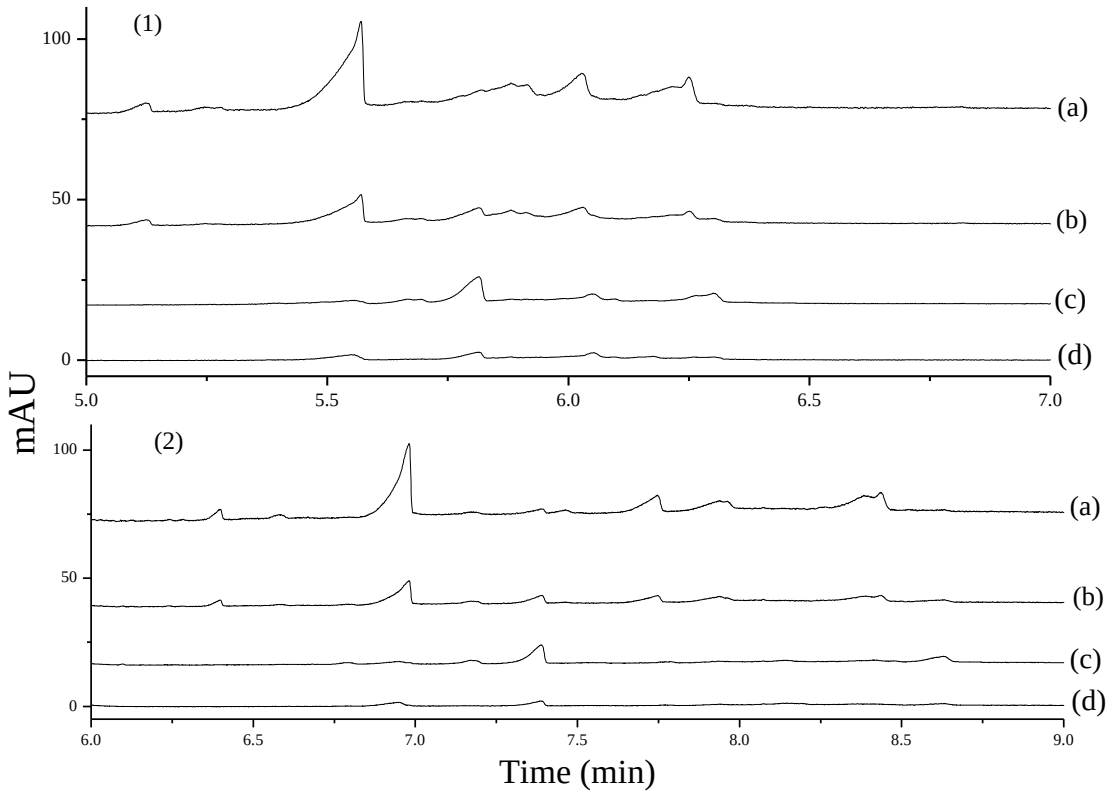

Figure 2-18 Electropherograms of 0.1% w/v rosin in methanol sample analysed in positive polarity, 20 kV, capillary 58 cm (49.5 cm to detector), 50 µm i.d., 25°C and 50 mbar 4 s injection times. Buffer consists of (1) 5 mM MECD 5 mM SBCD in 20 mM MES buffer pH 6 and (2)10 mM MECD 10 mM SBCD in 20 mM MES buffer pH 6. Detection at (a) 200 nm, (b) 214 nm, (c) 240 nm and (d) 265 nm.

The peak at 5.8 min was at its highest intensity at 240 nm, possibly corresponding to abietic acid. There were peaks at 5.51 and 6.05 min that are seen at all the wavelengths. Using a 10 mM MECD 10 mM SBCD MES buffer, there was also a peak visible at all the wavelengths with its strongest intensity at 240 nm corresponding to abietic acid [92].

Tris has a pK_a of 8.1 according to product specification so a tris buffer at pH 8 was prepared to investigate its use as a suitable buffer.

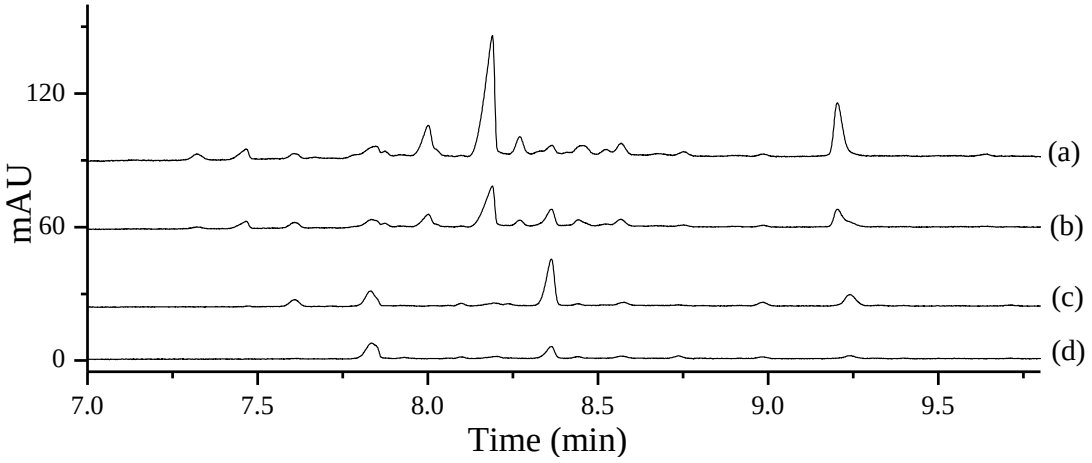

Figure 2-19 Electropherograms of 0.1% w/v rosin in methanol sample analysed in positive polarity, 20 kV, capillary 58 cm (49.5 cm to detector), 50 µm i.d., 25°C and 50 mbar 4 s injection times. Buffer consists of 10 mM MECD 10 mM SBCD in 20 mM Tris buffer pH 8. Detection at (a) 200 nm, (b) 214 nm, (c) 240 nm and (d) 265 nm.

In the electropherogram for the rosin sample analysed using the 10 mM MECD 10 mM SBCD tris buffer (Figure 2-19), the peak at 8.3 min whose intensity was highest at 240 nm is the ABA peak. As was seen with the phosphate buffers, there was a large peak with much stronger intensities at 200 and 214 nm at 8.2 min and the last migrating peaks was visible at all wavelengths. As with the majority of buffers, resolution was improved for the sample when analysed with 10 mM CD compared to 5 mM CD, and the efficiency values were also higher.

As the tris buffer can be used at a pH sufficient to keep the acids in their charged state, and based on the best resolution and efficiency values, and which electropherogram showed the most peaks, the optimum buffer was chosen to be 10 mM MECD 10 mM SBCD in 20 mM Tris buffer pH 8. Up to 16 fully resolved and coeluting peaks were observed and the resolution and efficiency values can be seen in Table 2-9.

Table 2-9 Resolution and efficiency values for a rosin sample analysed using a 10 mM MECD 10 mM SBCD 20 mM tris buffer pH 8, detection at 200 nm.

Peak number	Resolution (R_s)	Efficiency (N)
1		117296
2	2.1	116444
3	2.0	54556
4	1.5	109746
5	1.2	74731
6	1.1	183787
7	0.9	136849
8	1.1	128026
9	1.0	397578
10	0.5	105846
11	1.6	260678
12	0.8	125566
13	1.1	126793
14	0.8	122454
15	0.3	127579
16	1.0	104118
17	1.0	113254
18	1.1	65439
19	0.8	252765
20	0.4	302284

The optimum separation conditions were found to be a 4s injection time at 50 mbar, 20 kV separation voltage, positive polarity and a temperature of 25°C. Further studies analyse 0.1% w/v gum rosin in methanol samples using a 10 mM MECD 10 mM SBCD 20 mM tris buffer at pH 8.

2.3.3 Buffer additive study

A 20 mM tris buffer at pH 8 containing 10 mM MECD 10 mM SBCD was found to give the highest number of resolved peaks so far. Buffer additives were then further investigated.

2.3.3.1 SDS-tris buffer

As micellar electrokinetic chromatography is also used for the separation of compounds according to their hydrophobicity, SDS as a buffer additive was briefly investigated.

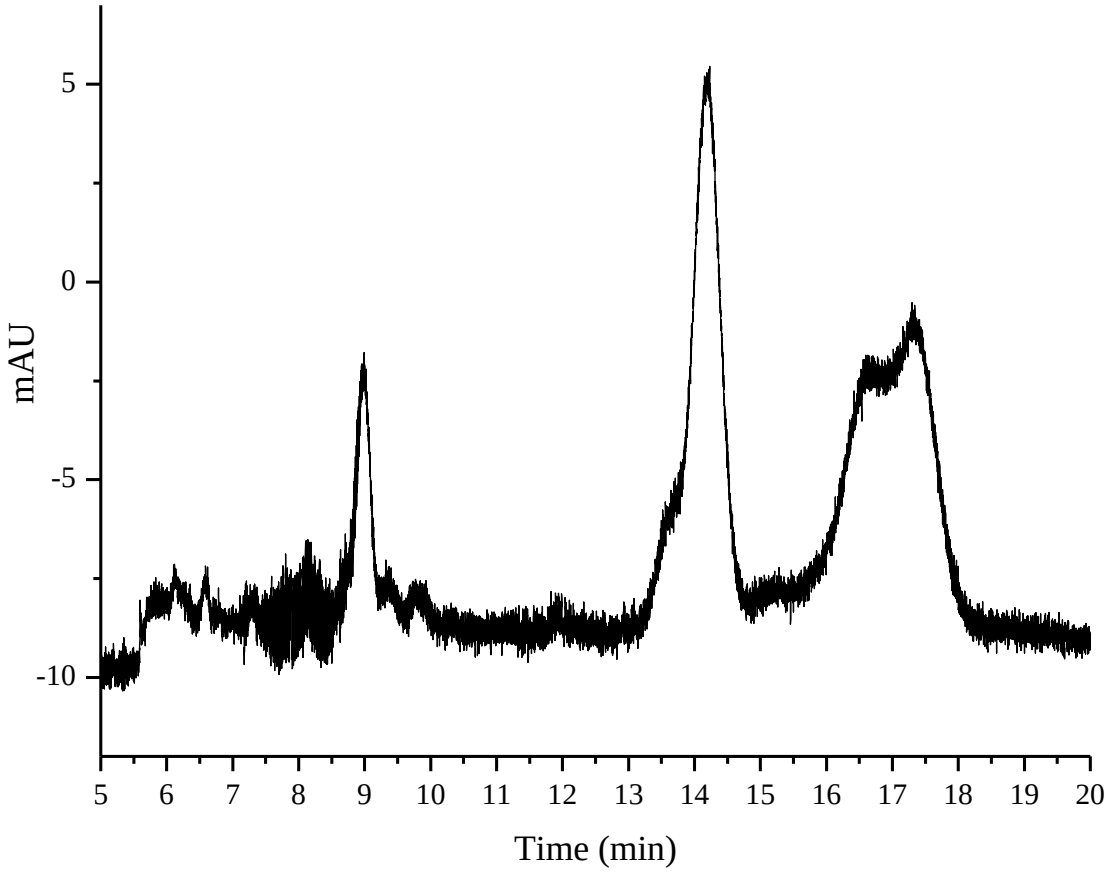

Figure 2-20 Electropherogram of 0.1% w/v rosin sample analysed in positive polarity, 20 kV, capillary 58 cm (49.5 cm to detector), 50 µm i.d., 25°C, 50 mbar 4 s injection times. Buffer consists of 50 mM SDS in 20 mM tris buffer pH 8. Detection was at 200 nm.

A rosin sample was analysed using a 50 mM SDS in 20 mM tris buffer at pH 8. As can be seen in Figure 2-20, the separation was not comparable with the separation achieved with a CD-tris buffer. The rosin separated into 4 masses of peaks compared

to the up to 20 partially resolved peaks obtained using a CD-tris buffer. The low analysis wavelength may be contributing to the significant baseline noise.

2.3.3.2 Cyclodextrin concentration variation

As the addition of cyclodextrins to the CE run buffer resulted in separation, the effect of varying the concentration of one cyclodextrin relative to the other was investigated. Numerous publications report that a combination of a neutral and a charged cyclodextrin added to a buffer greatly increase separation when compared to either one added on its own [31, 90]. The neutral CD provides the structural difference for compounds to separate while the charged CD provides mobility. Thus far all buffers contained equal concentrations of MECD and SBCD. A short study was carried out to see if varying the ratio of their concentration relative to each other improved separation. Tris buffers containing 10 mM SBCD and 1-10 mM MECD were prepared and rosin samples in MeOH were analysed.

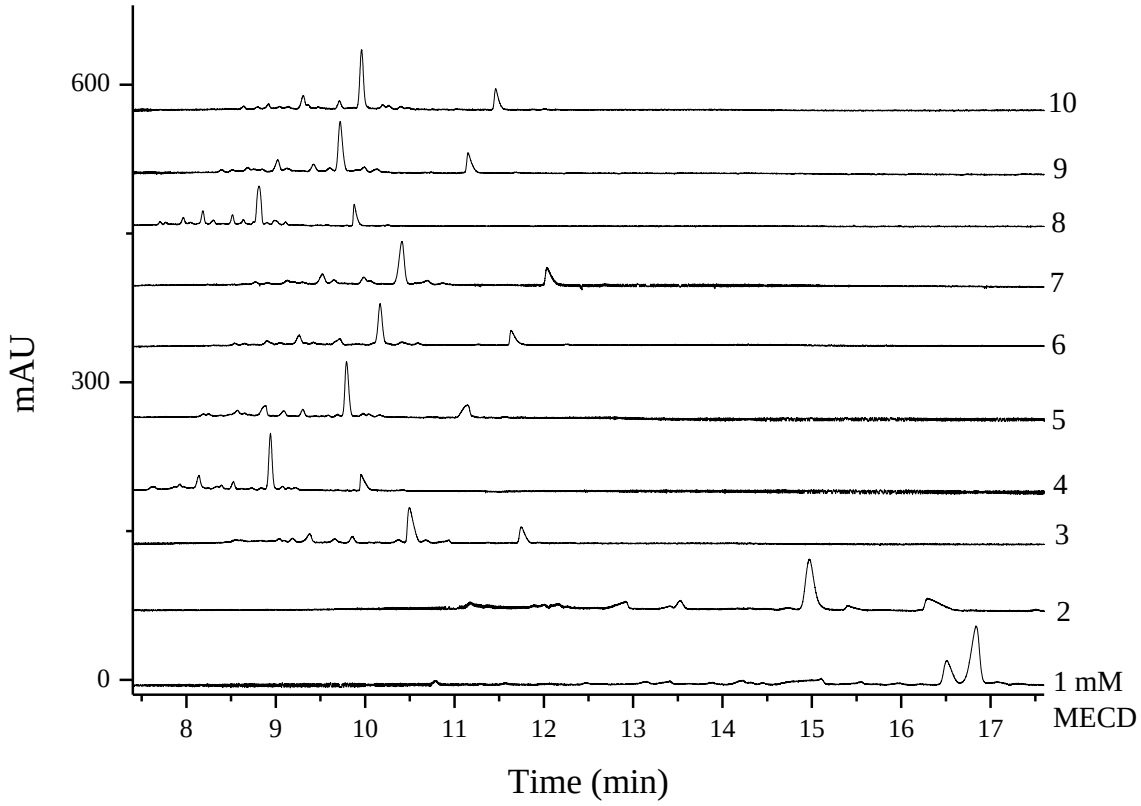

Figure 2-21 Electropherograms of 0.1% w/v rosin sample analysed in positive polarity, 20 kV, capillary 58 cm (49.5 cm to detector), 50 µm i.d., 25°C, 50 mbar 4 s injection times. Buffer consists of 20 mM tris buffer pH 8 containing 10 mM SBCD and varying concentrations of MECD from 1 mM to 10 mM. Detection at 200 nm.

As seen in Figure 2-21, the electropherogram changes over the range of cyclodextrin concentration ratios investigated in terms of resolution and efficiency (Table 2-10). When the concentration of MECD was increased, the analysis times decreased. This could suggest that the analytes favour interacting with MECD over SBCD, and do so when it is available thus reducing their interactions with SBCD which would result in later migration times as the SBCD travels against the EOF. When there is more MECD present in the buffer, the analytes can interact more with this neutral cyclodextrin which moves with the EOF. Higher elution times were seen when 1 mM MECD 10 mM SBCD was used in the buffer which suggests that the lack of MECD leads to the compounds interacting more with the negatively charged SBCD.

The earlier elution times make the 10 mM MECD concentration more attractive as a separation method. While both buffers show a similar number of coeluting and baseline resolved peaks, the efficiencies are much greater for the peaks seen using 10 mM MECD 10 mM SBCD tris buffer compared to those of the 1 mM MECD 10 mM SBCD buffer tris buffer. The higher MECD concentration results in 13 peaks with efficiencies over 100000 while all but three of the peaks in the 1 mM MECD buffer are fewer than 100000. In comparison with HPLC, 10119 was the highest efficiency achieved in this chapter, while the majority of efficiency values were an order of magnitude less.

Table 2-10 Resolution and efficiency values for the peaks seen in Figure 2-21

SBCD conc. (mM)	MECD conc. (mM)	Average R_s	SD	Average N	SD
10	1	1.3	0.4	58247	44556
10	2	1.3	0.9	62913	39656
10	3	1.4	0.6	78401	37703
10	4	1.7	2.0	100427	35096
10	5	1.4	0.9	132104	70671
10	6	1.6	1.5	92247	32254
10	7	1.2	0.7	79070	28823
10	8	1.7	1.6	150030	54648
10	9	1.7	1.7	102745	37289
10	10	1.8	1.5	141051	46515

A 1:1 concentration ratio of MECD: SBCD was selected for further analysis, using a 10 mM MECD 10 mM SBCD in 20 mM tris buffer at pH 8. The cyclodextrin ratio is consistent with literature reports. Luong *et al.* also came to the conclusion that the concentration of MECD and SBCD had to be at or near equal in order to optimise separation [31].

2.3.4 Resin acid standards and mixture

In order to develop a CE method specifically for the separation and quantification of acids in rosin samples, acid standards were analysed using the 10 mM MECD 10 mM SBCD in 20 mM tris buffer at pH 8 both individually (see Figure 2-22) and as a mixture (see Figure 2-23).

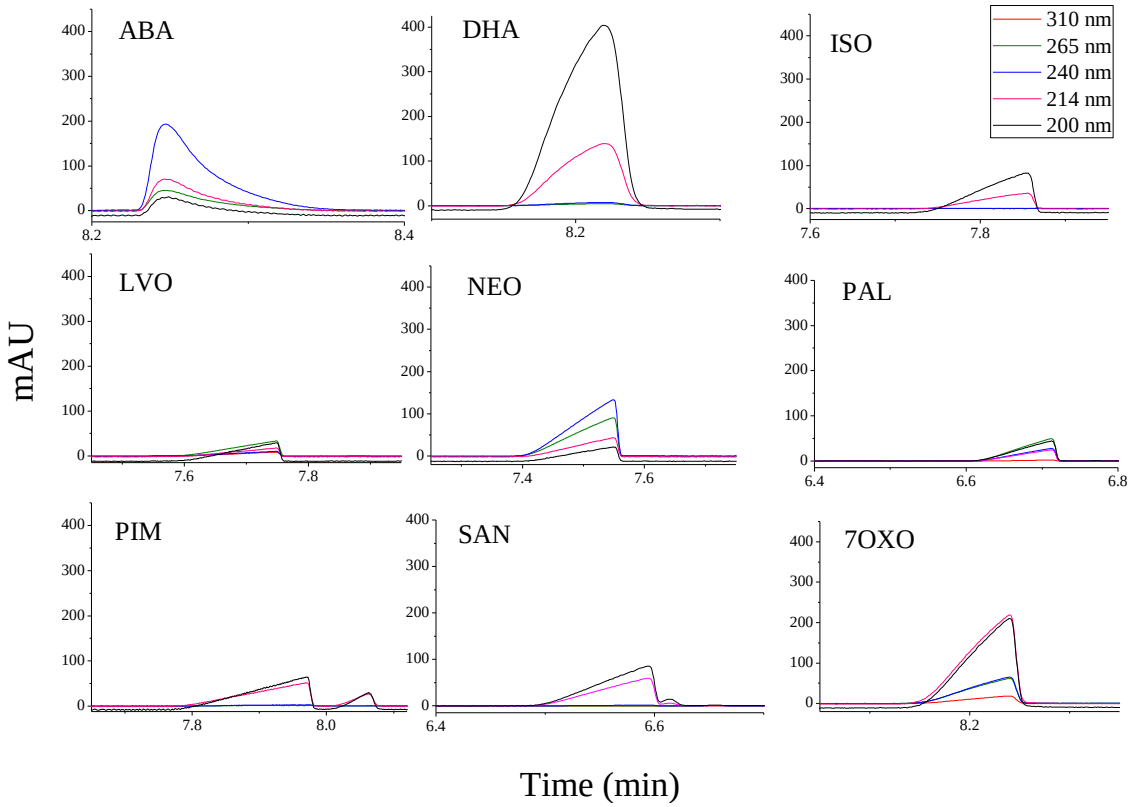

Figure 2-22 Electropherograms of acid standards analysed in positive polarity, 20 kV, capillary 58 cm (49.5 cm to detector), 50 µm i.d., 25°C, 50 mbar 4 s injection times. Buffer consists of 10 mM MECD 10 mM SBCD in 20 mM tris buffer pH 8. Detection at wavelengths as described in legend.

All of the acids were detected at 200 nm, some more strongly than others, as expected. DHA demonstrates the strongest absorbance at 200 nm, at least twice that of the next strongest absorbing acid, 7OXO. It shows weaker absorbance at 214 nm and practically none at the other wavelengths. It also elutes at the same time as the 7OXO standard which could pose problems in their separation. The ABA standard absorbs most strongly at 240 nm as reported in literature [92]. 7OXO absorbs strongly at both 200 and 214 nm. It also has a small absorbance at 310 nm while most of the acids show no absorbance at this wavelength. ISO only absorbs at 200 and 214 nm. LVO acid absorbs strongest at 200 nm, followed by 265 nm. Like 7OXO, it has a small absorbance at 310 nm. NEO shows strongest absorbance at 240 and 265 nm. PAL absorbs strongest at 265 nm. There are some impurities also seen in its electropherogram. PIM and SAN only show UV absorbance at 200 and 214 nm.

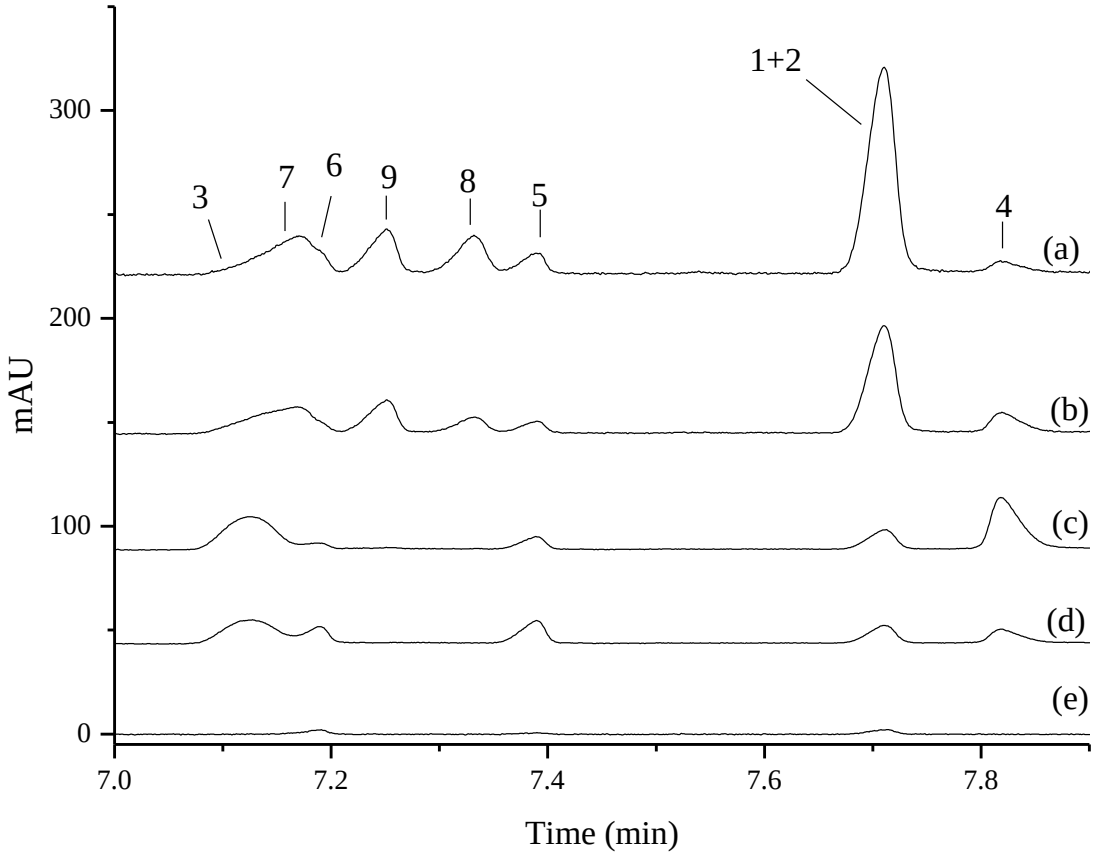

Figure 2-23 Electropherogram of a 0.01% w/v resin acid mixture analysed in positive polarity, 20 kV, capillary 58 cm (49.5 cm to detector), 50 µm i.d., 25°C, 50 mbar 4 s injection times. Buffer consists of 10 mM MECD 10 mM SBCD in 20 mM tris buffer pH 8. Wavelengths are (a) 200 nm, (b) 214 nm, (c) 240 nm, (d) 265 nm and (e) 310 nm. Numbers indicate (1) 7OXO, (2) DHA, (3) NEO, (4) ABA, (5) PAL, (6) LVO, (7) SAN, (8) ISO and (9) PIM.

As seen in Figure 2-23, some of the acids were found to coelute. The acids different spectral properties were used to aid their identification in this electropherogram. The nine resin acids were not all baseline resolved so further optimisation of the buffer was necessary. Resolution values are seen in Table 2-11. NEO was the first peak to migrate so its resolution value is taken from the following peak.

Table 2-11 Average resolution values for 10 mM MECD 10 mM SBCD in 20 mM tris buffer pH 8 separations

NEO	SAN	LVO	PIM	ISO	PAL	DHA	7-OXO	ABA
0.5	0.5	0.2	1.9	1.6	1.1	0.9	0.9	2.4

2.3.5 (2-Hydroxypropyl)-γ-cyclodextrin modified buffer

As changing the concentration of MECD, the neutral cyclodextrin, was found to affect peak efficiency and resolution (see Table 2-10), the use of a different neutral cyclodextrin was investigated as an alternative additive for the separation of the resin acids.

(2-Hydroxypropyl)-γ-cyclodextrin (HPγCD) is a neutral cyclodextrin with a larger cavity width than that of MECD (from 0.6-0.65 nm to 0.75-0.83 nm). A 20 mM tris buffer at pH 8 was prepared with 10 mM HPγCD and 10 mM SBCD and the resin acid mixture and standards analysed (see Figure 2-24 and Figure 2-25).

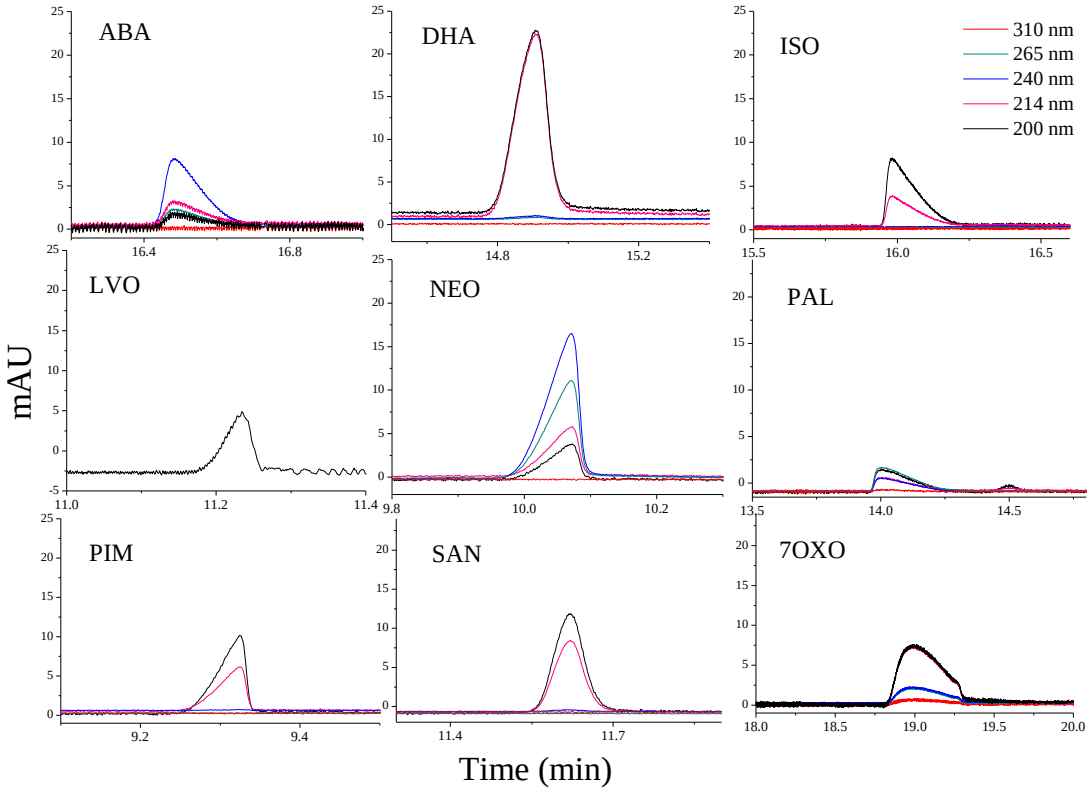

Figure 2-24 Electropherograms of acid standards analysed in positive polarity, 20 kV, capillary 58 cm (49.5 cm to detector), 50 µm i.d., 25°C, 50 mbar 4 s injection times. Buffer consists of 10 mM HPγCD 10 mM SBCD in 20 mM tris buffer pH 9. Detection at wavelengths as described in legend.

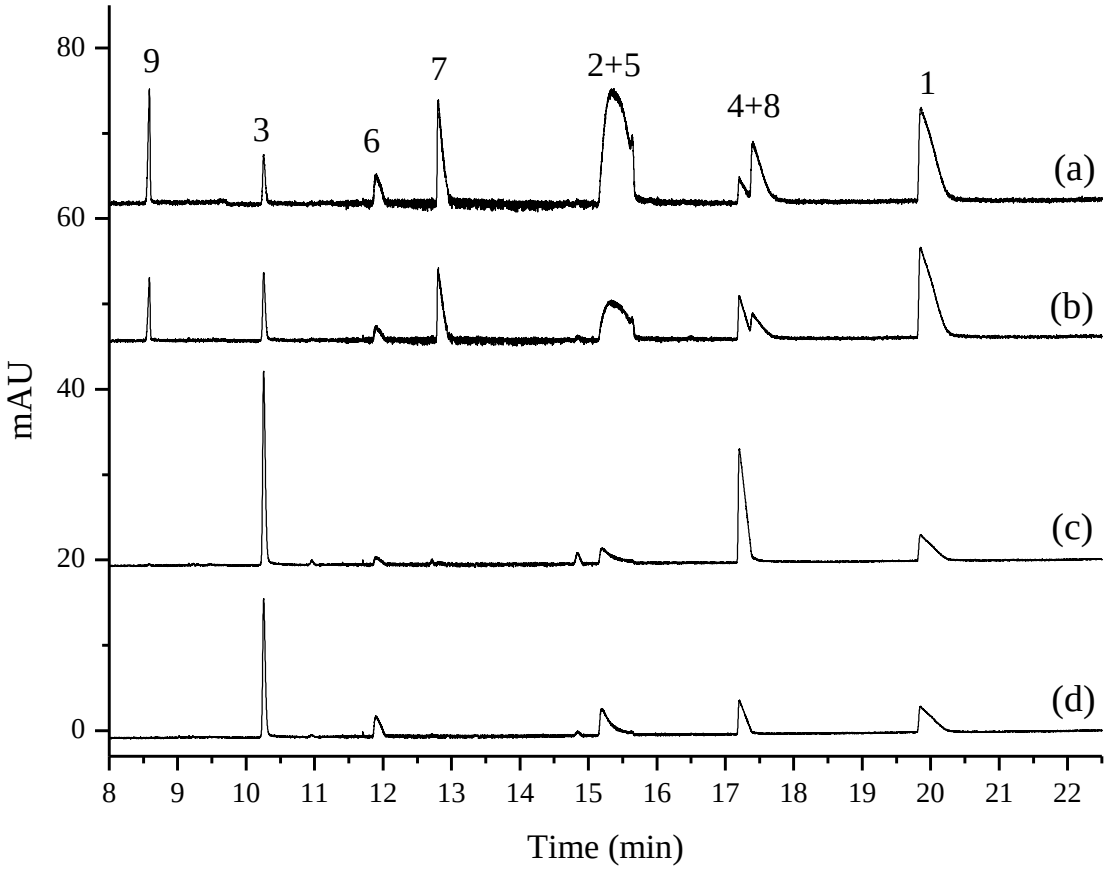

Figure 2-25 Electropherograms of a 0.01% w/v resin acid mixture analysed in positive polarity, 20 kV, capillary 58 cm (49.5 cm to detector), 50 µm i.d., 25°C, 50 mbar 4 s injection times. Buffer consists of 10 mM HPγCD 10 mM SBCD in 20 mM tris buffer pH 9. Wavelengths are (a) 200 nm, (b) 214 nm, (c) 240 nm and (d) 265 nm. Numbers indicate (1) 7OXO, (2) DHA, (3) NEO, (4) ABA, (5) PAL, (6) LVO, (7) SAN, (8) ISO and (9) PIM.

As shown in Figure 2-25 eight peaks are seen at 200 nm, two coeluting at 17.5 min and two coeluting at 15.7 min. While it is not obvious at 200 nm that the peak at 15.7 min is coeluting, at 240 and 265 nm two peaks are seen in its place. The migration order of the acids is different from that when MECD was used in the buffer. DHA and PAL, the peaks at 15.7 min, now have very close migration times while 7OXO is now found to migrate last. PIM, NEO, LVO and SAN are now separated, and PIM is the acid which migrates from the capillary first.

2.3.5.1 Cyclodextrin concentration

The concentration of the charged cyclodextrin, SBCD, was modified and the mixture of the nine resin acids analysed. Figure 2-26 shows that as the concentration of the charged cyclodextrin decreases, the migration times of the acids decrease as expected as they are being pulled towards the anode and away from the detector less. However, little improvement was seen in the separation of the nine peaks.

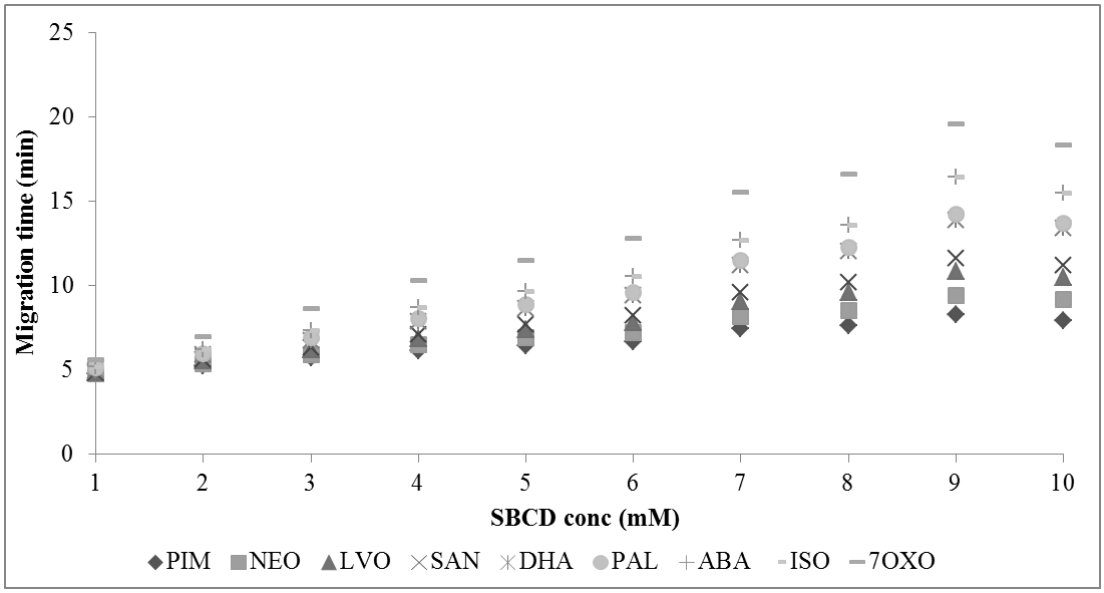

Figure 2-26 Plot of acid migration times versus SBCD concentration. Resin acid mixtures were analysed in positive polarity, 20 kV, capillary 58 cm (49.5 cm to detector), 50 µm i.d., 25°C, 50 mbar 4 s injection times. Buffer consists of 20 mM tris buffer pH 9 containing 10 mM HPγCD and varying concentrations of SBCD from 1 mM to 10 mM.

As can be seen in Figure 2-27, by varying the concentration of the neutral cyclodextrin a more selective effect is observed rather than simply affecting the migration times. While the first four peaks remain separated at each concentration, DHA and PAL were often found to coelute as were ISO and ABA. The resolution values are seen in Table 2-12. The majority of resolution values are above 1.5 with the buffer containing 5 mM HPγCD 10 mM SBCD resulting in the baseline resolution of eight of the resin acids. However, the resolution between the PAL and DHA peak is 1.3 so further buffer optimisation was carried out.

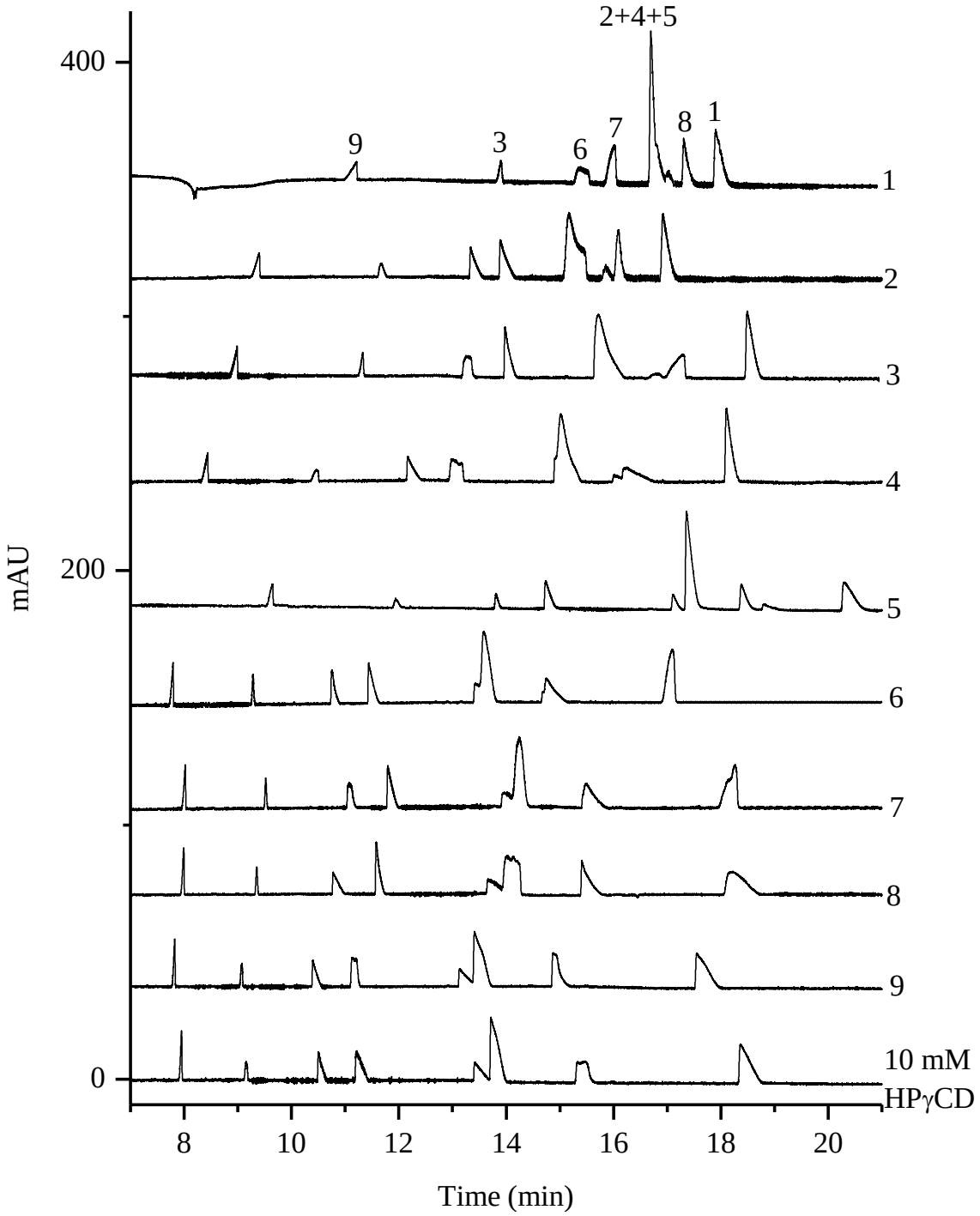

Figure 2-27 Electropherograms of a 0.01% w/v resin acid mixture analysed in positive polarity, 20 kV, capillary 58 cm (49.5 cm to detector), 50 µm i.d., 25°C, 50 mbar 4 s injection times. Buffer consists of 20 mM tris buffer pH 9 containing 10 mM SBCD and varying concentrations of HPγCD from 1 mM to 10 mM. Detection at 200 nm. Numbers indicate (1) 7OXO, (2) DHA, (3) NEO, (4) ABA, (5) PAL, (6) LVO, (7) SAN, (8) ISO and (9) PIM.

Table 2-12 Resolution values for the electropherograms seen in Figure 2-27.

10 mM SBCD								
HP-y-CD (mM)	**Peaks 1-2**	**P2-3**	**P3-4**	**P4-5**	**P5-6**	**P6-7**	**P7-8**	**P8-9**
1	16.5	6.5	2.1	3.3	1.9	1.5		2.6
2	14.5	9.1	2.6	3.8	2.1	1.1		3.8
3	20.9	9.8	2.8	5.5	2.6	1.4		3.3
4	14.8	8.8	2.9	5.3		3.3	0.6	4.8
5	18.3	13.1	6.4	13.9	1.3	5.4	1.7	4.5
6	24.0	15.2	4.3	11.1	0.9	3.1		7.1
7	25.4	12.6	4.2	8.9	1.1	3.6		7.4
8	23.5	11.2	5.0	8.9	0.9	3.6		6.2
9	20.6	11.9	4.0	8.3	0.9	5.1		8.1
10	17.7	12.0	3.9	8.7	1.1	5.1		7.3

2.3.5.2 Tris buffer pH

A high pH is required in order for the analytes to remain in their charged form (pK_a values range from 5.7-7.25 [1, 31, 84]). Analysis using a tris buffer over a range of pH 7.2-9 was investigated for further optimisation of the separation method (see Figure 2-28).

Table 2-13 Resolution, efficiency and RSD values for electropherograms of varying tris pH in Figure 2-28, n=3

Peak	**PIM**	**NEO**	**LVO**	**SAN**	**PAL**	**DHA**	**ISO**	**ABA**	**7OXO**
Resolution									
pH 7.2		25.3	13.4	6.6	13.4		7.7	1.4	5.4
pH 8		16.1	14.9	5.2	15.3	0.9	4.5		7.5
pH 9		12.5	11.3	3.7	8.6	0.8	3.5	1.7	5.3
Efficiency									
pH 7.2	267875	310451	247208	179954	184139		138475	68950	192585
pH 8	183499	214951	255099	182735	312401	165122	69278		162608
pH 9	194968	184085	137042	147190	72125	96405	106703	99024	80366
RSD (%)									
pH 7.2	0.54	1.25	0.77	0.98	0.94		1.32	1.65	1.06
pH 8	0.31	0.39	0.35	0.39	0.41	0.34	0.31		0.32
pH 9	0.42	0.45	0.50	0.50	0.57	0.57	0.57	0.76	0.73

A change in migration order was observed for some of the acids at different pH values as the degree to which they are ionized was affected. At pH 7.2, PAL and DHA coeluted and were followed by ABA and ISO. At pH 8, PAL migrates before DHA however ABA and ISO now coelute. At pH 9, these four acids migrate in the order PAL, DHA, ISO and ABA. PAL and DHA are still not completely baseline resolved. The migration order of the other acids did not change with the pH of the buffer. Luong *et al.* also observed a change in the migration order of the acids influenced by the buffer pH. They reported that the solubilities of the resin acids increased as pH increased. The acids were found to be more soluble in a buffer containing neutral MECD at pH 7, but at pH 9 several of the acids were reported to be more soluble in the charged SBCD [31]. As seen in Table 2-13 there was good reproducibility of the migration times at pH 9; 0.42-0.76% relative standard deviation (RSD). As pH 9 resulted in at least partial separation of all the acids in the mixture, it was chosen for further optimisation.

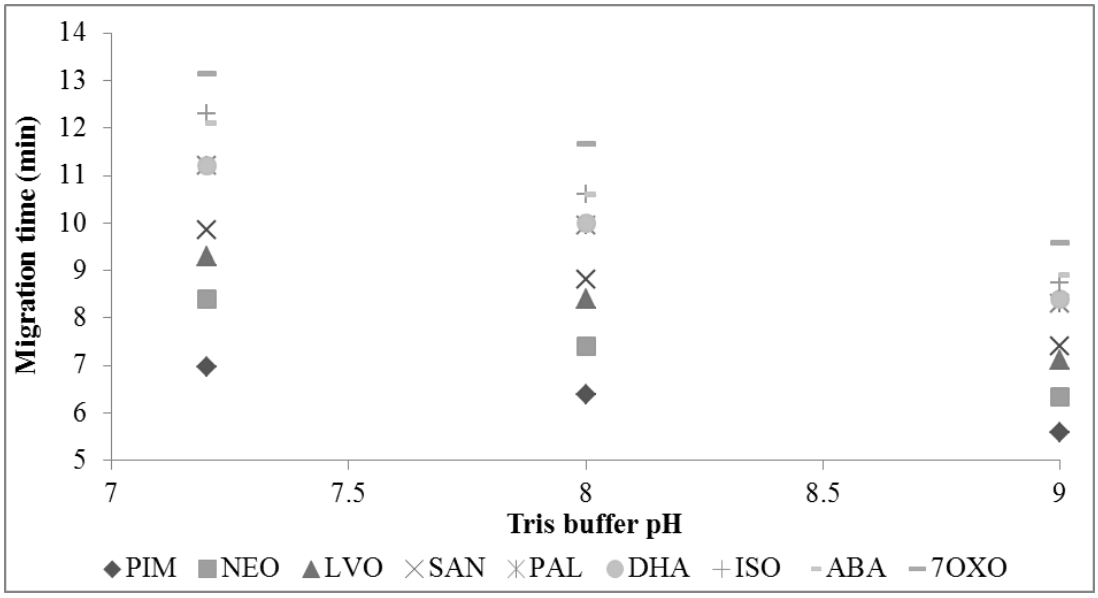

Figure 2-28 Plot of acid migration times versus tris buffer pH. Resin acid mixtures were analysed in positive polarity, 20 kV, capillary 58 cm (49.5 cm to detector), 50 µm i.d., 25°C, 50 mbar 4 s injection times. Buffer consists of 20 mM tris buffer at pH 9, pH 8 and pH 7.2 containing 10 mM SBCD 5 mM HPγCD.

2.3.5.3 Tris buffer concentration

The optimisation of concentration of the buffer was investigated over the range 10-50 mM for further optimisation of the separation (see Figure 2-29).

Table 2-14 Resolution, efficiency and RSD values for electropherograms with varying concentrations of tris in Figure 2-29, n=3

Peak	PIM	NEO	LVO	SAN	PAL	DHA	ISO	ABA	7OXO
Resolution									
10 mM		18.1	17.6	5.1	10.9	1.2	4.1	2.0	6.7
20 mM		12.5	11.3	3.7	8.6	0.8	3.5	1.7	5.3
50 mM		9.4	8.5	3.1	7.5	1.2	3.4	1.5	5.2
Efficiency									
10 mM	299203	403362	312563	207842	109664	172873	105502	107873	150940
20 mM	194968	184085	137042	147190	72125	96405	106703	99024	80366
50 mM	71076	104314	55249	82287	45774	53785	72715	83750	52718
RSD (%)									
10 mM	1.27	1.45	1.50	1.51	1.71	1.70	1.79	1.87	2.14
20 mM	0.42	0.45	0.50	0.50	0.57	0.57	0.57	0.76	0.73
50 mM	1.17	1.47	1.95	2.08	2.68	2.57	2.89	2.92	3.15

At lower tris concentrations the migration times were found to be less reproducible than 20 mM tris (1.3-2.1% RSD, n=3) and at higher concentration the peaks became broader decreasing efficiencies (see Table 2-14). Although resolution values were higher at 10 mM, PAL and DHA were still not baseline resolved and the resolution values for all other peaks at 20 mM tris were above 1.5. 20 mM tris also had the most reproducible migration times and was determined as the optimum concentration.

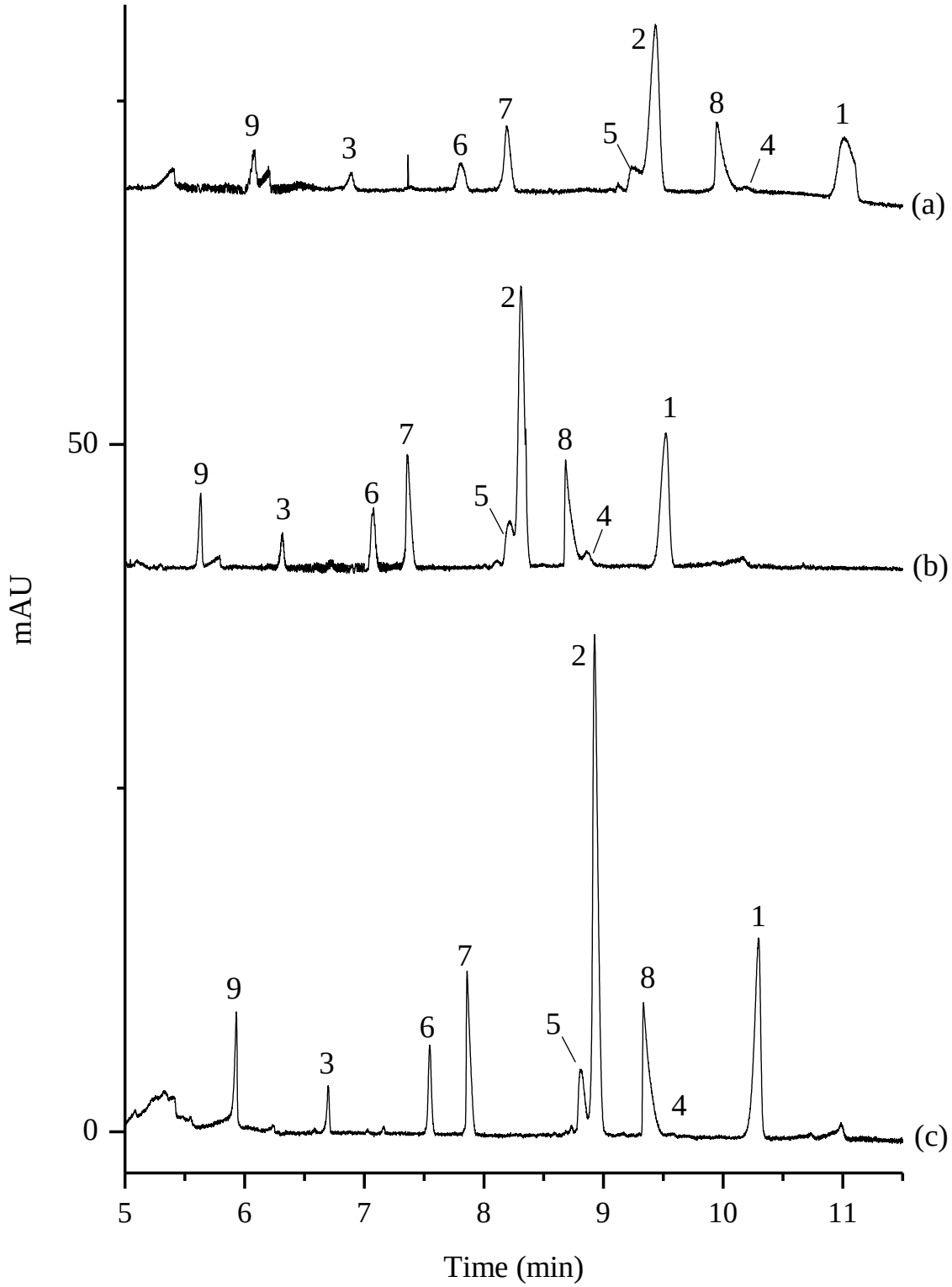

Figure 2-29 Electropherograms of resin acid mixture analysed in positive polarity, 20 kV, capillary 58 cm (49.5 cm to detector), 50 µm i.d., 25°C, 50 mbar 4 s injection times. Buffer consists of (a) 50 mM, (b) 20 mM and (c) 10 mM tris buffer at pH 9 containing 10 mM SBCD 5 mM HPγCD. Detection at 200 nm. Numbers indicate (1) 7OXO, (2) DHA, (3) NEO, (4) ABA, (5) PAL, (6) LVO, (7) SAN, (8) ISO and (9) PIM.

2.3.5.4 Effect of organic modifier

The acid mixture was analysed using buffers containing 10-30% MeOH. The addition of a solvent changes the equilibrium between the host-guest complexes by affecting the affinity of the analyte for the CD and so changes the complexes mobilities. The separation was improved with the presence of MeOH up to 30% as the PAL and DHA peaks were now baseline separated. At 30% MeOH the ISO and DHA peaks began to coelute (see Figure 2-30).

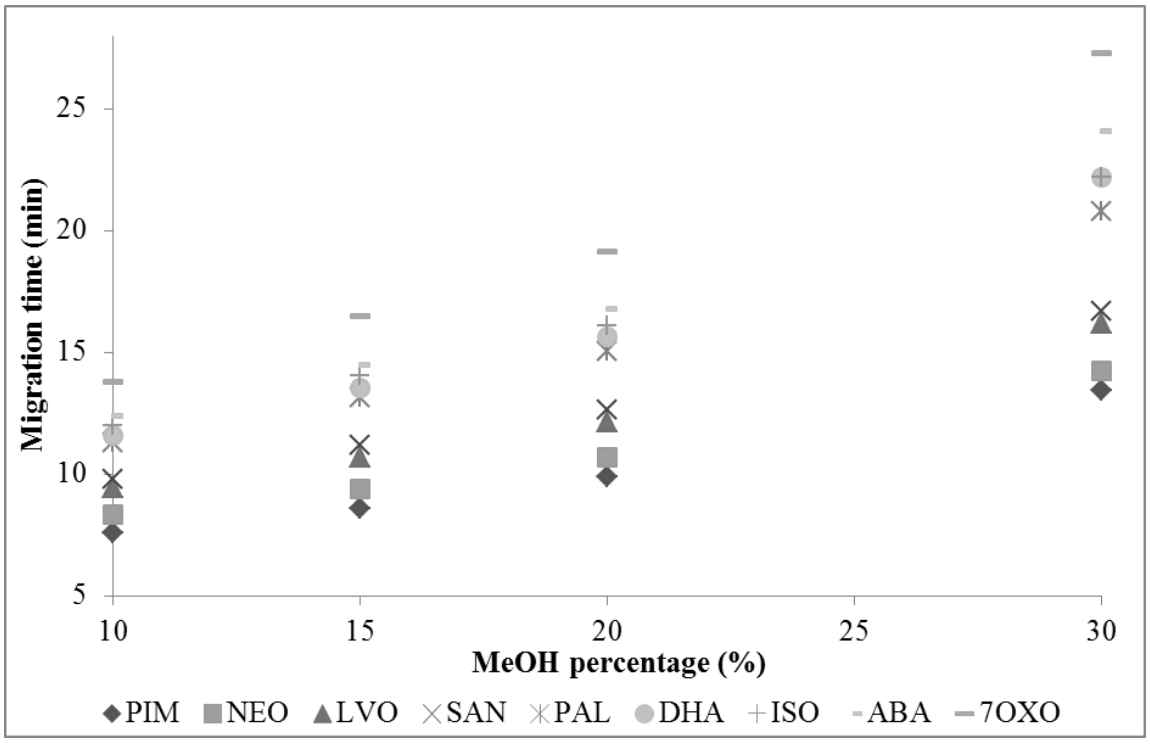

Figure 2-30 Plot of acid migration times versus the percentage of MeOH in the buffer. Resin acid mixtures in MeOH were analysed in positive polarity, 20 kV, capillary 58 cm (49.5 cm to detector), 50 µm i.d., 25°C, 50 mbar 4 s injection times. Buffer consists of 10-30% MeOH 20 mM tris buffer at pH 9 containing 10 mM SBCD 5 mM HPγCD.

15% MeOH was considered optimum as it resulted in baseline separation of the nine acids with good reproducibility of their migration times (0.2-1.2% RSD, n=3), good resolution values (2.3-18.3) and good efficiencies (60613-241875) (see Table 2-15). The separation of the nine resin acids using the optimum buffer; 15% MeOH 5 mM HPγCD 10 mM SBCD 20 mM tris buffer at pH 9, is seen in Figure 2-31.

Table 2-15 Resolution, efficiency and RSD values for electropherograms with varying MeOH percentages in Figure 2-30, n=3

Peak	PIM	NEO	LVO	SAN	PAL	DHA	ISO	ABA	7OXO
Resolution									
10 %		11.2	16.9	5.6	16.4	2.8	2.8	2.0	8.1
15 %		10.2	15.3	5.1	18.3	3.3	3.2	2.3	9.8
20 %		10.7	17.2	5.7	23.8	4.9	3.0	3.9	13.3
30 %		6.3	13.1	2.6	19.1	3.8		5.0	10.3
Efficiency									
10 %	217128	257084	346752	292977	175952	197277	74669	46518	195660
15 %	208786	203536	226614	241875	186078	165664	104347	60613	145126
20 %	383146	267183	296401	377365	257135	240433	145979	147173	180417
30 %	172950	197152	150216	88905	172531	26994		202796	71009
RSD (%)									
10 %	0.98	0.88	0.98	1.01	1.13	1.18	1.14	0.96	1.30
15 %	0.14	0.40	0.66	0.82	1.52	1.01	0.91	1.18	1.13
20 %	0.60	0.70	0.82	0.86	0.94	0.97	1.02	1.00	1.05
30 %	2.19	2.16	1.96	2.11	1.61	1.35		1.35	1.03

A 20 mM tris buffer at pH 9 containing 15% MeOH 5 mM HPγCD 10 mM SBCD resulted in the baseline resolution of the nine resin acids for the first time. The use of a γ cyclodextrin in place of a β cyclodextrin resulted in a different migration order and baseline resolution all the acids, possibly due to the increased cavity size of the larger cyclodextrin. The elution order of the acids in a mixture was found to be PIM, NEO, LVO, SAN, PAL, DHA, ISO, ABA, 7OXO. The higher molecular weight of 7OXO results in it eluting last.

Table 2-16 Resolution, efficiency, peak asymmetry and RSD values for Figure 2-31, n=3

Peak ID	N	R_s	A_s	Migration time (min)	RSD (%)
PIM	208786		2.4	8.6	0.1
NEO	203536	10.2	2.8	9.4	0.4
LVO	226614	15.3	2.2	10.7	0.7
SAN	241875	5.1	0.9	11.2	0.8
PAL	186078	18.3	0.2	13.1	1.5
DHA	165664	3.3	0.3	13.6	1.0
ISO	104347	3.2	0.2	14.1	0.9
ABA	60613	2.3	0.8	14.5	1.2
7OXO	145126	9.8	0.3	16.5	1.1

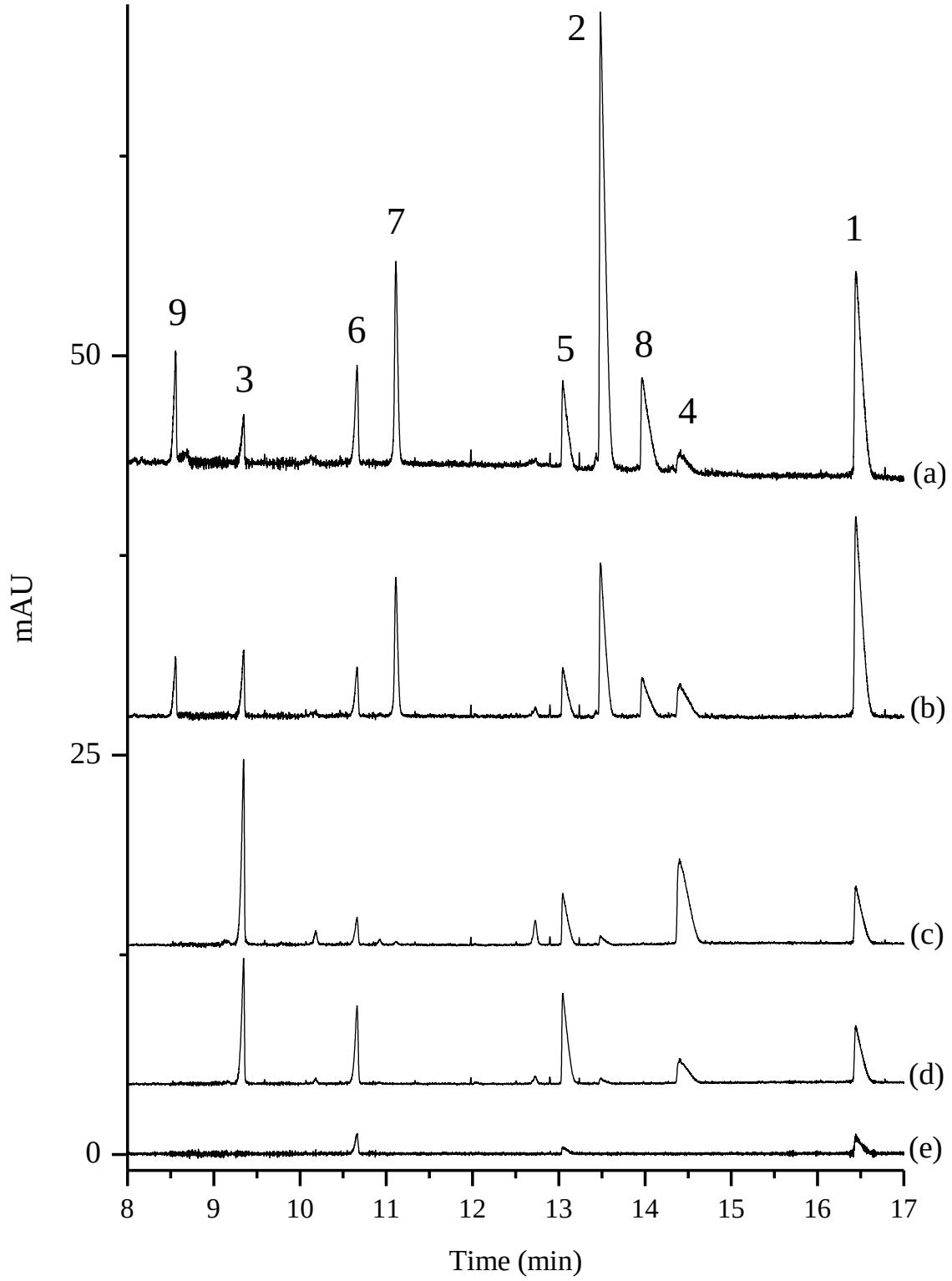

Figure 2-31 Electropherogram of a 0.01% w/v resin acid mixture analysed in positive polarity, 20 kV, capillary 58 cm (49.5 cm to detector), 50 µm i.d., 25°C, 50 mbar 4 s injection times. Buffer consists of 15% MeOH 5 mM HPγCD 10 mM SBCD in 20 mM tris buffer pH 9. Wavelengths are (a) 200 nm, (b) 214 nm, (c) 240 nm and (d) 265 nm. Numbers indicate (1) 7OXO, (2) DHA, (3) NEO, (4) ABA, (5) PAL, (6) LVO, (7) SAN, (8) ISO and (9) PIM. Detection at 200 nm.

Some of the peaks show some tailing, as seen by the peak asymmetry factor (A_s) in

Table 2-16. This may be a result of the mobility of the buffer ions being greater than the mobility of the analyte ions. Tailing can also result from interactions between the analytes and the capillary walls [73]. Good reproducibility of the migration times is achieved, less than 1.3% RSD, n=3. This reproducibility is seen in Figure 2-32.

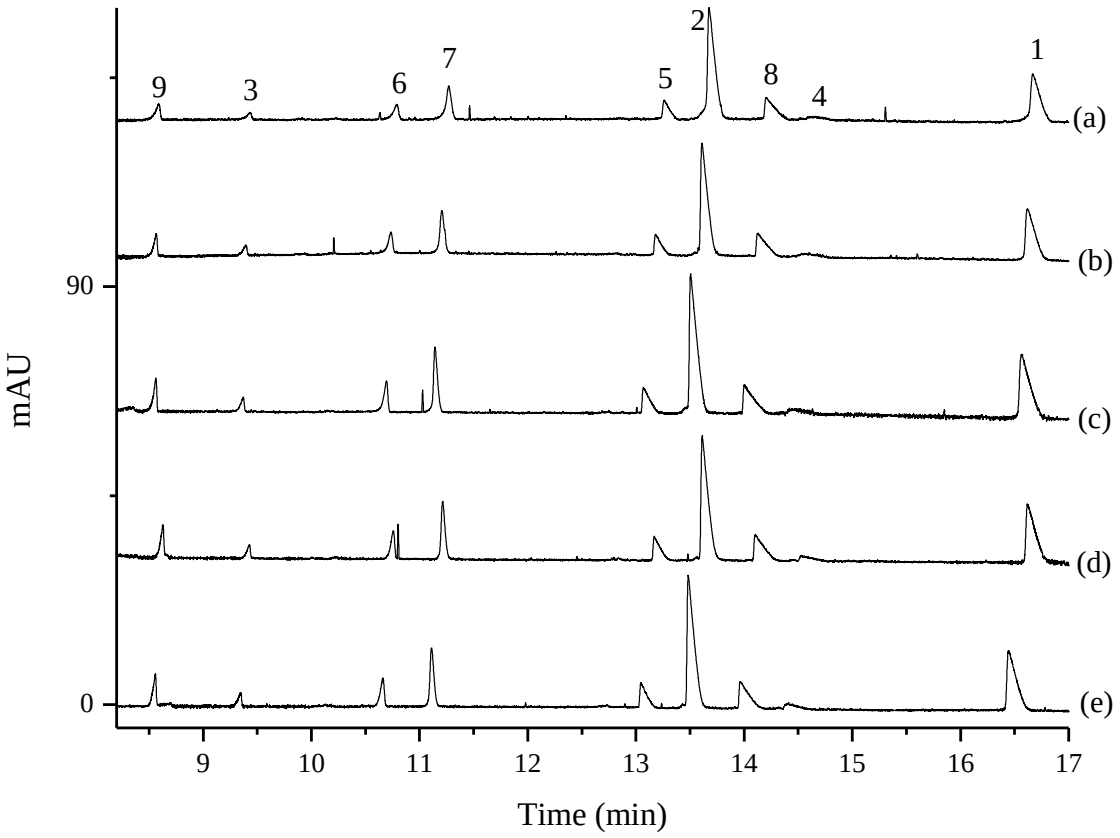

Figure 2-32 Repeat electropherograms of the resin acid analysed in positive polarity, 20 kV, capillary 58 cm (49.5 cm to detector), 50 µm i.d., 25°C, 50 mbar 4 s injection times. Buffer consists of 15% MeOH 5 mM HPγCD 10 mM SBCD in 20 mM tris buffer pH 9, detection at 200 nm.

2.3.6 Resin acid calibrations

Using the optimum buffer and separation conditions, calibration curves for the nine resin acids were constructed using triplicate analysis of five different concentrations of each acid at 5, 10, 50, 100 and 1000 mg L^{-1}. The use of corrected peak area (peak area/migration time) compensates for any run to run shift in migration times. It is also used because as a result of the detection being online, the analytes which pass the detector later are moving slower and so their peaks are broader than earlier migrating analyte [97]. All calibration curves were found to be linear over the range tested and LODs varied from 0.15-1.24 mg L^{-1} (see Figure 2-33 and Table 2-17). LODs were calculated from as 3 times the baseline noise.

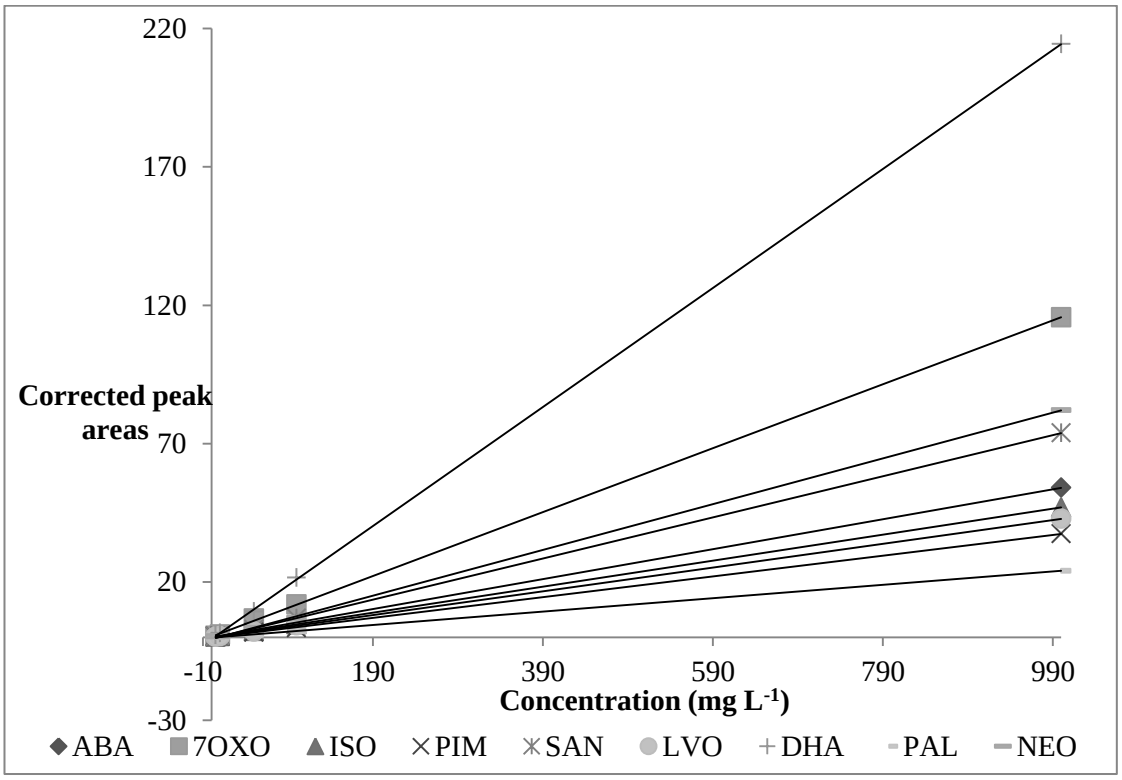

Figure 2-33 Calibration curves for the resin acids.

The method shows greatest sensitivity towards DHA, as seen by comparing the slopes of the curves. As seen in Table 2-17 there is good linearity observed for the acids over the range 5-1000 mg L^{-1}.

Table 2-17 Linearity and LOD values for the nine resin acids

Acid	Analysis wavelength (nm)	R^2 (n=3)	LOD (mg L^{-1})	Line equation
ABA	240	0.99	0.15	y=0.0541x-0.076
7-OXO	200	0.99	0.25	y=0.1154x+0.2792
ISO	200	1	0.73	y=0.047x-0.0194
PIM	200	0.99	0.65	y=0.0375x-0.0801
SAN	200	0.99	0.48	y=0.0742x-0.4241
LVO	200	1	1.24	y=0.0429x-0.0488
DHA	200	1	0.25	y=0.2149x-0.5548
PAL	265	0.99	0.35	y=0.0242x-0.1538
NEO	240	0.99	0.79	y=0.0826x-0.603

Luong *et al*. achieved LODs of 5 ppm (5 mg L^{-1}) for resin acids using CE-UV at 214 nm for their separation and Dell'mour *et al.* reported the LOD of DHA to be 400 pg μL^{-1} (0.4 mg L^{-1}), comparable to those seen in this work [31, 57].

Axelsson *et al.* compared GC-FID and HPLC/ESI-MS as methods for the determination of 7OXO, DHA and ABA in air samples. They reported LODs of 0.42 ng m^{-3}, 5.2 ng m^{-3} and 9.4 ng m^{-3} respectively using LC/MS, which are lower than those achieved by GC-FID (24, 115 and 89 ng m^{-3}) [98].

The LODs achieved by Axelsson *et al.* are an order of magnitude lower than those reported for this CE method, highlighting one of the drawbacks of CE; its sensitivity. The sensitivity of CE relative to other analytical methods is quite low due to the very small optical path length in the detector which is usually UV, and the minute sample volume injected (nanolitres). However, CE also offers certain advantages over other techniques. Minimal sample preparation was necessary while for GC-FID derivatization of the analytes was required. The amount of sample and buffer consumed is much lower than the volume of mobile phase used in HPLC, and the high efficiency values achievable using CE allow for the baseline separation of nine resin acids in the same analysis time that Axelsson *et al.* separate three.

2.4 Conclusions

The crystallisation of rosins in certain industrial applications is an on-going problem and the specific composition of rosins which tend to crystallise has not yet been defined. In this work, an effective method was developed for the separation of nine resin acids, abietic-, neoabietic-, dehydroabietic-, pimaric-, isopimaric-, levopimaric-, sandaracopimaric-, palustric- and 7-oxo-dehydroabietic acid using CE.

A reversed-phase HPLC method using an amide column and an ACN:water mobile phase with 0.1% acetic acid was found to be unable to separate the resin acids with the exceptions of DHA and 7OXO. The very similar structures of the remaining acids resulted in them coeluting in two peaks. The CE method resulted in improved separation and higher efficiency. As a chromatographic approach to the separation of the analytes present in rosin samples achieved less baseline resolution than the orthogonal electrophoretic approach, the CE method was the focus of further optimisation for the analysis of rosin samples.

It was found that a range of buffers investigated containing no cyclodextrins did not achieve separation. A tris buffer containing a charged and a neutral cyclodextrin, MECD and SBCD, resulted in the separation of several of the acids but LVO, SAN and NEO coeluted, as did DHA and 7OXO. When MECD was replaced by a γ cyclodextrin, HPγCD, the nine resin acids were separated using a 15% MeOH 5 mM HPγCD 10 mM SBCD in 20 mM tris buffer at pH 9. LODs of 0.15-1.25 mg L^{-1} were reported. For the first time a CE method was able to separate PIM, SAN and 7OXO, as well as the other important resin acids present in rosins.

The CE method allows for the first time a simple and rapid separation of a mixture of nine resin acids present in rosin samples. It is also the first use of CE for the quantification of resin acids in rosin samples. This method can then be applied to modified and unmodified rosin samples in order to screen for the presence and concentration of acids in each sample. CE provides an alternative separation method with high efficiencies and fast resolution to the use of GC which requires a sample derivatisation step. CE can also be used to analyse non-volatile compounds.

Chapter 3

A capillary electrophoresis method for the separation of terpenes and other neutral compounds in rosin samples

3.1 Introduction

While rosins consist mainly of acidic compounds, they also contain roughly 10% neutral compounds, including terpenes, terpene alcohols and aldehydes [1, 36, 57]. Longifolene, terpineol and 4-allylanisole make up 50-60% of the volatiles present in gum rosins [1]. Terpenes are natural hydrocarbons formed by the head to tail joining of at least two isoprene units. They are grouped based on their number of isoprene units e.g. monoterpenes contain two and sesquiterpenes three. They are primarily found in nature in plants such as pine trees and are the main component of turpentine and many essential oils. Terpenes are generally found in low concentrations in samples, are soluble in organic solvents but insoluble in water [99]. Terpenes known to be present in rosins include monoterpenes such as camphene, 3-carene, α- and β-pinene and sesquiterpenes such as longifolene and aromadendrene (see Figure 3-2) [23, 100].

To the author's knowledge, there are limited publications of the determination of the neutral fraction of rosins. In various other natural samples terpenes are generally analysed by GC, often with a flame ionisation detector (FID) or with mass spectrometry (GC-MS) with analysis times of 25-60 min reported [99, 101, 102]. HPLC is also used for terpene analysis but to a lesser extent, usually when the separation of more polar compounds cannot be achieved by GC [99, 103, 104]. Capillary electrophoresis (CE) is an alternative separation technique for the rapid determination of neutral components. As neutral analytes do not have their own electrophoretic mobility, charged compounds including cyclodextrins, micelles and microemulsions are used in the separation medium as pseudo-stationary phases providing mobility to the neutrals as they interact. Such modified CE methods can provide a rapid and simple method for the analysis of neutral compounds.

In this chapter, HPLC, cyclodextrin-CE (CD-CE), micellar electrokinetic chromatography (MEKC) and microemulsion electrokinetic chromatography (MEEKC) were studied for the separation of a mixture of nine compounds including monoterpenes, sesquiterpenes, a phenylpropene and a monoterpene alcohol. These were chosen as they have all been detected in rosin samples.

3.1.1 HPLC

Although GC is most often used for the analysis of the volatile terpenes, HPLC has been used for their separation, usually with CDs either included in the mobile phase or bonded to the stationary phase [104]. HPLC was used for the separation of α-pinene, β-pinene, camphene and limonene while determining the association constants they form with cyclodextrins. Only the presence of α-CD in the 0.1% orthophosphoric acid 55:45 water:methanol (MeOH) mobile phase resulted in the separation of the chiral enantiomers [104]. Capillary liquid chromatography was used to separate α- and β-pinene in an acetonitrile (ACN):water mobile phase without the need for CD additives [103].

3.1.2 CE

CE is becoming a more widely used method for the analysis of neutral compounds due to the ease of changing the mode of separation i.e. a different additive such as a CD or micelles are placed in the buffer, compared to other techniques where a new column may be required, which is costly. Both MEKC and MEEKC have been used for the analysis of terpenes. Their hydrophobic nature allows them to partition easily into micelles and microemulsions. The same can be said for the use of CDs in CE.

MEKC was used for the determination of monoterpenes in marjoram plants. A buffer containing 10% ACN 10 mM NaH_2PO_4, 6 mM $Na_2B_4O_7$, 50 mM SDS, 7 mM γ -cyclodextrin at pH 8 resulted in the separation of camphene, α pinene and β pinene among other terpenes. α-Terpineol was also separated from other monoterpene alcohols and determined by this method [105]. Camphene, α-pinene, β-pinene and limonene were separated with the addition of 5 mM α-CD and 6.5 mM sulphated β-CD to a 10 mM phosphate buffer at pH 3.3 [90]. Cao *et al.* investigated the use of oil-in-water and water-in-oil MEEKC methods for the analysis of five diterpenoids [106].

The analysis of terpenes, including 3-carene, α- and β-pinene, present in pepper extracts by capillary electrochromatography (CEC) was reported. The 50 mM ammonium acetate/ACN (10:90 v/v) mobile phase at pH 6 separated 11 compounds with a run time of 25 min [107].

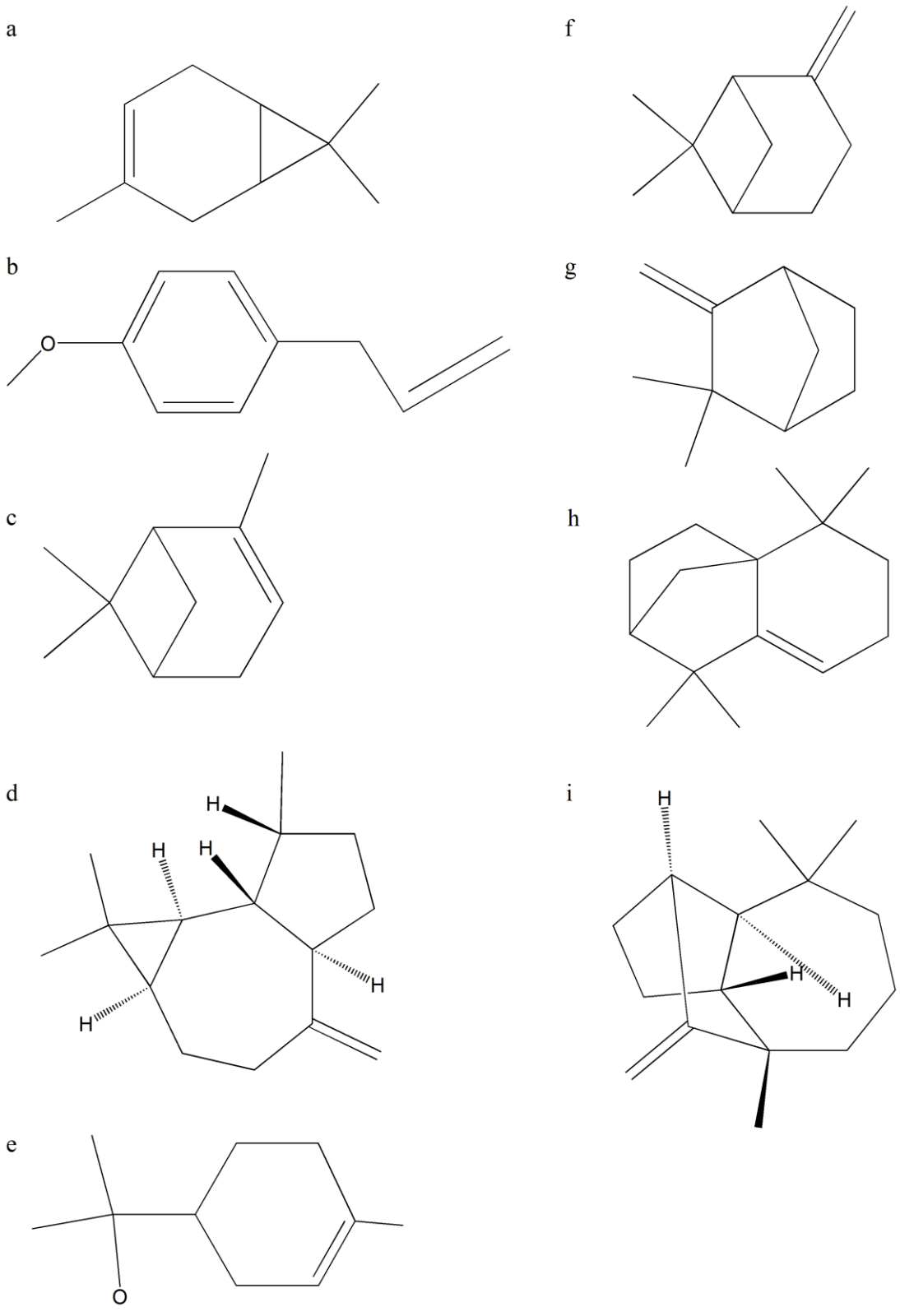

Figure 3-1 Structures of the neutral analytes in planar geometry. Letters indicate (a) 3-carene, (b) 4-allylanisole, (c) α-pinene, (d) aromadendrene, (e) terpineol, (f) β-pinene, (g) camphene, (h) isolongifolene and (i) longifolene.

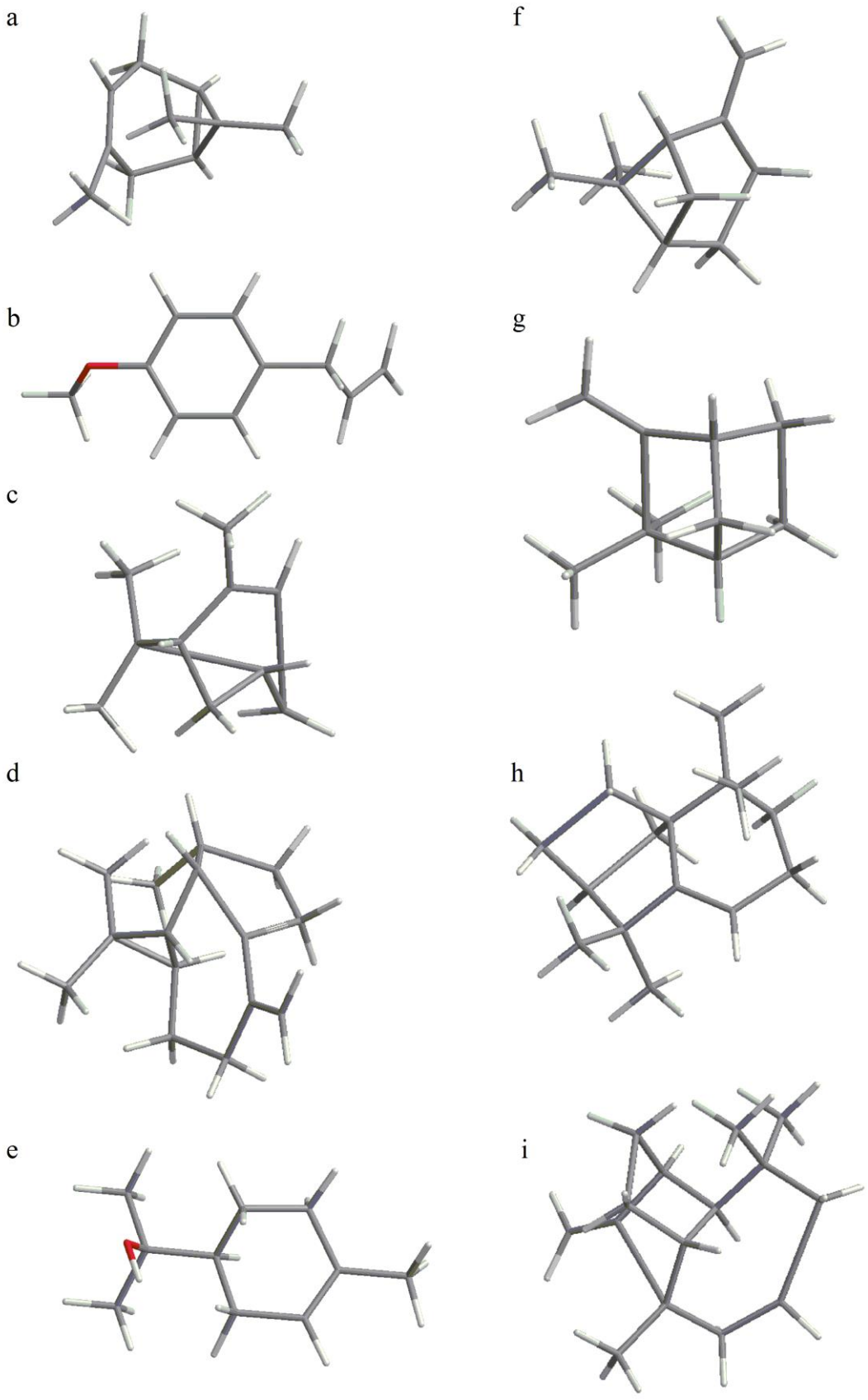

Figure 3-2 Structures of the neutral analytes in 3D. Letters indicate (a) 3-carene, (b) 4-allylanisole, (c) α-pinene, (d) aromadendrene, (e) terpineol, (f) β-pinene, (g) camphene, (h) isolongifolene and (i) longifolene.

3.1.1 Aims

The aim of this research is to investigate analytical techniques for the separation of some of the neutral compounds found in rosin samples. The objectives are to investigate the use of HPLC and several CE modes which involve the use of pseudo-stationary phases for the separation of the analytes, and to optimise a method for the separation of a mixture of nine terpenes and other neutral compounds for future application to rosin samples.

3.2 Experimental

3.2.1 Instrumentation

HPLC analysis was carried out on an Agilent 1100 HPLC system (Agilent Technologies Ireland Ltd., Unit 3, Euro House, Euro Business Park, Little Island, Cork, Ireland). The system uses a DAD (range 190-600 nm) and a fluorescence detector (excitation range is 200-700 nm and emission range is 280-900 nm). The software used was Agilent Chemstation. The column used was a Supelco Ascentis RP-Amide column (15 cm x 4.6 mm, 3 μm particles). CE analysis was carried out on an Agilent Capillary Electrophoresis System G1601A (Agilent Technologies Ireland Ltd., Unit 3, Euro House, Euro Business Park, Little Island, Cork, Ireland). The CE system uses a DAD which has a range of 191-599 nm. Peaks were manually integrated using the Agilent 3D-CE Chemstation software. Capillaries used were 58 cm (49.5 cm effective length) fused silica capillaries, 50 μm inner diameter (CMScientific, Silsden, BD20 0DL, UK). The pH meter used was a HI2211 pH/ORP meter (Hanna Instruments, Rhode Island, USA) with a calomel reference electrode (Metrohm AG, Switzerland).

3.2.2 Reagents

All reagents used were of analytical grade, including anhydrous sodium phosphate monobasic, sodium tetraborate, disodium tetraborate, Tris(hydroxymethyl)aminomethane, trizma® hydrochloride, (2-hydroxypropyl)- γ-cyclodextrin (HP-γ-CD), methyl- β-cyclodextrin (MECD), β-cyclodextrin, boric acid, ACN, acetic acid, sodium dodecyl sulphate, 1-butanol, heptane, ethyl acetate, cyclohexane, isopropanol, sodium hydroxide (NaOH), MeOH and hydrochloric acid (HCl) and were purchased from Sigma Aldrich Ireland Ltd. (Vale Road, Arklow, Wicklow, Ireland). Sulfobutylether -β-cyclodextrin (SBCD) was donated by CyDex Pharmaceuticals, Inc. (Ligand Pharmaceuticals, Inc. 11119 North Torrey Pines Road, Suite 200 La Jolla, CA 92037). Camphene, α-pinene (98% purity), β-pinene (98%), α-terpineol (97%), 4-allylanisole (98%), longifolene (99%), isolongifolene (98%), aromadendrene (97%), 3-carene (99%) and rosin samples were donated by Henkel Ireland Ltd., Dublin, Ireland.

3.2.3 HPLC separation conditions

Unless stated otherwise, separations were carried out at a flow rate of 1 mL min^{-1} with 20 μL injections. UV detection was at 254 nm and fluorescence excitation was at 250 nm with emission at 410 nm. The mobile phase consisted of 0.1% acetic acid 97:3 ACN: water. The mobile phase was filtered through a 0.45 μm nylon membrane and sonicated before use. Methanol blanks were run between each sample. The column was stored in ACN overnight at room temperature.

3.2.4 CE separation conditions

CE separations, unless stated otherwise, were carried out at 20 kV and the temperature was maintained at 25°C. Separations were all repeated 3 times. Pre-injection rinse consisted of 3 min 0.1 M NaOH, 3 min water and 5 min buffer. The optimum injection time was found to be 2 s, however, injections under 3 s are subject to instrumental injection pressure and voltage variability. In order to avoid this but have the same injection volume, hydrodynamic injections of 20 s at 5 mbar were carried out. Detection was set at 200 nm.

3.2.5 Sample and buffer preparation

In sections 3.3-3.3.4.4 the terpene mixture consists of 4-allylanisole, β-pinene, α-pinene, camphene, 3-carene, isolongifolene, α-terpineol, aromadendrene and longifolene at 0.01% v/w dissolved in 100% MeOH. From section 3.3.4.5 onwards they were dissolved in MeOH and diluted to 0.01% with 5 mM β-CD 10 mM SDS 50 mM tris buffer at pH 8.

Tris buffers were prepared to the required concentration and pH by mixing appropriate amounts of tris HCl and tris base in distilled water following the Sigma-Aldrich tris buffer mixing table e.g. a 50 mM tris buffer at pH 8 was prepared by mixing 4.44 g L^{-1} tris HCl and 2.65 g L^{-1} tris base. All buffers were filtered through a 0.2 μm nylon membrane filter. MEKC buffers were prepared by dissolving appropriate amounts of SDS and CDs in the tris buffer and were sonicated for 15 min. MEEKC buffers were prepared by mixing appropriate amounts of surfactant,

oil and co-surfactant in tris buffer e.g. a 6% butanol 4% SDS 1% ethyl acetate buffer in 10 mM tris at pH 8 was prepared by mixing 370 μL butanol, 0.2 g SDS and 55 μL ethyl acetate in 5 mL tris buffer and sonicated for 30 min.

3.3 Results and Discussion

Both HPLC and CE were investigated for their ability to separate a mixture of neutral compounds, with more success found using the CE methods. MEEKC, MEKC and CD-MECK all showed varying degrees of separation of the mixture with CD-MEKC giving the eventual optimised method. As the specific cause of rosin crystallisation is not known, the analysis of the neutral components of rosin could potentially provide information on any links between their presence and concentration and the rosins tendency to crystallise.

3.3.1 HPLC method

The HPLC method developed in chapter 3 was used to analyse terpene standards individually and in a mixture to investigate if it was more suitable for terpene separation than for acids.

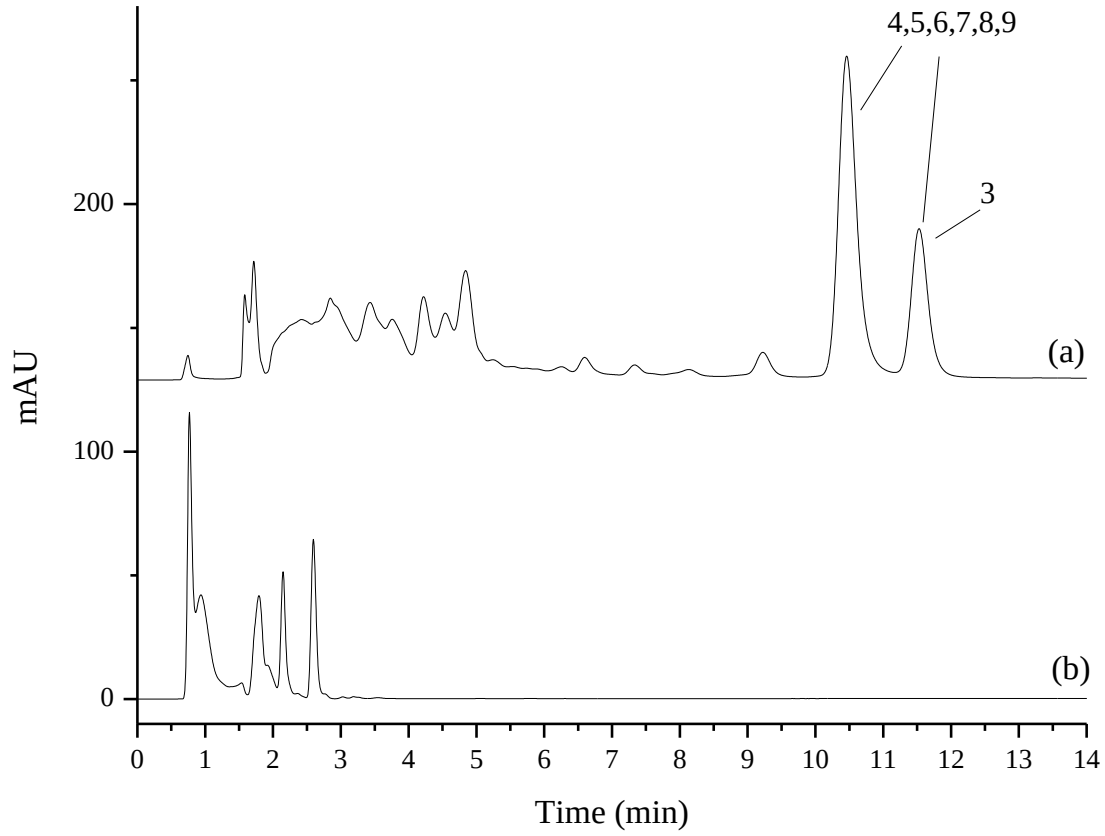

Figure 3-3 Chromatograms of (a) 0.1% w/v gum rosin in MeOH and (b) 0.1% terpene mixture analysed at 0.1% acetic acid 97:3 ACN: water mobile phase, 20 µL injection at 1 mL min^{-1}, UV detection at 254 nm. Numbers indicate acids as follows: (3) neoabietic acid, (4) abietic acid, (5) palustric acid, (6) levopimaric acid, (7) sandaracopimaric acid, (8) isopimaric acid and (9) pimaric acid.

The terpene mixture containing 4-allylanisole, β-pinene, α-pinene, camphene, 3-carene, isolongifolene, α-terpineol, aromadendrene and longifolene in MeOH was analysed using an RP-Amide column with a 0.1% acetic acid 97:3 ACN:water mobile phase (see Figure 3-3).

The terpenes were found to elute earlier than the acids. This was expected as they are less polar and the RP-amide column retains polar compounds longer. The terpene standards were then analysed separately.

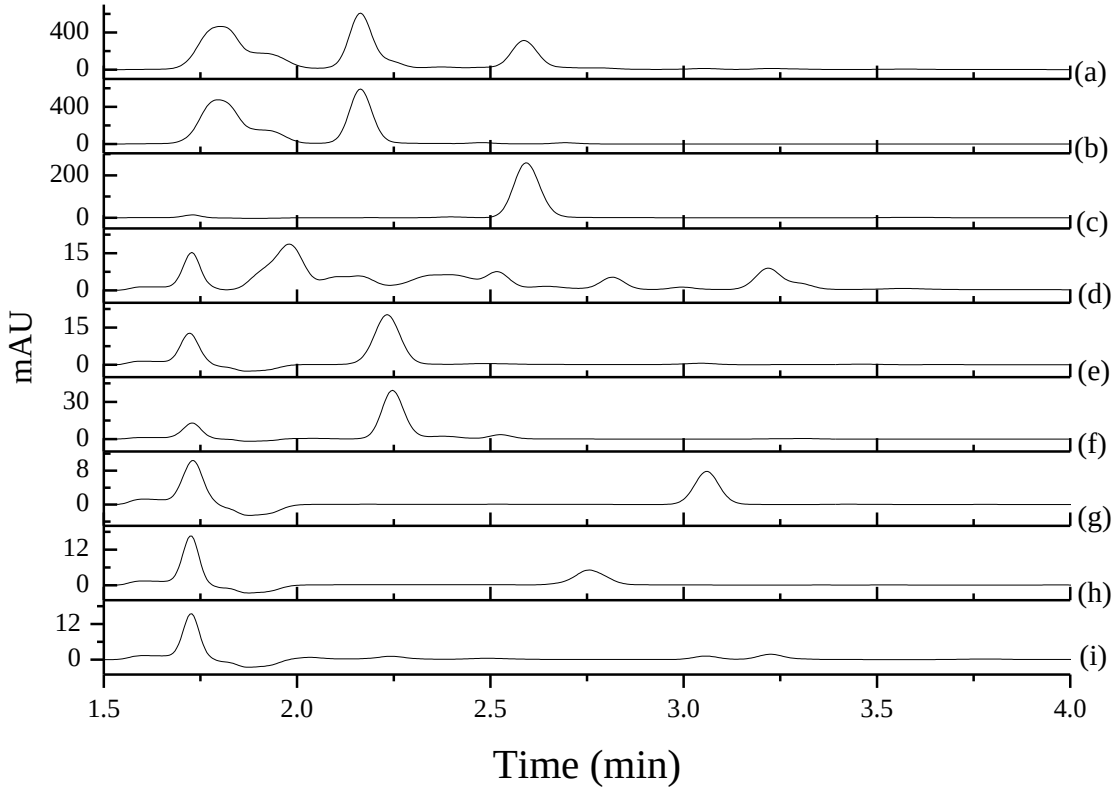

Figure 3-4 Chromatograms of 0.01% terpene mixture overlaid with single terpene standards. Samples analysed at 0.1% acetic acid 97:3 ACN:water mobile phase, 20 µL injection at 1 mL min^{-1}, UV detection at 254 nm. (a) terpene mix, (b) 4-allylanisole, (c) isolongifolene, (d) 3-carene, (e) β-pinene, (f) terpineol, (g) camphene, (h) longifolene and (i) α-pinene.

As can be seen in Figure 3-4, when the individual terpene standards were overlaid with the chromatogram of the standard mixture it became clear that the 3 peaks corresponded to 4-allylanisole and isolongifolene. As 4-allylanisole contains an aromatic ring it was expected to have stronger signal intensity due to the conjugated bonds present which increase absorption intensity [108]. The other terpenes have much lower peak areas. The initial peak at 1.7 min is the MeOH peak.

3.3.2 CE method development

Initial CE separations had shown more potential than HPLC separations. As a variety of CE modes including CD-CE and MECK were suited to the separation of neutrals, the use of CE for the analysis of terpenes in rosin samples was then investigated.

3.3.2.1 Capillary Zone Electrophoresis (CZE)

The mixture of nine neutral compounds reported to be present in rosin samples was analyed using a simple CZE method.

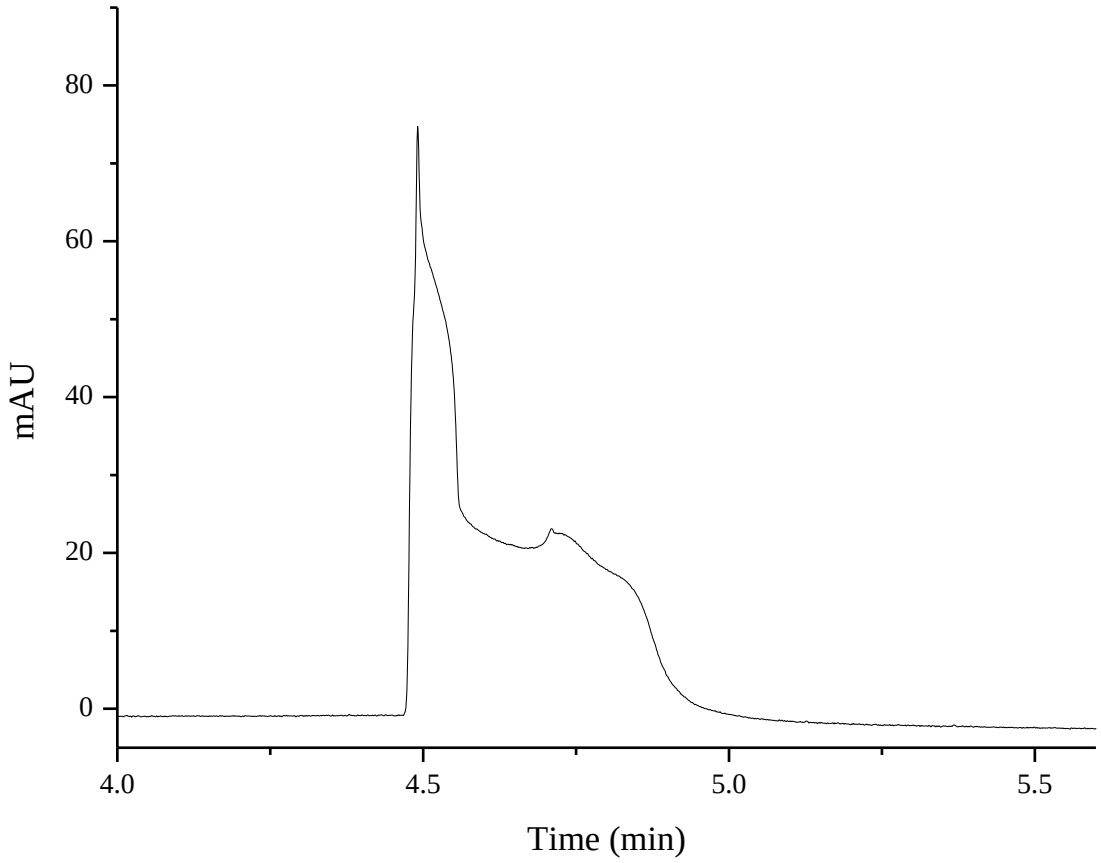

Figure 3-5 Electropherogram of a 0.01% w/v terpene mixture in MeOH analysed in positive polarity, 20 kV, capillary 58 cm (50 cm to detector), 50 µm i.d., 25°C, 50 mbar 2 s injection times, detection at 200 nm. Buffer consists of 20 mM tris pH 8.

As expected, the nine compounds coelute owing to their neutral nature, they all migrate with the EOF (see Figure 3-5). They do not possess electrophoretic mobilities and so cannot be separated by this CE mode. LogP is the logarithmic form of the octanol-water coefficient (P), which is the ratio of analytes solubility in octanol and in water. The higher the LogP value, the more hydrophobic the analyte. As seen in Table 3-1, all the analytes of interest are hydrophobic and so will partition into the hydrophobic cavities of cyclodextrins, microemulsions and micelles.

Table 3-1 Compounds as denoted in Figure 3-2.

Analyte	Formula	Molecular weight ($g\ mol^{-1}$)	LogP[a]	Compounds
α-Terpineol	$C_{10}H_{18}O$	154.25	2.79±0.36	Monoterpene alcohol
***p*-Allylanisole**	$C_{10}H_{12}O$	148.20	3.15±0.22	Phenylpropene
β-Pinene	$C_{10}H_{16}$	136.23	4.37±0.24	Monoterpene
α-Pinene	$C_{10}H_{16}$	136.23	4.37±0.24	Monoterpene
Camphene	$C_{10}H_{16}$	136.23	4.37±0.24	Monoterpene
3-Carene	$C_{10}H_{16}$	136.24	4.37±0.24	Monoterpene
Isolongifolene	$C_{15}H_{24}$	204.36	6.15	Sesquiterpene
Longifolene	$C_{15}H_{24}$	204.36	6.17	Sesquiterpene
romadendrene	$C_{15}H_{24}$	204.36	6.41	Sesquiterpene

[a]LogP values for neutral compounds determined experimentally or predicted by ACD/Labs

3.3.2.2 Cyclodextrin-modified capillary electrophoresis (CD-CE)

As the addition of CDs to a tris buffer had successfully separated nine resin acids as described in chapter two, the same CD-CE method using a 15% MeOH 5 mM HP-γ-CD 10 mM SBCD in 20 mM tris buffer pH 9 was applied to the terpene mixture (see Figure 3-6).

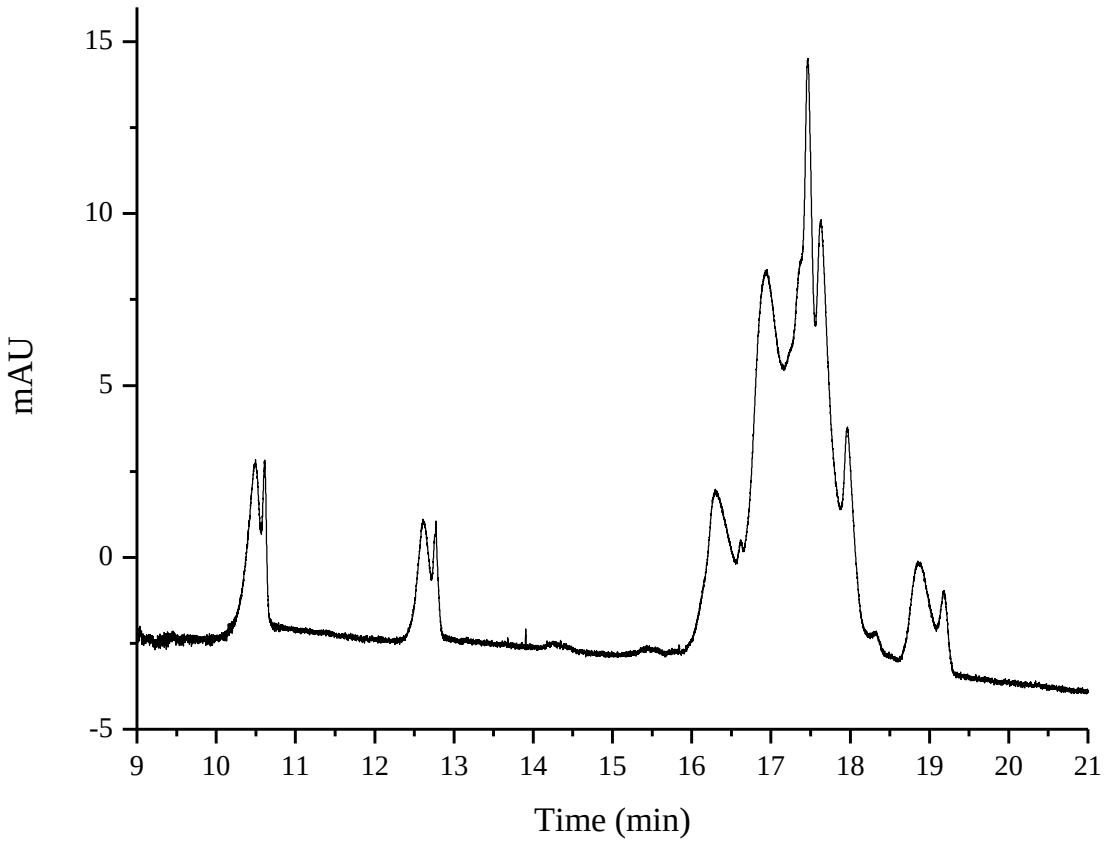

Figure 3-6 Electropherogram of a 0.01% w/v terpene mixture in MeOH analysed in positive polarity, 20 kV, capillary 58 cm (49.5 cm to detector), 50 µm i.d., 25°C, 5 mbar 20 s injection times, detection at 200 nm. Buffer consists of 15% MeOH 5 mM HP-γ-CD 10 mM SBCD in 20 mM tris pH 9.

Using this particular buffer, the majority of the terpenes coelute. Two were separated and eluted before the others at 10.5 and 12.7 min. While the acids separated under these conditions, terpenes do not have functional groups to interact with the hydroxyls on the CDs and so may interact less with the CDs than the acids [109]. It was found that many of the analytes formed double peaks on elution. This peak splitting can be explained by the use of methanol as the sample matrix, as noted by Stapf *et al.* [110]. When an analyte is prepared in an organic solvent, the equilibrium constant of the analyte-cyclodextrin complex is different for the complex in the organic sample plug and in the aqueous buffer. This leads to two mobilities and therefore two peaks for the analyte. In order to combat this peak splitting, the sample should be prepared in a matrix as similar as possible to the separation buffer. As the terpenes are not very water soluble, they were first dissolved in methanol and then diluted with the tris buffer. This resulted in samples with the same terpene concentration as in Figure 3-6 but with the sample matrix now 80:20 buffer:methanol.

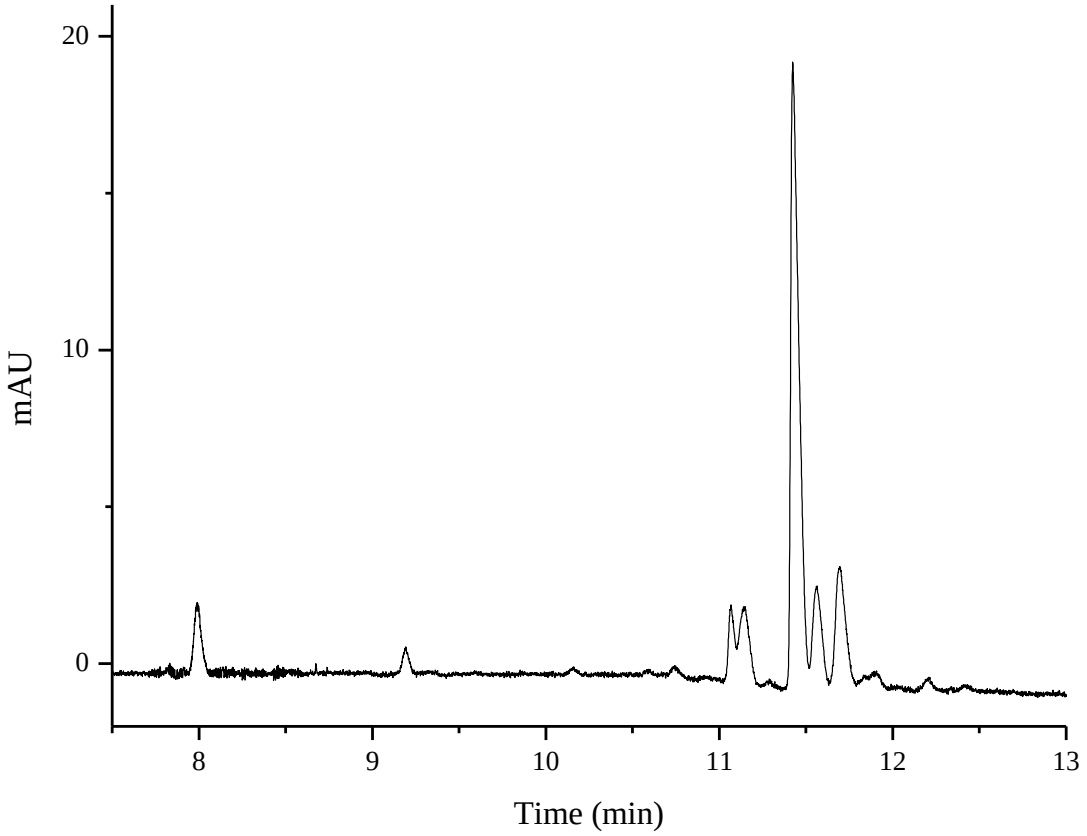

Figure 3-7 Electropherogram of a 0.01% w/v terpene mixture in 80:20 buffer:methanol analysed in positive polarity, 20 kV, capillary 58 cm (49.5 cm to detector), 50 µm i.d., 25°C, 5 mbar 20 s injection times, detection at 200 nm. Buffer consists of 15% MeOH 5 mM HP-γ-CD 10 mM SBCD in 20 mM tris pH 9.

As seen in Figure 3-7, there is no longer peak splitting in the two separated peaks while the later coeluting mass of peaks show more baseline resolution and defined peaks. The nine neutrals were not all separated using this method so other CE methods were investigated.

When this method was used for the separation of the less hydrophobic acids, peak splitting was not observed. This may be because more hydrophobic analytes have a higher tendency to show peak splitting. Ràfols *et al.* noted that while the chemical structure and functional groups also played a part, analytes hydrophobicity was the principle property contributing to peak-splitting [111].

3.3.3 Microemulsion electrokinetic chromatography

MEEKC is a mode of CE which uses microemulsions (ME), usually oil droplets, as a pseudo-stationary phase in the background electrolyte to provide a means of separation for analytes based on their hydrophobicities. Although MEKC is a more commonly used technique and generally considered before MEEKC, the use of oil droplets in MEEKC results in a larger area for analytes to interact with and is considered less rigid than a micelle with easier partitioning into the hydrophobic phase [78]. There are several parts to the microemulsion (ME) composition which can be optimised in MEEKC allowing for many opportunities to further improve separation methods or adjust them for specific analytes. In general a high pH is used in order to benefit from a strong EOF.

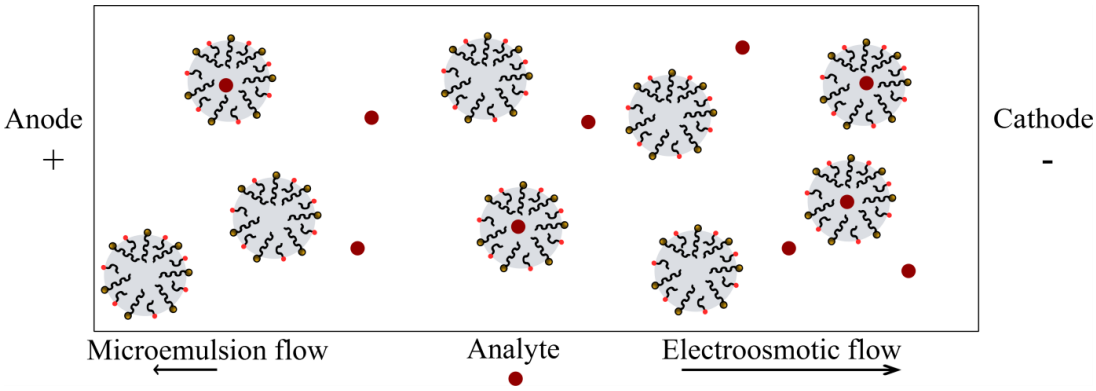

Figure 3-8 Schematic of a capillary during MEEKC of neutral analytes.

Figure 3-8 shows the neutral analytes partition in and out of the hydrophobic MEs. As the MEs are negatively charged their mobility is towards the anode, however, the EOF is stronger and so the net direction is towards the cathode. The analytes which spend more time in the MEs will elute later.

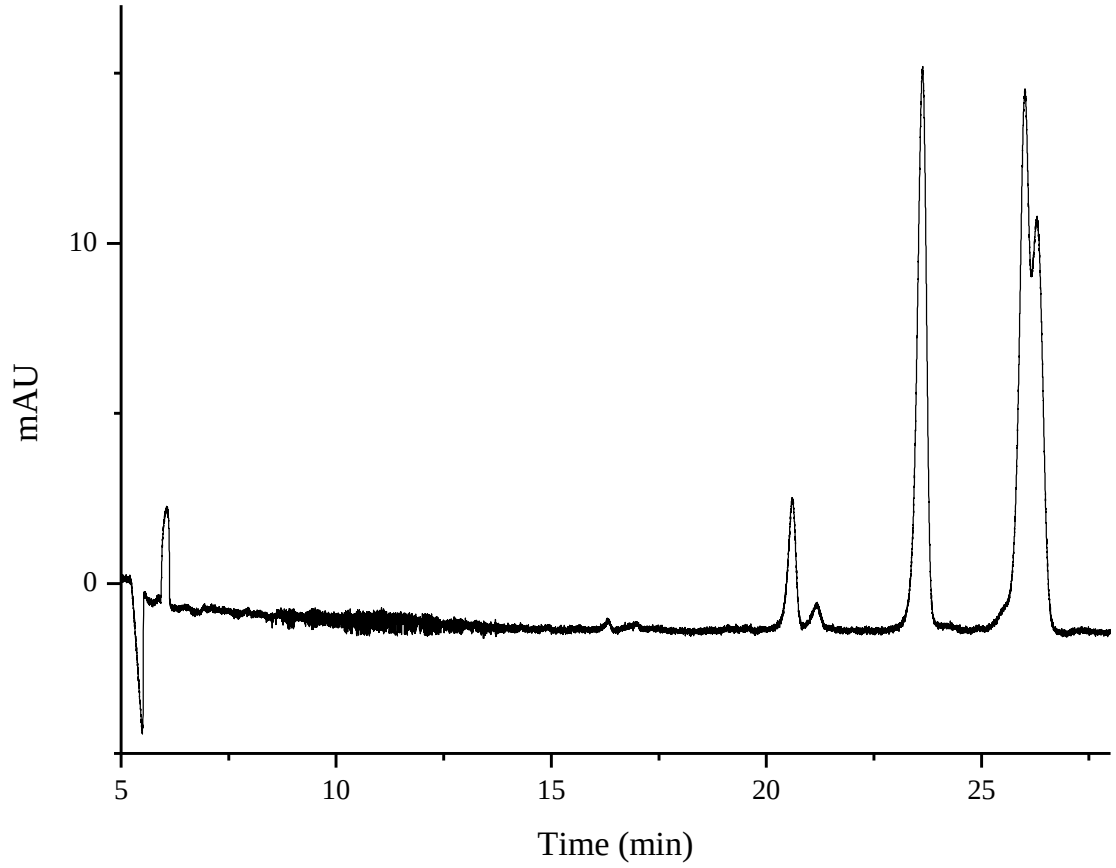

Figure 3-9 Electropherogram of a 0.01% w/v terpene mixture analysed in positive polarity, 20 kV, capillary 58 cm (49.5 cm to detector), 50 µm i.d., 25°C, 5 mbar 20 s injection times, detection at 200 nm. Buffer consists of 6% 1-butanol, 3% SDS, 0.6% heptane in 10 mM borate buffer pH 8.

For the initial separation of a mixture of nine neutral analytes, a borate buffer was prepared at pH 8 and with a typical ME composition; 6% 1-butanol, 3% SDS and 0.6% heptane [79]. As can be seen in Figure 3-9 analysis times were almost 30 min and reproducibility of this electropherogram was found to be poor. The separation of the nine analytes was also not achieved. In order to shorten analysis time a short-end injection approach to MEEKC was explored.

In short-end injection the sample vial was placed at the outlet (cathode) end and injection was performed at negative pressure. The polarity was then reversed for the separation so the sample would move towards the other end of the capillary (now the cathode) and pass the detector.

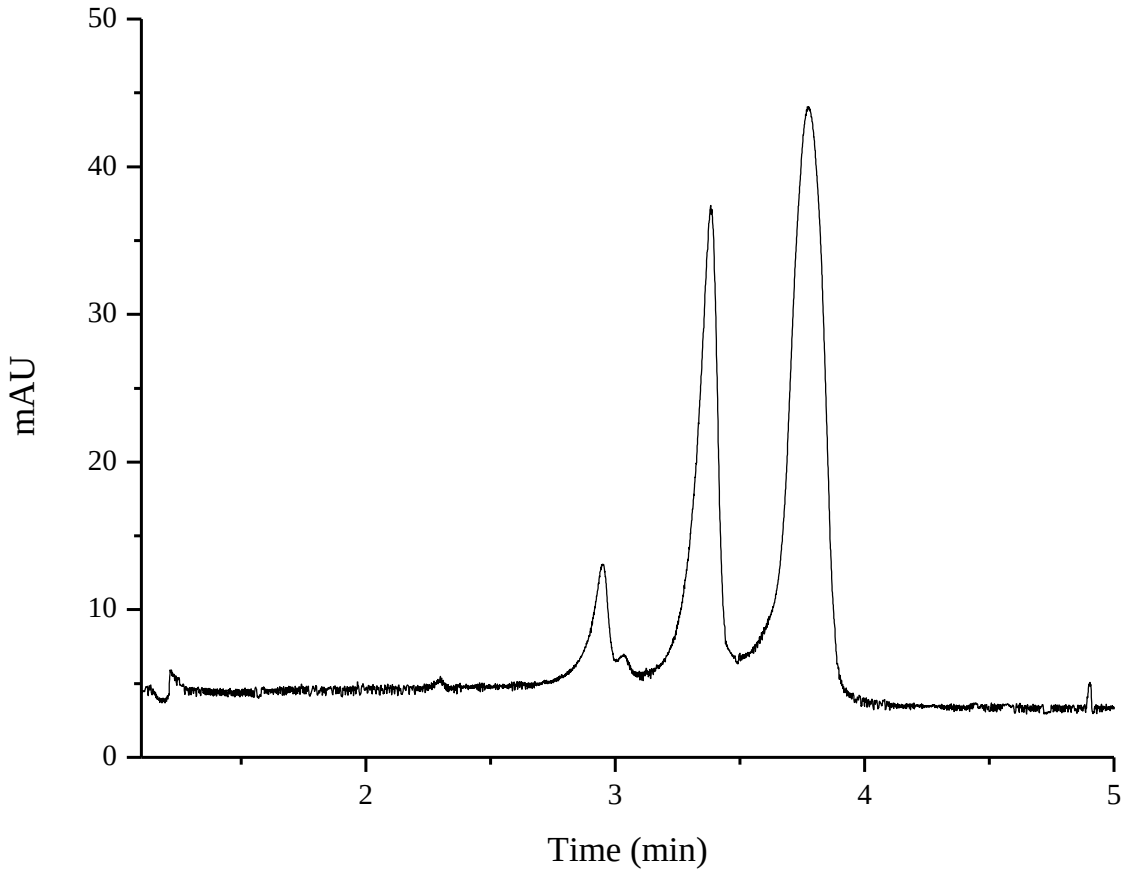

Figure 3-10 Electropherogram of a 0.01% w/v terpene mixture analysed in negative polarity, 20 kV, capillary 58 cm (49.5 cm to detector), 50 µm i.d., 25°C, -5 mbar 20 s injection times, detection at 200 nm. Buffer consists of 6% 1-butanol, 3% SDS, 0.6% heptane in 10 mM borate buffer pH 8.

As seen in Figure 3-10, the migration was reduced from 30 to 4 min, however, little separation of the analytes was observed.

3.3.3.1 Low pH MEEKC

In order to reduce the EOF a pH 2 buffer was prepared. As the MEs were prepared with negatively charged SDS, they have their own mobility towards the anode. The polarity was reversed so the anode was then located at the detector end of the capillary.

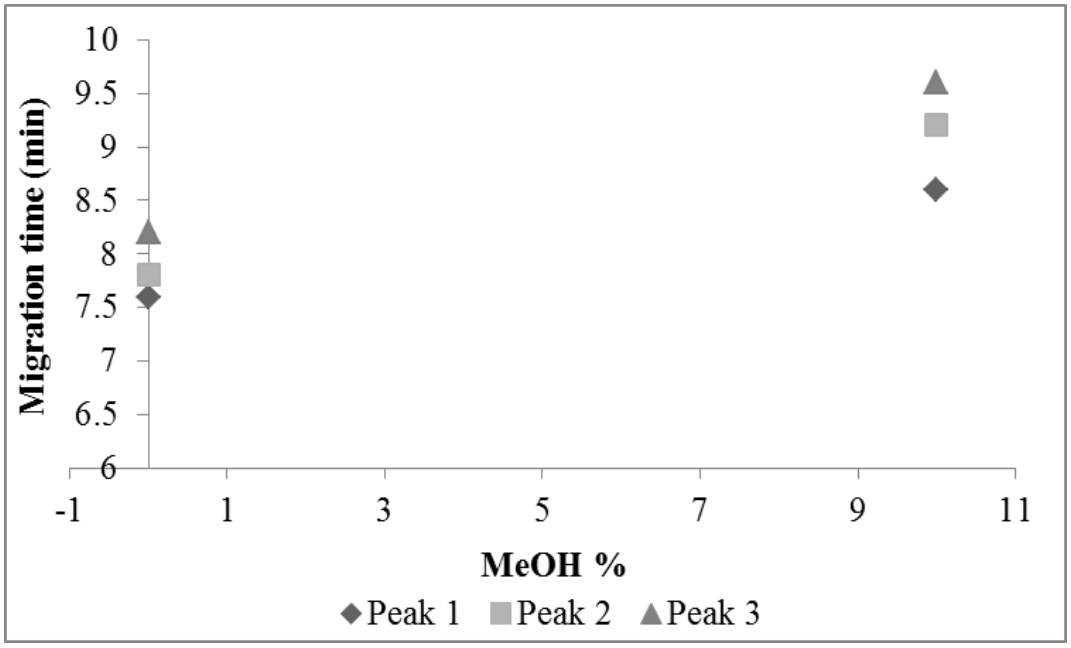

Figure 3-11 Electropherogram of a 0.01% w/v terpene mixture analysed in negative polarity, 20 kV, capillary 58 cm (49.5 cm to detector), 50 µm i.d., 25°C, 5 mbar 20 s injection times, detection at 200 nm. Buffer consists of (a) 6% 1-butanol, 3% SDS, 0.6% heptane in 10 mM phosphate buffer pH 2 and (b) 10% MeOH 6% 1-butanol, 3% SDS, 0.6% heptane in 10 mM phosphate buffer pH 2.

Figure 3-11 shows the electropherogram of the terpene mixture using a pH 2 phosphate buffer with and without MeOH. The analysis time was shorter than with a pH 8 borate buffer and more reproducible. The addition of MeOH showed no improvement in separation and the analysis time was increased. The various parameters for optimisation of the MEs were then investigated within normal range of use.

3.3.3.2 Surfactant concentration

The incorporation of the surfactant is reported to affect the stability, size and charge of the ME. SDS is an anionic surfactant and the most commonly used in MEEKC. Its charge gives mobility to the MEs so the separation of neutral compounds is possible.

The concentration of SDS was varied from 2 to 6% while keeping the oil, co-surfactant and buffer concentrations constant (Figure 3-12). Concentrations of lower than 2% have been reported to lead to poor reproducibility and the possible collapse of the droplets. Higher surfactant concentration was found to increase the charge density on the ME and so increases the capacity factor for neutral analytes [79].

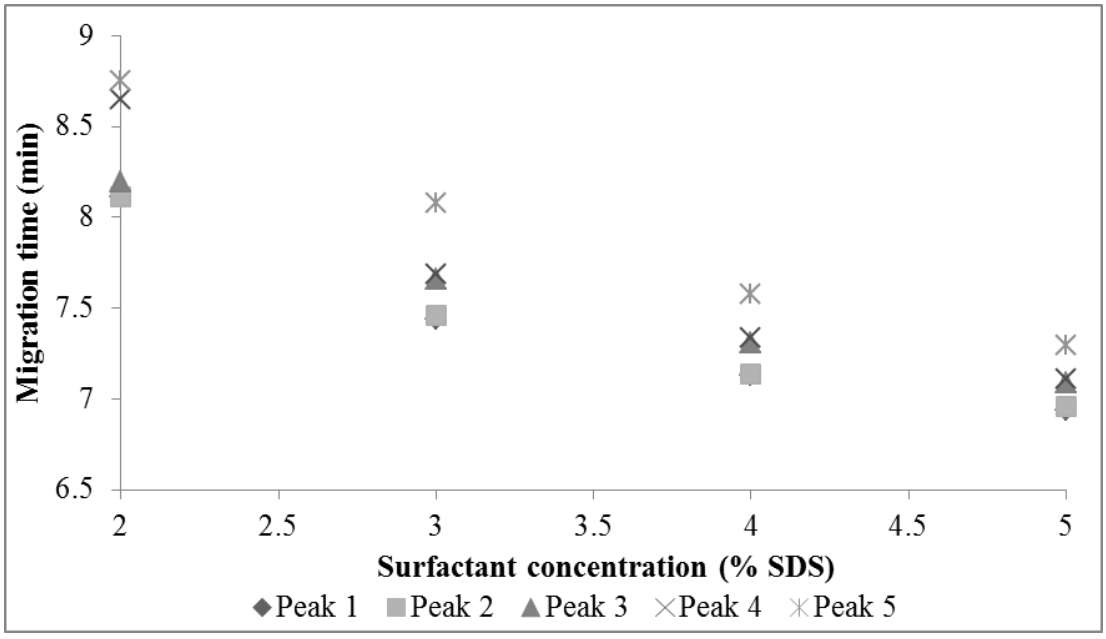

Figure 3-12 Plot of migration times versus the percentage of SDS in the buffer. The terpene mixture was analysed in negative polarity, 20 kV, capillary 58 cm (49.5 cm to detector), 50 µm i.d., 25°C, 5 mbar 20 s injection times,. Buffer consists of 6% 1-butanol, 0.6% heptane and 2-6% SDS in 10 mM phosphate buffer pH 2.

When the concentration is increased to 4 and 5% the first peak begins to separate into two coeluting peaks. However, when it is further increased to 6%, the separation deteriorates. This may be due to the high current resulting from the higher SDS concentration (the current increased from 50 µA with 2% SDS to 100 µA with 6% SDS). Generally, increasing SDS concentration increases analysis time, however, since negative polarity is being used, higher concentrations of SDS result in quicker mobilities towards the detector.

Table 3-2 Resolution values for the electropherograms in Figure 3-12.

2% SDS	3% SDS	4% SDS	5% SDS
		0.3	0.4
1.8	0.3	3.1	3.1
0.5	3.3	0.6	0.5
2.9	0.3	4.1	3.8
0.7	2.3	0.9	0.4

As seen in Table 3-2, slightly greater resolution values are seen with 4% SDS compared with 5% SDS so this concentration was used in further analysis.

3.3.3.3 Oil type and concentration

Long chain alkanes including 1-hexane and 1-heptane are the most often used oil types. Water-insoluble cyclohexane and water-soluble ethyl acetate were also investigated.

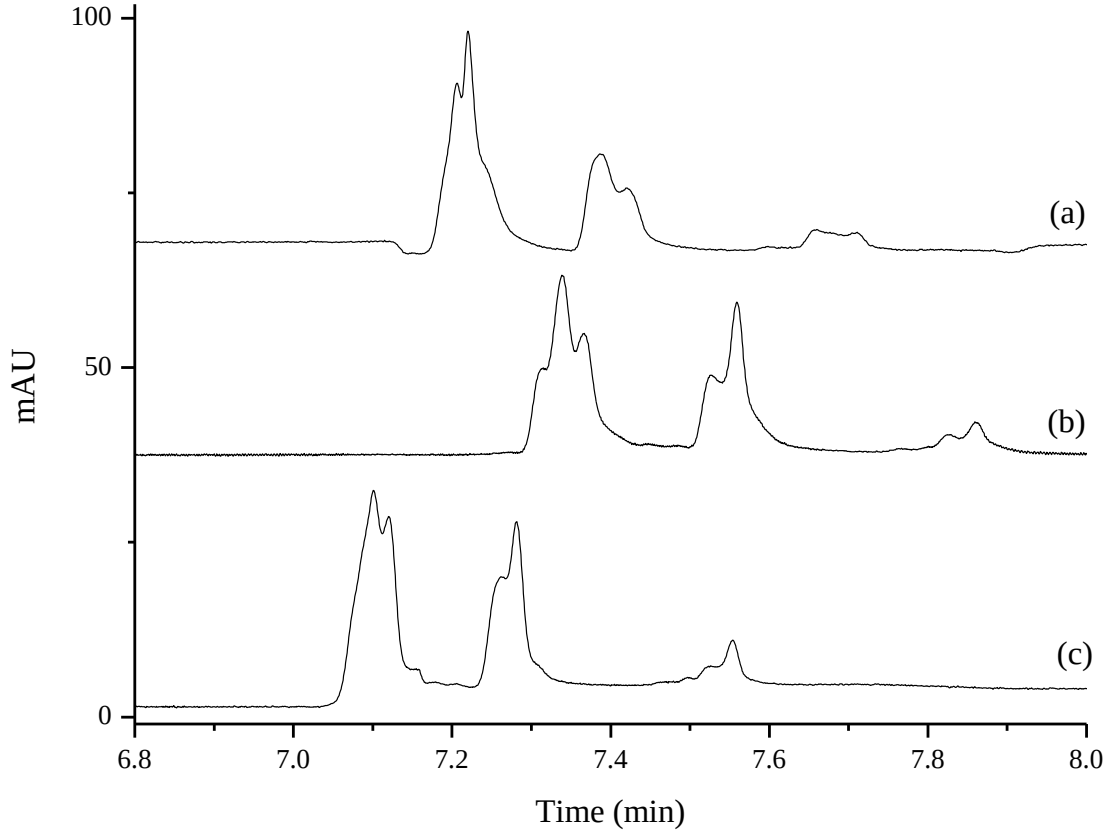

Figure 3-13 Electropherogram of a 0.01% w/v terpene mixture analysed in negative polarity, 20 kV, capillary 58 cm (49.5 cm to detector), 50 µm i.d., 25°C, 5 mbar 20 s injection times, detection at 200 nm. Buffer consists of 6% 1-butanol, 4% SDS and 0.6% (a) heptane, (b) ethyl acetate and (c) cyclohexane.

Three different oils were shown in Figure 3-13. As expected, there was little difference in analyte selective effect [112]. As ethyl acetate showed a further coeluting shoulder on the first peak it was chosen for future analysis. Ethyl acetate has lower interfacial tension than the long chained alkanes and so can form a stable ME with a lower surfactant concentration if necessary [78].

There are conflicting reports on whether or not the oil concentration has a significant effect on separation efficiency [78]. While in general the oil concentration has not

shown an effect on separation [78, 79, 113, 114], Cao *et al*. varied the concentration of cyclohexane from 0.3-1.2% and observed a decrease in separation resolution when the concentration was increased [106]. Oledzka *et al.* also reported deterioration in separation when n-octane was increased [115].

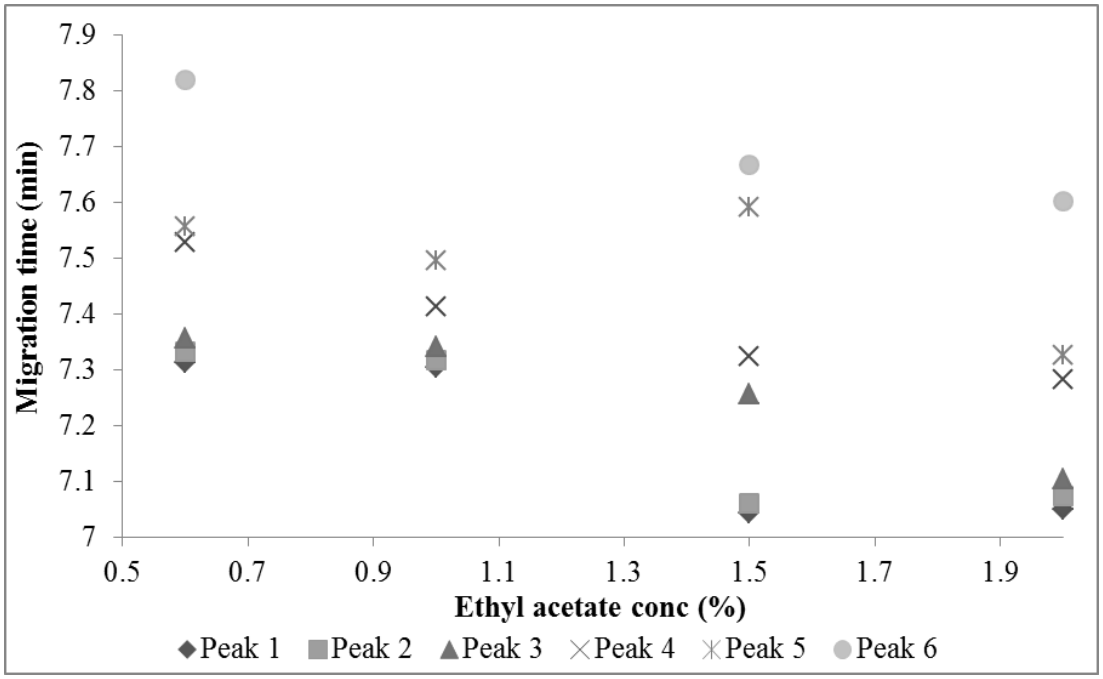

Figure 3-14 Plot of migration times versus the percentage of ethyl acetate in the buffer. The terpene mixture was analysed in negative polarity, 20 kV, capillary 58 cm (49.5 cm to detector), 50 µm i.d., 25°C, 5 mbar 20 s injection times. Buffer consists of 6% 1-butanol, 4% SDS and 0.6-2% ethyl acetate in 10 mM phosphate buffer pH 2.

The concentration of ethyl acetate was investigated from 1 to 2% (see Figure 3-14). As observed in most literature reports, in this study the concentration of oil had very little effect on separation. The oil concentration has little effect on the size of the ME, thought to be due to its flexible structure [112]. A pseudo-stationary phase with a more rigid structure such as a cyclodextrin could provide more selectivity through steric interactions, while the flexible ME does not.

3.3.3.4 1-butanol concentration

The co-surfactant coats and partitions into the oil droplet, reduces interfacial tension and increases the size of the ME, allowing more access to the hydrophobic core [112]. The use of 1-butanol as a co-surfactant is reported to result in a more stable

ME than those prepared with other co-surfactants including propanol and methanol [116]. 1-butanol, 2-hexanol and cyclohexanol tend to give good reproducibility. Pomponio *et al.* reported different analyte migration orders depending on the co-surfactant used due to different selectivities. They also noted that cyclohexanol and 2-hexanol resulted in good peak symmetry, with cyclohexanol giving the best resolution values [117].

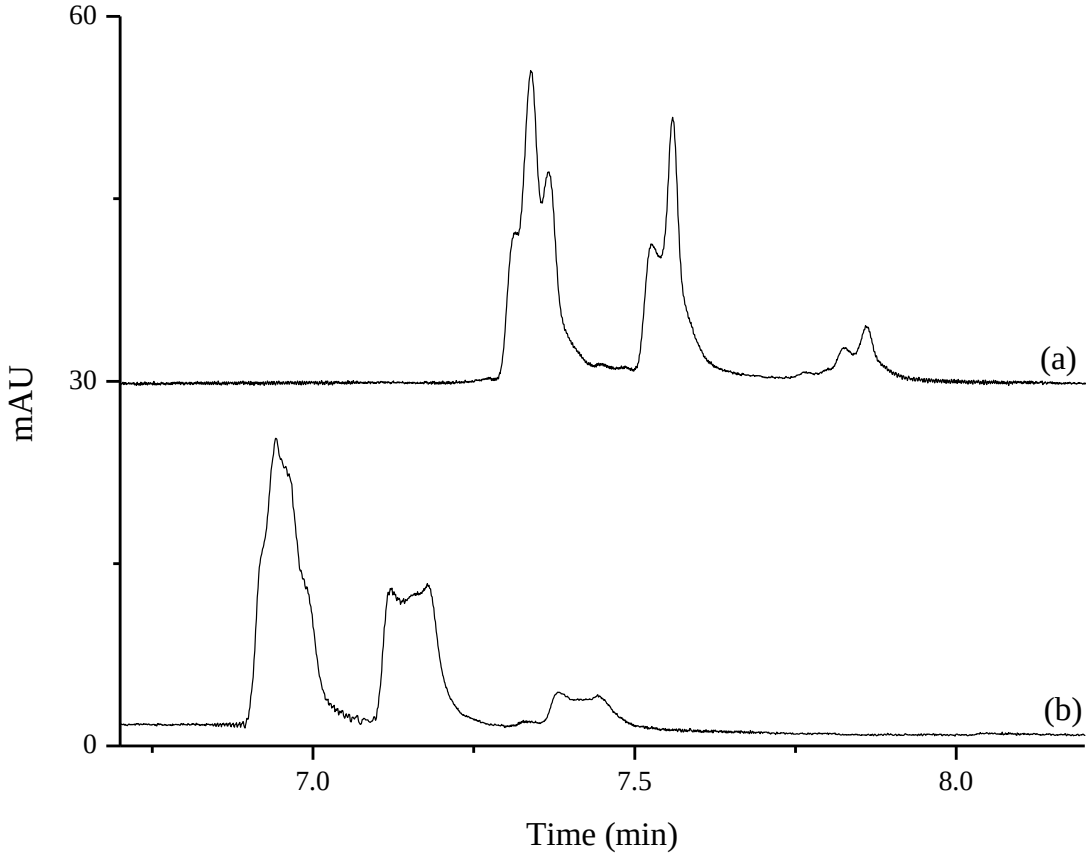

Figure 3-15 Electropherogram of a 0.01% w/v terpene mixture analysed in negative polarity, 20 kV, capillary 58 cm (49.5 cm to detector), 50 µm i.d., 25°C, 5 mbar 20 s injection times, detection at 200 nm. Buffer consists of 4% SDS, 0.6% ethyl acetate and (a) 6% and (b) 5% 1-butanol.

The concentration of 1-butanol was investigated at 5 and 6% but reducing the concentration was found to result in more coelution of the peak shoulders (see Figure 3-15). This may be due to the smaller size and higher surface tension of the ME when there is less co-surfactant present. The change in migration time due to 1-butanol is expected as it affects buffer viscosity and so affects the EOF [79].

3.3.3.5 Organic additive

As little separation was thus far achieved using MEEKC, isopropanol (IPA) was added to the MEEKC system to investigate if it improved selectivity by aiding solubility of the terpenes and potentially affecting their partition coefficient with the ME [112]. The addition of organic additives can also affect the physicochemical properties of the ME. Where some analytes are very water insoluble they will remain primarily in the micelle and be poorly resolved. The addition of organic solvent can improve resolution by reducing retention in the micelle. Less than 30% organic solvent is recommended in order to avoid disruption of the micelle. While the addition of MeOH to an MEEKC buffer had already been investigated, IPA was considered as it was suggested that it aided analytes in moving from the oil to buffer [78].

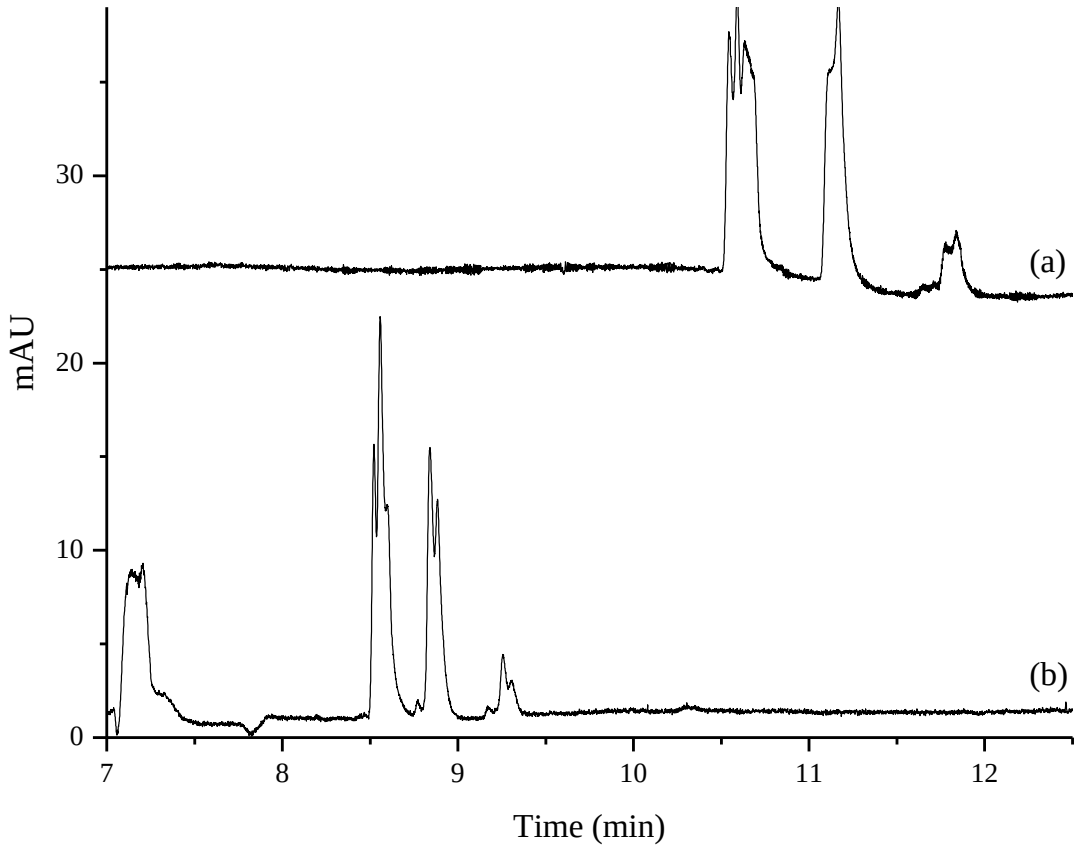

Figure 3-16 Electropherogram of a 0.01% w/v terpene mixture analysed in negative polarity, 20 kV, capillary 58 cm (49.5 cm to detector), 50 µm i.d., 25°C, 5 mbar 20 s injection times, detection at 200 nm. Buffer consists of 6% 1-butanol, 4% SDS, 1% ethyl acetate in 10 mM phosphate buffer pH 2, (a) 10% IPA and (b) 5% IPA.

When the concentration of IPA was increased there was high baseline noise and peaks were no longer separated (Figure 3-16), suggesting that the MEs had been disrupted which can happen with excessive amounts of organic additives as it makes the MEs unstable. Cao *et al*. found 10% ACN to be the highest amount that could be used while still avoiding demulsification [112].

From results obtained using MEEKC little separation of the nine neutral analytes was achieved. Therefore, MEKC was then investigated as an alternative separation technique.

3.3.4 Micellar electrokinetic chromatography

As previous attempts to separate the terpenes using a cyclodextrin based buffer and MEEKC were unsuccessful, an alternative CE mode was then investigated. In hindsight, MEKC should have been investigated before MEEKC (section 3.3.3). MEKC is an established technique for the separation of neutral and charged compounds. The use of a charged surfactant provides mobility to analytes which have no charge and therefore no electrophoretic mobility of their own. SDS is the most commonly used, cheaply available and one of the most effective surfactants reported in literature [75].

A 20 mM tris buffer pH 8 was prepared and the concentration of SDS varied from 10-50 mM. A 0.01% w/v terpene mixture was analysed with each buffer (see Figure 3-17). SDS is an anionic surfactant. As expected, the lower SDS concentration resulted in shorter migration times as there was less SDS interacting with the terpenes and moving against the EOF. Increasing SDS concentration also increased the ionic strength of buffer, reducing the EOF which resulted in longer migration times [106].

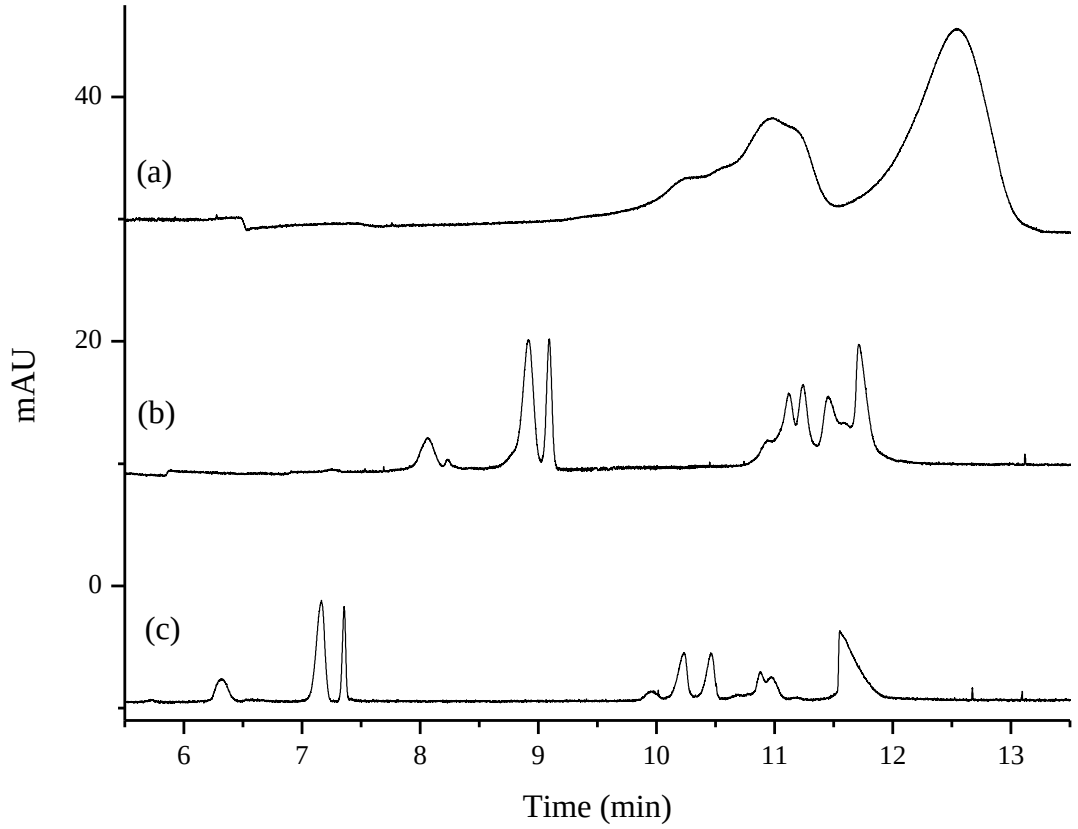

Figure 3-17 Electropherograms of a 0.01% w/v terpene mixture analysed in positive polarity, 20 kV, capillary 58 cm (49.5 cm to detector), 50 µm i.d., 25°C, 5 mbar 20 s injection times, detection at 200 nm. Buffer consists of 20 mM tris pH 8 containing (a) 50 mM SDS, (b) 20 mM SDS and (c) 10 mM SDS.

It was found that 50 mM SDS resulted in little separation. The 10 mM SDS buffer results in improved resolution values and the baseline resolution of more peaks than the 20 mM SDS 20 mM tris buffer and so was used for further buffer optimisation. Average resolution values for 10 mM SDS were 3.4, while 20 mM SDS resulted in only two peaks with resolution values above 1.5. SDS concentrations lower than 10 mM resulted in decreased resolution and efficiency values. It was initially suspected that this was because the critical micelle concentration (CMC) had not been reached and micelles were not stably formed which resulted in less separation. The CMC of SDS in water has been reported as 8.1-8.4 mM; however, the CMC is affected by buffer composition [118]. CMC values in buffers are lower than in pure water e.g. CMC decreased from 8.08 mM in water to 1.99 mM in 50 mM phosphate buffer [119]. The CMC is decreased because the buffer ions neutralise the micelle charge which reduces electrostatic repulsions between the surfactant monomers by reducing the thickness of the ionic atmosphere around the monomers ionic heads, aiding micellisation [120]. It would be expected therefore that the CMC of SDS in a 20 mM

tris buffer is lower than its value in water, so lower than 8.1 mM. This suggests that the CMC had been reached as 10 mM was the lowest SDS concentration investigated.

The concentration of the tris buffer was varied to observe if the increased buffer capacity would improve separation. The SDS concentration was kept at 10 mM (Figure 3-18). When the concentration of tris was increased from 20 to 50 mM, the migration time increased as expected. However, the baseline resolution of several peaks was increased to above 1.5 (see Table 3-3). When the concentration was further increased to 75 mM the migration time increased again, however there was not as significant an improvement in the resolution of the peaks. Also, the small peaks at 16 and 16.6 min seen in the 50 mM tris electropherogram are now coeluting in the 75 mM tris electropherogram. A 50 mM tris buffer was used for further studies.

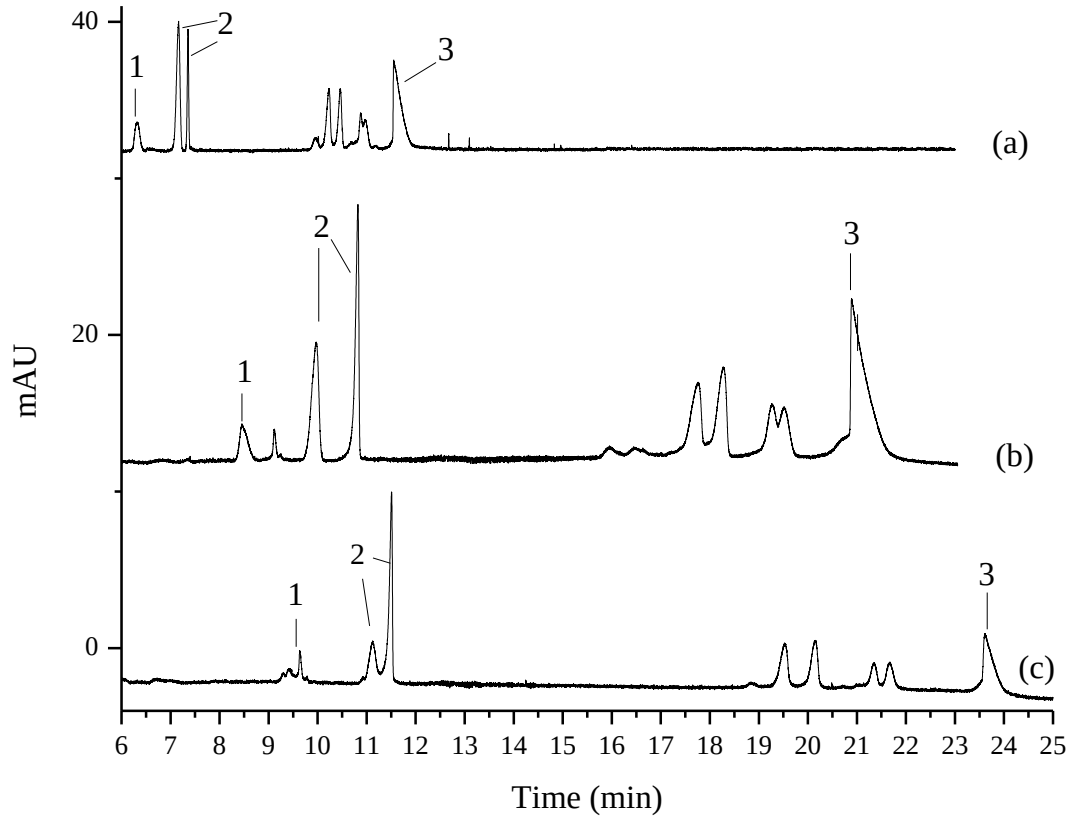

Figure 3-18 Electropherograms of a 0.01% w/v terpene mixture analysed in positive polarity, 20 kV, capillary 58 cm (49.5 cm to detector), 50 µm i.d., 25°C, 5 mbar 20 s injection times, detection at 200 nm. Buffer consists of 10 mM SDS in (a) 20 mM tris pH 8, (b) 50 mM tris pH 8 and (c) 75 mM tris pH 8. Numbers indicate (1) terpineol, (2) 4-allylanisole and (3) aromadendrene.

Table 3-3 Resolution values for the peaks in electropherograms seen in Figure 3-18. Buffers all contain 10 mM SDS, 20 and 30 kV analysis using 10 mM SDS 50 mM tris

20 mM tris	50 mM tris	75 mM tris	20 kV	30 kV
1.2	2.5	0.9	2.3	1.7
3.6	5.1	6.8	2.0	3.0
1.8	2.7	1.7	2.9	2.4
19.6	6.7	26.8	16.2	18.2
1.3	13.4	1.8	1.2	1.2
1.4	1.3	1.9	1.9	1.7
2.3	2.0	3.8	1.3	0.8
0.5	1.2	1.1	3.0	1.5
1.2	2.5	5.0	0.8	
1.5	0.5		4.1	1.7
	2.8			

A higher voltage was investigated with the 10 mM SDS 50 mM tris buffer pH 8 to investigate if shorter migration times could be achieved without a loss in resolution. While the migration times were reduced with a higher voltage, several resolution values were also reduced as a result (see Table 3-3) so 20 kV was used for further analysis.

3.3.4.3 Buffer type

Other buffers were investigated for the separation of the terpene mixture, however, none resulted in higher resolution than the tris buffer. An acetate buffer at pH 4 resulted in too low an EOF. Little separation was achieved and run times were up to 35 min. A phosphate buffer at pH 7.5 and a borate buffer at pH 9 were also investigated; however, the tris buffers resulted in a significantly higher number of resolved peaks than either of these.

3.3.4.4 CD-MEKC

There have been several reports of the use of cyclodextrins both on their own and in combination with SDS in a CE buffer (see Figure 3-19) for the separation of monoterpenes, namely α-pinene, β-pinene, terpineol and camphene [105, 121, 122]. Several derivatized CDs were added to the SDS tris buffer to investigate if they would result in more separation than with SDS alone.

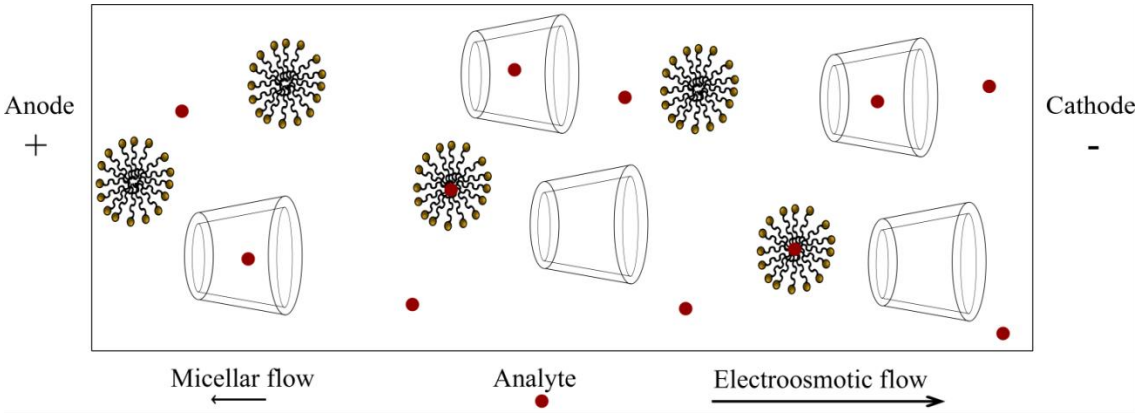

Figure 3-19 Schematic of a capillary containing micelles and cyclodextrins.

Little separation was achieved with the use of any of the derivatized CDs so the addition of native α, β and γ cyclodextrins to the SDS tris buffer was then examined for their use in separating the terpene mixture.

All three native CDs were investigated as there have been mixed reports on the appropriate CD cavity size for some of the compounds in question. Rodrigues *et al.* used γ-CD in combination with SDS and ACN for the separation of camphene, α-pinene and β-pinene [122]. However, α- and β-CD are more commonly reported for the separation of monoterpenes [102, 104, 121, 123, 124]. As seen in Figure 3-20, the addition of γ-CD results in very poor peak shapes. The cavity size may be too big to form stable inclusion complexes with the neutral analytes. While α-CD results in some peak separation, the β-CD buffer results in more baseline separation. α-CD has the smallest cavity size and so may be too small for a sterical fit with the analytes. Table 3-4 shows the resolution and efficiency values for the three cyclodextrins; β-CD also results in the best efficiency values.

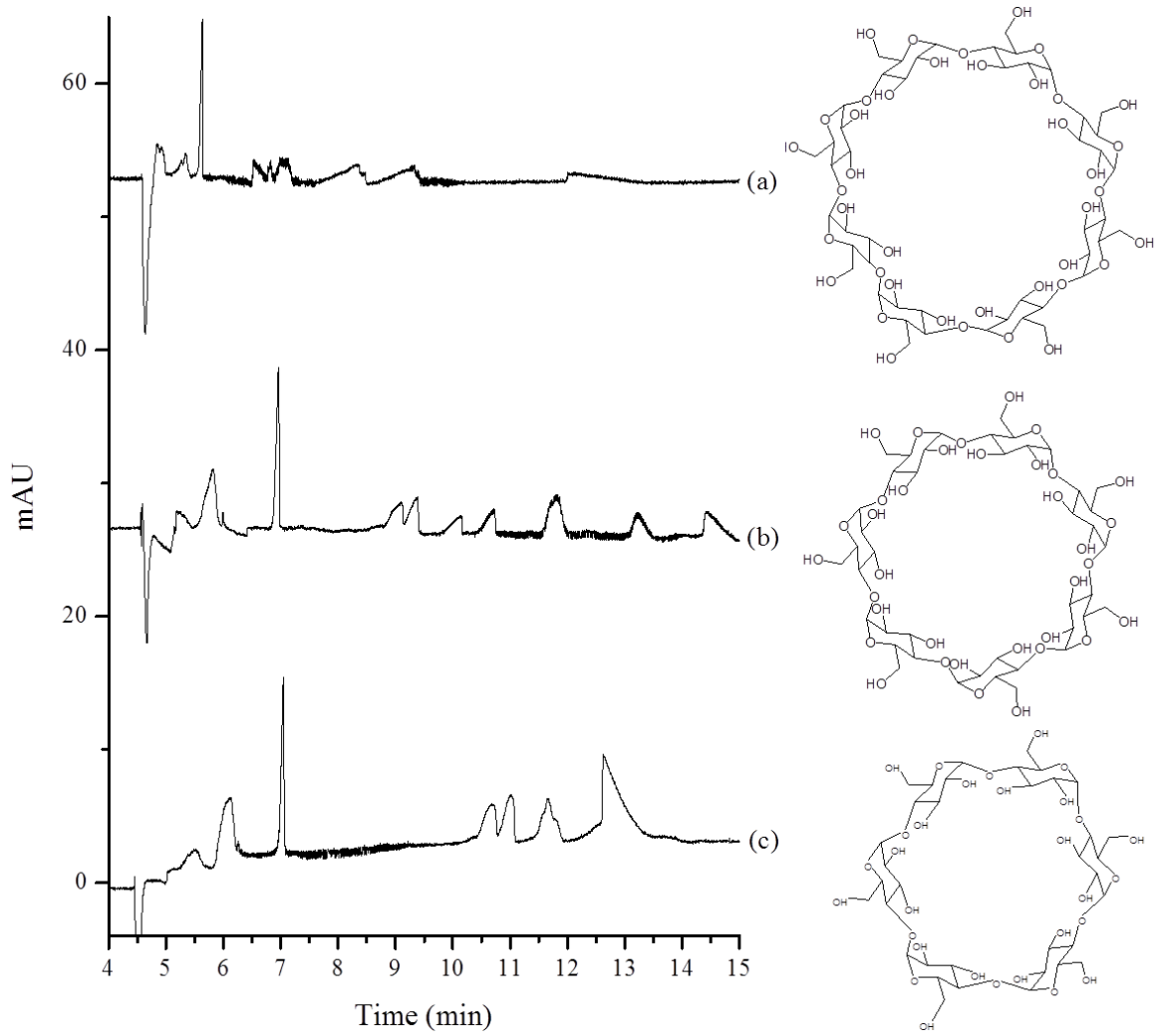

Figure 3-20 Electropherograms of a 0.01% w/v terpene mixture analysed in positive polarity, 20 kV, capillary 58 cm (49.5 cm to detector), 50 µm i.d., 25°C, 5 mbar 20 s injection times, detection at 200 nm. Buffer consists of 10 mM SDS 50 mM tris buffer pH 8 containing (a) 5 mM γ-cyclodextrin, (b) 5 mM β-cyclodextrin and (c) 5 mM α-cyclodextrin.

Table 3-4 Resolution and efficiency values for the peaks shown in the electropherograms in Figure 3-20.

	α-CD		**β-CD**		**γ-CD**
R_s	**N**	R_s	**N**	R_s	**N**
	2936		10728		3219
1.6	4404	1.7	3110	2.0	16888
3.7	78974	1.2	156155	3.0	41308
14.6	11343	11.3	71652	6.6	40813
0.9	19471	7.7	7365	1.0	4476
2.0	18081	0.8	18256	1.1	1405
0.4	82669	2.4	12933	1.4	1163
2.2	6573	1.7	19885	0.9	1828
		2.9	9926	3.3	3251
		2.7	13417		
		2.4	12335		

The concentration of the β-CD in the buffer was varied over 1-5 mM and the terpene mixture analysed (Figure 3-21). It was found that as the concentration of β-CD is increased, the peak which migrated at 13 min began to separate into three separate peaks. However, the two peaks seen at 10 and 10.4 min in 1 mM β-CD were no longer seen as the concentration increased.

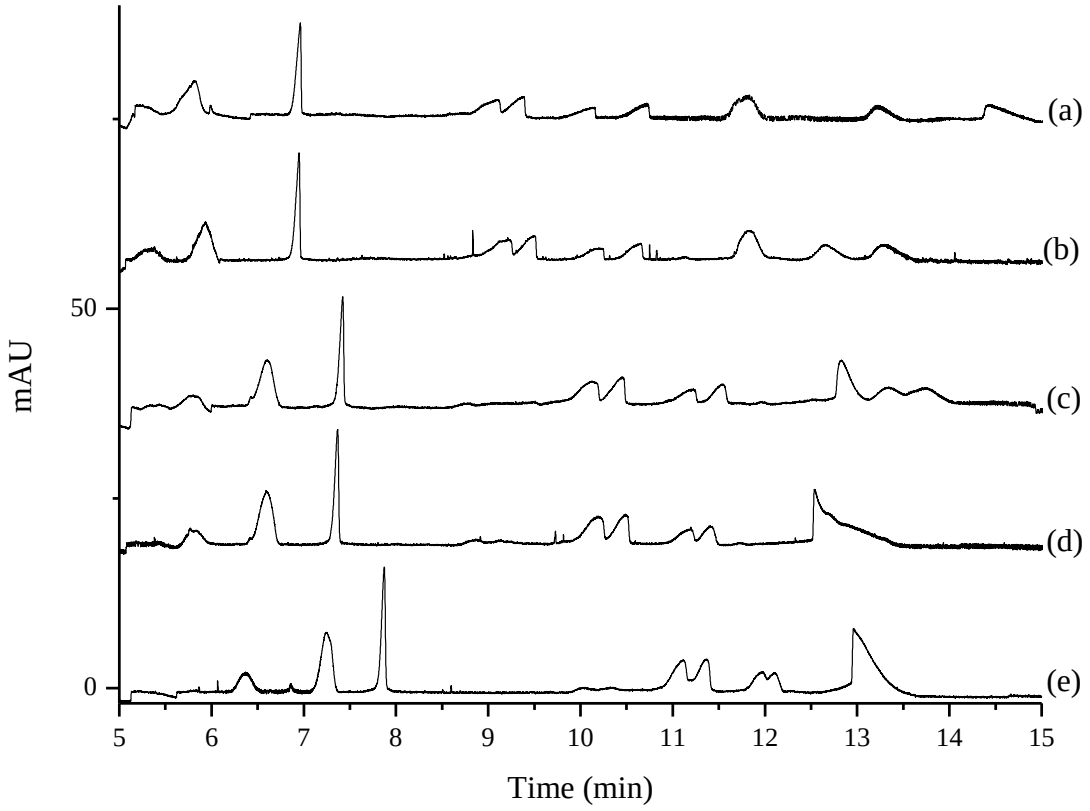

Figure 3-21 Electropherogram of a 0.01% w/v terpene mixture analysed in positive polarity, 20 kV, capillary 58 cm (49.5 cm to detector), 50 µm i.d., 25°C, 5 mbar 20 s injection times, detection at 200 nm. Buffer consists of (a) 5 mM, (b) 4 mM, (c) 3 mM, (d) 2 mM and (e) 1 mM β-CD in 10 mM SDS 50 mM tris.

Although the 5 mM β-CD buffer had a 2 min longer run time than 4 mM, it had one more peak with resolution above 1.5 (see Table 3-5). For all buffers, the efficiencies were quite poor for CE separations with the exception of the peak at 7.9 min. When the CD concentration was further increased a deterioration of the separation was observed. The separation of the mixture using a 5 mM β-CD 10 mM SDS 50 mM tris buffer at pH 8 is shown in Figure 3-22.

Table 3-5 Resolution and efficiency values for the electropherograms seen in Figure 3-21 where the β-CD concentration is varied.

Efficiency values				
1 mM β-CD	**2 mM β-CD**	**3 mM β-CD**	**4 mM β-CD**	**5 mM β-CD**
9178	4626	3943	3909	4567
157654	108926	7392	4990	4401
14018	9171			75029
109615	98293	94863	93155	223043
17690	14804			
20877	14604			
16799	10480	7374	9195	6863
35587	25934	22121	27174	17380
34602	17897	13819	18090	12089
57261	33909	25787	24368	17264
11872	13399	29113	19079	11427
		12817	13159	15725
		10379	19744	13106
Resolution values				
1 mM β-CD	**2 mM β-CD**	**3 mM β-CD**	**4 mM β-CD**	**5 mM β-CD**
2.8	2.9	2.5	1.9	1.6
2.7	1.2	4.2	4.3	0.8
3.4	4.0			13.1
11.1	8.1	9.5	9.1	7.9
0.9	0.8			
2.3	2.8			
0.9	0.9	0.9	1.3	0.8
2.4	2.3	2.3	2.8	2.3
0.7	0.8	1.0	1.5	1.7
2.6	3.5	4.4	3.9	2.8
		1.4	2.2	3.3
		0.8	1.4	2.6

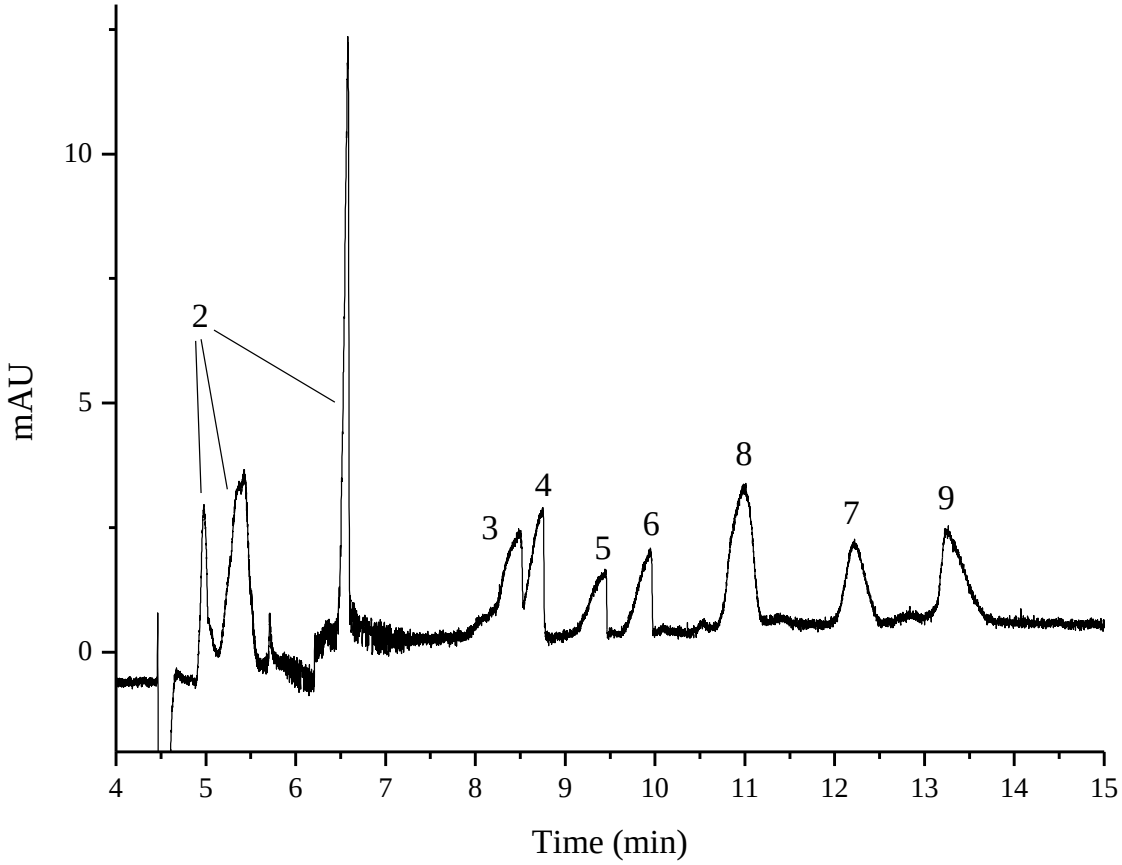

Figure 3-22 Electropherogram of a 0.01% w/v terpene mixture analysed in positive polarity, 20 kV, capillary 58 cm (49.5 cm to detector), 50 µm i.d., 25°C, 5 mbar 20 s injection times, detection at 200 nm. Buffer consists of 5 mM β-CD 10 mM SDS 50 mM tris buffer pH 8. Numbers indicate (2) 4 allylanisole, (3) camphene, (4) β-pinene, (5) 3 carene, (6) α-pinene, (7) isolongifolene, (8) longifolene and (9) aromadendrene.

The peaks were identified by spiking the mixture with 0.1% w/v standards (see Figure 3-22). Terpineol was not separated and 4-allylanisole produced several peaks.

3.3.4.5 Peak splitting in MEKC

In section 3.3.2.2, peak splitting was observed in CD-CE due to the sample being prepared in MeOH. At this stage individual terpene standards were prepared in methanol and analysed using the 10 mM SDS 50 mM tris pH 8 to investigate if the same was occurring with the MEKC buffer. It became apparent that several analytes were resulting in multiple peaks (see Figure 3-23).

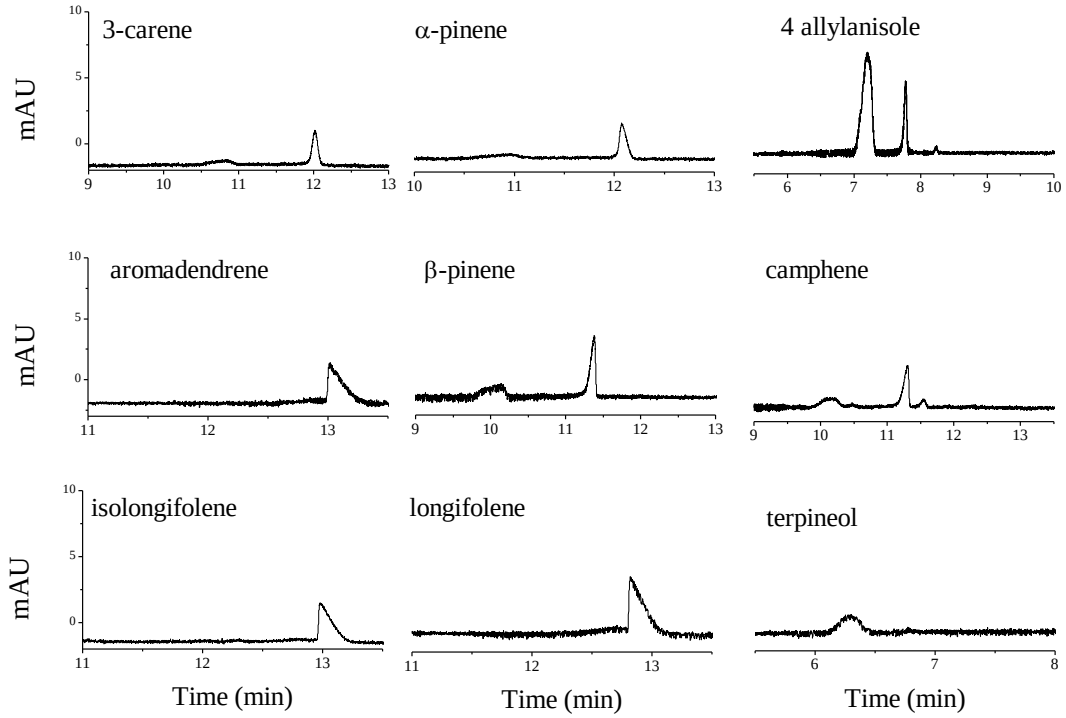

Figure 3-23 Electropherograms of 0.01% w/v terpene standards in methanol analysed in positive polarity, 20 kV, capillary 58 cm (49.5 cm to detector), 50 µm i.d., 25°C, 5 mbar 20 s injection times, detection at 200 nm. Buffer consists of 10 mM SDS 50 mM tris pH 8.

With regards to MEKC, the phenomenon of peak splitting has been primarily reported when the sample is prepared in an organic matrix [110, 111, 125]. When the sample is injected, micelles at either end of the sample plug begin interacting with the analytes and so two areas form containing high concentrations of analytes (see Figure 3-24 b). As the organic plug migrates more quickly than the analytes and micelles, it overtakes the complexes at the front of the plug which are disrupted (Figure 3-24 c). The analytes form new dynamic complexes at the front of the plug and migrate ahead of those at the end (Figure 3-24 d). Gradually, due to longitudinal diffusion, the organic solvent will no longer be concentrated enough in one area to disrupt the micelles and two separate peaks can be observed (Figure 3-24 e). Ràfols *et al.* found that naphthalene showed a split peak when the sample was prepared in more than 20% MeOH [111].

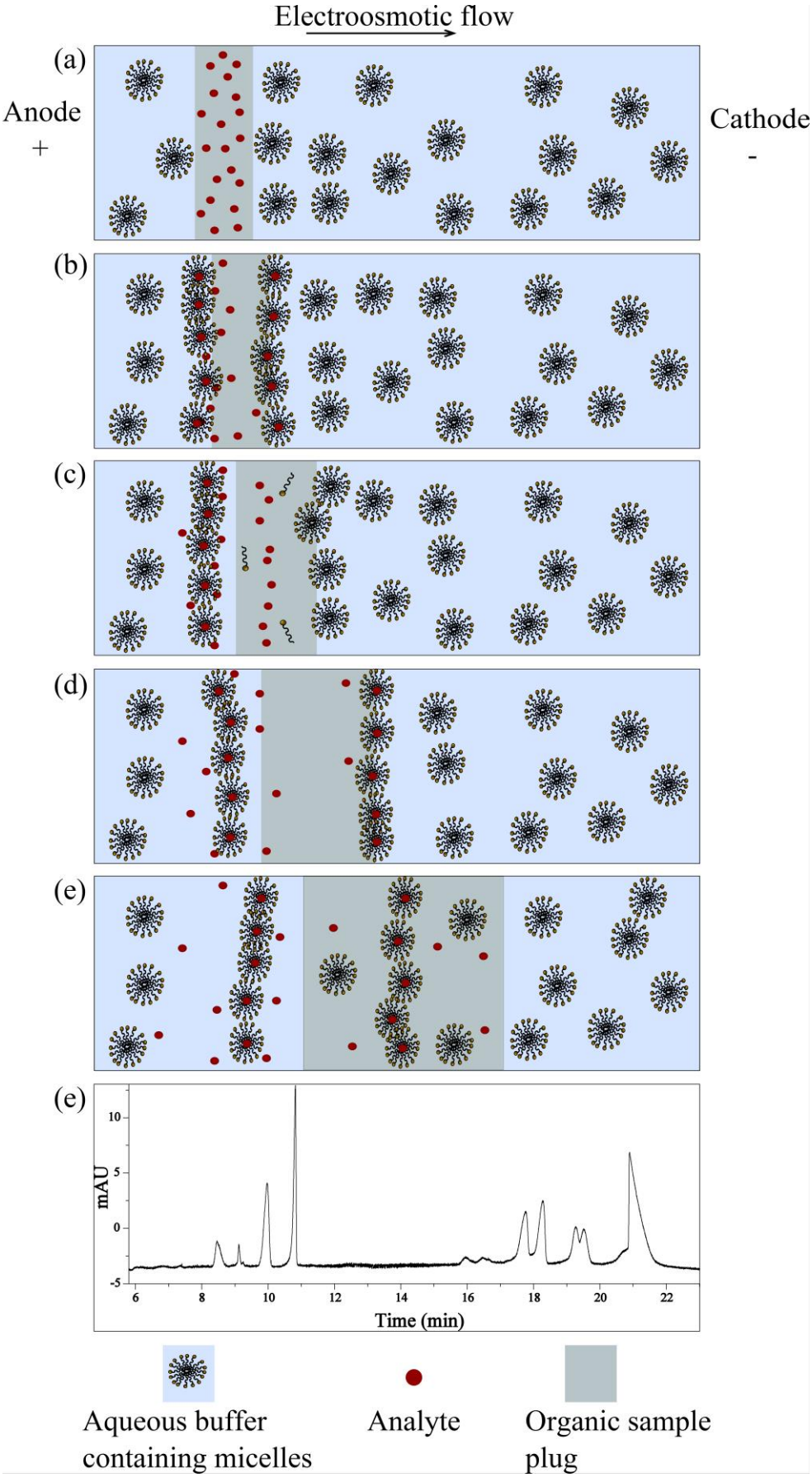

Figure 3-24 Schematic showing how peak splitting occurs in MEKC

If it is necessary for the analytes to be dissolved in 100% organic solvent, increasing the concentration of the surfactant in the buffer so more MeOH is required to disrupt the micelle, or choosing a solvent which decreases the CMC of the surfactant can help avoid peak splitting [111]. Adjusting injection time has also been shown to affect peak splitting in the case of sweeping MEKC when micelles cannot be introduced as part of the sample matrix [125]. In this case, the terpene standards were prepared by dissolving them in 400 µL MeOH and diluting this to 0.005% using the SDS tris buffer (see Figure 3-25).

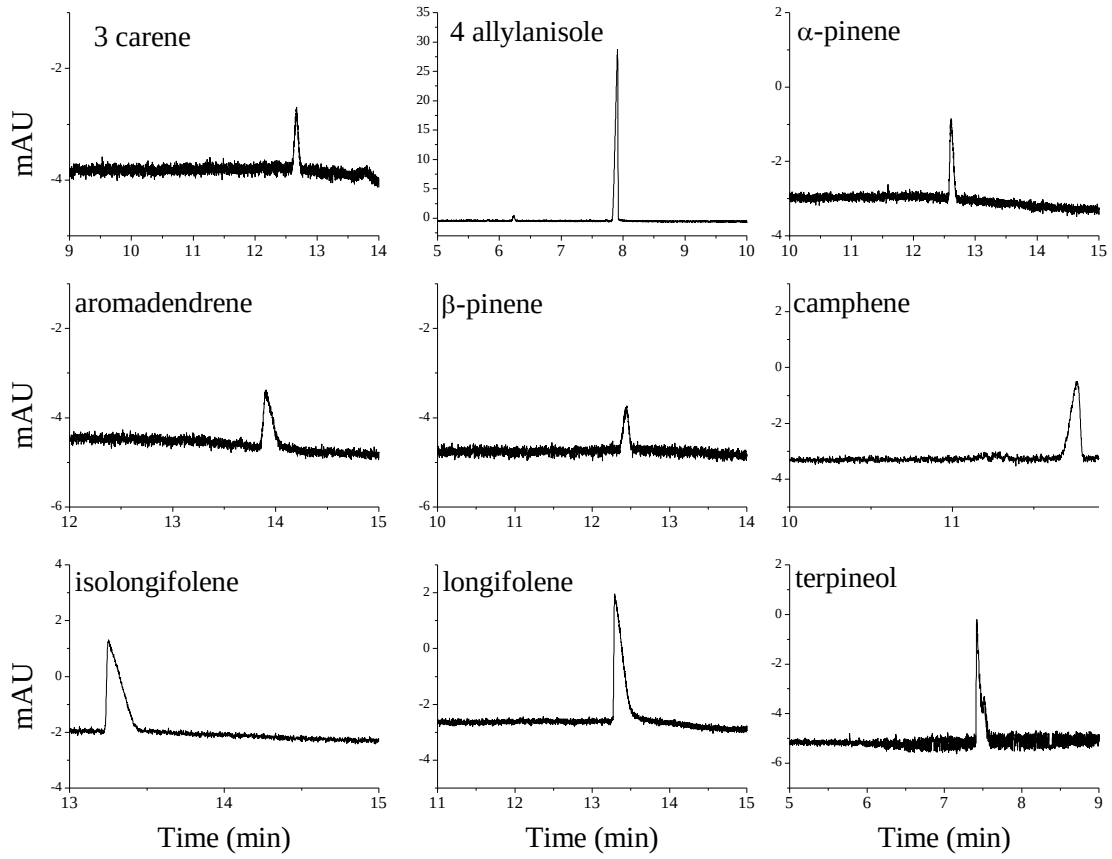

Figure 3-25 Electropherograms of 0.01% w/v terpene standards in 1:5 MeOH:SDS tris buffer, analysed in positive polarity, 20 kV, capillary 58 cm (49.5 cm to detector), 50 µm i.d., 25°C, 5 mbar 20 s injection times, detection at 200 nm.

Following this procedure it was found that a single peak is seen for each analyte, confirming the 100% organic sample solvent was the cause of the peak splitting. For all further work, samples were prepared in methanol and then diluted with the SDS tris buffer so that the final sample matrix was 1:5 MeOH:buffer.

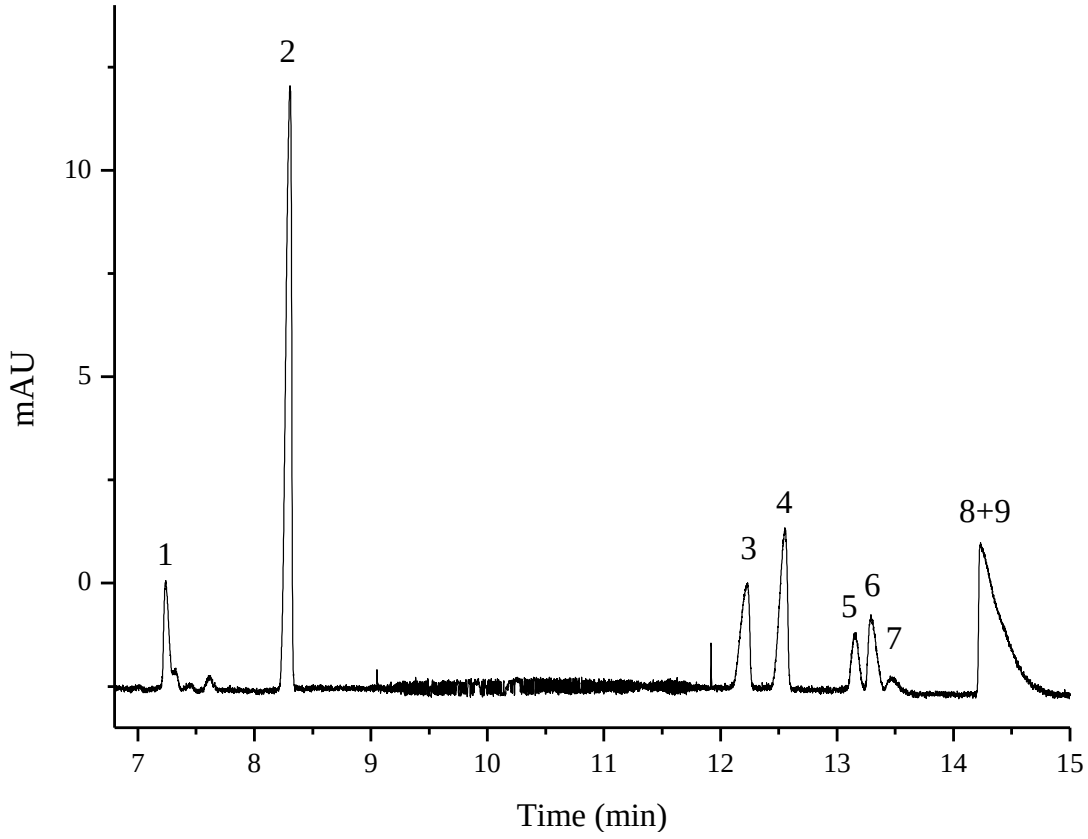

Figure 3-26 Electropherogram of 0.005% w/v terpene mixture in 1:5 MeOH:SDS tris buffer, analysed in positive polarity, 20 kV, capillary 58 cm (49.5 cm to detector), 50 µm i.d., 25°C, 5 mbar 20 s injection times, detection at 200 nm. Buffer consists of 10 mM SDS 50 mM tris pH 8. Numbers indicate (1) Terpineol, (2) 4 allylanisole, (3) camphene, (4) β-pinene, (5) 3 carene, (6) α-pinene, (7) isolongifolene, (8) longifolene and (9) aromadendrene.

Table 3-6 Resolution, efficiency and migration time %RSD values for the electropherogram seen in Figure 3-26 and Figure 3-27, n=3

10 mM SDS 50 mM tris pH 8								
N	83896	144204	194855	259547	231077	287500	144632	64092
R_s		11.3	38.7	3	5.8	1.3	1.3	4
RSD (%)	1.2	1.2	0.8	0.7	0.6	0.6	0.5	0.4
5 mM β-CD 10 mM SDS 50 mM tris buffer pH 8								
N	47675	52606	55994	93238	47675	97328	102892	91154	45526
R_s		6.6	12.8	2.2	5.6	4.8	8.3	11.1	7.2
RSD (%)	**0.5**	0.6	0.7	0.6	0.5	0.6	0.6	0.7	0.6

Figure 3-26 shows the electropherogram of the terpene mixture prepared in 1:5 MeOH:buffer. Terpineol and 4-allylanisole migrate first while the terpenes migrate

later, with longifolene and aromadendrene coeluting. The resolution and efficiency values are shown in Table 3-6.

For the first time, all nine neutral analytes are baseline resolved. Terpineol and 4-allylanisole have the lowest LogP values (see Table 3-1). The more hydrophobic terpenes were found to interact with the SDS more and so migrate later. The migration order has changed slightly with the addition of the β-CD. The first six analytes migrate in the same order however with the presence of the CD, longifolene now migrates before isolongifolene. This suggests that the longifolene has a higher affinity for the β-CD which reduces its interactions with the SDS micelles. The optimum buffer for the separation of the neutral analyte mixture was 5 mM β-CD 10 mM SDS 50 mM tris pH 8.

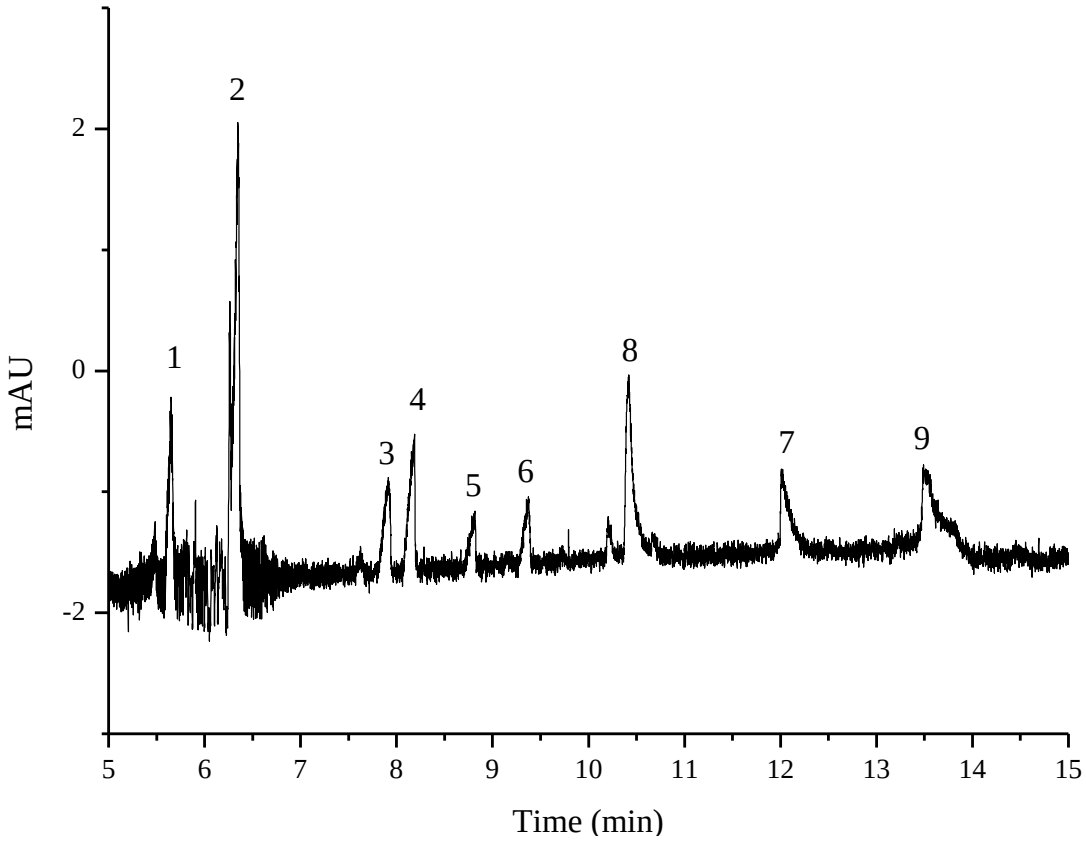

Figure 3-27 Electropherogram of 0.005% w/v terpene mixture in 1:5 MeOH:β-CD SDS tris buffer, analysed in positive polarity, 20 kV, capillary 58 cm (49.5 cm to detector), 50 µm i.d., 25°C, 5 mbar 20 s injection times, detection at 200 nm. Buffer consists of 5 mM β-CD 10 mM SDS 50 mM tris pH 8. Numbers indicate (1) Terpineol, (2) 4 allylanisole, (3) camphene, (4) β-pinene, (5) 3 carene, (6) α-pinene, (7) isolongifolene, (8) longifolene and (9) aromadendrene.

3.3.5 Analysis of rosin samples for occurrence of neutral compounds

Modified and unmodified rosin samples were then analysed using the optimised separation conditions described above (see Figure 3-28). All samples were prepared in a 1:5 MeOH:buffer matrix. This is the first report of the use of CE to analyse the neutral fraction of rosin samples.

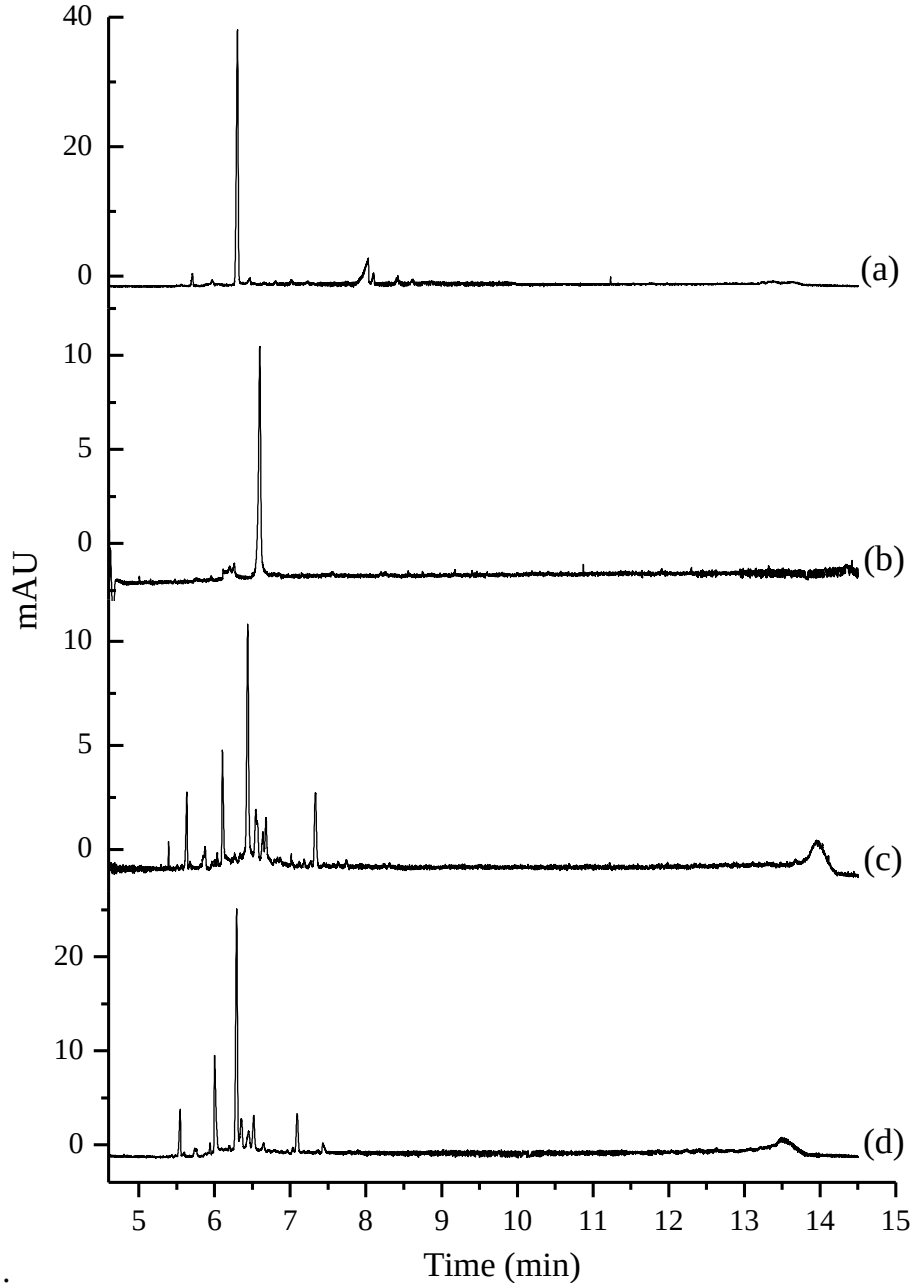

.

Figure 3-28 Electropherograms of 0.1% (a) acid modified rosin, (b) disproportionated rosin, (c) bad gum rosin and (d) good gum rosin analysed in positive polarity, 20 kV, capillary 58 cm (49.5 cm to detector), 50 µm i.d., 25°C, 5 mbar 20 s injection times, detection at 200 nm. Buffer consists of 5 mM β-CD 10 mM SDS 50 mM tris pH 8.

As rosins are known to consist of 90% resin acids, a gum rosin sample was spiked with acid standards in order to identify which peaks corresponded to acids and which may correspond to the neutral analytes being analysed (see Figure 3-29).

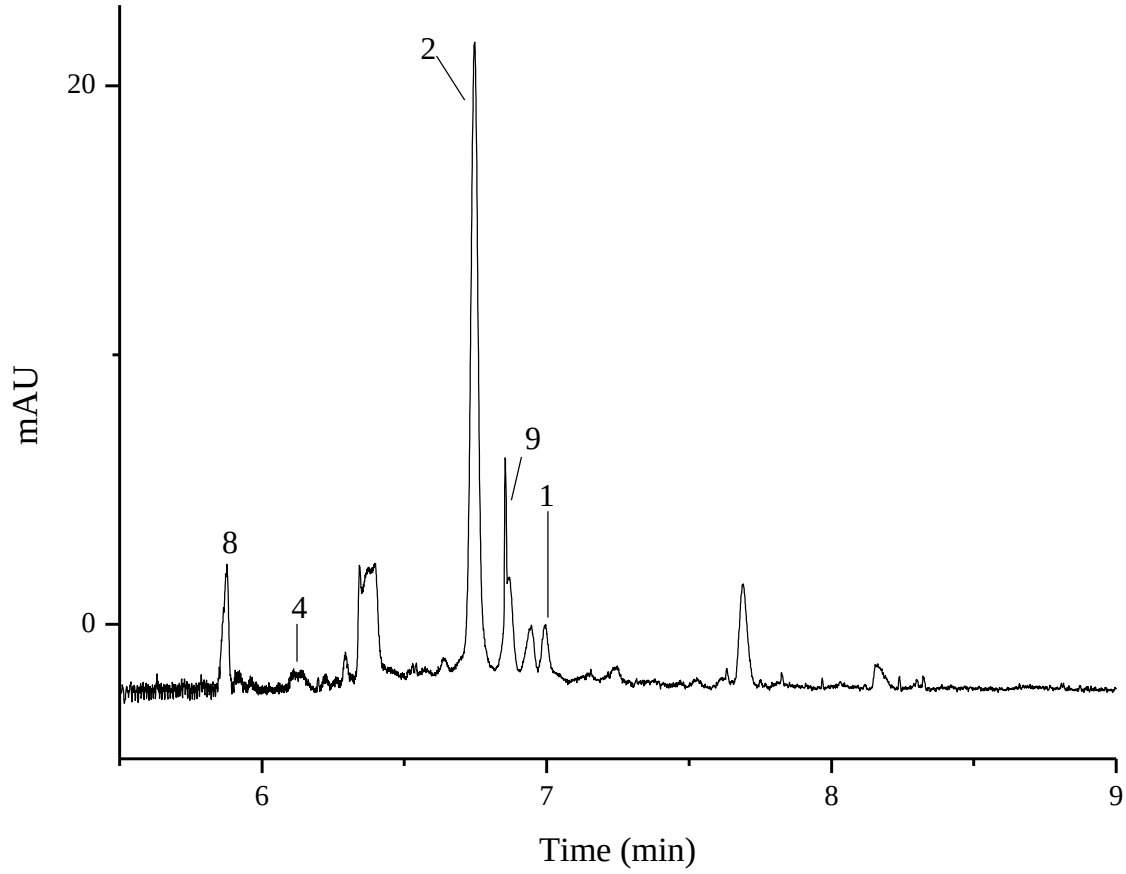

Figure 3-29 Electropherogram of a 0.1% w/v gum rosin sample analysed in positive polarity, 20 kV, capillary 58 cm (49.5 cm to detector), 50 µm i.d., 25°C, 5 mbar 20 s injection times, detection at 200 nm. Buffer consists of 5 mM β-CD 10 mM SDS 50 mM tris pH 8. Numbers indicate (1) 7OXO, (2) DHA, (4) ABA, (8) ISO and (9) PIM.

Several of the resin acids were not baseline resolved using this separation buffer.

3.3.5.1 Terpene spiked rosin samples

The rosin samples were spiked with the terpenes in order to investigate if they corresponded to any of the peaks in the rosin electropherograms.

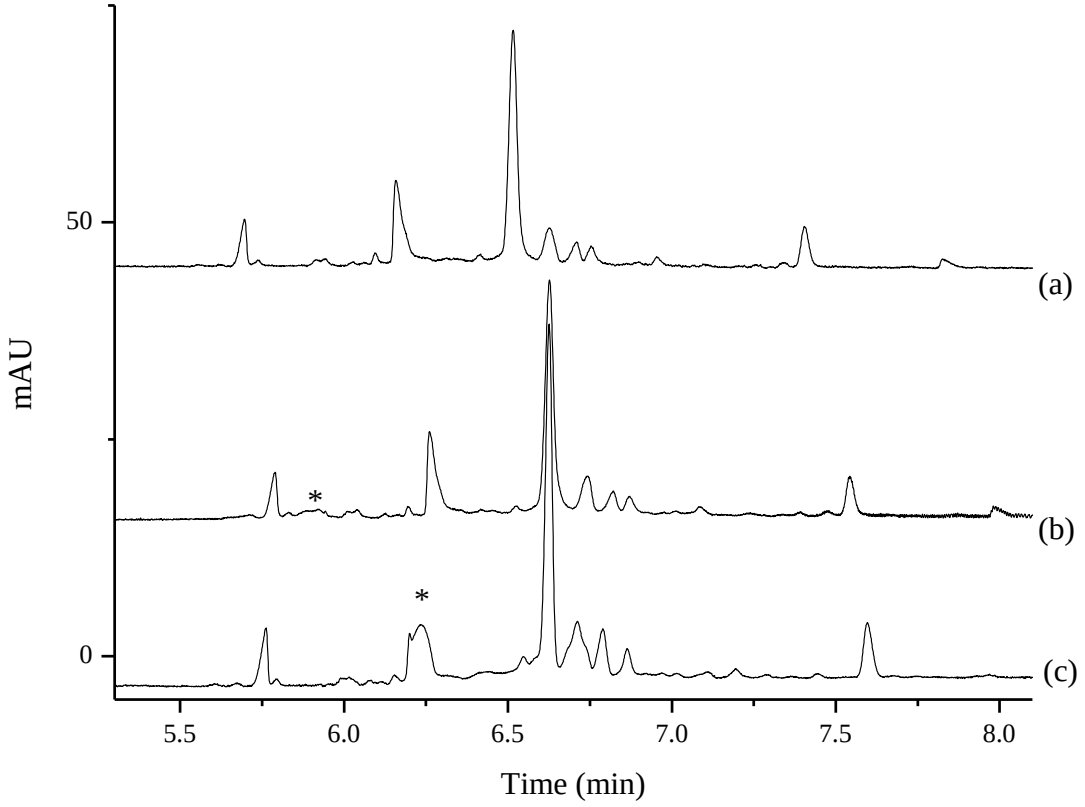

Figure 3-30 Electropherograms of (a) a gum rosin sample, (b) a terpineol spiked gum rosin sample and (c) a 4-allylanisole spiked gum rosin sample analysed in positive polarity, 20 kV, capillary 58 cm (49.5 cm to detector), 50 µm i.d., 25°C, 5 mbar 20 s injection times, detection at 200 nm. Buffer consists of 5 mM β-CD 10 mM SDS 50 mM tris pH 8. Stars indicate spikes.

As seen in Figure 3-30, the terpineol spiked peak does not correspond to any of the peaks in the gum rosin electropherogram. The 4-allylanisole spike is seen at 6.25 min coeluting with another peak.

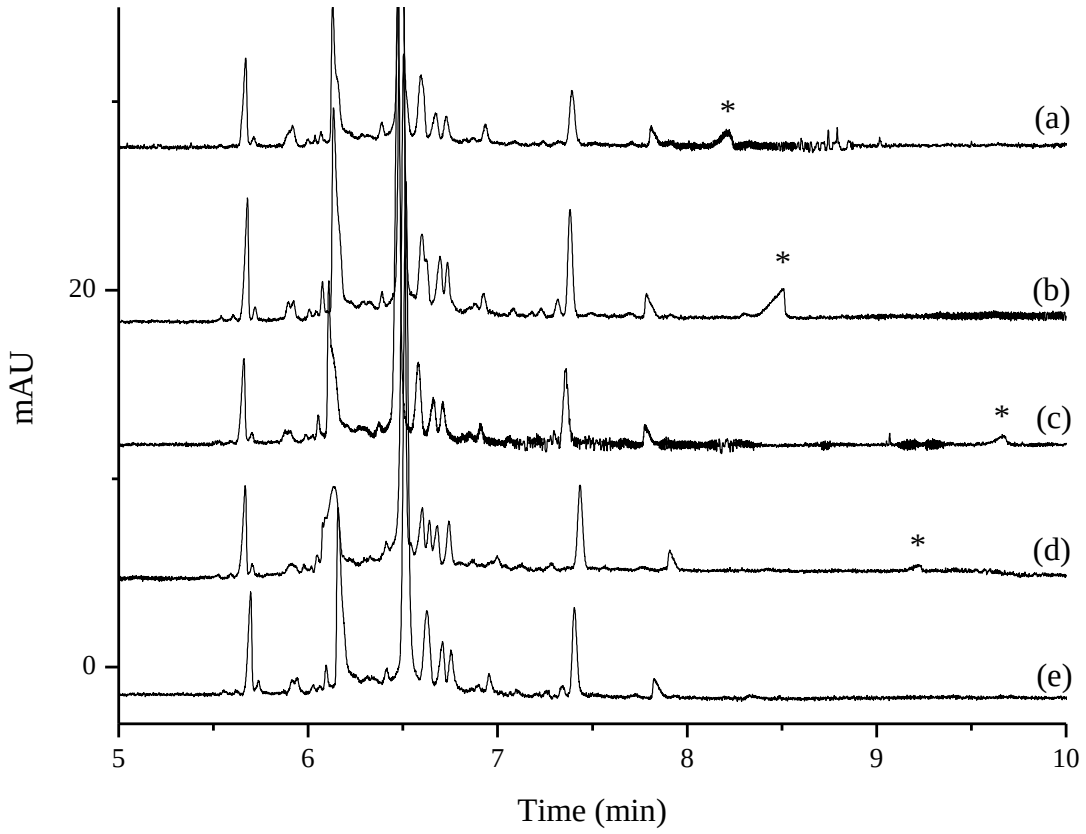

Figure 3-31 Electropherograms of a gum rosin sample spiked with (a) camphene, (b) β-pinene, (c) α-pinene, (d) 3-carene and (e) an unspiked gum rosin sample analysed in positive polarity, 20 kV, capillary 58 cm (49.5 cm to detector), 50 µm i.d., 25°C, 5 mbar 20 s injection times, detection at 200 nm. Buffer consists of 5 mM β-CD 10 mM SDS 50 mM tris pH 8. Stars indicate spikes.

Figure 3-31 shows the spike of camphene, β-pinene, α-pinene and 3-carene, all of which elute between 8 and 10 min. None of these spikes correspond to peaks in the gum rosin electropherogram.

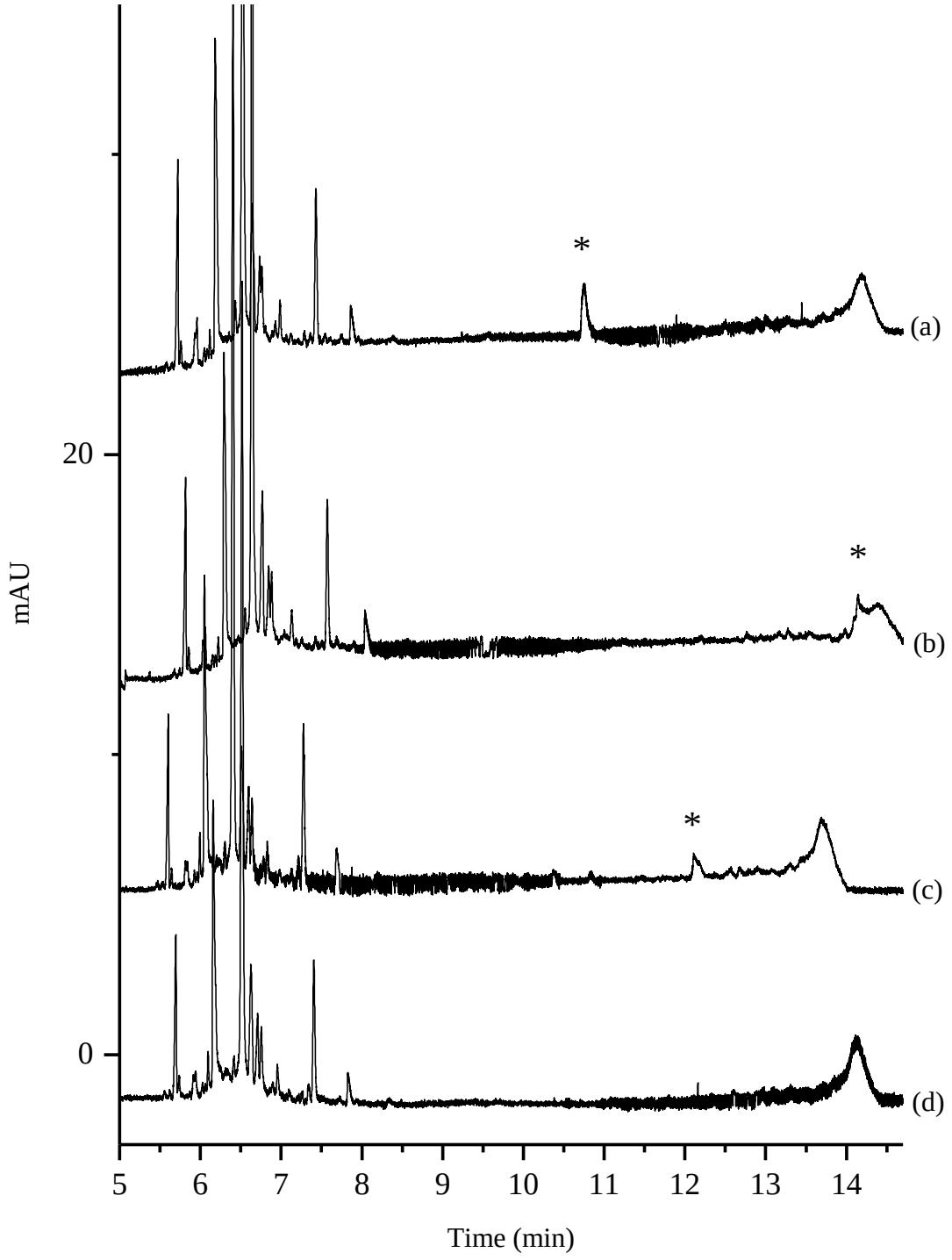

Figure 3-32 Electropherograms of gum rosin samples spiked with (a) longifolene, (b) aromadendrene, (c) isolongifolene (d) an unspiked gum rosin sample analysed in positive polarity, 20 kV, capillary 58 cm (49.5 cm to detector), 50 µm i.d., 25°C, 5 mbar 20 s injection times, detection at 200 nm. Buffer consists of 5 mM β-CD 10 mM SDS 50 mM tris pH 8. Stars indicate spikes.

As seen with the other terpene spikes longifolene and isolongifolene do not correspond to any of the gum rosin peaks (Figure 3-32). The aromadendrene spike is

seen at the peak eluting at 14 min, however, it does not appear to be the sole component of that peak, it is coeluting with another compound.

All of the analysed neutral compounds have been detected in rosin samples and some quantified [1, 23]. Zinkel *et al.* report that terpineol, 4-allylanisole and longifolene make up 50-60% of the volatile neutral compounds present [1]. Through analysis by GC-MS head space analysis, Hadi identified the presence of many of the neutral compounds in several rosin samples; however, none were found to be present in every rosin sample [23]. This highlights the fact that the neutral compounds being investigated in this work are not always present in the rosin sample. The spiked samples show where the neutral compounds peaks would be expected, showing that the compounds are not present in these particular rosin samples.

3.4 Conclusions

As the main components of rosins are acidic, the majority of research on their composition investigates the acidic fraction and not the neutral fraction. The exact reason for rosin crystallisation is not yet known so it is worth investigating these neutral compounds to explore if their presence or concentration is linked to rosin crystallisation. In this work a novel CE method for the separation of nine neutral compounds including terpenes, alcohols and phenylpropenes was developed.

HPLC was found to be unsuitable for the separation of these compounds. A range of CE methods were then investigated, including CZE, MEEKC, MEKC and CD-CE.

The buffer pH, oil type and concentration, co-surfactant concentration, organic additive and surfactant concentration of the microemulsions used in MEEKC were all varied, however, little separation was achieved using this technique.

In MEKC, the buffer type, concentration and SDS concentration was optimised and the use of cyclodextrins investigated. The addition of 5 mM β-CD to the MEKC buffer resulted in the baseline resolution of many peaks, however, some of those peaks were suspected to be resulting from peak splitting.

The peak splitting was found to be as a result of the samples being prepared in 100% MeOH. When the sample preparation was changed to dissolution in MeOH and then dilution with the running buffer, peak splitting was avoided. With the neutral mix prepared this way, the MEKC buffer of 10 mM SDS 50 mM tris pH 8 resulted in the separation of all but longifolene and aromadendrene. As these particular compounds had previously been separated with the use of β-CD, it was reintroduced into the buffer. A buffer containing 5 mM β-CD 10 mM SDS 50 mM tris pH 8 resulted in the baseline separation of a mixture of α-pinene, β-pinene, camphene, 3-carene, terpineol, 4-allylanisole, longifolene, isolongifolene and aromadendrene for the first time. To the author's knowledge, this is also the first report of the use of CE for the analysis of the neutral fraction of rosin samples.

This work highlights some of the advantages of CE, its speed, versatility and robustness. Several CE techniques were investigated by changing the buffer

composition only, while the same range of investigation in another analytical technique may require different columns which can be costly.

Both modified and unmodified rosin samples were analysed using the optimised CE conditions. The samples were spiked to confirm if any of the peaks in the rosin electropherograms corresponded to the neutral analytes. It was observed that the spiked peaks did not match any of the rosin peaks, indicating that the neutral analytes in question were not present in these particular rosin samples.

Chapter 4

Investigation of cyclodextrin association constants with terpenes and other natural compounds by affinity capillary electrophoresis

4.1 Introduction

The formation of inclusion complexes between cyclodextrins (CDs) and hydrophobic guest molecules forms the basis of many electrophoretic and chromatographic separations, including the methods developed in chapters 2 and 3. However, there are still gaps in the quantitative knowledge of the association constants of many cyclodextrin-analyte complexes. Investigating complexation constants can provide useful information on the fundamental behaviour of the inclusion complexes formed as several properties of analytes are affected when in a complex, including spectral properties, solubility, stability and reactivity [80, 82, 126-129]. Information on the stability and stoichiometry of inclusion complexes can aide in the use of cyclodextrins to their full potential. In electrophoretic separations, this data can aid in the comprehension of analyte behaviour when CDs are added to the background electrolyte. The terms formation, association, binding, complexation and stability constant are all used in literature to describe the binding interactions [80, 127, 130, 131]. The term association constant will be used in this thesis. This work details the first report of the use of affinity capillary electrophoresis for the determination of the association constants of CD-terpene inclusion complexes.

4.1.1 Determination of association constants

In order to investigate association constants between analytes and complexing agents such as cyclodextrins, micelles or proteins, the analyte in question needs a measurable property that differs when in a complex and when free in solution such as mobility [132]. Many techniques have been employed for this including spectroscopy, potentiometry, mass spectrometry and chromatography [104, 124]. The simplest and most commonly used CE method for the determination of association constants is affinity capillary electrophoresis, where the effective mobility of the analyte is determined as the concentration of the cyclodextrin in the background electrolyte is varied [130, 133]. Three linearization plot types, double-, X- and Y-reciprocal plots, are generally used to express this data as they are considered one of the most convenient methods [132, 134-142]. Although the plots all contain the same equation in different forms, the resulting correlations will be affected differently by the variable, depending on where it is found in the equation.

The X-reciprocal fit is more affected by CD concentration variation as the dependent variable is on both axis. The Y-reciprocal plot has the independent variable on both axis, while data acquired at low cyclodextrin concentrations are emphasised by the double-reciprocal plot as deviations from linearity are masked [132, 136, 141]. Good linearity supports the 1:1 binding stoichiometry of the complexes [134, 141].

4.1.2 Cyclodextrins

The properties of the native CDs are seen in Table 4-1. CD inclusion complexes usually form a stoichiometric ratio of 1:1 but this is not always the case [126, 143, 144]. The larger γ-CD can form complexes in with two or more guest molecules in each CD cavity [145] e.g. Brocos *et al.* indicated the existence of complexes containing two SDS molecules per γ-CD [146] (see Figure 4-1) . The smaller α-CD has also been known to form a complex containing two CD molecules with one analyte molecule e.g. a 2:1 α-CD:camphene complex [147]. Sometimes the inclusion complex is formed with a hydrophobic section of the analytes as opposed to the entire structure [80, 148, 149].

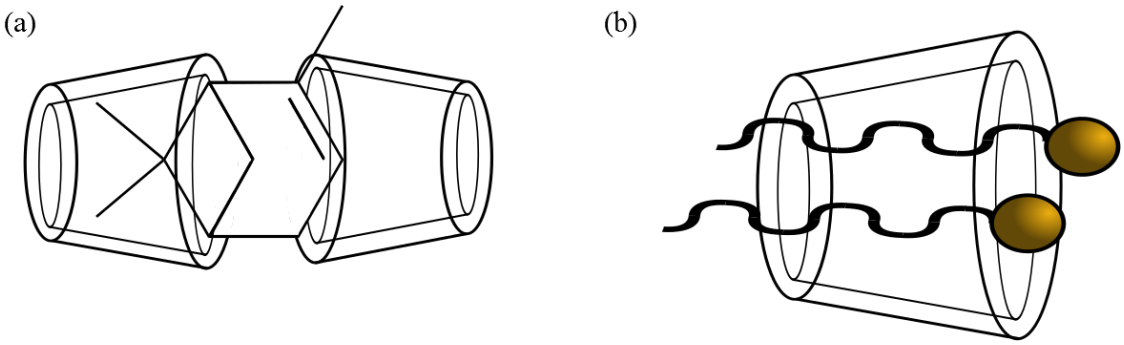

Figure 4-1 Schematic illustration of (a) 2:1 α-CD:α-pinene inclusion complex and (b) 1:2 γ-CD:SDS molecule inclusion complex.

Table 4-1 Properties of the native CDs [82]

	α-CD	**β-CD**	**γ-CD**
Inner diameter	4.7-5.3 Å (0.47-0.53 nm)	6-6.5 Å	7.5-8.3 Å
Outer diameter	13.7 Å	15.3 Å	16.9 Å
Cavity depth	7-8 Å	7-8 Å	7-8 Å
Cavity volume	174 $Å^3$	262 $Å^3$	427 $Å^3$
Solubility	14.5g/100mL water	1.85g/100mL water	23.2g/100mL water
Molecular weight (g M^{-1})	972	1135	1297

4.1.3 Cyclodextrin-Terpene inclusion complexes

The structures of the terpene analytes are shown in Figure 3-2. While some terpenoids have functional groups e.g. the α-terpineol has a hydroxyl group, the terpenes do not and therefore lack charge transfer interactions, π-π, dipole, and hydrogen bonding. Terpenes are generally analysed by GC-FID or GC-MS, and are separated by GC using CD bonded stationary phases, by HPLC with CDs as additives in the mobile phase, or by CD-CZE [101, 104]. A combination of α-CD and sulphated β-CD were used to separate the bicyclic monoterpenes camphene, α-pinene and β-pinene where the β-CD alone was not successful [121]. Rodrigues *et al.* found a combination of SDS, ACN and γ-CD was required to separate camphene, α-pinene and β-pinene amongst other terpenes using CE (see Figure 4-2) as α- and β-CD could not [122].

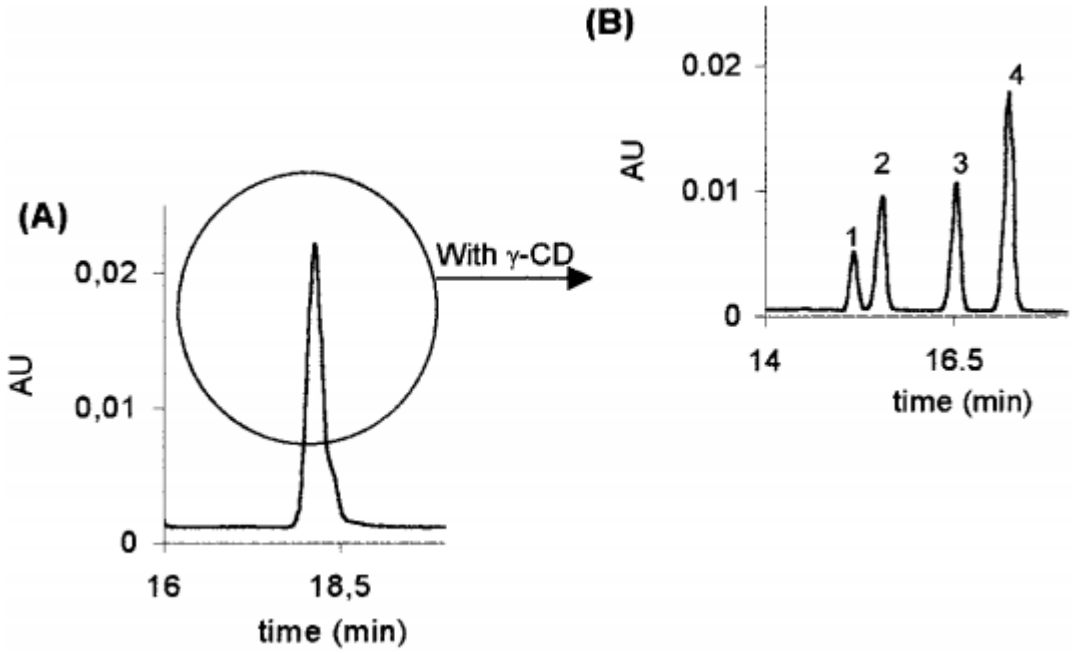

Figure 4-2 Electropherograms of (1) camphene, (2) β-pinene, (3) α-pinene and (4) γ-terpinene. Separation at 20 kV, capillary 57 cm (50 cm to detector), 75 µm i.d., 25°C, 5 mbar 20 s injection times, detection at 200 nm, buffer consists of 10 mM phosphate 6 mM borate at pH 8 containing 50 mM SDS 5% ACN and (A) 10 mM α-CD or (B) 10 mM γ-CD [122].

The formation constants of some terpenes were investigated using reverse-phase HPLC with α- and β-CD in the mobile phase. It was found that α-pinene, β-pinene and camphene tend to form a 1:2 guest:CD ratio with α-CD but a 1:1 ratio with β-CD [104]. A study by Asztemborska *et al.* also reported the formation of a 1:2 guest:CD ratio between α-pinene, β-pinene and camphene and α-CD [102]. The bicyclic structure of some of the terpenes may be too rigid to fully fit into an α-CD cavity. Ceborska *et al.* determined that camphene formed a 1:1 guest:CD ratio with β-CD using GC, NMR and X-ray crystallography studies [123]. Chatjigakis *et al.* found a 1:1 guest:CD ratio between α-terpineol and β-CD using reverse-phase HPLC [124].

To the authors' knowledge, there are only a few reports of association constants reported in literature for terpene-cyclodextrin analytes. Association constants of 6080, 6120 and 6040 M^{-1} for α-, β-pinene and camphene respectively with β-CD were determined by HPLC [104]. While others mentioned in the literature reported 1:2 guest:CD complexes, Ciobanu *et al*. reported 1:1 complexes forming between α-pinene, β-pinene and camphene and α-CD as well as with β-, γ-CD and MECD.

They used a static headspace GC titration method to determine stability constants of 1778, 2588, 214 and 2395 M^{-1} for α-pinene with α-, β-, γ-CD and MECD respectively. β-pinene stability constants of 1018, 4587, 633 and 4450 M^{-1} with α-, β-, γ-CD and MECD respectively were reported. Camphene pinene stability constants of 598, 4825, 360 and 6625 M^{-1} with α-, β-, γ-CD and MECD respectively were reported. The methylated and native β-CD complexes gave the highest stability constants and complexation efficiencies [150]. MEKC was used to analyse neutral plant metabolites and reported the partition coefficient of terpineol into an SDS micelle as 785±48 [151].

4.1.4 Aims

The aim of this research is to investigate the association constants of the inclusion complexes formed between resin acids, monoterpenes, sesquiterpenes and other neutral natural components found in natural rosin samples with cyclodextrins of different cavity sizes and modifications using affinity capillary electrophoresis and three linearization methods. The objectives are to record the mobilities of the analytes when analysed in buffers containing increasing concentrations of CD, and to plot the data using 3 linear plotting methods and calculate association constants. The effects of surfactant and cyclodextrin concentrations and the addition of methanol to the buffer will also be investigated.

4.2 Experimental

4.2.1 Instrumentation

CE instrumentation is as described in section 3.2.1.

4.2.2 Reagents

The reagents used are as described in section 3.2.2. In addition, α-, β- and γ-cyclodextrin were purchased from Sigma Aldrich Ireland Ltd. (Vale Road, Arklow, Wicklow, Ireland).

4.2.3 Separation conditions

CE separation conditions are as described in section 3.2.4.

4.2.4 Buffer and sample preparation

Tris buffers were prepared to the required concentration and pH by mixing appropriate amounts of tris HCl and tris base in distilled water following the Sigma-Aldrich tris buffer mixing table e.g. a 50 mM tris buffer at pH 8 was prepared by mixing 4.44 g L^{-1} tris HCl and 2.65 g L^{-1} tris base. The concentration of 10 mM SDS was kept constant in all buffers while the CD concentration was varied. All buffers were sonicated for 15 min and filtered through a 0.2 μm nylon membrane filter. Terpene and acids samples were prepared by first dissolving in 100% MeOH, and then diluting with 10 mM SDS 50 mM tris buffer at pH 8.

4.2.5 Data evaluation

In order to correct for any changes in viscosity as the cyclodextrin concentration was increased, mobility ratios (M) were determined by mobility values using the following equation [152, 153]:

$$M = \mu_{net}/\mu_{eof} = (\mu + \mu_{eof})/\mu_{eof} \quad (1)$$

Where μ_{eof} is the mobility due to EOF, μ is the mobility of the analyte and μ_{net} is the net measured mobility of the analyte.

$$\mu = IL/tV \quad (2)$$

When the mobility equation (2) is substituted into the mobility ratio equation (1) the following equation is observed:

$$M = t_{eof}/t + 1 \quad (3)$$

Where t_{eof} is the migration time of the neutral marker and t is the migration time of the analyte [154]. These mobility ratios were used in place of mobility values when plotting the double, Y and X reciprocal plots.

The 1:1 molecular association of an analyte (A) and a cyclodextrin (CD) can be described by the following equilibrium equation [126]:

$$A+CD = ACD \quad (4)$$

Where K = the association constant (M^{-1}), which describes the bonding affinity of two molecules at equilibrium. A and CD are the free analyte and cyclodextrin respectively and ACD is the inclusion complex formed. The experimentally measured mobility (μ_a) is a weighted average of the mobility of the free (μ_f) and complexed analyte (μ_c). At a given cyclodextrin concentration (mM), the mobility of the analyte is described in Eq. 5 [132, 136]:

$$\mu_a = \frac{1}{1+K[C]}\mu_f + \frac{K[C]}{1+K[C]}\mu_c \quad (5)$$

In order to linearise the data, Eq.5 can be rearranged to suit three mathematical plotting models: double reciprocal, Y-reciprocal and X-reciprocal plots. This also allows the avoidance of necessitating the use of μ_c which is difficult to measure experimentally [136, 141].

Double reciprocal plot:

$$\frac{1}{(\mu_a-\mu_f)} = \frac{1}{(\mu_c-\mu_f)K}\frac{1}{[C]} + \frac{1}{(\mu_c-\mu_f)} \quad (6)$$

Plotting $1/(\mu_a - \mu_f)$ versus 1/[C] gives a double reciprocal plot where K=intercept/slope.

Y-reciprocal plot:

$$\frac{[C]}{(\mu_a-\mu_f)} = \frac{1}{(\mu_c-\mu_f)}\frac{[C]}{1} + \frac{1}{(\mu_c-\mu_f)K} \quad (7)$$

Plotting [C] /(μ_a- μ_f) versus [C] gives a Y-reciprocal plot where K=slope/intercept.

X-reciprocal plot:

$$\frac{(\mu_a-\mu_f)}{[C]} = \frac{-K(\mu_a-\mu_f)}{1} + \frac{K(\mu_C-\mu_f)}{1} \quad (8)$$

Plotting (μ_a- μ_f)/[C] versus (μ_a- μ_f) gives an X-reciprocal plot where K=-slope.

4.3 Results and discussion

Association constants can indicate the binding strength of an inclusion complex, information which could potentially be used to predict any property changes the analytes might experience. The constants could also be used to select the appropriate cyclodextrin size for the analysis [134]. The appropriate CD size depends on favourable thermodynamic interactions, and a favourable steric fit depending on the size of the guest molecule and any functional groups present [82].

4.3.1 Initial separation

A mixture of α-pinene, β-pinene, isolongifolene, aromadendrene, camphene, α-terpineol, 4-allylanisole, longifolene and 3-carene was analysed in 10 mM SDS 50 mM tris buffers at pH 8 containing 1-5 mM of α-, β-, γ-CD or MECD and in a buffer containing no CD. As the guest:CD ratio of many of these compounds with β- and γ-CD was previously determined to be 1:1 [104, 123, 124], it was assumed the same was true for the other compounds of similar structure and hydrophobicity. As both the analytes and cyclodextrins are neutral, the presence of negatively charged SDS in the buffer was required to provide mobility to the analytes and allow separation; without it they would all coelute with the EOF. LogP is logarithmic form of the octanol-water partition coefficient (P). The logP values of the analytes range from 2.79-6.4 (predicted values from ACD/Labs, see Table 3-1), indicating their hydrophobicity. Cyclodextrins and micelles demonstrate similar separation mechanisms, in that the interior of their structures are hydrophobic and allow interactions with hydrophobic analytes. Therefore, it is clear that the analytes will interact with the SDS micelles as well as the CDs. Figure 4-3e shows the separation of the analyte mixture in an SDS tris buffer without CD. The presence of SDS allows the separation of some of the neutral analytes. The concentration of SDS was kept constant throughout all the experiments; therefore any difference in mobilities was attributed to the change in cyclodextrin concentration [136].

While some properties such as the critical micelle concentration (CMC) are affected by analyte-buffer interactions [129], the complexation thermodynamics are not significantly affected by other interactions before complexation [136, 148]. Figure 4-3 a-d shows the separation of the analyte mixture using buffers containing 5 mM of each CD. Figure 4-4 shows schematics of the proposed mechanisms involved in each separation. It is clear from the figure that there is analyte-CD interaction taking place as the migration times and migration order change with different CD types. The analytes appear to elute earlier due to the presence of neutral CDs as they spend less time in the negatively charged micelles travelling away from the detector so more interactions with the CDs result in shorter migration times. The migration order can change if a different CD cavity size is a better steric fit for certain analytes and result in more interaction with the CD while another analyte now interacts less. The association constants calculated by the three linearization methods for each CD concentration are shown in Table 4-2.

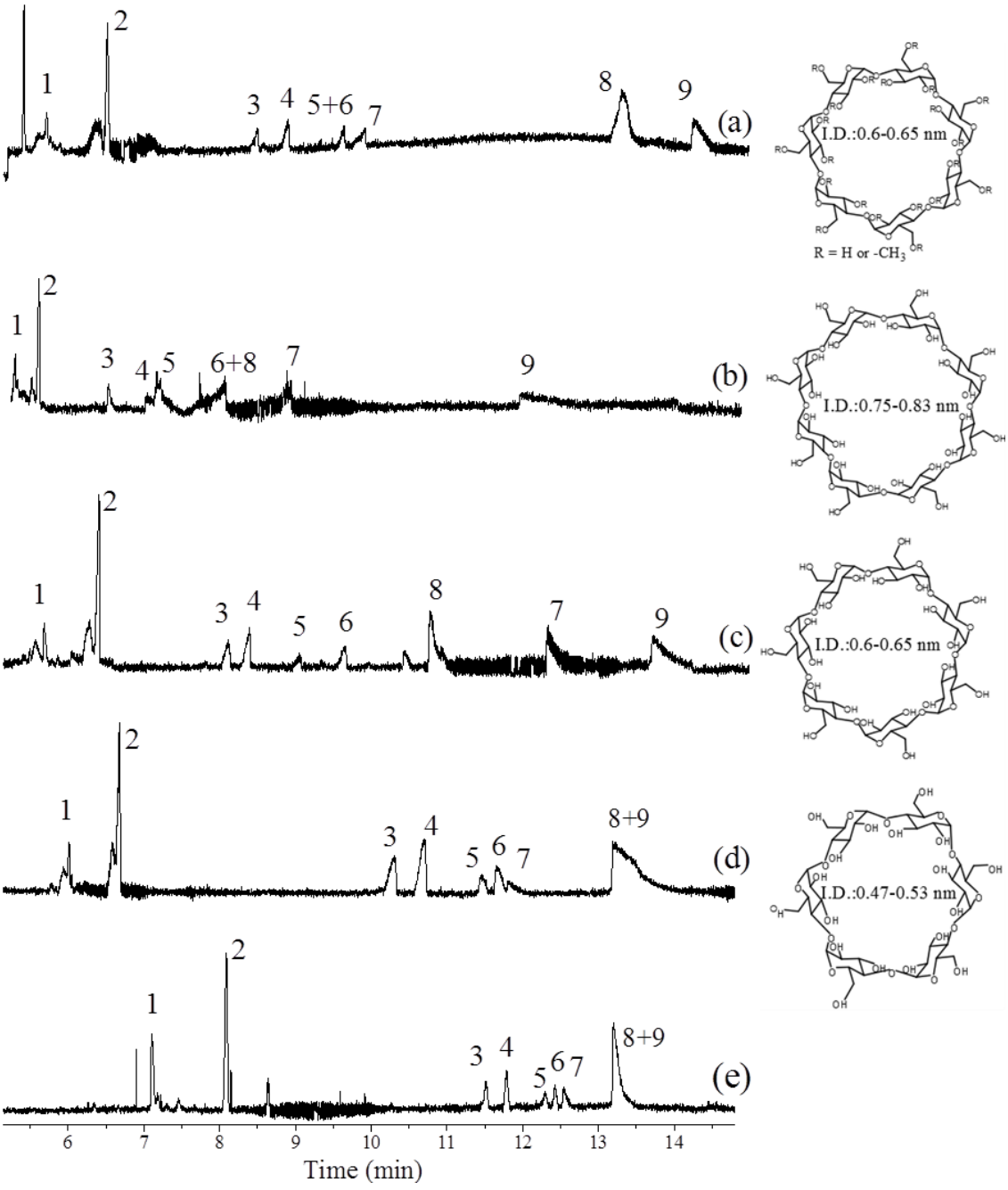

Figure 4-3 Electropherograms of the mixture of nine neutrals analysed in buffers composed of 10 mM SDS 50 mM tris pH 8 and 5mM (a) MECD, (b) γ-CD, (c) β-CD, (d) α-CD and (e) no CD. Separation at 20 kV, capillary 58 cm (49.5 cm to detector), 50 µm i.d., 25°C, 5 mbar 20 s injection times, detection at 200 nm. Numbers indicate analytes as follows; (1) terpineol, (2) 4-allylanisole, (3) camphene, (4) β-pinene, (5) 3-carene, (6) α-pinene, (7) isolongifolene, (8) longifolene and (9) aromadendrene.

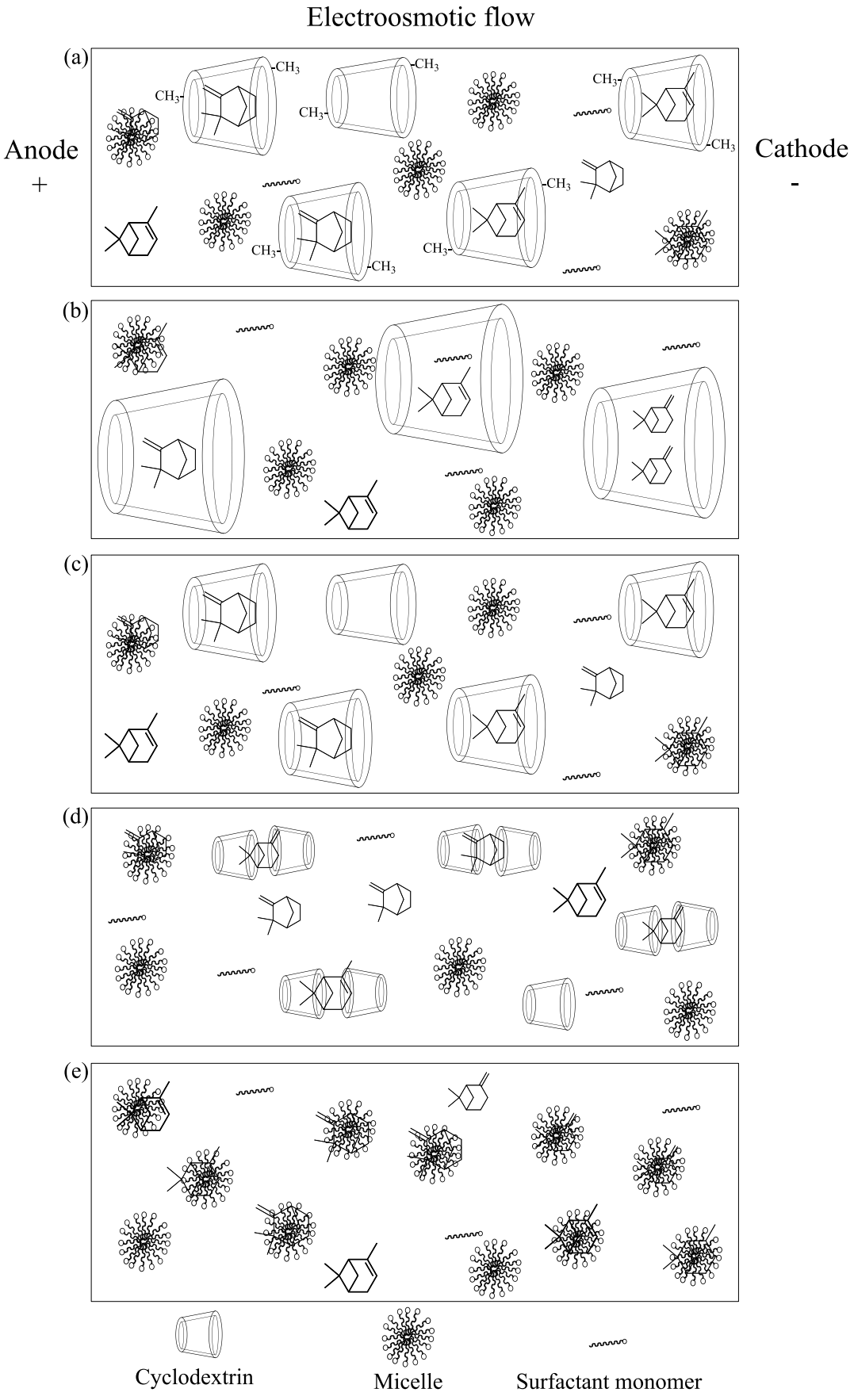

Figure 4-4 Schematic of proposed separation mechanisms for the electropherograms in Figure 4-3.

4.3.2 α-cyclodextrin

The mobilities of the analytes were found to increase with an increase of α-CD concentration, consistent with their behaviour in the presence of other CD types (see Figure 4-5). Aromadendrene is an exception here as the CD concentration was found to have little effect on its mobility. However, the guest:CD binding ratio of the analytes was reported to be 1:2. This is due to the small inner diameter of the CD (4.7-5.3Å [82, 147]). The double-, Y- and X-reciprocal linearization plots cannot be applied as they are based on 1:1 stoichiometry complexes.

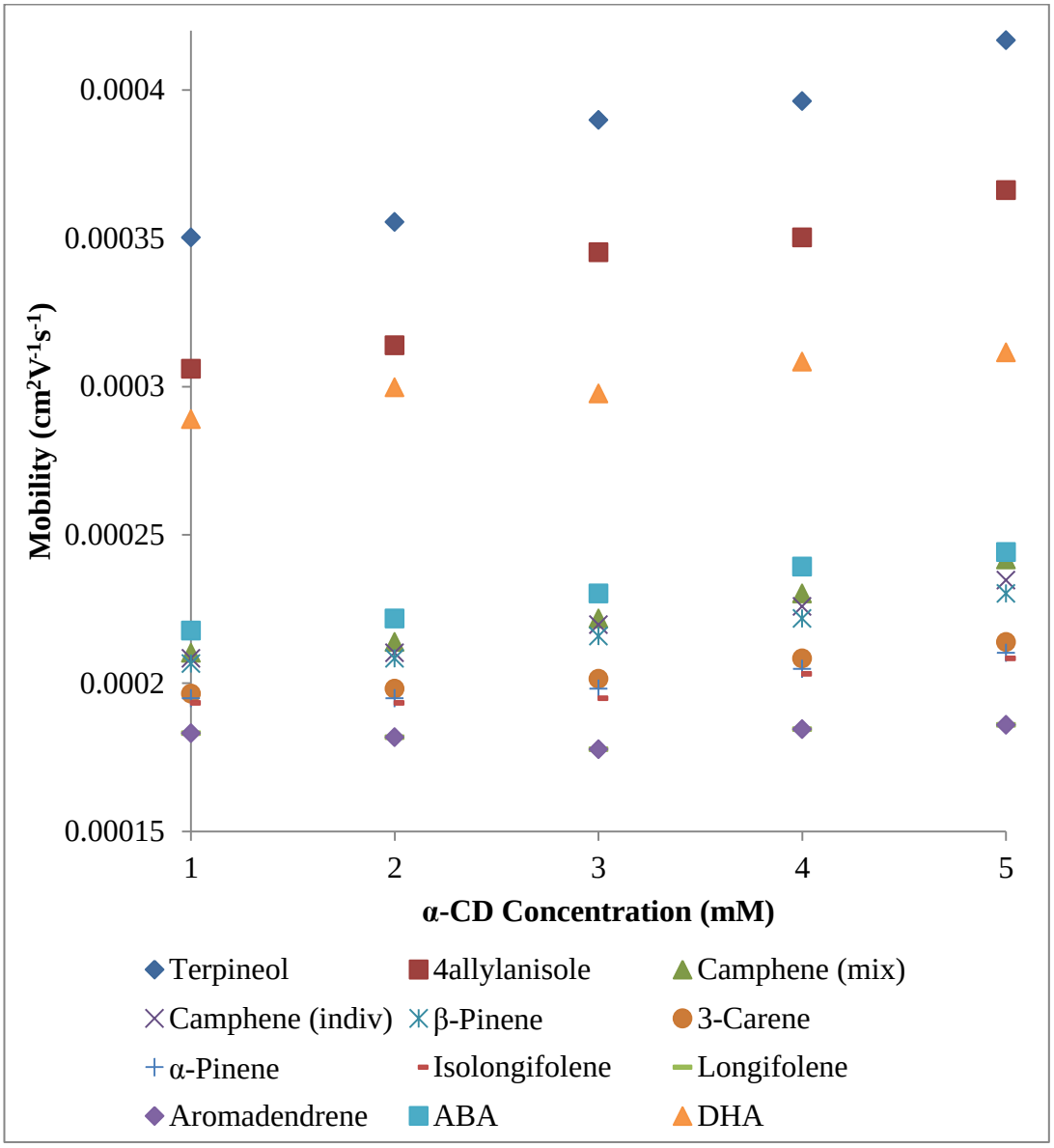

Figure 4-5 Plots of mobility ($cm^2V^{-1}s^{-1}$) versus α-CD concentration

4.3.3 β-cyclodextrin

The buffer containing β-CD was found to separate all of the analytes in the study (see Figure 4-3). The inner cavity of β-CD is 6-6.5 Å [82] which is more suitable to facilitate the size of the monoterpenes (the monoterpenes studied range from 5.8-6.6 Å at their widest axis, sizes calculated in ChemDraw 3D) and other analytes, in particular cyclic aliphatic compounds [148].

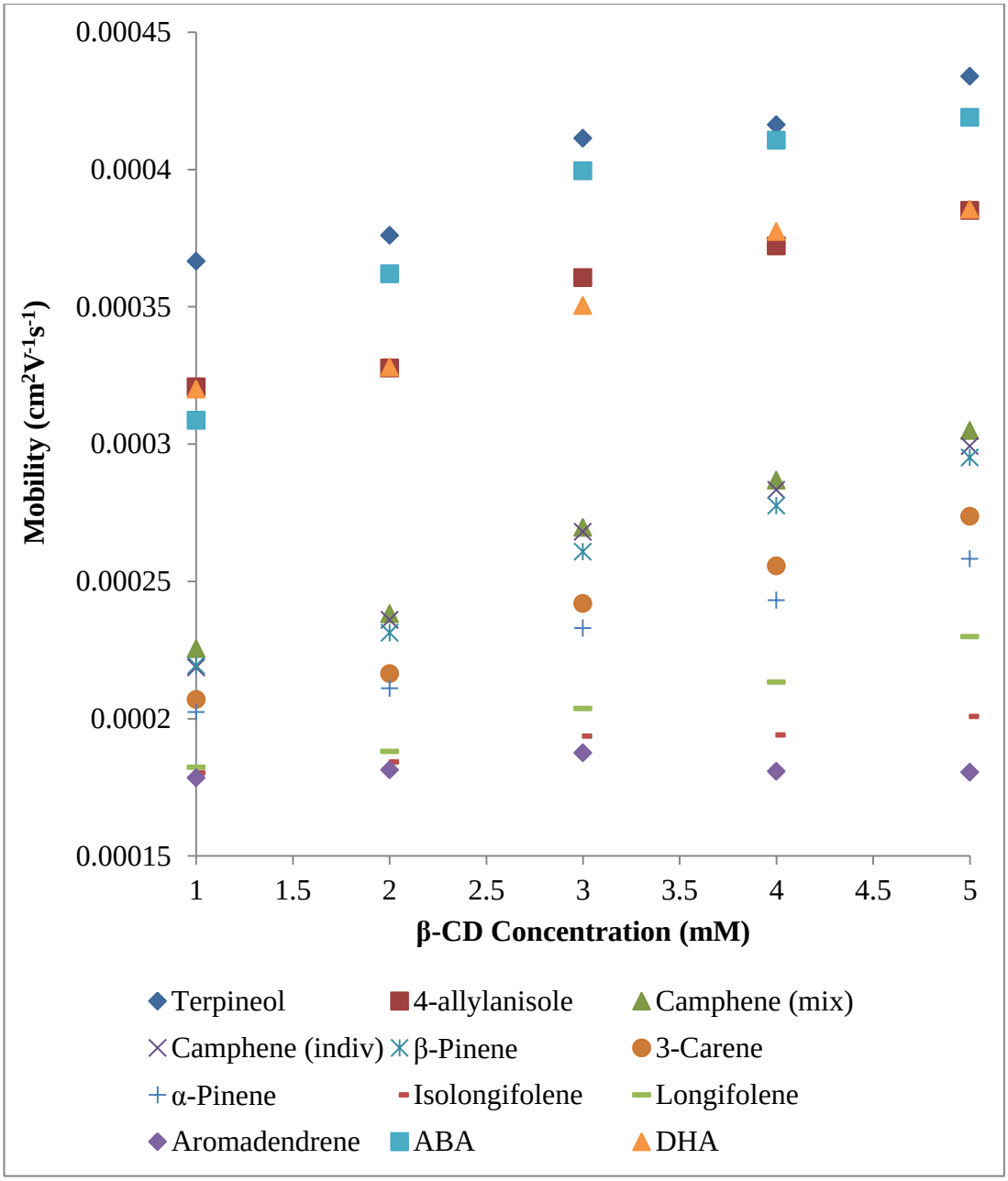

Figure 4-6 Plots of mobility ($cm^2V^{-1}s^{-1}$) versus β-CD concentration

The analyte mobilities were found to increase with increasing concentration of β-CD (see Figure 4-6), indicating that they spend less time migrating towards the anode with the SDS micelles (R^2 values given in Table 4-2). The exception is aromadendrene, suggesting there is little or no interaction between aromadendrene and β-CD. This is unexpected as aromadendrene has the highest LogP value and so would be expected to interact with the hydrophobic inner cavity of the CD. Aromadendrene is a three-ringed structure with three methyl and one methylene groups. The lack of interaction may be due to steric hindrance, as the aromadendrene molecule is 7.5 Å across at its widest. Longifolene was found to migrate before isolongifolene in β-CD modified buffer, indicating that it interacts more with the CD, likely due to the double bond found on the exterior of its structure. The higher molecular weight sesquiterpenes are predictably the last to elute. However, terpineol and 4-allylanisole which have slightly higher molecular weights than the monoterpenes, elute before them. Terpenoid alcohols have been reported to be included more into β-CD than terpene hydrocarbons [80]. The hydrophilic hydroxyl group of terpineol would likely be orientated pointing out of the hydrophobic CD cavity [148]. The aromatic ring in the 4-allylanisole is para-substituted which may increase interactions with the CD cavity as an additional methyl group in the para position of phenethylamine increased its affinity to α- and β-CD four-fold [148]. Aromatic rings – except for imidazole interact more with β-CD than α-CD [148]. The methoxy group present in 4-allylanisole also contributes more to the association constant of a CD complex than a methyl group as suggested in another paper by Rekharsky *et al*. [155]. The migration order of the analytes was found to correlate with their LogP values (see Table 3-1); the lower the value the earlier the analytes migration time. This shows that, in this case, the analytes hydrophobicity is more significant than molecular weight in influencing their migration order. Studies found that LogP values generally did not correlate with CD complex stability [149].

Table 4-2 Association constant values for analyte:CD complexes for the three linearization methods

	β-CD			MECD		γ-CD	
	K (M^{-1})	R^2	K(M^{-1}) [a]	K (M^{-1})	R^2	K (M^{-1})	R^2
Terpineol							
Double reciprocal	113.9	0.934		121.2	0.999	242.3	0.708
Y reciprocal	56.7	0.251		128.1	0.960	4.8	0.001
X reciprocal	43.1	0.137		1235	0.930	-2.2	0.000
4-allylanisole							
Double reciprocal	77.4	0.914		30.4	0.997	213.7	0.756
Y reciprocal	11.8	0.012		35.2	0.487	-8.2	0.003
X reciprocal	2	0.000		295	0.363	-23.9	0.031
Camphene							
Double reciprocal	-56.5	0.987	6040	-94.9	0.998	-4.0	0.948
Y reciprocal	-61.6	0.558		-83.8	0.870	-77.4	0.489
X reciprocal	-65.5	0.674		-826	0.905	-89.2	0.791
β-pinene							
Double reciprocal	-65.7	0.989	6120	-112.2	0.997	-44.7	0.959
Y reciprocal	-68.6	0.625		-96.9	0.870	-105.1	0.675
X reciprocal	-71.8	0.729		-941	0.909	-118.4	0.930
3-carene							
Double reciprocal	-89.1	0.989		-144.1	0.994	-165.9	1.000
Y reciprocal	-90.1	0.729		-122.4	0.864	-163.6	0.996
X reciprocal	-91.6	0.822		-1163	0.920	-163.7	1.000
α-pinene							
Double reciprocal	-113.4	0.993	6080	-146.4	0.995	-138.6	0.995
Y reciprocal	-100.6	0.764		-126.7	0.883	-156.1	0.964
X reciprocal	-101.2	0.821		-1206	0.937	-162.2	0.998
Longifolene							
Double reciprocal	-336.8	0.802		-588.9	0.529	-126.9	0.995
Y reciprocal	-290.6	0.367		-573.8	0.653	-128.1	0.900
X reciprocal	-204.2	0.890		-5647	0.869	-141.8	0.983
Isolongifolene							
Double reciprocal	-707.2	0.401		13.4	0.985	-570.7	0.357
Y reciprocal	-879.6	0.393		-19.7	0.142	279.5	0.021

X reciprocal	-602.4	0.843		-240	0.250	-219.8	0.901
Aromadendrene							
Double reciprocal	-970.8	0.163		-418.5	0.592	-803.9	0.410
Y reciprocal	-943.7	0.239		468.6	0.220	518.3	0.106
X reciprocal	-558.6	0.810		-3156	0.941	-269	0.769
Abietic acid							
Double reciprocal	338.1	0.984		-95.1	0.996	1034.9	0.998
Y reciprocal	449.9	0.971		-77.0	0.825	1001.6	0.999
X reciprocal	358.6	0.852		-769	0.892	1023.1	0.995
Dehydroabietic acid							
Double reciprocal	292.1	0.773		-214.5	0.943	553.0	0.865
Y reciprocal	54.1	0.085		-174.8	0.675	369.1	0.833
X reciprocal	19.6	0.012		-1639	0.911	302.8	0.510

a) Association constant values found in literature [104]

However, the association constants calculated from the double, Y and X reciprocal plots were negative values for all the neutral compounds except terpineol and 4-allylanisole. This is unexpected as negative association constants generally indicate a lack of complexation between the CD and analytes. Contrary to this, the earlier migration times of the analytes and the improved separation of some of the analytes with increasing CD concentration support the hypothesis that the analytes are interacting with the CDs. The double bond in α-pinene is located in a ring, making it more rigid than its structural isomer β-pinene which may contribute to a more stable complex so a higher association constant would be expected [104]. Similarly, 3-carene also contains a ring with a double bond and so its association constant would be expected to be higher than that of β-pinene [104]. β-CD has been shown to form more stable complexes with cycloalkanes compared to α- and γ-CD with higher association constants than their corresponding linear equivalents [80]. The constants formed between β- and γ-CD and cyclic compounds increases with an increasing number of carbons in the ring [80].

4.3.4 MECD

As seen with β-CD, the analyte mobilities increased with increasing concentration of MECD (Figure 4-7), again indicating that the presence of CDs result in the analytes interacting less with the micelles.

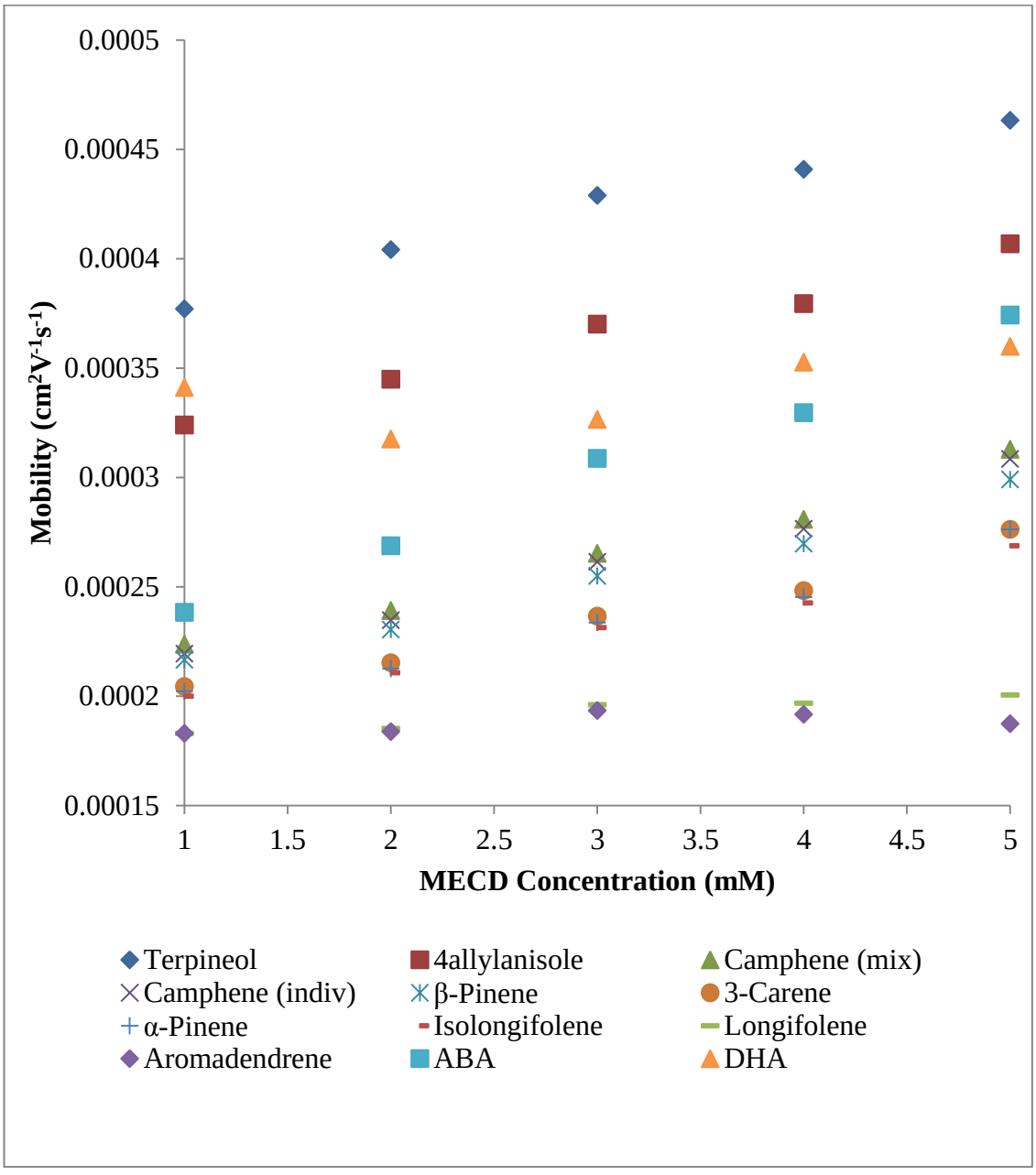

Figure 4-7 Plots of mobility ($cm^2V^{-1}s^{-1}$) versus MECD concentration

In general, modification of a CD improves its solubility and interactions [82]. MECD has methyl groups substituted on carbons 2, 3 or 6 which converts some of the hydrophillicity of the CD cavity ends to a more hydrophobic nature [80]. The modification of CDs usually improves the separation of analytes, with a methylated CD possibly allowing for additional hydrophobic interactions. However, in this case the majority of analytes are terpenes which have no functional groups to interact with. As seen in Figure 4-3, the elution order of the analytes is the same with and without MECD present. 3-carene and α-pinene were found to coelute, unsurprising due to their similar structures which both contain a six-membered ring with a double bond. However, these two analytes separate in a buffer containing SDS without MECD suggesting that the CD is reducing the analytes interaction with the micelles. Another noticeable change is that longifolene and aromadendrene were separated with MECD present whereas SDS alone could not achieve this separation. The methyl groups on the CD provide more interaction for the analytes. When compared with the non-derivatized β-CD, it appears that the presence of the methyl groups has the effect of reducing the interactions between the CD and longifolene.

As seen in Table 4-2, the association constants for the majority of the neutral compounds are negative. Terpineol and 4-allylanisole show the highest association constant from the X-reciprocal plots, 1235 and 295 M^{-1} respectively. In this case, isolongifolene also gives a positive value of 13.4 M^{-1} from the double reciprocal plot while the Y and X reciprocal plots give negative values.

4.3.5 γ-cyclodextrin

It was found that (Figure 4-3) there is little separation and poor peak shapes when a γ-CD buffer was used for analysis. The inner diameter of a γ-CD cavity is 7.5-8.3 Å [82], and while it is large enough to accommodate the analytes it is perhaps less sterically suitable as its large cavity can be unsuitable for complexing with a single guest molecule [80]. If the analyte is too small relative to the CD size it will not bind tightly, often seen with small organic compounds which form weaker complexes with γ-CD than with α-CD [88, 156]. An example is adamantane, which is too big to fully fit into α-CD but fits in both β- and γ-CD. The affinity for adamantane to β-CD

is rough 100 times higher than its affinity for α-CD, but its affinity decreases slightly for γ-CD [148].

However, it is also clear from Figure 4-3 that the migration times of the analytes have been reduced greatly, indicating that the analytes interactions with the micelles are being reduced. As stated earlier, micelle-like aggregates can be formed by the CDs [129]. It is also possible that more than one analyte is entering the CD cavity at one time, decreasing migration time but with little resolution or efficiency as γ-CD is known to form 1:2 guest:CD complexes [145]. The larger cavity width of γ-CD could also allow both an analyte and a surfactant molecule to enter the cavity at the same time [157] (see Figure 4-4d). Again terpineol and 4-allylanisole are the only neutrals to produce positive association constants. The analyte mobilities increased with increasing cyclodextrin concentration as seen in Figure 4-8.

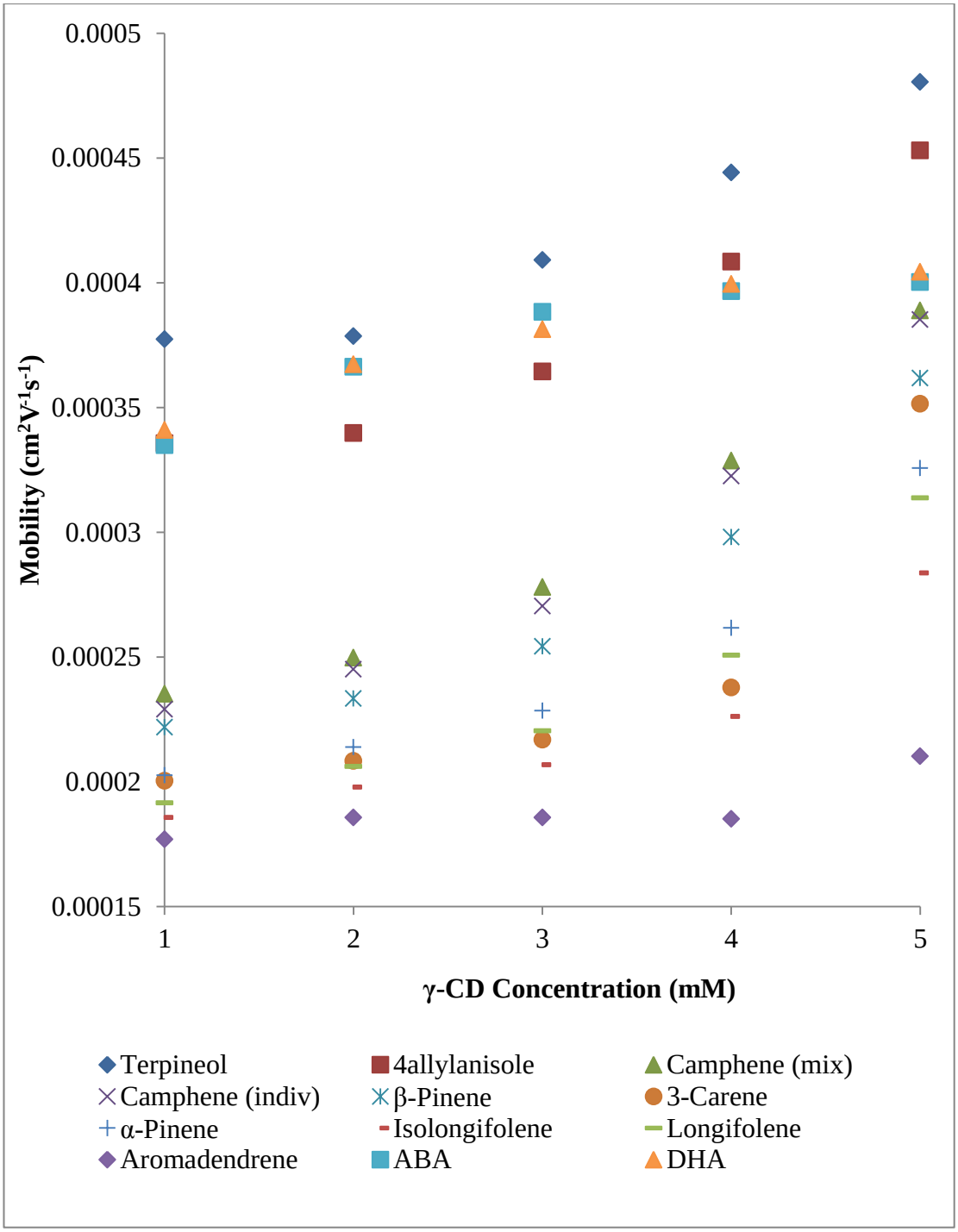

Figure 4-8 Plots of mobility ($cm^2V^{-1}s^{-1}$) versus γ-CD concentration

4.3.6 Comparison of acid and terpene association constants

In order to compare how charged and neutral analytes interact with the CD types, abietic- (ABA) and dehydroabietic acid (DHA) were analysed in the buffers with varying CD concentration. To the authors' knowledge, the stoichiometric guest:CD ratio of resin acids has not been reported previously. However, other terpenic acids including oleanolic acid were reported to form 1:1 guest:CD complexes with β-CD [158].

The acid:CD inclusion complexes form with the charged carboxyl group pointing out of the CD cavity still exposed to the aqueous buffer [148] and the isopropyl part of the acids in the cavity. This isopropyl group is about 4.3 Å in diameter and so can fit into the cavity of all three CD sizes. Dehydroabietic acid has an aromatic ring attached to the isopropyl group which can form a hydrogen bond with one of the hydroxyl groups on the CD. The acids are negatively charged at this high pH unlike the neutral compounds and so they will have their own mobility towards the anode.

The association constants of the inclusion complexes formed between ABA and DHA and several different CD types are reported for the first time in Table 4-2. Unlike the terpenes, positive association constants are seen for the complexes formed between the two acids and the CDs. In general the double reciprocal plots show the highest values with the γ-CD forming higher association constants than the β-CD complexes. The values are higher than those for terpineol and 4-allylanisole. The fused three ring structure of the acids are larger than the neutral compounds investigated and so more suited to form inclusion complexes with the larger cavity where the terpenes could not.

Negative association constants are seen for the acids with MECD. This must be due to the methyl groups on the β-CD as positive constants were seen for the complexes formed with the underivatised CD.

The Y- and X-reciprocal plots of the acids with γ- and β-CD gave positive slopes where the terpenes gave negative slopes and vice-versa (see Figure 4-9). This indicates that the acids and neutral compounds interact with the CDs by different mechanisms, and that the Y- and X-reciprocal plots are less suited to analysing the data of the neutral association constants with CDs.

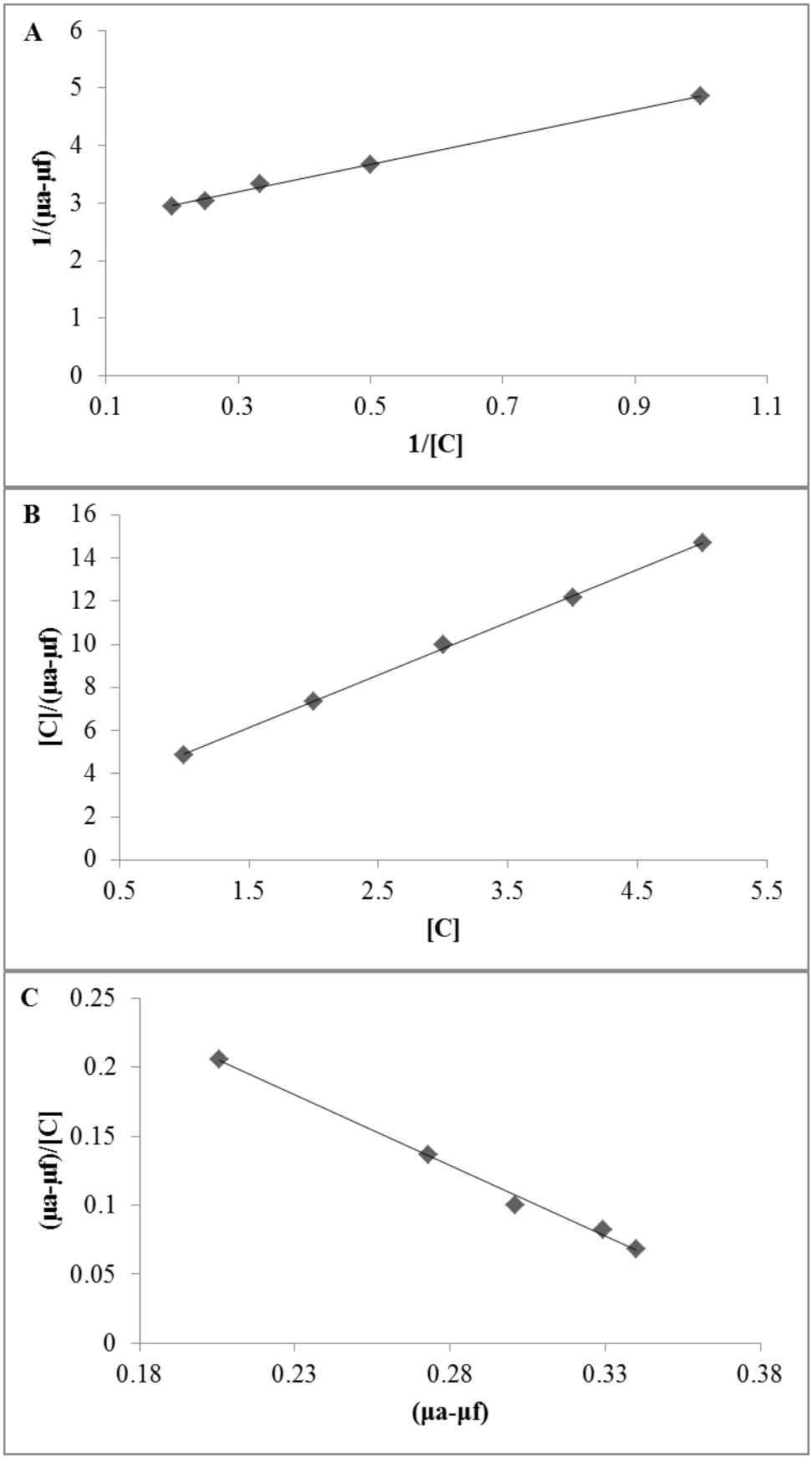

Figure 4-9 (A) Double, (B) Y and (C) X reciprocal plots for ABA. R^2 values were (A) 0.9983, (B) 0.9993 and (C) 0.9945.

4.3.7 Addressing the negative association constants

In order to address the negative association constants, a higher CD concentration was investigated. Although other reports had determined association constants over similar and even smaller CD concentration ranges [132, 136], other papers suggest high CD concentrations are required [132, 137], therefore CD concentrations up to 10 mM were then investigated to contribute more data points to the double, Y and X reciprocal plots.

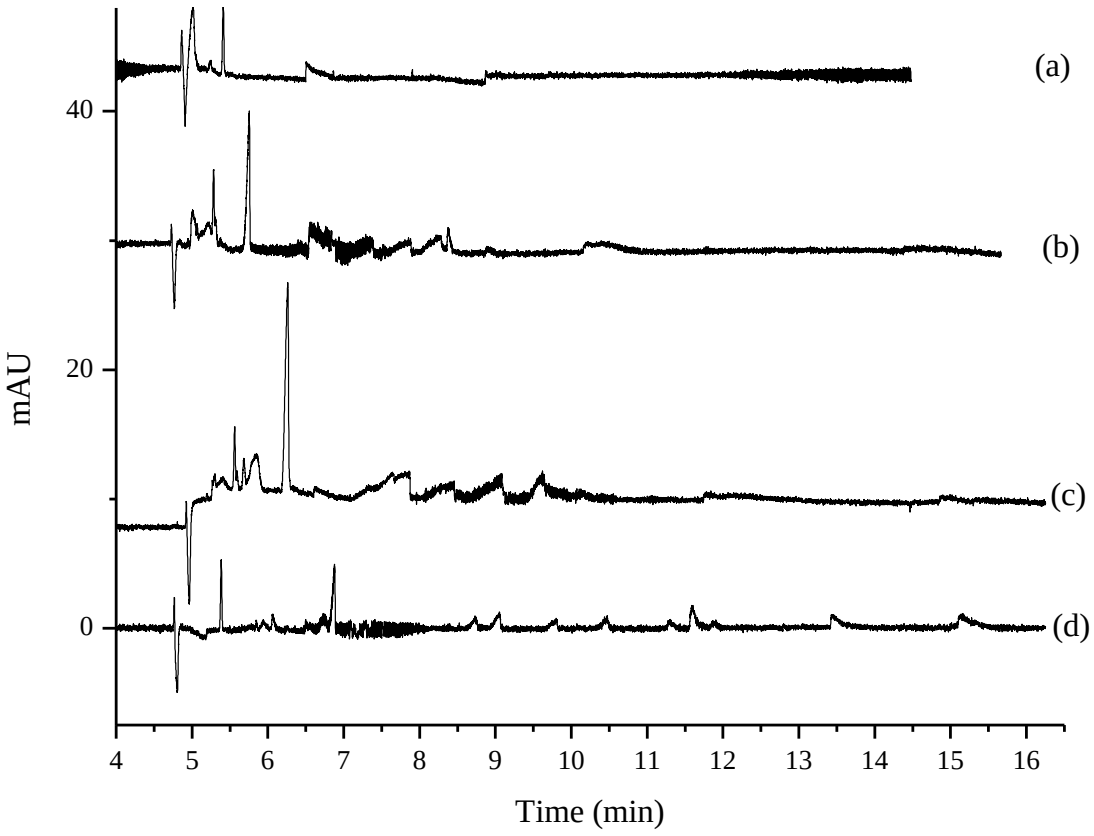

Figure 4-10 Electropherograms of the mixture of nine neutrals analysed at 20 kV, capillary 58 cm (49.5 cm to detector), 50 µm i.d., 25°C, 5 mbar 20 s injection times, detection at 200 nm. Buffers consist of 10 mM SDS buffer with (a) 10 mM, (b) 7 mM, (c) 6 mM and (d) 5 mM β-CD.

From this study it was found that, rather than increased separation, the separation of the neutral mixture deteriorated as the CD concentration was increased (see Figure 4-10).

Consideration was given to the fact that the micelles were being influenced by the increased presence of the CDs and possibly being disrupted. In order to investigate this possibility, the concentration of the SDS was increased to 20 mM and the neutral mixture analysed. The schematic in Figure 4-12 shows the proposed mechanism for the separation in Figure 4-11.

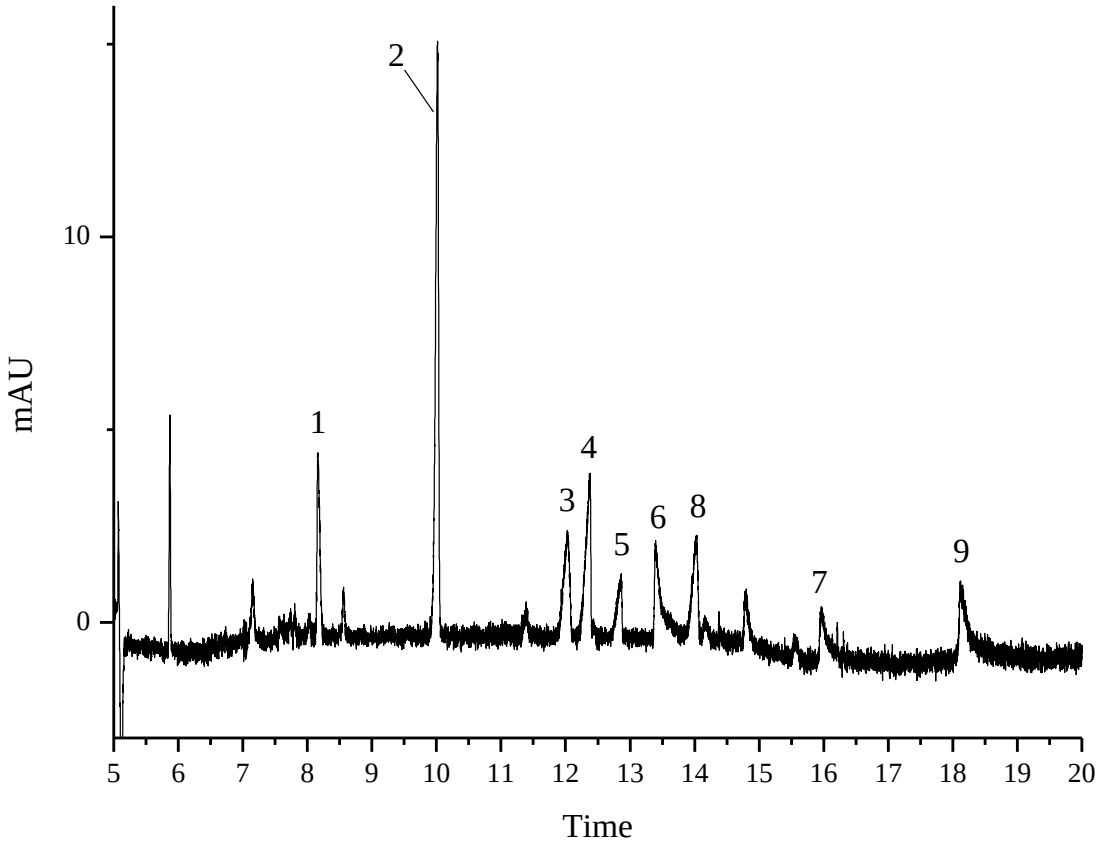

Figure 4-11 Electropherogram of the mixture of nine neutrals analysed at 20 kV, capillary 58 cm (49.5 cm to detector), 50 µm i.d., 25°C, 5 mbar 20 s injection times, detection at 200 nm. Buffer consists of 10 mM β-CD 20 mM SDS 50 mM tris buffer pH 8. Numbers indicate analytes as follows; (1) terpineol, (2) 4-allylanisole, (3) camphene, (4) β-pinene, (5) 3-carene, (6) α-pinene, (7) isolongifolene, (8) longifolene and (9) aromadendrene.

As seen in Figure 4-11, when the SDS concentration was increased to 20 mM, separation of the analytes was achieved with a higher CD concentration where it had not been with 10 mM SDS. This confirms that, as the CD concentration was increased, the critical micelle concentration (CMC) was also increased and so the micelles were no longer being formed at the 10 mM SDS. This is in agreement with

a paper by Cifuentes *et al*. who reported the CMC of SDS in a 10 mM β-CD buffer to be 14.8 mM [118]. The resolution and efficiency values of the electropherogram are seen in Table 4-3.

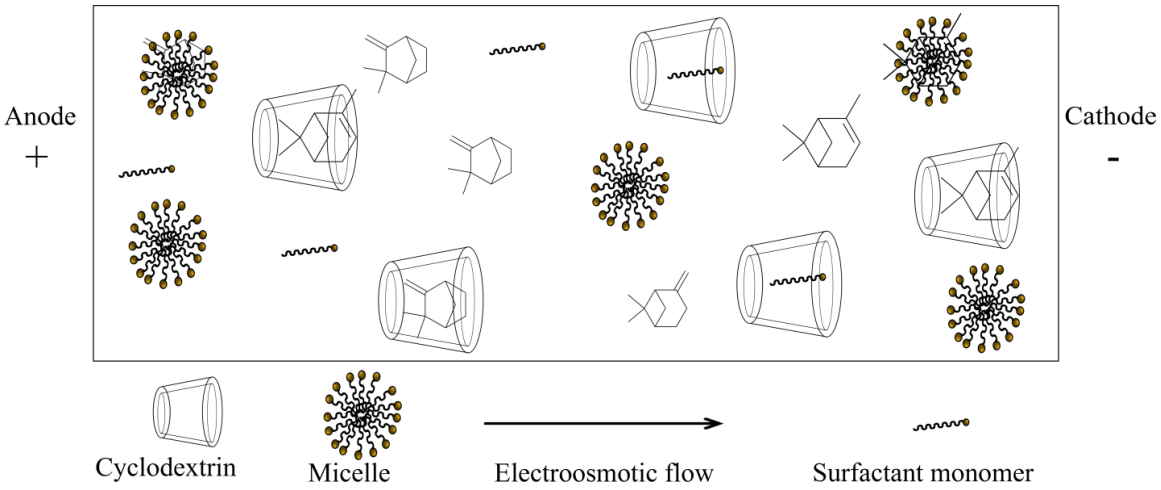

Figure 4-12 Schematic of the proposed mechanism for the separation shown in Figure 4-11.

Table 4-3 Resolution and efficiency values for the electropherogram in Figure 4-11

Resolution (R_s)	**Efficiency (N)**
	121005
19.1	159284
13.9	70574
2.1	120992
3.2	141476
3.6	102771
3.8	111689
10.5	108335
9.0	64518

Although micelles themselves will not partition into a CD cavity due to its hydrophilic outer surface, surfactant molecules (monomers) can form inclusion complexes with CDs. This increases the CMC as the CD cavity competes with the self-aggregation of the surfactants for monomers. When the surfactant concentration is below the CMC, the surfactant monomers and cyclodextrins form a complexation equilibrium (Figure 4-13 a). The concentration of surfactant is increased until it reaches the CMC and micelles can form (Figure 4-13 c). The CMC when CDs are

present is the combination of the concentration of surfactant monomers complexed with the CDs and the concentration of the free surfactants in equilibrium with the micellised surfactants. The analyte partitions into three phases; into the micelle, into the CD and in free solution [129, 159-162]. In this case the neutral analytes partition into the SDS micelles, the β-CD and the aqueous buffer.

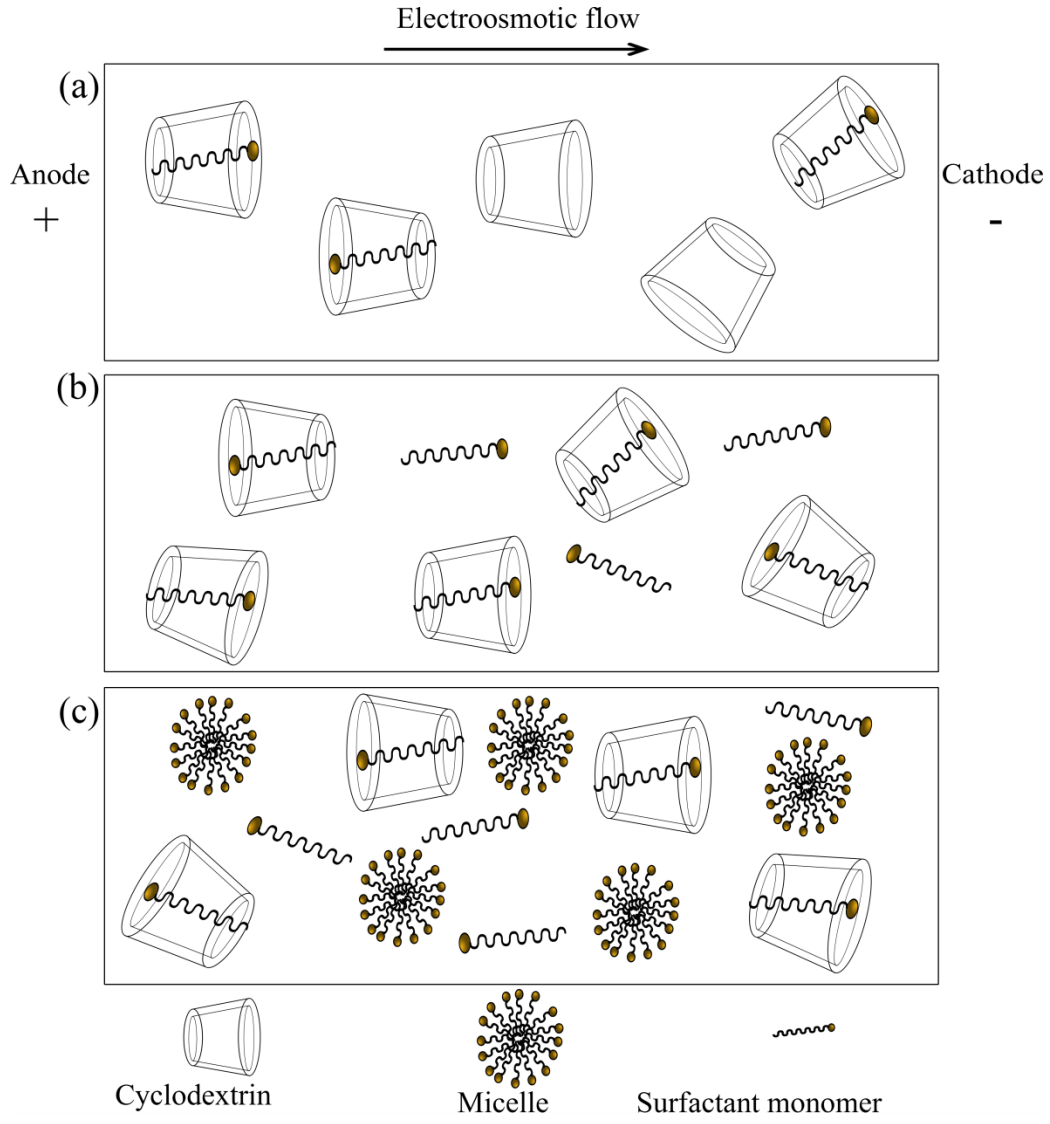

Figure 4-13 Schematic representation of buffer as SDS concentration is increased, adapted from [129].

In the same way that the CMC is increased by surfactant monomers partitioning into CDs instead of micellising, the presence of surfactant monomers in the CD cavities also reduces the interactions between analytes and CDs. α-CD forms mainly a 2:1

CD:surfactant complex while β-CD forms primarily 1:1 complexes with a much lesser amount (>10%) of 2:1 CD:surfactant formed. γ-CD can also form 1:2 CD:surfactant complexes [143, 144, 146, 160]. This suggests that the greatest CMC increase is expected in the γ-CD modified buffer, followed by the β-CD modified and then the α-CD modified buffer as it complexes with less surfactant monomers [163]. The neutrals partition into the CDs less as surfactant monomers are also partitioning into them.

Association constants for SDS-β-CD complexes have been reported from 210 to 25600 M^{-1} [163]. However, the wide range of values reported do not address the formation of complexes other than the 1:1 complexes – with some techniques potentially not sensitive enough to detect the presence of lesser formed 2:1 CD:surfactant complexes [146]. As there is such a wide range of association constants for SDS-CD complexes and so few reported constants for terpene-CD complexes it is difficult to say with certainty which complex will be favoured.

As a higher SDS concentration resulted in separation even when higher CD concentration was used (Figure 4-11), buffers were prepared containing SDS concentrations from 5-30 mM to investigate how separation was affected.

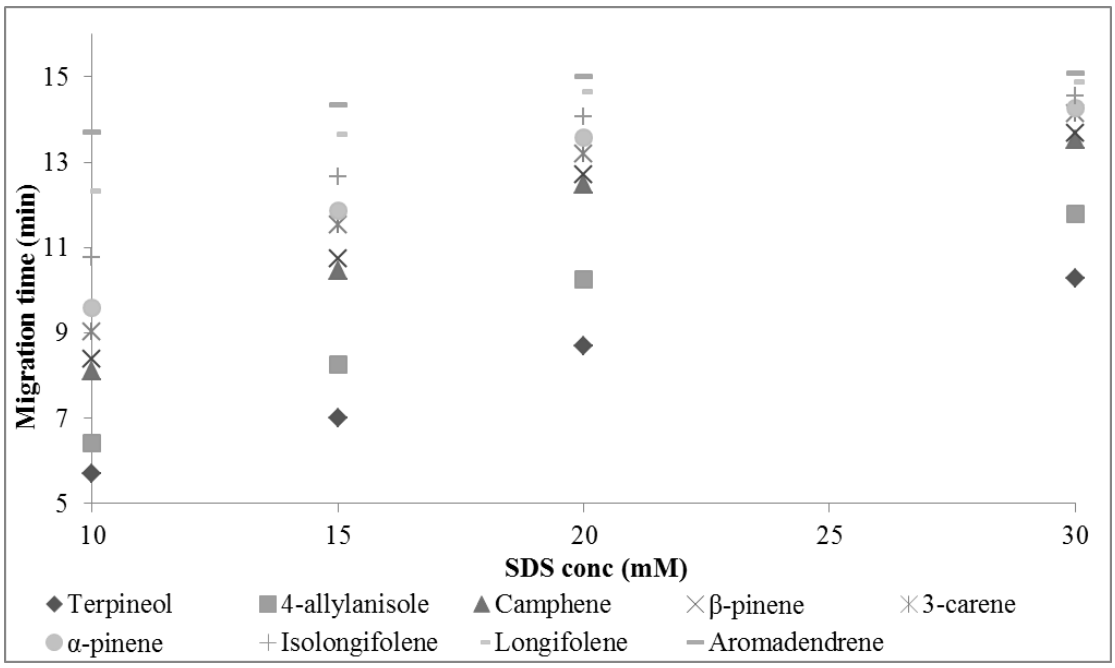

Figure 4-14 Plot of migration times versus the SDS concentration in the buffer. The neutral mixture was analysed at 20 kV, capillary 58 cm (49.5 cm to detector), 50 µm

i.d., 25°C, 5 mbar 20 s injection times. Buffer consists of 5 mM β-CD 50 mM tris pH 8 with 10-30 mM SDS.

Figure 4-14 shows the migration times of the neutral analytes when the β-CD was kept constant at 5 mM and the SDS concentration varied. When the SDS was decreased to 5 mM SDS (10 mM having been used throughout the cyclodextrin concentration variation) there was no separation seen as this was clearly below the CMC. When the SDS concentration was increased the analytes migrate later as expected as the SDS moves against the EOF and the resolution was decreased for all analytes except terpineol and 4 allylanisole (see Table 4-4).

Table 4-4 Resolution and efficiency values for the electropherogram as seen in Figure 4-14.

Resolution (R_s)				**Efficiency (N)**			
10 mM SDS	**15 mM SDS**	**20 mM SDS**	**30 mM SDS**	**10 mM SDS**	**15 mM SDS**	**20 mM SDS**	**30 mM SDS**
7.8	13.9	17.7	17.0	90880	102040	141028	192612
15.6	19.8	20.4	20.6	56570	131726	239495	329846
2.6	2.2	1.8	1.6	90727	100689	138851	388036
5.4	6.9	4.0	4.6	108763	133513	167654	303166
4.1	2.4	3.1	1.1	67344	167123	209201	307164
8.5	4.7	3.0	2.5	89121	83464	189010	372545
9.1	5.7	3.2	2.3	82232	79735	78515	147128
6.0	3.7	2.1	1.6	67822	109592	128857	214358
				40941	75615	105197	261396

The γ-CD buffer was then prepared with a higher SDS concentration to investigate if earlier separations had been carried out containing SDS at a concentration lower than the CMC.

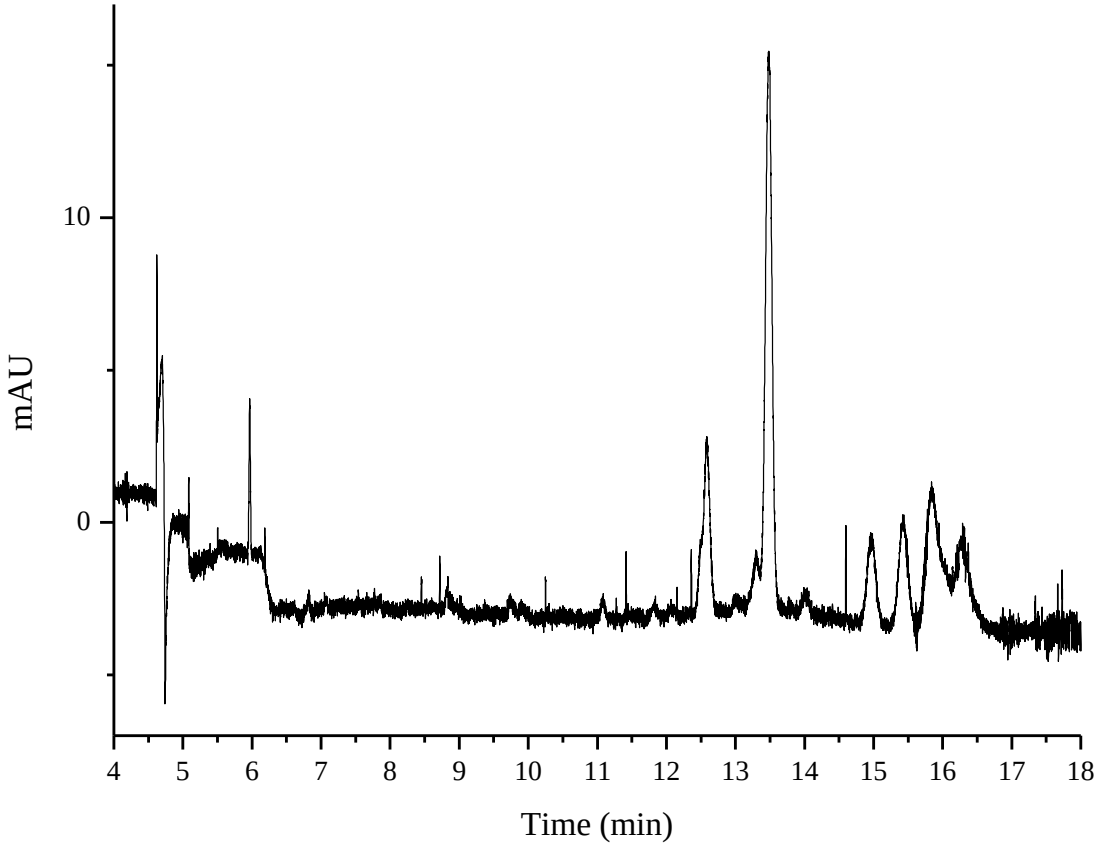

Figure 4-15 Electropherogram of the mixture of nine neutrals analysed at 20 kV, capillary 58 cm (49.5 cm to detector), 50 µm i.d., 25°C, 5 mbar 20 s injection times, detection at 200 nm. Buffer consists of 5 mM γ-CD 50 mM SDS 50 mM tris pH 8.

Figure 4-15 shows the electropherogram of the separation of the mixture of neutrals by a tris buffer containing 5 mM γ-CD 50 mM SDS. In contrast with the separation using a 5 mM γ-CD 10 mM SDS tris buffer (see Figure 4-3b), the peaks are sharper and better resolved. The migration times are also longer, suggesting that in a buffer containing γ-CD the CMC was not reached at 10 mM SDS while at 50 mM SDS micelles have formed. They travel against the EOF as the analytes partition in and out, resulting in longer migration times. This is consistent with literature, as Bendazzoli *et al.* determined the CMC of SDS in a buffer containing 10 mM γ-CD to be 21.4 mM [163].

As the association constants were not giving positive values as expected from the separation, different possible causes were investigated. The present of the SDS was clearly more involved in the separation than initially hypothesised so the effect of the addition of alcohol on the separation was investigated. It was expected that as the

methanol percentage was increased it would increasingly disrupt the micelles as methanol has been reported to increase the CMC of SDS [143].

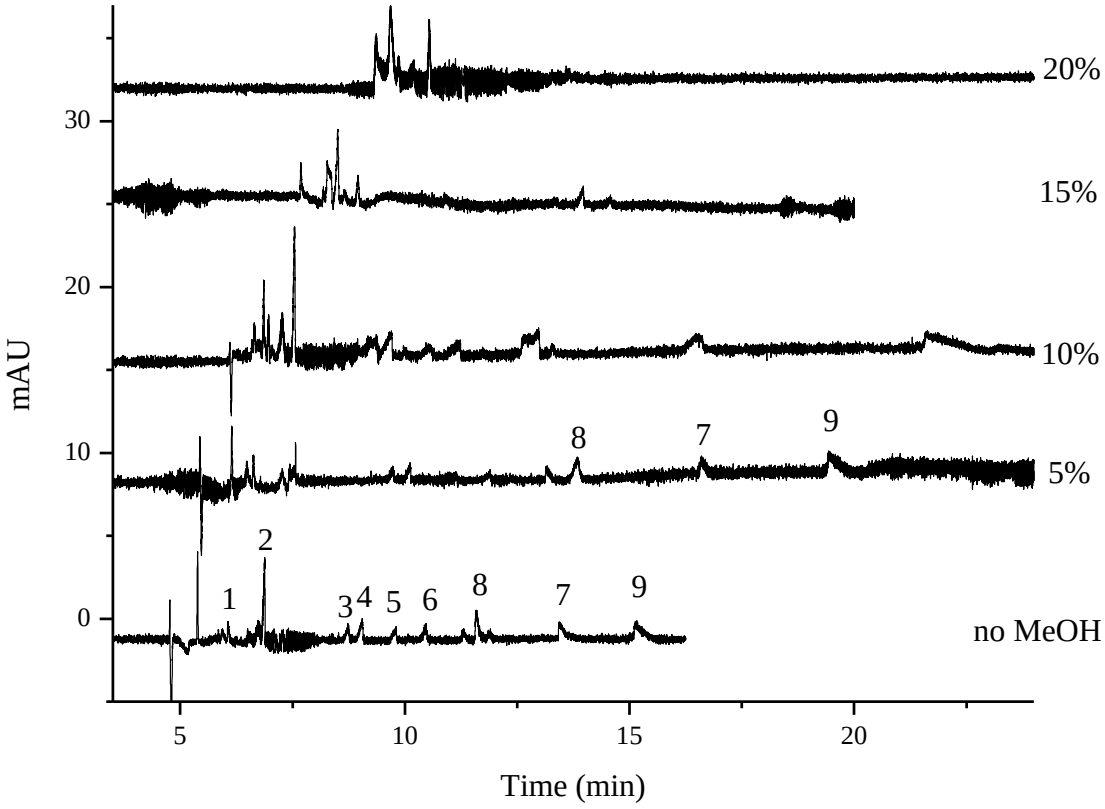

Figure 4-16 Electropherograms of the mixture of nine neutrals analysed at 20 kV, capillary 58 cm (49.5 cm to detector), 50 µm i.d., 25°C, 5 mbar 20 s injection times, detection at 200 nm. Buffer consists of 5 mM β-CD 10 mM SDS 50 mM tris pH 8 with varying % of MeOH as described in figure. Numbers indicate analytes as follows; (1) terpineol, (2) 4-allylanisole, (3) camphene, (4) β-pinene, (5) 3-carene, (6) α-pinene, (7) isolongifolene, (8) longifolene and (9) aromadendrene.

As seen in Figure 4-16, with 5% MeOH in the buffer there is slightly increased resolution for the last three peaks (longifolene, isolongifolene and aromadendrene) but as it is further increased the separation deteriorates with everything migrating at the EOF (the EOF migrates later with increased MeOH). This confirms that the MeOH has disrupted the micelles by increasing the CMC enough that 10mM is now below the CMC. Resolution and efficiency values are shown in Table 4-5.

Table 4-5 Resolution and efficiency values for the electropherogram as seen in Figure 4-16

Resolution			**Efficiency (N)**		
no MeOH	**5% MeOH**	**10% MeOH**	**no MeOH**	**5% MeOH**	**10% MeOH**
7.8	6.7	9.6	90880	171938	193801
15.6	15.4	11.5	56570	39979	171553
2.6	2.4	1.3	90727	54250	21125
5.4	6.2	3.6	108763	67089	21626
4.1	4.9	2.6	67344	89186	30151
8.5	8.9	6.4	89121	62623	28326
9.1	11.4	11.8	82232	50138	34210
6.0	9.5	11.3	67822	81753	35675
			40941	47155	21727

4.4 Conclusions

Affinity capillary electrophoresis was used for the first time to investigate the association constants for a range of natural products present in rosins with α-, β-, γ- and methyl-β-CD. The mobilities of the analytes in buffers containing 10 mM SDS and 1-5 mM CD were recorded. However, when three different linearization plotting methods were applied to the data, negative association constants were obtained for the majority of the neutral analytes. As the electropherograms showed that separation was in fact being achieved, it was concluded that the presence and concentration of the CDs was not the only significant contributing factor to the separation of the mixture.

The migration order of the neutral analytes correlated with their LogP values; the lower the value the shorter the analytes migration time. This shows that in this case the analytes hydrophobicity is more significant than molecular weight in influencing their migration order. However, the values could not be used to predict migration time as the analytes structures also affected their interactions with the CDs.

The association constants of two resin acids were determined by the use of affinity capillary electrophoresis and the double-,Y- and X-reciprocal plotting methods and reported for the first time. Inclusion complexes with γ-CD gave the highest values, 1035 and 553 M^{-1} for ABA and DHA respectively. The complexes formed with MECD were found to give negative association constants with the acids.

The effects of surfactant and cyclodextrin concentration in the separation buffer were also investigated. It was found that as the CD concentration was increased, surfactant monomers partitioned into the CD cavities, resulting in the formation of less micelles when the SDS concentration was not increased accordingly. The CMC increased as the CD cavities competed with self-aggregation of SDS for surfactant monomers. This had resulted in the disruption of micelles and poor resolution. During the determination of the association constants of the charged acids, the acids had their own mobility whereas the neutral compounds depended on the micelles for mobility and so were affected more as the CMC was increased. For this reason, this method of association constant determination was successful for the acids but not the neutral terpenes. The addition of methanol to the buffer was also found to reduce separation

by increasing the CMC of SDS. The CD-SDS interactions were found to be more significant to the separations than initially hypothesised.

Capillary electrophoresis was found to be a suitable method for the determination of association constants of charged analytes which provides quantitative information on the affinity of the analytes for the cyclodextrins. Association constant information could aid in the approach to optimising a separation method. The neutral analytes required the presence of a charged surfactant to provide mobility; however, the effect of the increased addition of CDs to the buffer inhibited the formation of micelles.

Chapter 5

Application of developed separation methods to natural and modified samples of rosins and resins

5.1 Introduction

5.1.1 Sources of natural samples

Natural products are produced through secondary metabolism by plants and animals [69], for example resins are produced by pine trees. As described in section 1.2, when the volatile oils have been distilled from resin, rosin is the solid that remains. The volatile portion removed is known as turpentine [1]. Resins are also known to contain resin acids.

Resins have a very wide range of applications in multiple industries including cosmetics, pharmaceuticals, glues, varnishes and adhesives. GC-MS and spectroscopic techniques are the most common analysis methods of natural resins [53, 164-166]. There are a few reports on the analysis of resins by CE [57, 59]. In this chapter the separation methods developed in chapters 2 and 3 are applied to a range of modified and unmodified rosins, and resin samples for the first time.

5.1.2 Rosin crystallisation

As described in section 1.2.2, problems can arise when natural rosin samples are used in industry. Their industrial applications include varnishes, adhesives and as solder flux. Reported issues in these areas are associated with the tendency of rosins to crystallise, which reduces the value of the raw material and may exclude it from certain applications.

At present there are rough tests carried out by Henkel to predict an unmodified rosins tendency to crystallise, such as the resin acid balance test (described in section 5.3.3) and the acetone crystallisation test (section 5.2.5). However, batches which pass these tests can sometimes crystallise at a later period and even after inclusion in a product which can have a significant impact on its efficacy.

5.1.3 Aims

The aim of this research is to investigate the composition of various natural and modified rosin and resin samples. The objectives are to apply the two separation methods developed in chapters 2 and 3 to the samples and to use spiked samples and multiwavelength analysis to identify specific acids in rosin and resin electropherograms. Calibration curves will be used to quantify the acids present. Links between the composition of rosins and their tendency to crystallise will be examined. The crystallisation of both modified and unmodified rosin samples will be investigated and any resulting precipitate analysed.

5.2 Experimental

5.2.1 Instrumentation

CE instrumentation is as described in section 3.2.1.

5.2.2 Reagents

The reagents used are as described in sections 2.2.2 and 3.2.2. In addition; rosin samples were donated by Henkel Ireland Ltd., (Dublin, Ireland). Music and cello rosins were purchased from Waltons, (69 South Great George's street, Dublin 2, Ireland). Turpentine oil was purchased from O'Sullivan Graphic Supplies, (Camden Street, Dublin 2, Ireland). Balsam resin and venetian turpentine were purchased from K&M Evans art supplies, (Meetinghouse Lane, Dublin 7). Buffers were prepared in deionised water.

5.2.3 Sample and buffer preparation

For analysis by the acid method fresh samples were prepared daily at 0.1% w/v by dissolution in 100% methanol. For analysis by the neutrals method, samples were dissolved in 1:5 MeOH: 5 mM β-CD 10 mM SDS 50 mM tris buffer at pH 8.

Tris buffers were prepared to the required concentration and pH by mixing appropriate amounts of tris HCl and tris base in distilled water following the Sigma-Aldrich tris buffer mixing table e.g. a 50 mM tris buffer at pH 8 was prepared by mixing 4.44 g L^{-1} tris HCl and 2.65 g L^{-1} tris base. All buffers were filtered through a 0.2 μm nylon membrane filter. Buffers were sonicated for 15 min.

5.2.4 CE separation conditions

For the acid method, CE separations are as described in section 2.2.4. For the terpene method, CE separations are as described in section 3.2.4.

5.2.5 Acetone test

The acetone test described in a Henkel internal test method calls for 10 g of the rosin sample (free from powder) to be placed in 10 mL of acetone in a sealed jar at room temperature.

5.3 Results and discussion

5.3.1 Rosin samples

Both natural and modified gum rosin samples were analysed using the optimised acid separation conditions described in chapter two (samples are listed in Table 5-1 and Table 5-2). The acids present were identified by spiking the rosin samples and their content quantified. The acids' different spectral properties were also exploited to aid in peak identification. The RSD values for the acids' migration times were found to increase slightly to 1.7-3.2% when the method was applied to the natural samples compared to the values when applied to a standard mixture (0.2-1.2%). Peak shapes can be affected by the concentration of other analytes by electromigration dispersion.

Table 5-1 Names of rosin and resin samples from sources other than Henkel

Sample ID	Name	Source
Music	Music rosin	Waltons music
Cello	Hidersine 3C Cello rosin	Waltons music
Turpentine oil	Daler-Rowney turpentine oil	O'Sullivan Graphic Supplies
Venetian turpentine	Sennelier Terebenthine de Venise	K&M Evans art supplies
Balsam resin	Oudt-Hollandse Olie-verwenmakerij Balsam Hars	K&M Evans art supplies

Table 5-2 Rosin samples provided by Henkel

Sample ID	Name	Batch	Acid value (mg KOH g^{-1})	Softening point (°C)	Notes	CAS	Rosin type
YT201A	YT-201 (A)	1310074	130.9	100		65997-05-9	Polymerised
YT201B	YT-201 (B)	1220465	123.0	100	Low acid value	65997-05-9	Polymerised
YT201C	YT-201 (C)	1320591	129.0	102	Low acid value	65997-05-9	Polymerised
YT201D	YT-201 (D)	1241218	139.0	101		65997-05-9	Polymerised
YT201E	YT-201 (E)	1220617	130.6	102	Close to lower specification limit	65997-05-9	Polymerised
YT201F	YT-201 (F)	1310220	142.5	102		65997-05-9	Polymerised
Dymerex	Dymerex	DB11070170	146-158	132-142	Eastman,	65997-05-9	Fully-dimerised
Poly-pale	Poly-pale	650980A	130-155	138-151	Eastman,	65997-05-9	Partially dimerised
Resine K10	Resine K10	1068860	146-158	132-142	Granel S.A.	65997-05-9	Dimerised
RA	RES132	Drum4 IDH380627	n.a.[1]	70-80	Good gum rosin	8050-09-7	Gum
RB	RES132	RN87444A	n.a.	70-80	Good gum rosin	8050-09-7	Gum
RC	RES132	Drum46 IDH380627	n.a.	n.a.	Crystallising	8050-09-7	Gum
RD	RES132	Drum52 IDH380627	n.a.	n.a.	Crystallising	8050-09-7	Gum
RES155	RES155/Disprosin A-100	RN10090457	n.a.	80	Marlin chemicals Ltd	8050-09-7	Disproportionated
Gresinox	Gresinox 578M		n.a.	n.a.		8050-09-7	Disproportionated
A-mod	RES134/KE-604	RN505101	n.a.	129	Marlin chemicals Ltd	8050-09-7	Acid-modified hydrogenated rosin

[1]n.a.= not available

5.3.1.1 Natural gum rosin samples

Four gum rosin samples were analysed using the optimised CE method as described in chapter 2. These included two samples from batches successfully incorporated in industrial products (samples RA and RB) and two from batches known to crystallise (samples RC and RD). The acid peaks in the electropherograms were identified (see Figure 5-1) by spiking the rosin samples.

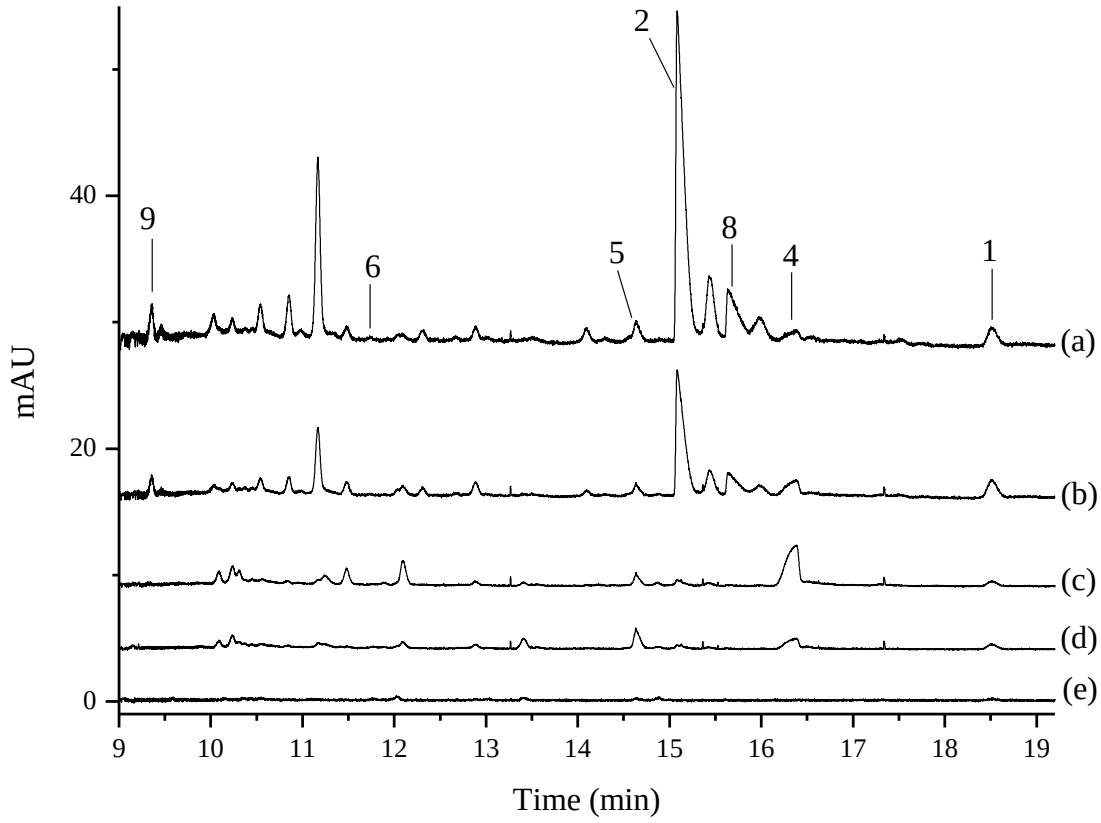

Figure 5-1 Electropherograms of 0.1% w/v gum rosin sample RB, a non-crystallising rosin, analysed in positive polarity, 20 kV, capillary 58 cm (49.5 cm to detector), 50 µm i.d., 25°C, 50 mbar 4 s injection times. Buffer consists of 15% MeOH 5 mM HPγCD 10 mM SBCD in 20 mM tris buffer pH 9. Wavelengths are (a) 200 nm, (b) 214, (c) 240 nm, (d) 265 nm and (e) 310 nm. Numbers indicate (1) 7OXO, (2) DHA, (4) ABA, (5) PAL, (6) LVO, (8) ISO and (9) PIM.

The acid standard calibration curves (seen in section 2.3.6) were used to calculate the concentrations of the acids present in the rosin samples. In the non-crystallising rosin samples it was determined that ABA, DHA and ISO are present in greatest concentrations (see Table 5-3) with the ABA concentration being determined at 240 nm and PAL at 265 nm. PIM, PAL and 7OXO are present in lower amounts. While some of the other acid peaks were also identified, they were present below their LODs and so could not be confidently quantified e.g. LVO. This is the first application of a CE method to rosin samples with the aim of quantifying the resin acids present.

The resin acid concentrations relative to each other can vary between different pine tree species and between different trees of the same species [1]. Different batches of a single gum rosin can also have different relative acid concentrations due to different processing and storage conditions. This is seen in the concentration of ABA and PAL which varied by 33% and 40.8% respectively between non-crystallising samples RA and RB. The other acid concentrations were more constant. The concentrations of ABA and PAL are less consistent as the majority of LVO present in the oleoresin precursor is converted to ABA and PAL, hence the final concentration depends on the extent of isomerisation undergone within the individual rosins [32, 167]. Initially LVO is isomerised in equal measure to PAL and ABA and then PAL can be further isomerised to ABA [33]. While sample RA contained more DHA than ABA, the opposite was true for sample RB. The other peaks present in the electropherogram could be attributed to the neutral compounds present in rosin, such as terpenes and aldehydes. Derivatives of resin acids such as tetrahydroabietic acid may also be present [87]. Some NEO would be expected, but its absence can be explained by its possible isomerisation to ABA [13]. Together ABA and NEO generally comprise 10-20% of the resin acid fraction [1]. Rosin samples RA and RB contain 18.5 and 25.7% ABA, higher than expected for the RB sample. The crystallising samples were found to contain significantly higher concentrations of ABA (40.3 and 51.5%) than anticipated. PIM is normally 5-10% of the resin acid faction as seen here in the RC and RD samples [1]. However, the acid fractions of the non-crystallising samples were determined to contain 12.8 and 13.2% PIM (see Table 5-3). SAN is normally present as 3% or less of the acid fraction of rosins [1, 49]. None of the gum rosin samples analysed were found to contain SAN. PAL

generally comprises around 20% of the acid fraction [1]. In these samples, the percentage of PAL ranged from 8.1-13.1%, lower than expected.

Table 5-3 Average concentrations and standard deviations for gum rosin samples, n=3

Non-crystallising gum rosin samples						
Acid	Sample RA (mg L^{-1})	SD	% of acid fraction	Sample RB (mg L^{-1})	SD	% of acid fraction
ABA[a]	34.5	2.3	18.5	45.9	4.9	25.7
ISO	53.6	8.5	28.7	51.2	6	28.7
PIM	23.8	3.2	12.8	23.5	2.1	13.2
DHA	47.1	3.9	25.2	38.1	4.5	21.4
PAL	24.5	1.2	13.1	14.5	0.6	8.1
7OXO	3.1	0.4	1.7	5.1	0.2	2.9
Crystallising rosin samples						
Acid	Sample RC (mg L^{-1})	SD	% of acid fraction	Sample RD (mg L^{-1})	SD	% of acid fraction
ABA	108.1	3	40.3	236.7	18.3	51.5
ISO	51	1.3	18.9	75.3	6.4	16.4
PIM	26.7	3.1	9.9	30.1	1.8	6.6
DHA	34.9	0.4	12.9	33.1	1.9	7.2
PAL[a]	21.7	0.8	8.1	40.3	1.5	8.8
7OXO	5.7	0.8	2.1	2.4	0.6	0.5
NEO[a]	20.5	1.9	7.6	41.5	2.2	9.0

[a]ABA and NEO determined at 240 nm, PAL determined at 265 nm, all others at 200 nm

The bar chart in Figure 5-2 highlights the concentration of ABA as the main composition difference of the samples; sample RD contains the highest concentration of ABA, with sample RC also containing more than twice the amount of ABA relative to samples RA and RB. Sample RD also contains higher concentrations of ISO, PAL and NEO. The concentrations of PIM, DHA and 7OXO are consistent in all the samples while NEO is only seen in samples RC and RD.

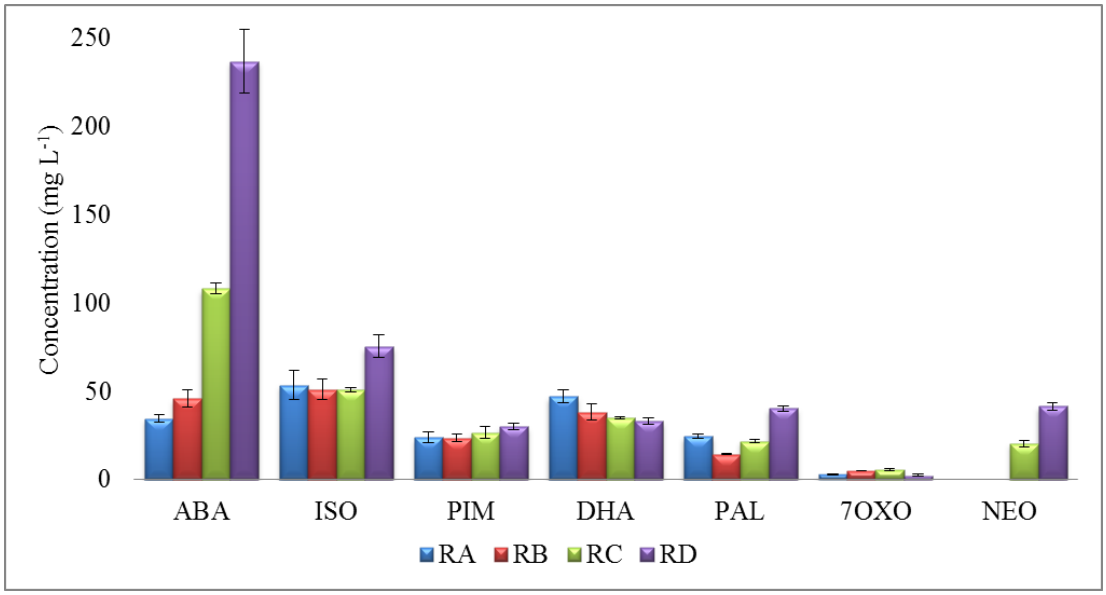

Figure 5-2 Acid concentration plots for samples RA-RD

Figure 5-3 shows the electropherograms for sample RD, a rosin Henkel have classified as crystallising. Greater variations in the compositions of the two crystallising rosin samples were observed in comparison to the non-crystallising samples (see Table 5-3) suggesting that such samples possess a more uniform composition. As with the non-crystallising samples, 7OXO was present in the smallest quantities with 5.7 and 2.4 mg L^{-1} in samples RC and RD. The acids present in highest quantities in both samples were ABA and ISO. The concentrations of PIM and DHA were comparable in samples RC and RD. The concentrations of PIM are 12.2% and 28.1% higher in samples RC and RD than in samples RA and RB. The RSD of the concentrations of ISO in samples RA, RB and RC is more consistent (1.2%). An increase of 48% is seen in the ISO concentration of sample RD. NEO was not identified in non-crystallising samples, however, it was present in notable amounts in both crystallising rosins. The presence of NEO could indicate a rosins tendency to crystallise.

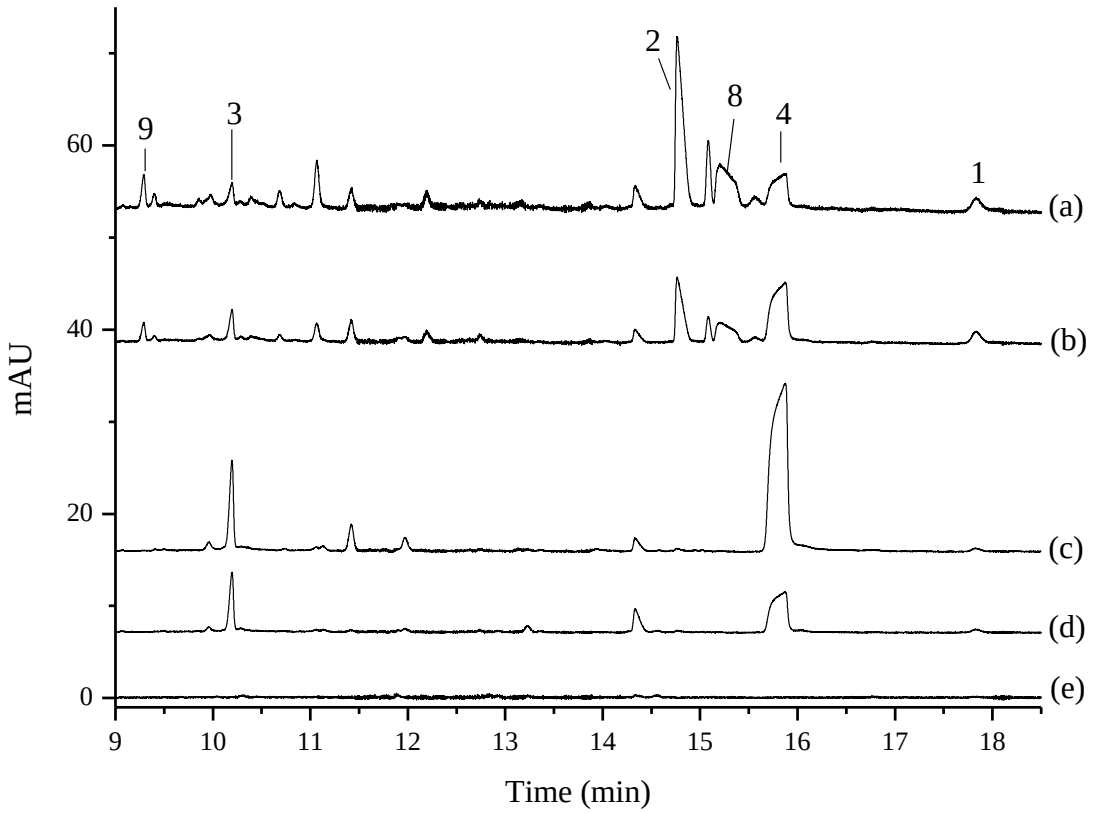

Figure 5-3 Electropherograms of 0.1% w/v gum rosin sample RD, a crystallising rosin, analysed in positive polarity, 20 kV, capillary 58 cm (49.5 cm to detector), 50 µm i.d., 25°C, 50 mbar 4 s injection times. Buffer consists of 15% MeOH 5 mM HPγCD 10 mM SBCD in 20 mM tris buffer pH 9. Wavelengths are (a) 200 nm, (b) 214, (c) 240 nm, (d) 265 nm and (e) 310 nm. Numbers indicate (1) 7OXO, (2) DHA, (3) NEO, (4) ABA, (8) ISO and (9) PIM.

RD was determined to contain twice the amount of NEO compared to RC. The highest PAL concentration was observed in RD, while its concentration in sample RC was similar to that in the non-crystallising rosins. The DHA concentrations in samples RA and RB were higher than those of RC and RD, suggesting that lower DHA concentrations are linked to rosin crystallisation. The concentration of ABA shows the greatest difference between crystallising and non-crystallising samples, from 34.5 and 45.9 mg/L in samples RA and RB to 108.1 and 236.7 mg/L in samples RC and RD. Sample RC contained three times more ABA than sample RA and sample RD contained five times more ABA than sample RB. Both crystallising rosin samples contained more than 30% ABA (Table 5-3) which is consistent with Zinkel's report that ABA contents above 30% is linked to a higher tendency to

crystallise [1]. Neither LVO nor SAN were found to be present above their LODs in any of the crystallising or non-crystallising samples.

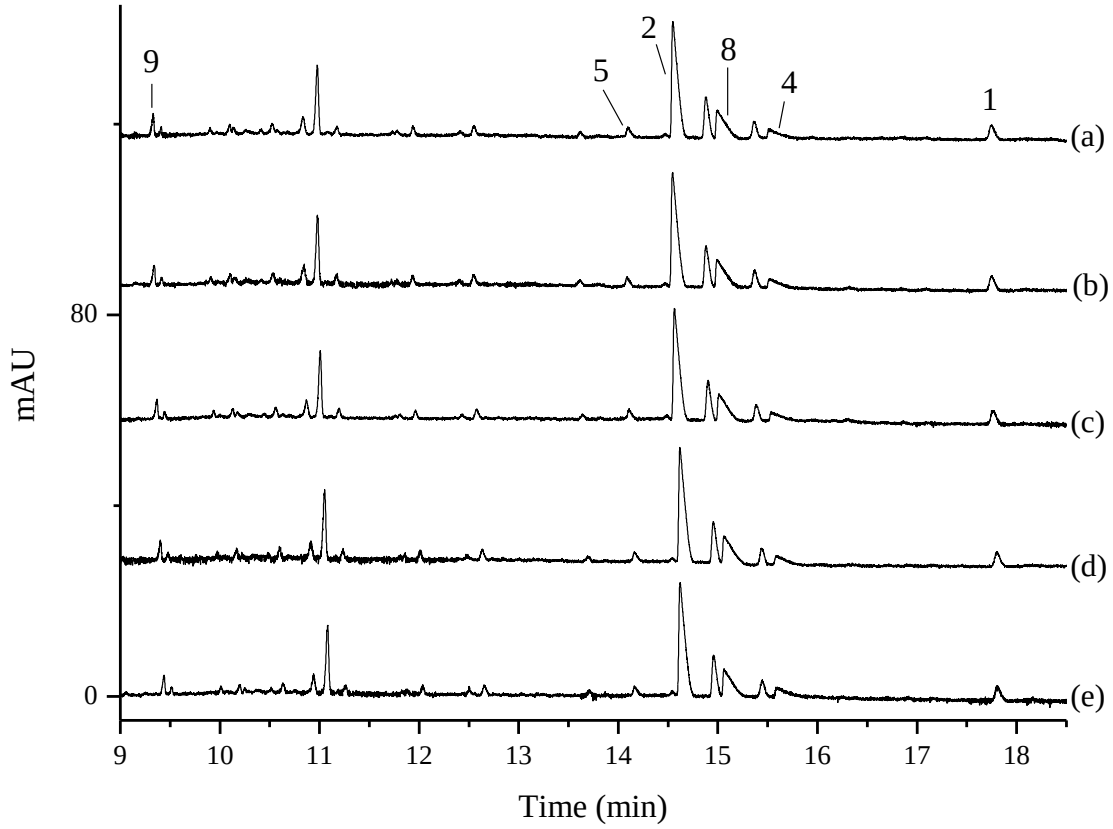

Figure 5-4 Repeat electropherograms a-e of gum rosin sample RB analysed in positive polarity, 20 kV, capillary 58 cm (49.5 cm to detector), 50 µm i.d., 25°C, 50 mbar 4 s injection times. Buffer consists of 15% MeOH 5 mM HPγCD 10 mM SBCD in 20 mM tris buffer pH 9, detection at 200 nm. RSD (%) were found to be 0.4 (PIM), 0.2 (PAL), 0.2 (DHA), 0.2 (ISO), 0.2 (ABA) and 0.2 (7OXO), n=5. Numbers indicate (1) 7OXO, (2) DHA, (4) ABA, (5) PAL, (8) ISO and (9) PIM.

The reproducibility of the method when applied to a gum rosin sample is seen in Figure 5-4 with the migration times RSD values remaining <1%. Considering that reproducibility is generally noted as a disadvantage of CE, these RSD values are comparable if not lower than typical RSD values achieved using GC or HPLC.

The variations of acid concentrations between rosin samples were also evaluated using acid ratios. The ratio of acid concentrations was investigated because of the current rosin suitability predictor test (an internal Henkel method), the resin acid balance (RAB) test. GC-MS is utilised to determine pentafluorobenzyl derivatives of the acids and their concentrations are included in the Equation 9;

$$[(PAL+NEO)/(DHA+ABA)] \qquad \text{Equation 9}$$

A value higher than one is indicative of a non-crystalizing gum rosin whereas a value under one predicts that crystallisation could be an issue. However, this test has only been validated for unmodified gum rosins and is not always accurate – rosins which have passed this test have been observed to crystallise at later stages of production.

When this equation was applied to the concentrations determined using the CE method, the resulting values were 0.3, 0.2, 0.3 and 0.3 for rosin samples RA-RD. Similar values are seen for both the crystallising and non-crystallising rosins, indicating that this equation is not suitable for use with CE analysis of resin acids. Higher ABA concentrations and the presence of Neo was noted in crystallising rosins, and the ABA:NEO ratios in samples RC and RD were 5.3 and 5.7:1.

In Table 5-4, ‘good’ rosin refers to a non-crystallising rosin and ‘bad’ rosin refers to one labelled by Henkel as crystallising. Some of the ratios highlight the differences between the ‘good’ and ‘bad’ rosin samples. The ABA:DHA, ABA:7OXO, ABA:PAL and ABA:PIM ratios show the higher ABA concentrations in the crystallising rosins (highlighted in Table 5-4). Only sample RD contains higher concentrations of PAL and NEO than DHA and their high concentrations are reflected in the PIM:NEO and PAL:7OXO ratios. Samples RA and RB have comparable concentration of ISO and DHA, while RC and RD have higher ISO concentrations. The DHA:PIM ratios show how the DHA concentrations are slightly higher in samples RC and RD while PIM has increased. Samples RA and RB contain more ISO than ABA while the reverse is true for the crystallising rosins. The ISO:PIM, ABA:NEO, NEO:PAL and, to a lesser extent, ISO:PAL ratios remain consistent for all samples. The DHA:7OXO, PIM:7OXO and ISO:7OXO ratios show the similar concentrations of 7OXO in Samples RA and RD and in samples RB and RC.

Table 5-4 Acid concentration ratios of gum rosin samples

	Good Rosin RA	Good Rosin RB	Bad rosin RC	Bad rosin RD
ABA:DHA	1:1.4	1.2:1	3.1:1	7.2:1
ABA:7OXO	11:1	9:1	19:1	98:1
ABA:PAL	1.4:1	3.2:1	5:1	5.9:1
ABA:PIM	1.5:1	2:1	4:1	7.9:1
DHA:PIM	2:1	1.6:1	1.3:1	1.1:1
DHA:ISO	1:1.1	1:1.3	1:1.5	1:2.3
ISO:PIM	2.3:1	2.2:1	1.9:1	2.3:1
ABA:ISO	1:1.6	1:1.1	2.1:1	3.1:1
DHA:7OXO	15.2:1	7.5:1	6.1:1	13.8:1
DHA:PAL	1.9:1	2.6:1	1.6:1	1:1.2
ISO:PAL	2.2:1	3.5:1	2.4:1	1.9:1
ISO:7OXO	17.3:1	10:1	8.9:1	31.4:1
PIM:PAL	1:1	1.6:1	1.2:1	1:1.3
PIM:7OXO	7.7:1	4.6:1	4.6:1	12.5:1
PAL:7OXO	7.9:1	2.8:1	3.8:1	16.8:1
PIM:NEO			1.3:1	1:1.4
7OXO:NEO			1:3.6	1:17.3
NEO:PAL			1:1.1	1:1
ABA:NEO			5.3:1	5.7:1
DHA:NEO			1.7:1	1:1.3
NEO:ISO			1:2.5	1:1.8

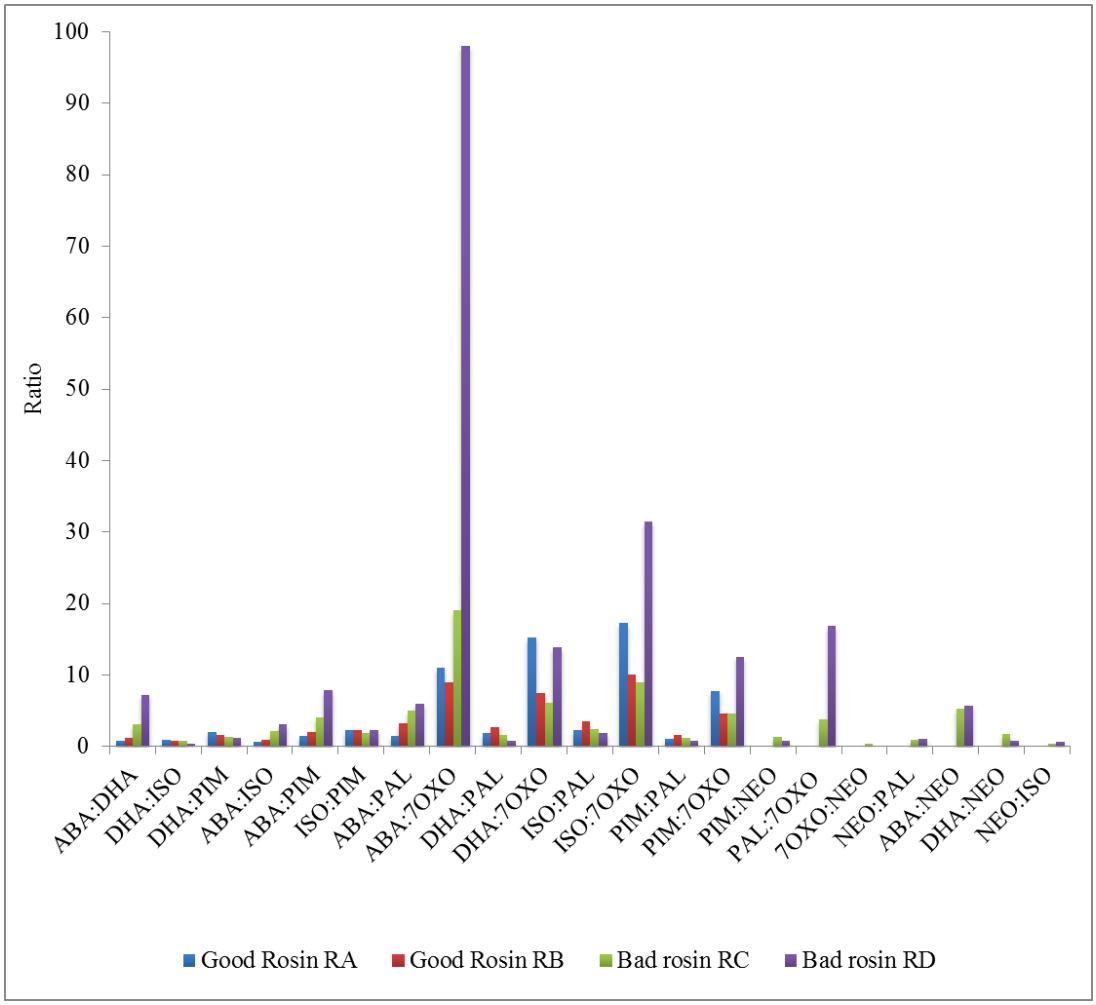

Figure 5-5 Bar plot of acid concentration ratios of gum rosin samples

The acid concentration ratios from Table 5-4 are plotted in Figure 5-5. The higher ABA concentrations of the crystallising rosin samples RC and RD are seen in the ABA:DHA, ABA:ISO, ABA:PIM, ABA:PAL and ABA:7OXO ratios. The DHA:7OXO, ISO:7OXO and PIM:7OXO ratios do not appear to be linked to a crystallisation tendency as in all cases samples RB (non-crystallising) and RC (crystallising) have close values.

As the ABA:7OXO ratio for sample RD is so high it is difficult to observe significant differences in the other ratios. Figure 5-6 highlights some of these ratios.

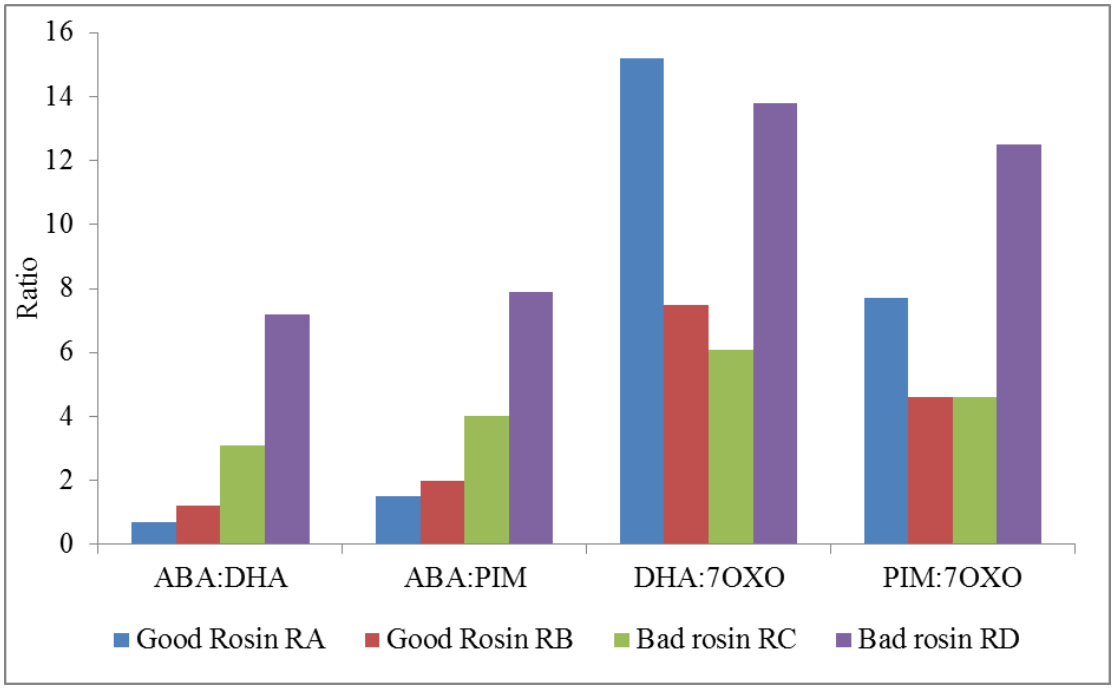

Figure 5-6 Bar plot of some of the acid concentration ratios of gum rosin samples

Rosin samples RC and RD both have higher ABA:DHA and ABA:PIM ratios than the 'good' rosin samples highlighting the increase in ABA concentration in the 'bad' rosin samples. However, the DHA:7OXO and PIM:7OXO ratios did not appear to be indicative of the rosins tendency to crystallise as samples RB and RC had similar ratio values while RA and RD were more comparable.

5.3.1.2 Rosin blocks for musical instruments

Another of the many applications of rosins is as a tool for influencing the friction of the bows of string instruments by rubbing a block of rosin along the bow strings. There are many suppliers of rosin block to music stores, each implying their own 'secret recipe' of additions to the rosin which is never disclosed. Two different rosin blocks were obtained for analysis, named here as 'music rosin' and 'cello rosin'.

5.3.1.2.1 Music rosin

The music rosin selected was a dark green block of rosin with no brand name (Table 5-1).

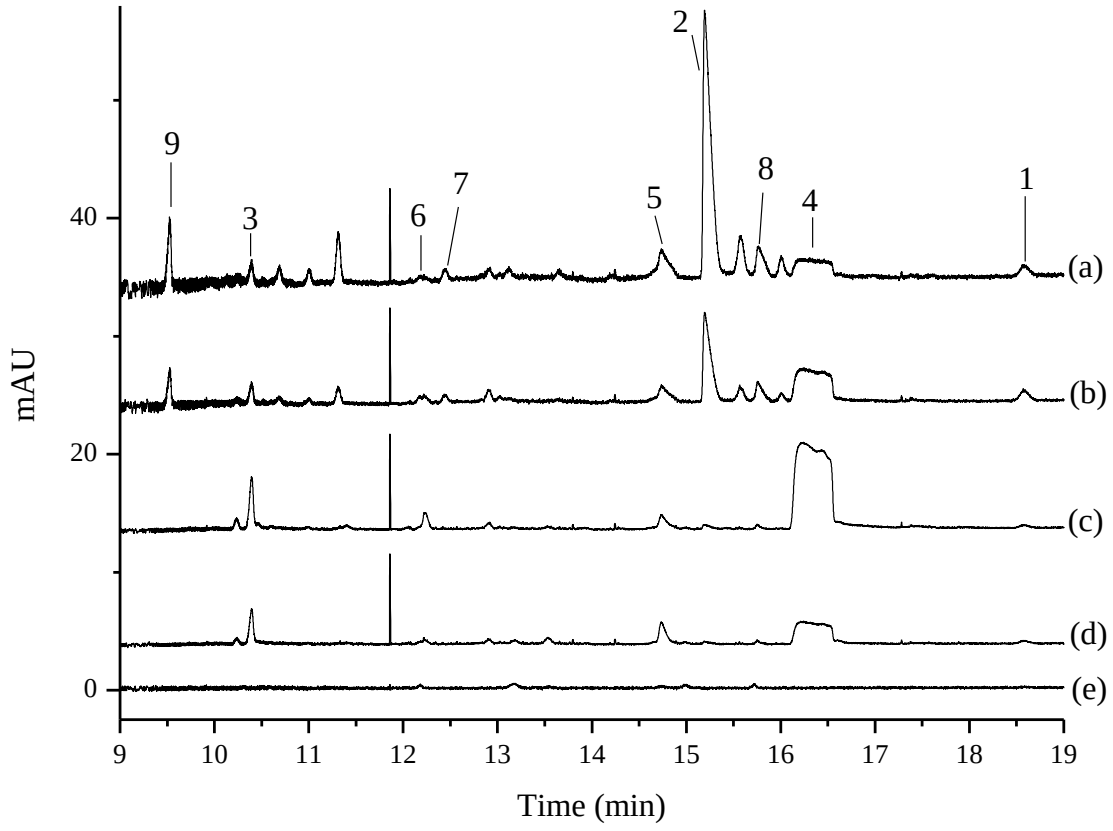

Figure 5-7 Electropherograms of 0.1% w/v music rosin sample analysed in positive polarity, 20 kV, capillary 58 cm (49.5 cm to detector), 50 µm i.d., 25°C, 50 mbar 4 s injection time. Buffer consists of 15% MeOH 5 mM HPγCD 10 mM SBCD in 20 mM tris buffer pH 9. Wavelengths are (a) 200 nm, (b) 214, (c) 240 nm, (d) 265 nm and (e) 310 nm. Numbers indicate (1) 7OXO, (2) DHA, (3) NEO, (4) ABA, (5) PAL, (6) LVO, (7) SAN, (8) ISO and (9) PIM.

Figure 5-7 shows the electropherogram of the music rosin. It is clear that the rosin in question is a natural gum rosin as opposed to a modified one. One of the main differences in this sample compared with samples RA and RB is the presence of NEO. NEO was found to be present in the crystallising samples RC and RD which suggests that this rosin may also have a tendency to crystallise. The NEO concentration was comparable to that of sample RC. Another notable difference is the quantifiable presence of both LVO and SAN which were not found in any of the natural gum rosins. SAN made up less than 3% of the acid as expected [1]. The concentrations of acids present in music rosin are seen in Table 5-5. The RSD values for all concentrations were under 10%. The concentration of PIM in the music rosin was found to be almost twice that of the samples RA-RD. It is also higher than the expected 5-10% of the acid fraction [1]. The ABA and PAL concentrations found in music rosin were higher than those determined in sample RA, RB and RC while the DHA concentration fell within the range seen in the gum rosins. ABA makes up 51.2 and 49.1% of the acid fraction of the music and cello rosin while it is generally reported to make up 10-20% of the acids with NEO [1]. As seen in the gum rosin samples, the percentage of the acid fraction comprised of PAL is lower than the 20% expected [1]. The ISO and 7OXO concentrations were greatly reduced, in the case of 7OXO to 1 mg L^{-1} and less. At 20 mg L^{-1}, the ISO concentration is at least half that found in the natural rosins. The acid concentration ratios are shown in Table 5-6.

Table 5-5 Average concentrations and standard deviations for music and cello rosin samples, n=3

	Music rosin				Cello rosin			
Acid	Conc. mg L^{-1}	SD	Migration time RSD (%)	% acid fraction	Conc. mg L^{-1}	SD	Migration time RSD (%)	% acid fraction
PIM	45.3	4.4	0.5	12.5	56.3	3.2	0.4	11.7
NEO	21.9	0.3	0.5	6.1	37.5	1.4	0.7	7.8
LVO	9.4	0.9	0.6	2.6	6.1	0.2	0.9	1.3
SAN	10.5	1	0.6	2.9	11.4	0.5	0.8	2.4
PAL	28.5	0.5	0.8	7.9	53.4	2	0.9	11.1
DHA	40.4	1.2	0.8	11.1	52.3	2.3	0.8	10.9
ISO	20.0	0.6	0.9	5.5	26.2	1.5	1.0	5.5
ABA	185.9	5	1.0	51.2	235.9	9.9	1.4	49.1
7OXO	0.9	0.1	1.6	0.2	1.0	0.2	0.8	0.2

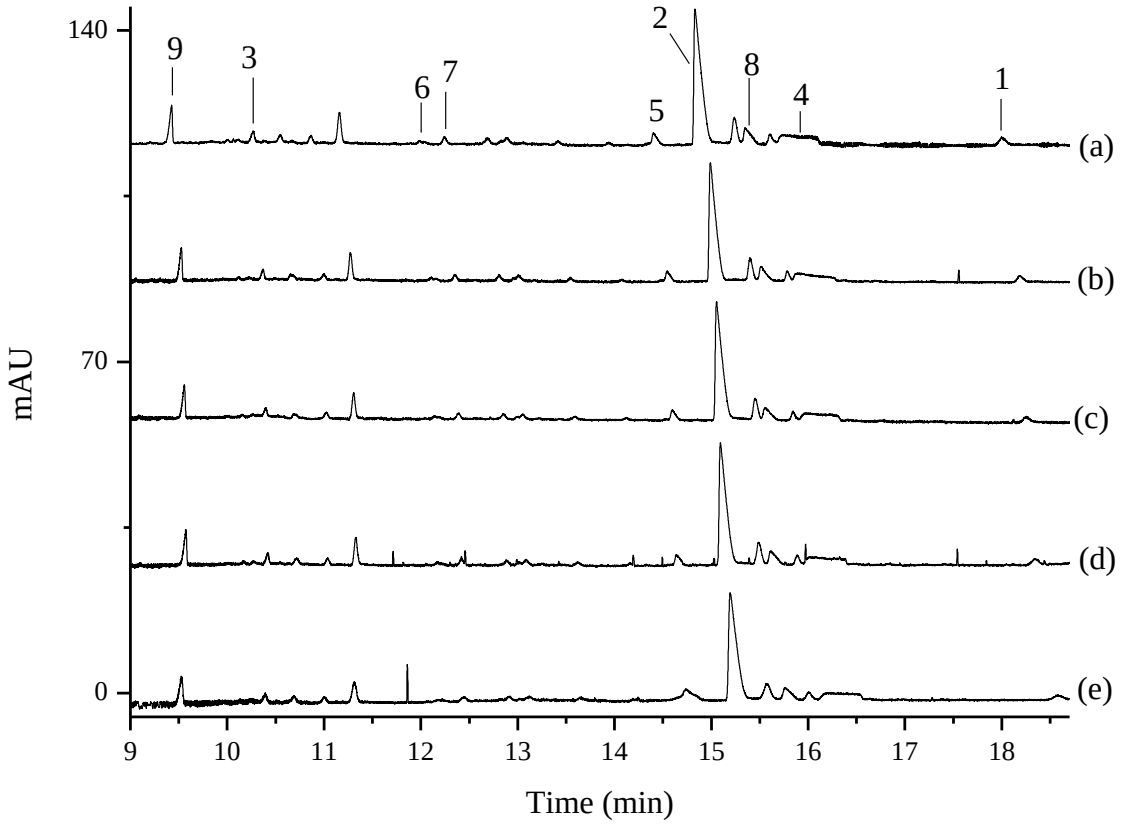

Figure 5-8 Repeat electropherograms a-e of music rosin sample analysed in positive polarity, 20 kV, capillary 58 cm (49.5 cm to detector), 50 µm i.d., 25°C, 50 mbar 4 s injection times. Buffer consists of 15% MeOH 5 mM HPγCD 10 mM SBCD in 20 mM tris buffer pH 9, detection at 200 nm. Numbers indicate (1) 7OXO, (2) DHA, (3) NEO, (4) ABA, (5) PAL, (6) LVO, (7) SAN, (8) ISO and (9) PIM.

The reproducibility of the method when applied to the music rosin sample is seen in Figure 5-8 with the migration time RSD values in Table 5-5 remaining under 2%.

5.3.1.2.2 Cello rosin

The cello rosin was an orange block of 'Hidersine 3C Cello rosin' (Table 5-1).

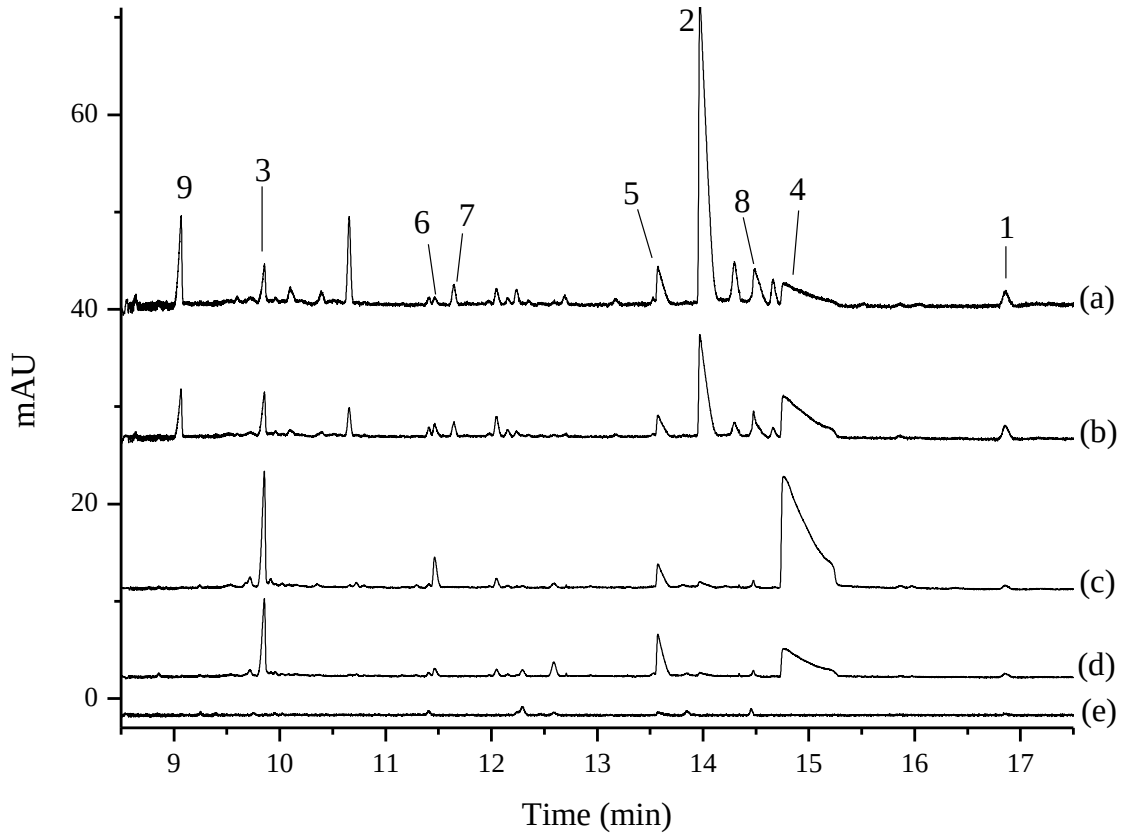

Figure 5-9 Electropherograms of 0.1% w/v cello rosin sample analysed in positive polarity, 20 kV, capillary 58 cm (49.5 cm to detector), 50 µm i.d., 25°C, 50 mbar 4 s injection time. Buffer consists of 15% MeOH 5 mM HPγCD 10 mM SBCD in 20 mM tris buffer pH 9. Wavelengths are (a) 200 nm, (b) 214, (c) 240 nm, (d) 265 nm and (e) 310 nm. Numbers indicate (1) 7OXO, (2) DHA, (3) NEO, (4) ABA, (5) PAL, (6) LVO, (7) SAN, (8) ISO and (9) PIM.

Again, it is clear from Figure 5-9 that the cello rosin is a natural gum rosin. The concentrations of acids determined are seen in Table 5-5. LVO and SAN are identified unlike in the gum rosin samples RA-RD, with a 35% lower LVO and a 8.6% higher SAN concentration compared to that of the music rosin. The cello rosin was found to contain the highest concentrations of PIM, PAL and DHA at 56.3, 53.4 and 52.3 mg L^{-1}. The NEO and ABA concentrations are equivalent to those of sample RD, a crystallising rosin. As with the music rosin, this could suggest a

tendency of the cello rosin to crystallise. The concentrations of ISO is 31% higher than in the music rosin, but still considerably lower than the concentrations determined in the natural gum rosins.

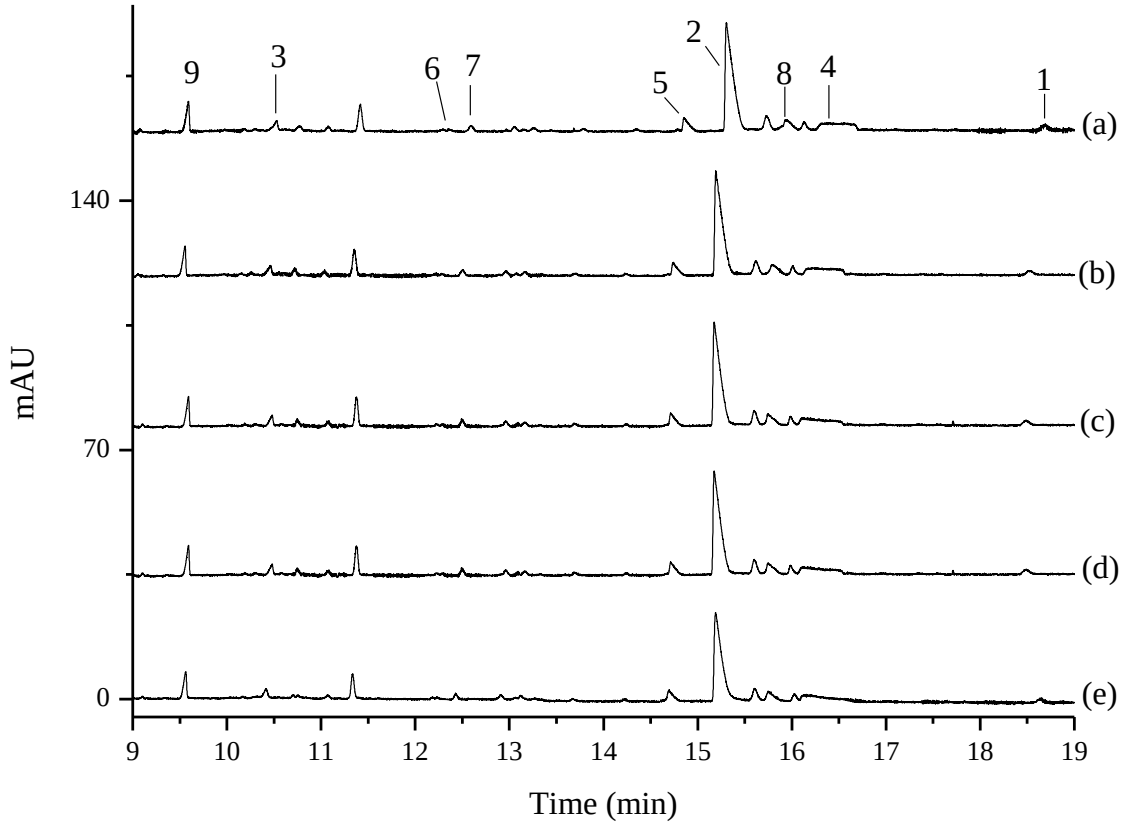

Figure 5-10 Repeat electropherograms a-e of cello rosin sample analysed in positive polarity, 20 kV, capillary 58 cm (49.5 cm to detector), 50 µm i.d., 25°C, 50 mbar 4 s injection times. Buffer consists of 15% MeOH 5 mM HPγCD 10 mM SBCD in 20 mM tris buffer pH 9, detection at 200 nm. Numbers indicate (1) 7OXO, (2) DHA, (3) NEO, (4) ABA, (5) PAL, (6) LVO, (7) SAN, (8) ISO and (9) PIM.

The reproducibility of the method when applied to the cello rosin sample is seen in Figure 5-10 with the RSD values in Table 5-5 remaining <2%.

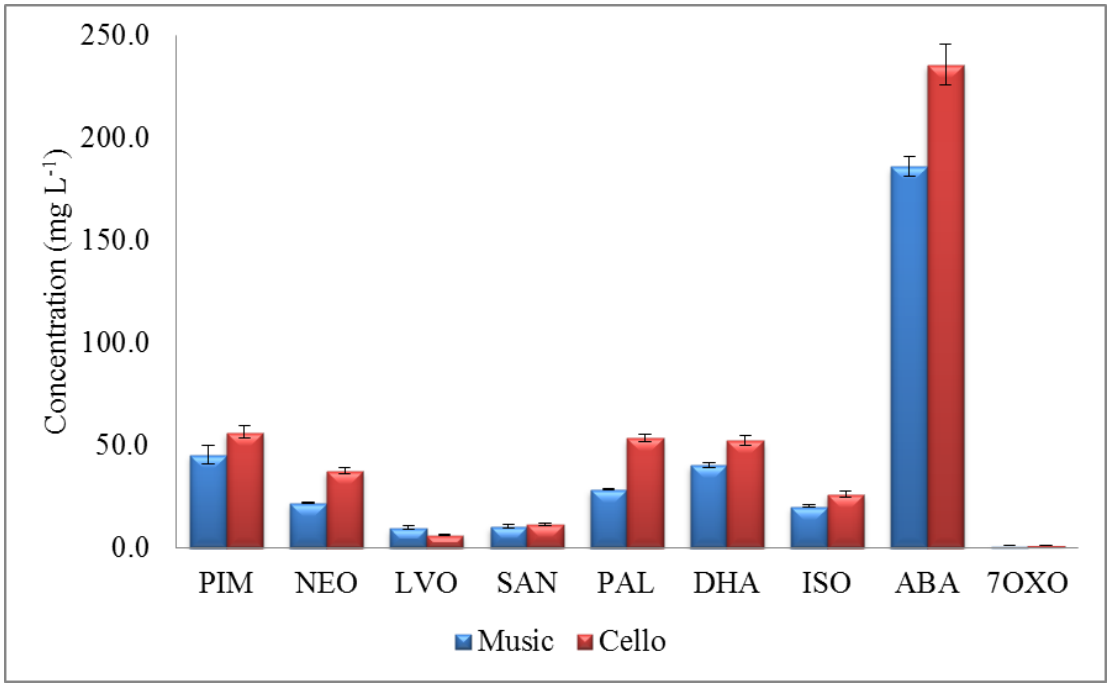

Figure 5-11 Acid concentration plots for music and cello rosin samples

The bar chart in Figure 5-11 also illustrates the differences in acid concentrations in the music and cello rosin. The main composition differences of the samples are the higher concentrations of PIM, NEO, PAL and ABA in the cello rosin samples. Only LVO is present in higher amounts in the music rosin sample.

The acid concentration ratios of the music and cello rosin samples (Table 5-6) are similar to the gum rosin samples (Table 5-4), with the main differences seen in the ratios containing 7OXO. The ABA:LVO ratio shows the higher ABA and lower LVO concentration of the cello rosin. The lower LVO concentration in the cello rosin is reflected in the LVO:PAL, NEO:LVO, DHA:LVO and PIM:LVO which are double for the cello rosin sample. The ABA:NEO ratios are higher than those of rosin samples RC and RD, the music rosin in particular at 8.5:1.

The ABA:DHA ratios of the music and cello rosin are higher for all except sample RD, which was the only gum rosin found to contain higher concentrations of ABA than the music and cello rosins. Many of the acid concentration ratios of the music and cello rosins are similar to those of rosin samples RC and RD. The DHA:PIM and ABA:PAL of the music and cello rosins and the PIM:PAL ratios of the cello rosin are all close to the acid ratio values of sample RD. The ABA:PIM, DHA:PAL and

PAL:NEO ratios of the music and cello rosins, and the DHA:NEO ratio of the music rosin are all close to the acid ratio values of sample RC. These similarities suggest that the music and cello rosins may share a source with rosin samples RC and RD, both crystallising rosin samples.

Table 5-6 Acid concentration ratios of music rosin samples

	Music rosin	Cello rosin		Music rosin	Cello rosin
ABA:DHA	4.6:1	4.5:1	DHA:NEO	1.9:1	1.4:1
DHA:ISO	2:1	2:1	ISO:NEO	1:1.1	1:1.4
DHA:PIM	1:1.1	1:1.1	ABA:LVO	19.8:1	38.7:1
ABA:ISO	9.3:1	9:1	PIM:LVO	4.8:1	9.2:1
ABA:PIM	4.1:1	4.2:1	PIM:SAN	4.3:1	4.9:1
ISO:PIM	1:2.3	1:2.2	ABA:SAN	17.7:1	20.7:1
ABA:PAL	6.5:1	4.4:1	NEO:LVO	2.3:1	6.2:1
ABA:7OXO	206:1	235:1	NEO:SAN	2.1:1	3.3:1
DHA:PAL	1.4:1	1:1	DHA:LVO	4.3:1	8.6:1
DHA:7OXO	44.9:1	52.3:1	DHA:SAN	3.9:1	4.6:1
ISO:PAL	1:1.4	1:2	LVO:SAN	1:1.1	1:1.9
ISO:7OXO	22.2:1	26.2:1	LVO:PAL	1:3	1:8.8
PIM:PAL	1.6:1	1.1:1	LVO:ISO	1:2.1	1:4.3
PIM:7OXO	50.3:1	56.3:1	LVO:7OXO	10.4:1	6.1:1
PIM:NEO	2.1:1	1.5:1	ISO:SAN	1.9:1	2.3:1
PAL:7OXO	31.7:1	53.4:1	SAN:PAL	1:2.7	1:4.7
7OXO:NEO	1:24.3	1:37.5	SAN:7OXO	11.7:1	11.4:1
PAL:NEO	1.3:1	1.4:1	ABA:NEO	8.5:1	6.3:1

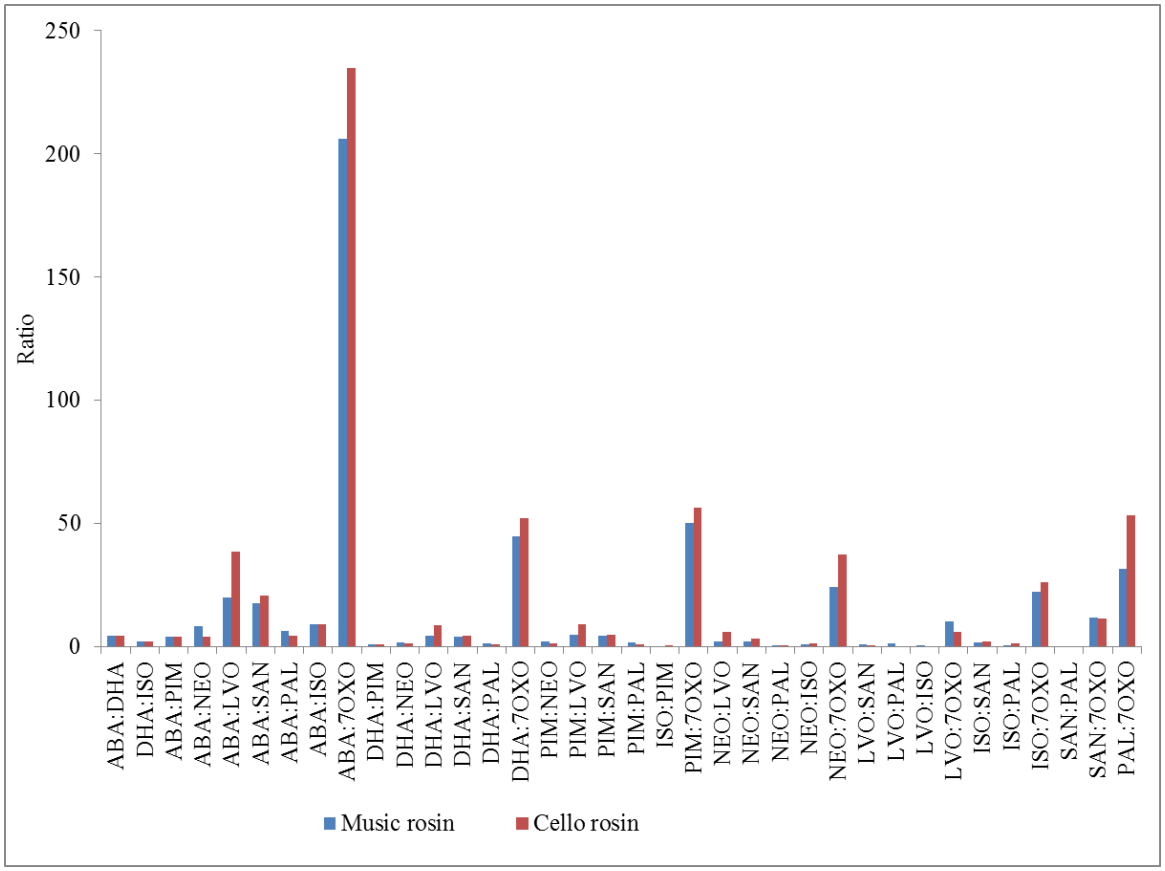

Figure 5-12 Bar chart of acid concentration ratios of music and cello rosin samples

The acid concentration ratios from Table 5-6 are plotted in Figure 5-12. The majority of ratios are the same magnitude as those of the gum rosin samples (Figure 5-5) with the ABA:7OXO ratios double those of sample RD.

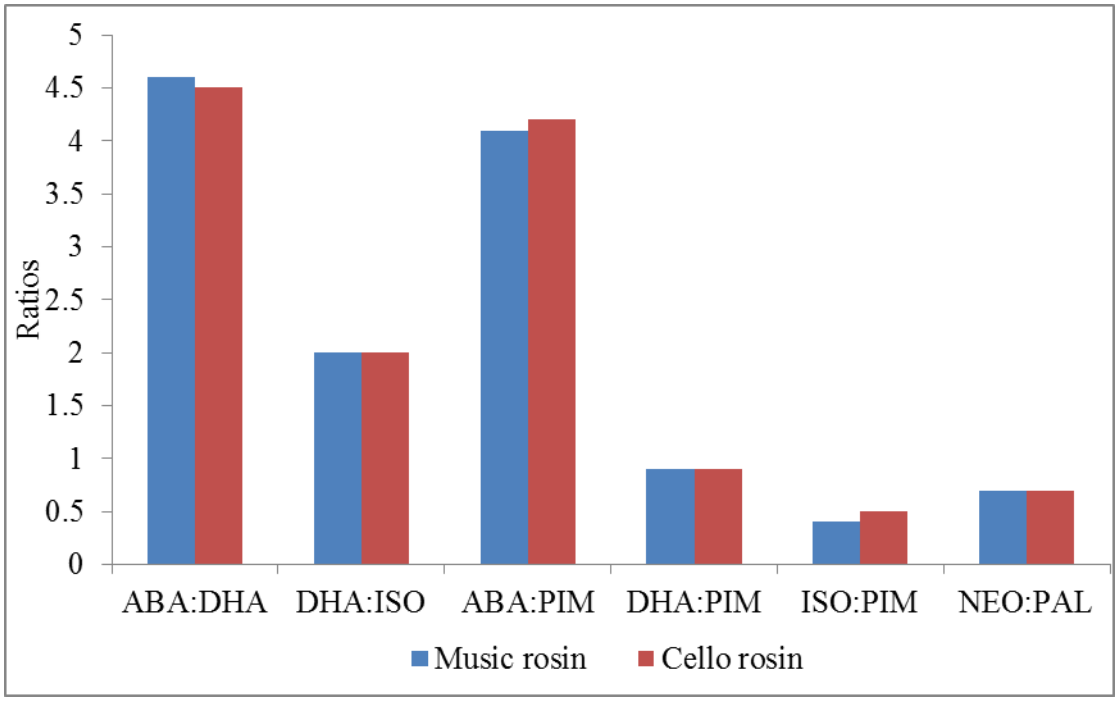

Figure 5-13 Bar chart of some of the acid concentration ratios of music and cello rosin samples

Some of the smaller ratios from Figure 5-12 are highlighted in Figure 5-13, showing that the cello and music rosin have several ratios of equal or very close values. While the cello rosin was found to contain higher concentrations of ABA and DHA than the music rosin sample, the ABA:DHA ratio was higher for the music sample.

5.3.1.3 Modified gum rosins

In many industrial applications the use of gum rosin is desirable as they are a lot less viscous than modified rosins. However, in other cases the modification of gum rosin can improve a desired aspect of the rosin which would make it more suitable for that particular purpose. Disproportionated rosin is reported to have good resistance to oxidation, low brittleness, lighter colour and high thermal stability as much of the ABA is converted to DHA [1, 30, 34]. It is used in industries such as polymers where high DHA concentrations are required and the presence of ABA can be an inhibitor [13]. Polymerised rosins are prepared by dimerising the ABA [35]. They are reported to have a longer shelf-life and higher softening point and are used as additives in inks, coatings, rubbers and food additives [1]. They also have improved film-forming properties and so are being investigated for their use in drug delivery systems [168, 169]. Hydrogenation is shown to improve rosin colour and also decreases susceptibility to oxidation and as a result they are used in industries including adhesives and chewing gum [1].

5.3.1.3.1 Acid modified hydrogenated rosin

The acid modified hydrogenated rosin (A-mod) was a translucent solid.

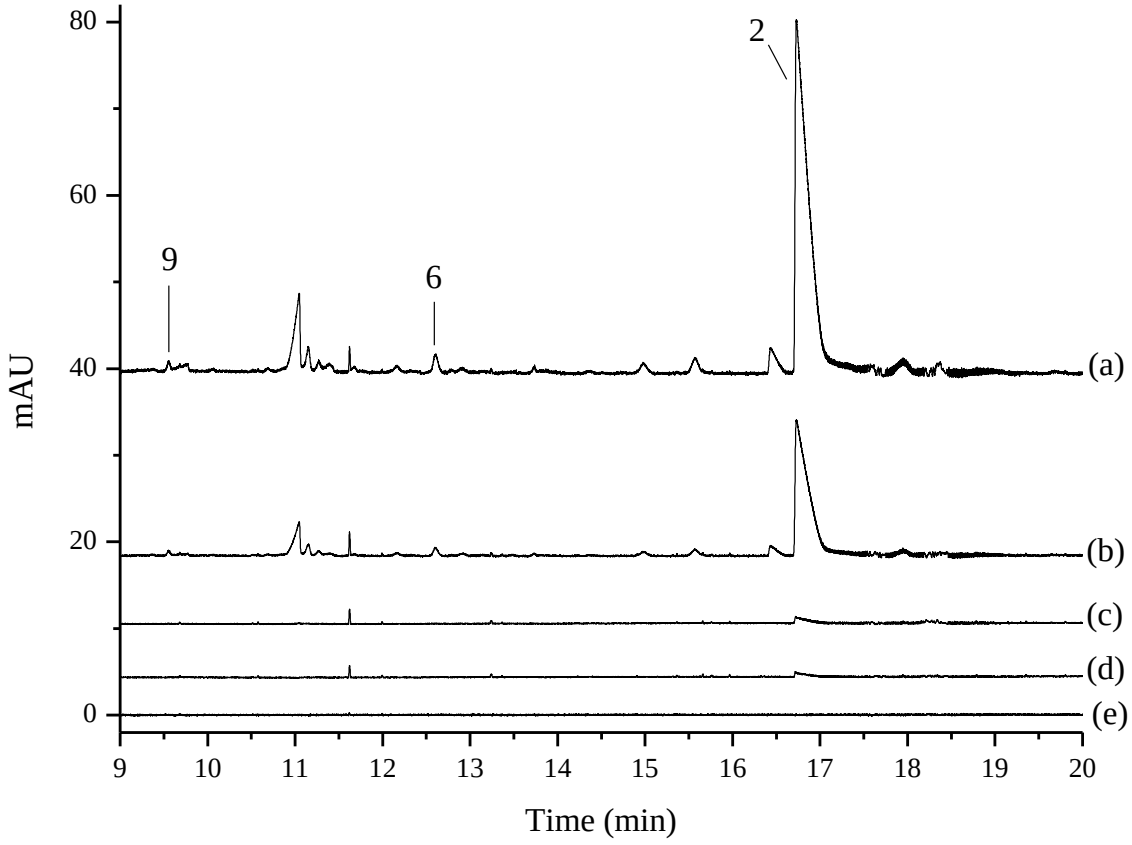

Figure 5-14 Electropherograms of 0.1% w/v acid modified rosin sample analysed in positive polarity, 20 kV, capillary 58 cm (49.5 cm to detector), 50 µm i.d., 25°C, 50 mbar 4 s injection times. Buffer consists of 15% MeOH 5 mM HPγCD 10 mM SBCD in 20 mM tris buffer pH 9. Wavelengths are (a) 200 nm, (b) 214, (c) 240 nm, (d) 265 nm and (e) 310 nm. Numbers indicate (2) DHA, (6) LVO and (9) PIM.

As expected, no ABA peak was observed in the electropherogram for the A-mod rosin as hydrogenation is known to convert ABA to DHA and dihydroabietic acid or tetrahydroabietic acid [30] (Figure 5-14). The unidentified peaks which do not correspond to any of the resin acid standards are most likely those of the dihydroabietic or tetrahydroabietic acid of which standards could not be obtained. As seen in Table 5-7, the primary acid present is DHA at 131.3 mg L^{-1}. PIM and LVO were also identified in smaller quantities.

Table 5-7 Average concentrations and standard deviations for modified rosin samples

	A-mod		Gresinox		RES155	
	Concentration (mg L^{-1})	**SD**	**Concentration (mg L^{-1})**	**SD**	**Concentration (mg L^{-1})**	**SD**
PIM	13.9	0.7	7.9	0.3	6.5	0.3
LVO	20.2	1.9				
DHA	131.3	6.4	204.2	10.5	444.5	13.3

The reproducibility of the method when applied to the A-mod rosin sample is seen in Figure 5-15. The RSD (%) values were 1.5, 1.7 and 2.3 for PIM, LVO and DHA respectively, n=5.

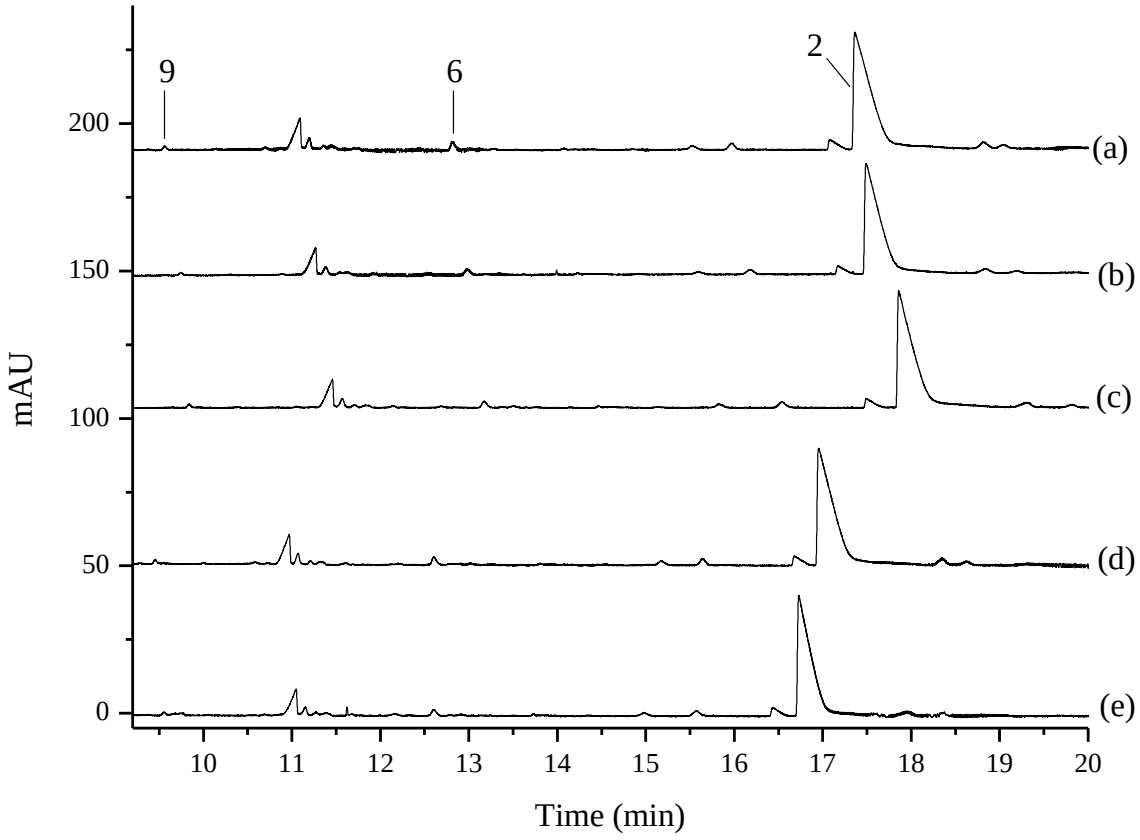

Figure 5-15 Repeat electropherograms a-e of A-mod rosin sample analysed in positive polarity, 20 kV, capillary 58 cm (49.5 cm to detector), 50 µm i.d., 25°C, 50 mbar 4 s injection times. Buffer consists of 15% MeOH 5 mM HPγCD 10 mM SBCD in 20 mM tris buffer pH 9, detection at 200 nm. Numbers indicate (2) DHA, (6) LVO and (9) PIM.

5.3.1.3.2 Disproportionated rosin Gresinox

Gresinox, a disproportionated rosin, was a pale yellow solid.

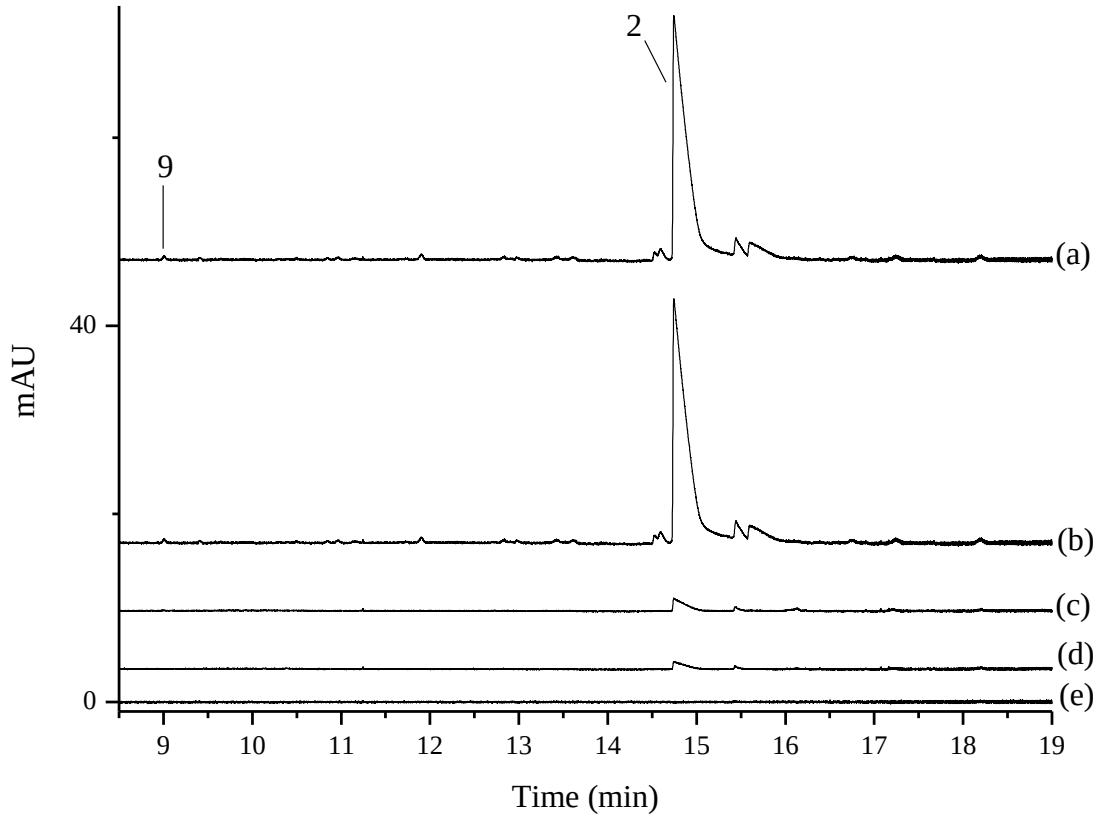

Figure 5-16 Electropherograms of 0.1% w/v Gresinox disproportionated rosin sample analysed in positive polarity, 20 kV, capillary 58 cm (49.5 cm to detector), 50 µm i.d., 25°C, 50 mbar 4 s injection times,. Buffer consists of 15% MeOH 5 mM HPγCD 10 mM SBCD in 20 mM tris buffer pH 9. Wavelengths are (a) 200 nm, (b) 214, (c) 240 nm, (d) 265 nm and (e) 310 nm. Numbers indicate (2) DHA and (9) PIM.

Disproportionation favours the most thermally stable isomers, in this case DHA. As expected, all ABA in this rosin sample was converted to DHA (see Figure 5-16). This is seen by the high DHA concentration, 204.2 mg L^{-1} and the absence of ABA. A small amount of PIM is also present (Table 5-7).

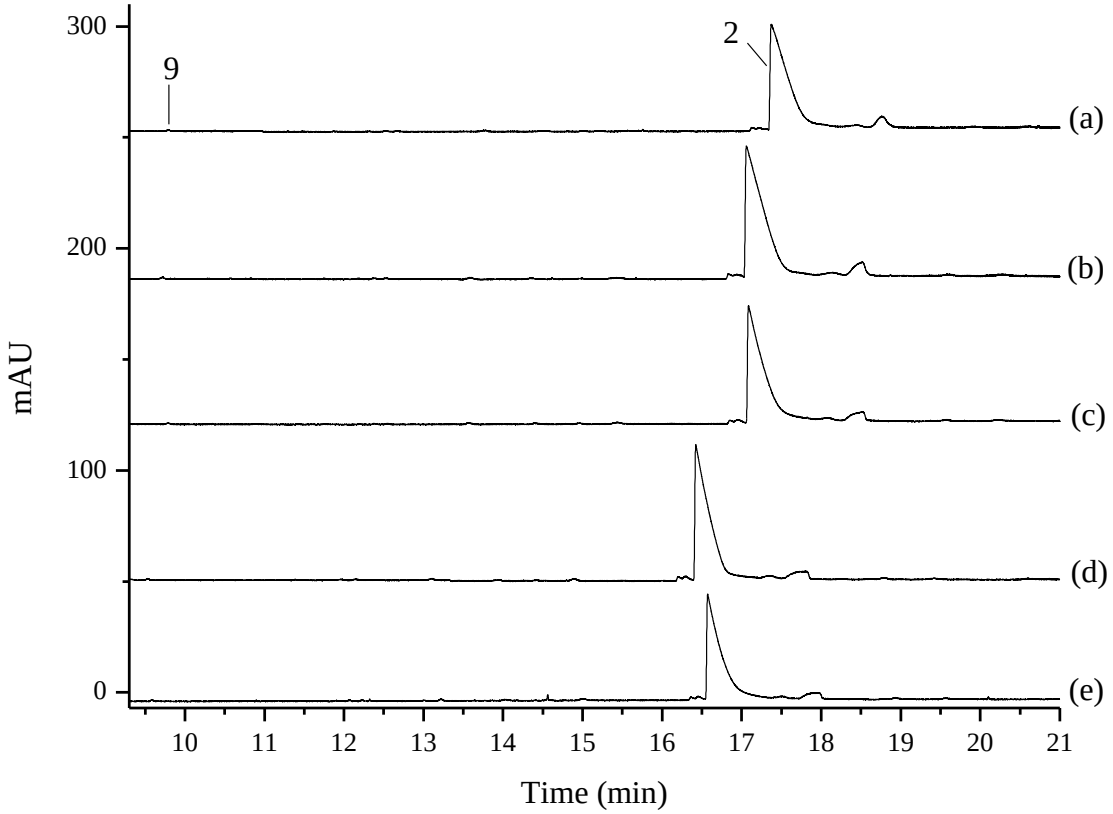

Figure 5-17 Repeat electropherograms a-e of a gresinox rosin sample analysed in positive polarity, 20 kV, capillary 58 cm (49.5 cm to detector), 50 µm i.d., 25°C, 50 mbar 4 s injection times. Buffer consists of 15% MeOH 5 mM HPγCD 10 mM SBCD in 20 mM tris buffer pH 9, detection at 200 nm. Numbers indicate (2) DHA and (9) PIM.

The reproducibility of the method when applied to the gresinox sample is seen in Figure 5-17. The RSD (%) values are 1.1 and 2.1% for PIM and DHA, n=5.

5.3.1.3.3 Disproportionated Rosin RES155

RES155 is another batch of disproportionated rosin, modified in the same way as Gresinox and with the same CAS number. It was a slightly more translucent yellow than the Gresinox sample.

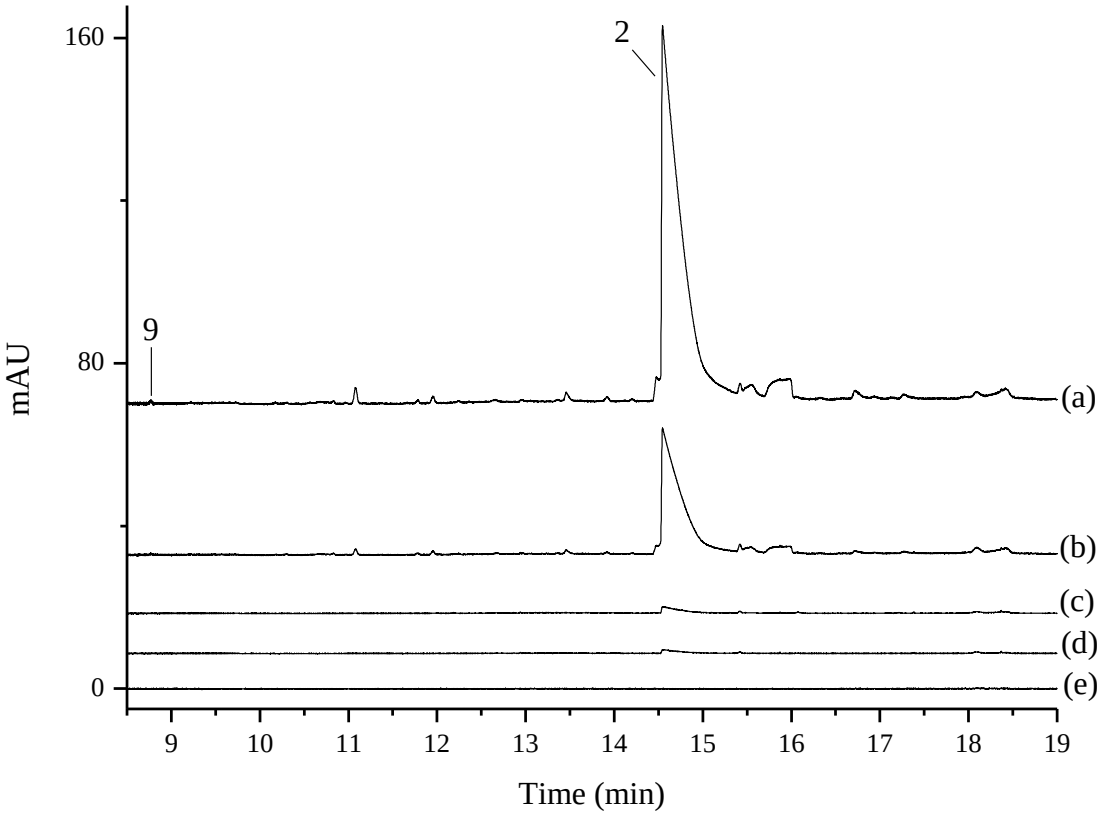

Figure 5-18 Electropherograms of 0.1% w/v disproportionated rosin sample analysed in positive polarity, 20 kV, capillary 58 cm (49.5 cm to detector), 50 µm i.d., 25°C, 50 mbar 4 s injection times. Buffer consists of 15% MeOH 5 mM HPγCD 10 mM SBCD in 20 mM tris buffer pH 9. Wavelengths are (a) 200 nm, (b) 214, (c) 240 nm, (d) 265 nm and (e) 310 nm. Numbers indicate (2) DHA and (9) PIM.

Consistent with Gresinox, DHA is the main acid present (see Figure 5-18). Although RES155 was modified in the same manner as the Gresinox sample, there are still differences in the concentrations of the acids found to be present. Its concentration in RES155 is 444.5 mg L^{-1} (see Table 5-7), more than double the amount found in Gresinox. This highlights the need for a rapid screening method to identify and quantify the acids present in rosin batches. For that particular purpose, this CE method could be suitable.

When these findings were presented to Henkel, it was remarked that RES155 was not suitable for use in some products because of its poor solubility. Moreover, Gresinox – which is modified in the same manner as RES155 – was much more soluble in the same solvents and its use in products was less restricted. Gresinox has less than half the amount of DHA present in RES155, indicating that it may be the presence of higher DHA concentrations that reduces the solubility of the rosin sample.

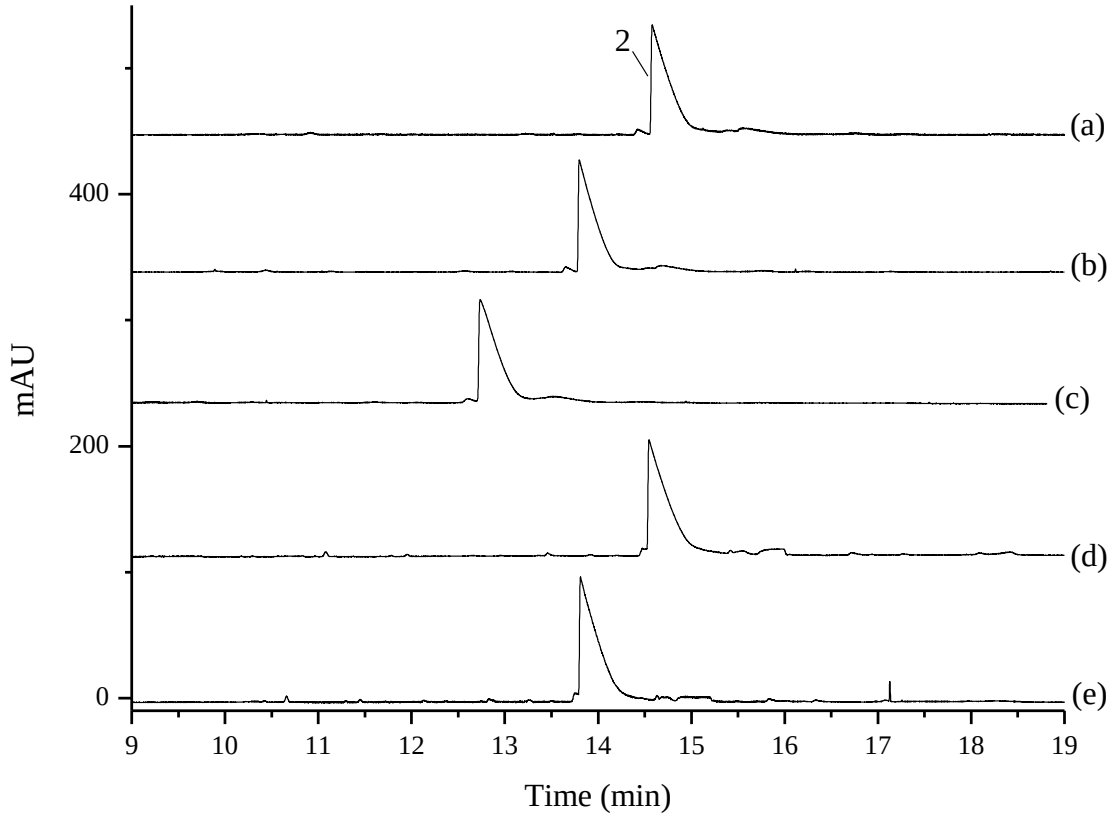

Figure 5-19 Repeat electropherograms a-e of RES155 rosin sample analysed in positive polarity, 20 kV, capillary 58 cm (49.5 cm to detector), 50 µm i.d., 25°C, 50 mbar 4 s injection times. Buffer consists of 15% MeOH 5 mM HPγCD 10 mM SBCD in 20 mM tris buffer pH 9, detection at 200 nm. (2) = DHA.

The RSD values for the migration times of PIM and DHA in the RES155 samples were found to be 3.7% and 3.5%, n=5 (see Figure 5-19).

5.3.1.3.4 Dimerised rosins

Three dimerised rosins, poly-pale (partially dimerised), resine k10 and dymerex (fully-dimerised) were analysed. As seen in Table 5-2, they all have the same CAS number as the polymerised rosins even though poly-pale is considered only partially dimerised, and has a different acid value and softening point to the two fully-dimerised rosins. Poly-pale was an orange colour while dymerex and resine K10 were pale amber.

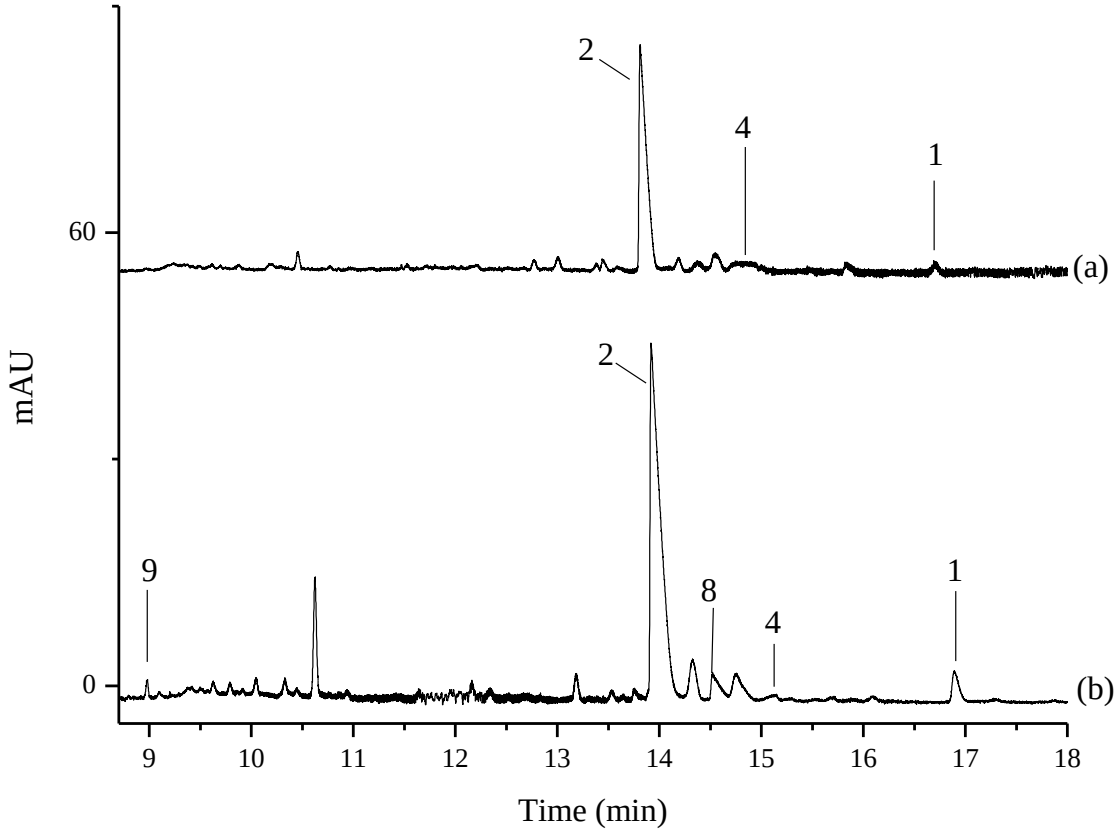

Figure 5-20 Electropherograms of 0.1% w/v (a) resine K10 fully-dimerised rosin sample and (b) partially dimerised poly-pale rosin sample analysed in positive polarity, 20 kV, capillary 58 cm (49.5 cm to detector), 50 µm i.d., 25°C, 50 mbar 4 s injection times. Buffer consists of 15% MeOH 5 mM HPγCD 10 mM SBCD in 20 mM tris buffer pH 9. Detection at 200 nm. Numbers indicate (1) 7OXO, (2) DHA, (4) ABA, (8) ISO and (9) PIM.

The different in compositions in the fully and partially dimerised rosins is evident in Figure 5-20. Dymerex and Resine K10, the fully-dimerised rosins, consist mainly of DHA and ABA. Resine K10 was also found to contain 0.7 mg L^{-1} 7OXO. Dymerex contains more DHA than ABA while the opposite is true for Resine K10. The decrease in DHA is less than 10%, and it may have been converted to 7OXO, an oxidation product of DHA. The fully-dimerised rosins have similar

electropherograms to the polymerised YT201 rosin batches as expected (see Figure 5-24), and this is reflected in the comparable DHA concentrations. Poly-pale, a partially-dimerised rosin, was found to also contain PIM and ISO, and a higher 7OXO concentration (see Table 5-8). No NEO, PAL or LVO was expected to be detected, as the modification process would have caused them to isomerise to ABA.

Table 5-8 Average concentration and standard deviation values for the dimerised rosin samples

	Poly-pale		Dymerex		Resine K10	
	Concentration (mg L^{-1})	SD	Concentration (mg L^{-1})	SD	Concentration (mg L^{-1})	SD
PIM	15.5	0.3				
DHA	104.3	6.3	55.7	5.4	50.5	1.1
ISO	28.7	0.1				
ABA	23.5	1.4	27.5	2.8	94.4	2.6
7OXO	6.9	0.1			0.7	0.3

The reproducibility of the method when applied to the polypale samples as seen in Figure 5-21 is shown by the migration time RSD values in Table 5-11.

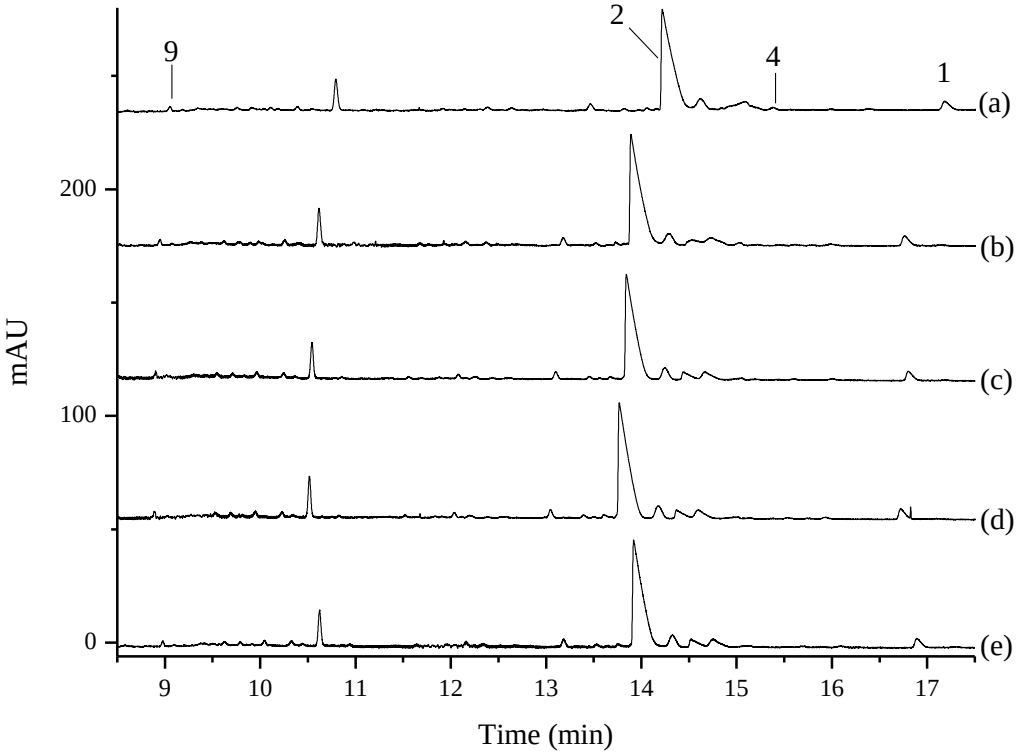

Figure 5-21 Repeat electropherograms a-e of polypale rosin sample analysed in positive polarity, 20 kV, capillary 58 cm (49.5 cm to detector), 50 µm i.d., 25°C, 50 mbar 4 s injection times. Buffer consists of 15% MeOH 5 mM HPγCD 10 mM SBCD in 20 mM tris buffer pH 9, detection at 200 nm. Numbers indicate (1) 7OXO, (2) DHA, (4) ABA and (9) PIM.

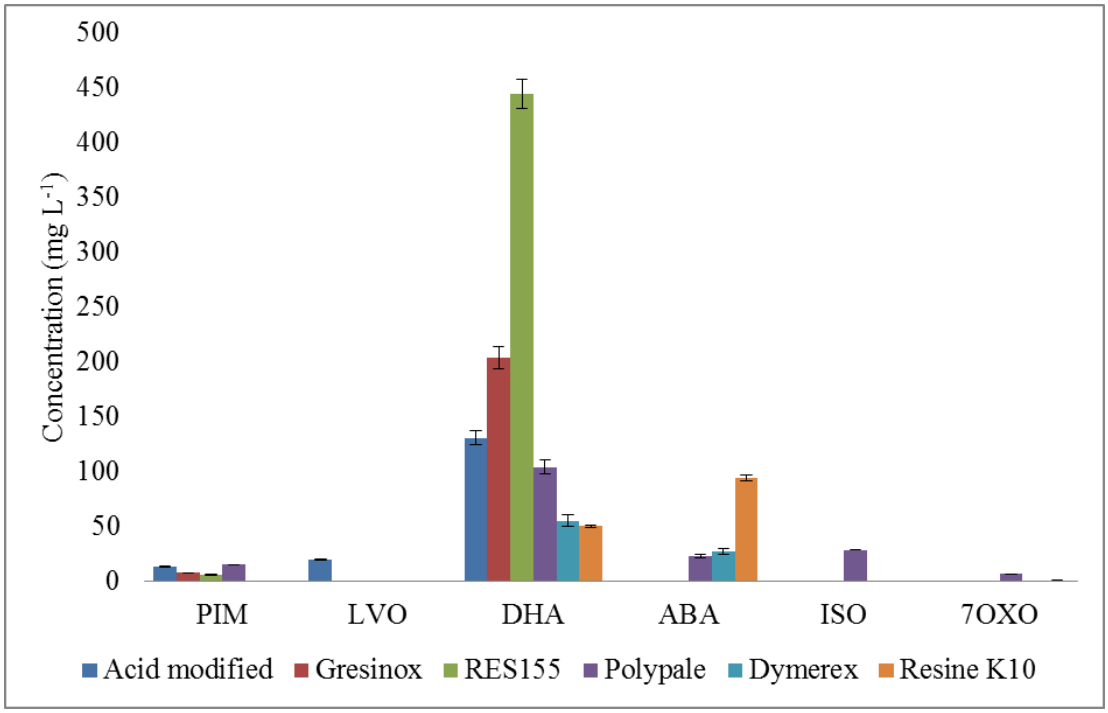

Figure 5-22 Acid concentration plots for modified rosin samples

A modified rosin is one which has been chemically modified by any of a variety of methods in order to improve a certain desirable feature such as resistance to oxidation. NEO, PAL and SAN were not found to be present in any of the modified rosin samples. The bar chart in Figure 5-22 illustrates the main composition differences of the samples. DHA was found to be present in the greatest concentration in RES155 sample. All of the modified rosins were found to have higher DHA concentrations than ABA except for Resine K10, while all except one gum rosin had more ABA than DHA (seen in Figure 5-2). Only the A-mod sample was found to contain LVO while only polypale was found to contain ISO. Both disproportionated rosins had comparable PIM concentrations while RES155 had a much higher DHA concentration.

All the batches of the polymerised rosin, and the two fully-dimerised rosins were found to have comparable DHA concentrations, while the partially-dimerised rosin poly-pale contained smaller quantities of ISO and PIM.

The ABA:ISO and ABA:PIM ratios of polypale are similar to those of rosin samples RA and RB, while the ISO:PIM ratio is equivalent to that of sample RC. It is possible that the polypale rosin was sourced from the same region as samples RA and RB before modification.

Table 5-9 Acid concentration ratios of modified rosin samples

	Acid modified	Gresinox	RES155	Polypale	Dymerex	Resine K10
ABA:DHA				1:4.4	1:2	1.9:1
DHA:ISO				3.6:1		
DHA:PIM	9.5:1	25.9:1	68.4:1	6.7:1		
ABA:ISO				1:1.2		
ABA:PIM				1.5:1		
ISO:7OXO				4.2:1		
ISO:PIM				1.9:1		
PIM:7OXO				2.3:1		
ABA:7OXO				3.4:1		134.9:1
PIM:LVO	1:1.5					
DHA:LVO	6.5:1					

The DHA:PIM ratios of the modified rosins illuminate their high DHA concentration relative to all other acids (see Table 5-9).

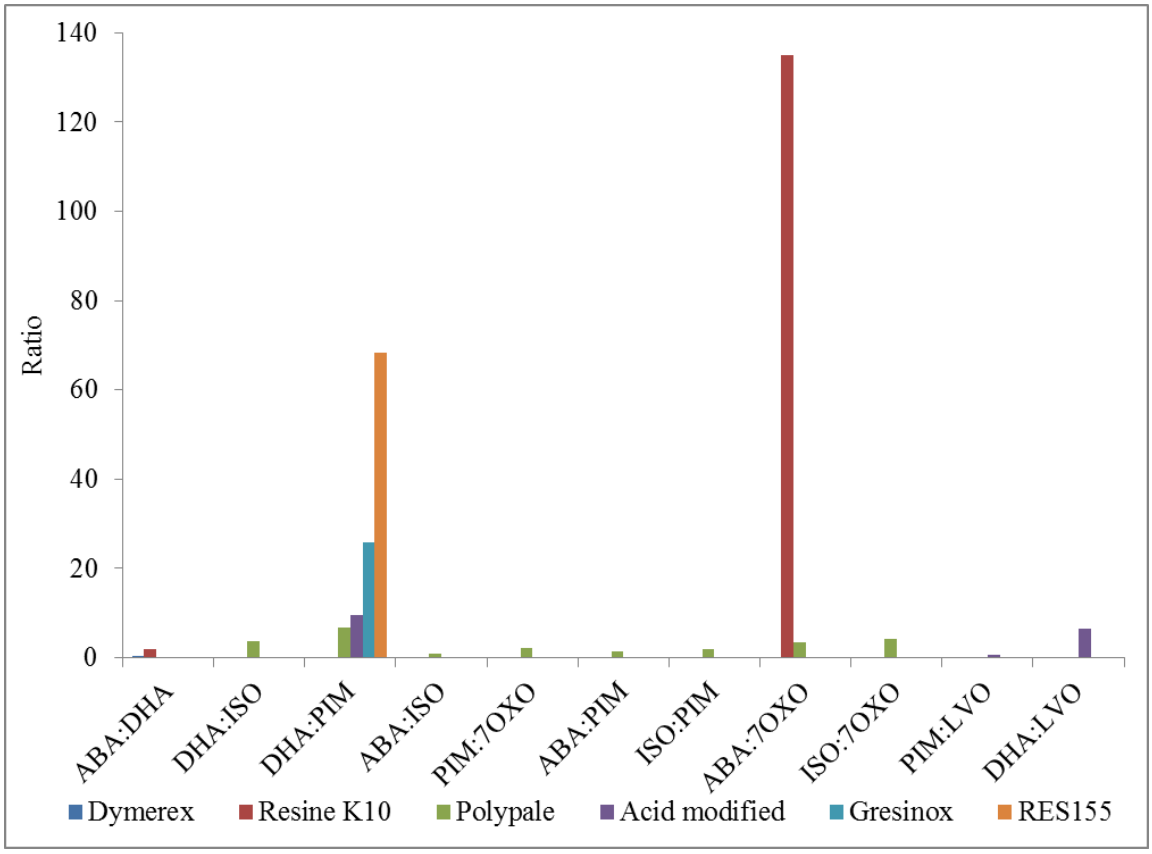

Figure 5-23 Bar chart of acid concentration ratios of modified rosin samples

The acid concentration ratios from Table 5-9 are plotted in Figure 5-23. The ABA:7OXO ratio is greater than that of gum rosin sample RD but lower than those of the music and cello rosins. Resine K10 and Dymerex are modified in the same way however Dymerex was not found to contain 7OXO. The DHA:PIM ratios of the acid-modified hydrogenated, disproportionated rosins and polypale sample are higher than those of the gum rosin samples with that of the RES155 sample the highest seen out of all the rosin and resin samples. The acid-modified hydrogenated rosin was the only modified rosin samples found to contain LVO. The DHA:ISO ratio of the polypale sample is also higher than those of the gum rosin samples.

5.3.1.3.5 Polymerised rosin

Six different batches (A-F) of polymerised rosin YT201 were analysed. The samples were a pale amber colour. Some were reported to have failed test specifications for product use. Test specifications included an acid value of 130-160 mg KOH g^{-1} and a softening point of 95-105°C. The individual batches values are seen in Table 5-2.

The acid number is described as the amount of milligrams of KOH needed to neutralise free acids in a gram of chemical substance [170]. The acid number of a rosin indicates its acid content by measuring the carboxylic acid groups present. It is determined by ASTM Method D465. Rosins with high acid numbers have been noted as more inclined to be oxidised. While rosins do not melt, they become a viscous liquid when heated and a certain degree of softness as described in the ASTM ring and ball method gives their softening point. This can be important in selecting a rosin of a certain level of viscosity [1].

Table 5-10 Average concentrations, standard deviations and ABA:DHA concentration ratios for YT201 batches, n=3

YT201 batch	DHA conc. (mg L^{-1})	SD	ABA conc. (mg L^{-1})	SD	ABA:DHA conc. ratio
A	63.8	0.4	74.8	0.8	1.2:1
B	57.5	3.4	62.5	3.4	1.1:1
C	49.9	2.9	64.9	2.2	1.3:1
D	47.2	4.1	113.5	12.9	2.4:1
E	67.4	0.6	72.1	1.2	1.1:1
F	50.2	0.2	120.9	1.6	2.4:1

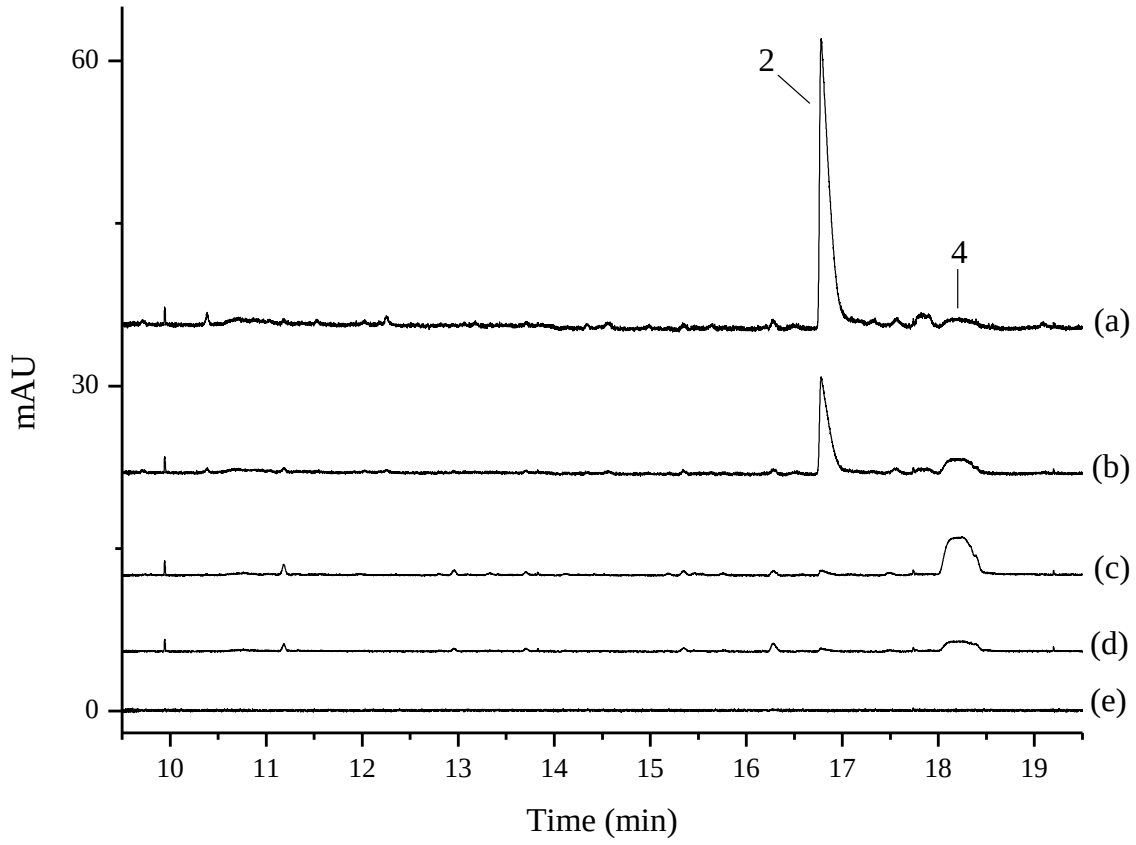

Figure 5-24 Electropherograms of 0.1% w/v YT201C polymerised rosin sample analysed in positive polarity, 20 kV, capillary 58 cm (49.5 cm to detector), 50 µm i.d., 25°C, 50 mbar 4 s injection times. Buffer consists of 15% MeOH 5 mM HPγCD 10 mM SBCD in 20 mM tris buffer pH 9. Wavelengths are (a) 200 nm, (b) 214, (c) 240 nm, (d) 265 nm and (e) 310 nm. Numbers indicate (2) DHA and (4) ABA.

Both DHA and ABA were found to be present in the polymerised rosin samples (the electropherogram of YT201C is seen in Figure 5-24). It is possible that the ABA peak may correspond to abietic acid dimer products resulting from the polymerisation process [35]. The electropherograms of all six batches are seen in Figure 5-25. The RSD of the DHA concentration in the YT201 batches was 13.5% while the ABA concentration varied by 27.6%, n=3. YT201B and YT201C failed the acid value test specification, and they were found to have the lowest ABA concentrations. YT201E also has a low ABA concentration and it was just above the lower specification limit of the acid value test. YT201D and YT201F had the highest ABA concentration, 113.5 and 120.9 mg L^{-1} (see Table 5-10).

The reproducibility of the method when applied to the YT201 polymerised rosin sample batches is shown by the migration time RSD values in Table 5-11.

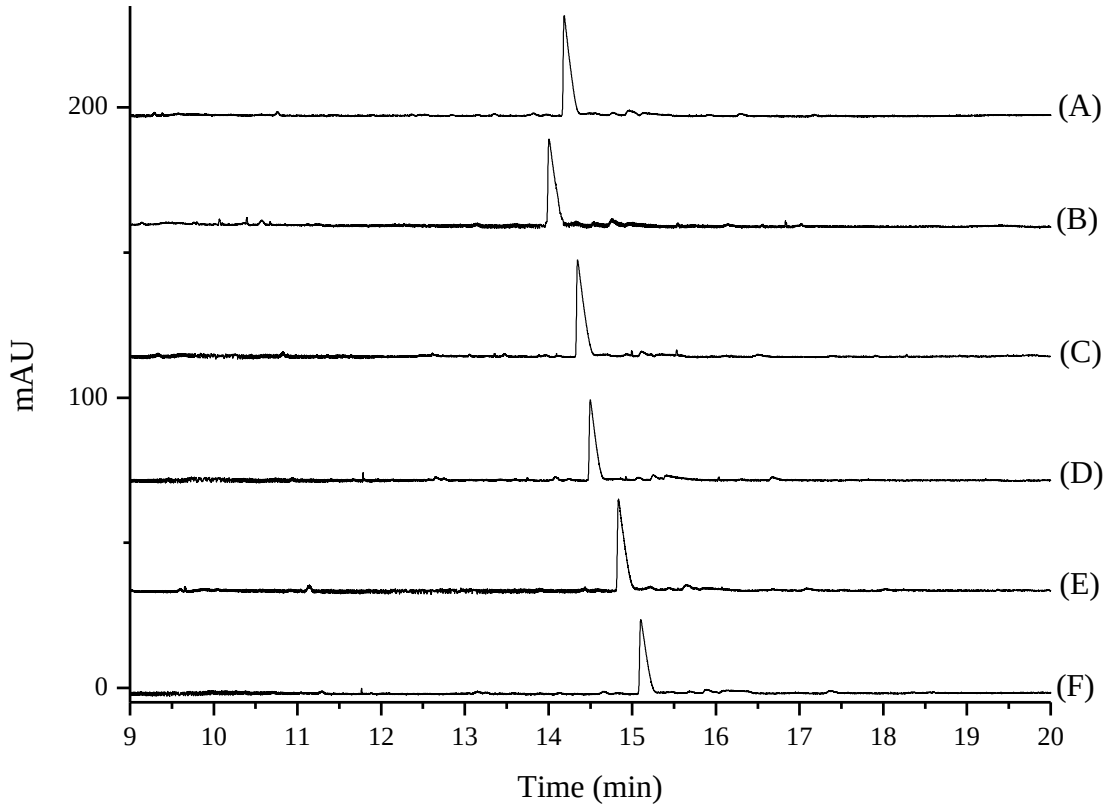

Figure 5-25 YT201 batches A-F analysed in positive polarity, 20 kV, capillary 58 cm (49.5 cm to detector), 50 µm i.d., 25°C, 50 mbar 4 s injection times, detection at 200 nm. Buffer consists of 15% MeOH 5 mM HPγCD 10 mM SBCD in 20 mM tris buffer pH 9.

Table 5-11 RSD values for the acids present in the dimerised rosin samples and YT201 batches A-F, n=5

RSD (%)	PIM	DHA	ISO	ABA	7OXO
Poly-pale	0.7	1.2	0.9	1.1	1.1
Dymerex		5.7		5.7	
Resine K10		2.4		2.8	2.7
YT201A		2.3		2.5	
YT201B		4.3		4.9	
YT201C		2.8		3.0	
YT201D		3.4		3.5	
YT201E		7.1		7.3	
YT201F		3.9		4.4	

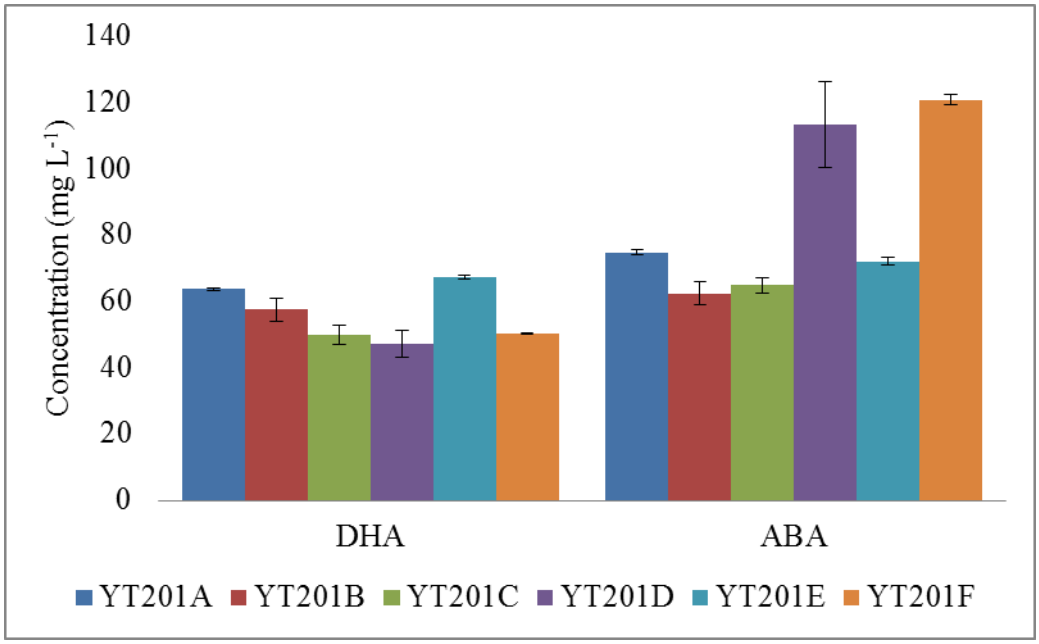

Figure 5-26 Acid concentration plots for the polymerised YT201 rosin samples

The bar chart in Figure 5-26 illustrates the differences in composition of the YT201 batches. All have higher concentrations of ABA than DHA. The ABA:DHA ratio of the YT201 batches varies from 2.4-1.1 (see Table 5-10). This is within the range of the ABA:DHA ratios of the gum rosin samples, however, no other similarities are observed between the YT201 rosin samples and other rosins.

5.3.3 Resin samples

Several resin samples were analysed using both the acid and terpene methods described in chapters two and three, demonstrating the potential of the separation methods for other natural products. The resin samples and sources are listed in Table 5-1.

5.3.3.1 Turpentine oil

Turpentine is the volatile part of resin, and consists of hydrocarbons, terpene alcohols and ethers. The main components are reported to be α-pinene and β-pinene (30-40%) and 3-carene (~50%) [1]. Other analytes of interest known to be found in turpentine include 4-allylanisole (in very small amounts), camphene, terpineol, and longifolene. A sample of turpentine oil, a clear liquid, was analysed using both the acid and terpene CE separation methods.

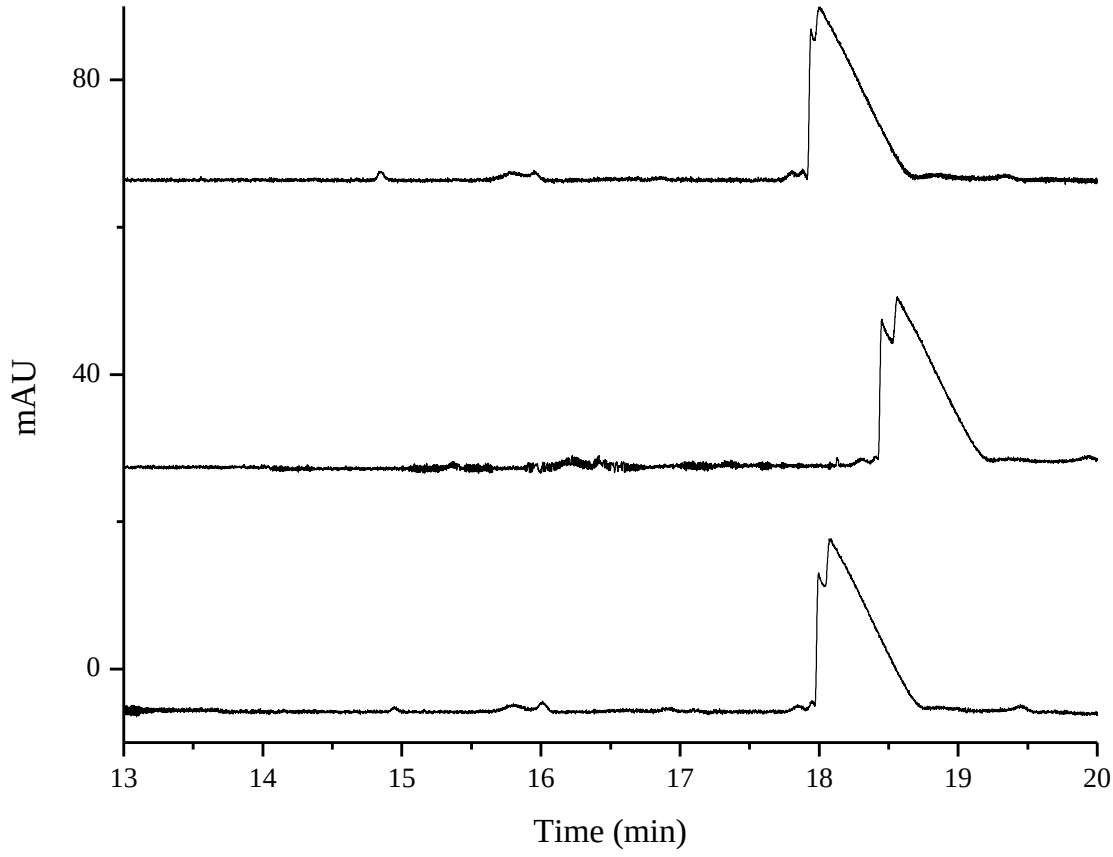

Figure 5-27 Electropherograms of a 0.1% v/v turpentine oil analysed in positive polarity, 20 kV, capillary 58 cm (49.5 cm to detector), 50 µm i.d., 25°C, detection at 200 nm. Sample prepared in MeOH, 50 mbar 4 s injection times, 15% MeOH 5 mM HPγCD 10 mM SBCD 20 mM tris buffer at pH 9.

When analysed with the acid method (see Figure 5-27), peak splitting is observed in the peaks at 15.9 and 17.8 min due to the sample being prepared in 100% MeOH as described in chapter 3.

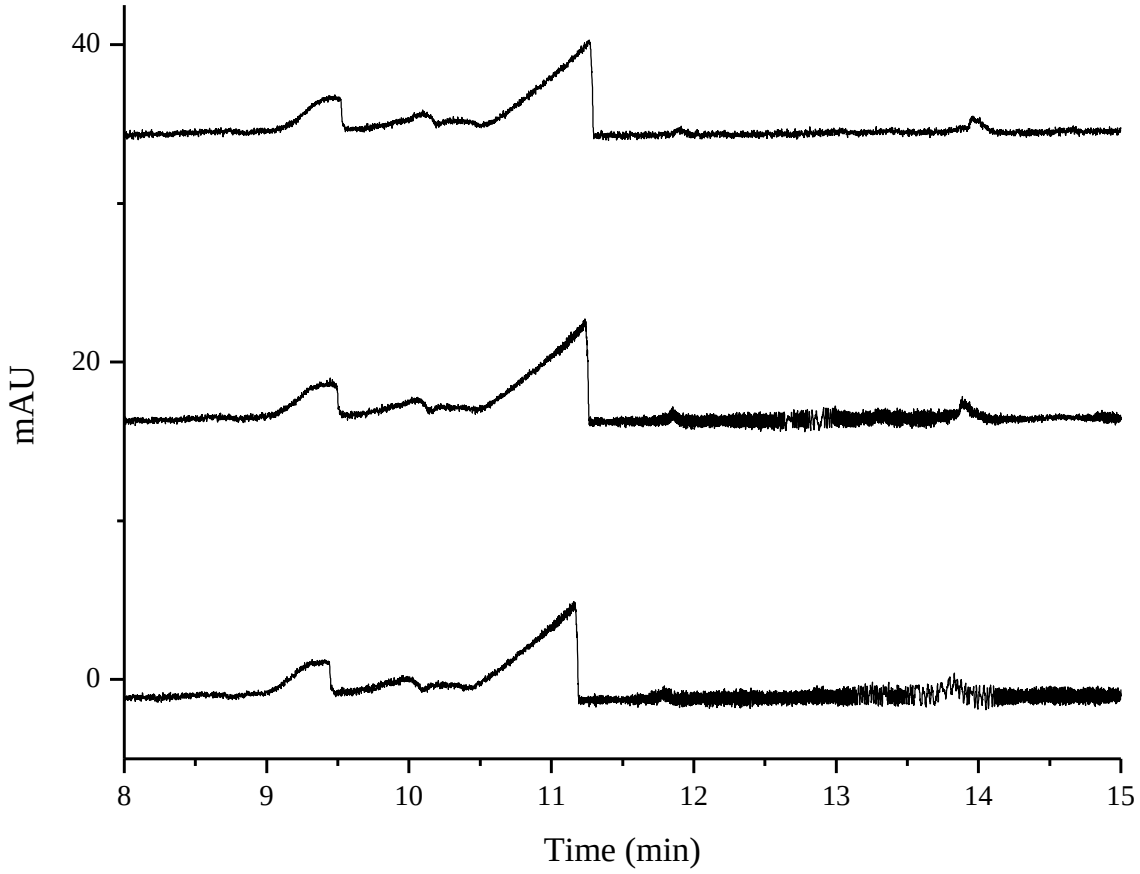

Figure 5-28 Electropherograms of a 0.1% v/v turpentine oil analysed in positive polarity, 20 kV, capillary 58 cm (49.5 cm to detector), 50 µm i.d., 25°C, detection at 200 nm., 5 mbar 20 s injection times, buffer consists of 5 mM β-CD 10 mM SDS 50 mM tris pH 8.

When analysed by the terpene method as shown in Figure 5-28, β-pinene coelutes at 9.8 min while 3-Carene elutes in the main peak at 11 min.

5.3.3.2 Venetian turpentine

Venetian turpentine is derived from larch trees (larix decidua). Its composition is very similar to that of rosin, with the exception of the presence of larixol and larixyl acetate. It has also been known to contain α-pinene, β-pinene, 3-carene, terpineol and longifolene [57, 171]. A sample of venetian turpentine, a viscous amber liquid, was analysed using both the acid and terpene CE separation methods.

5.3.3.2.1 Acid method

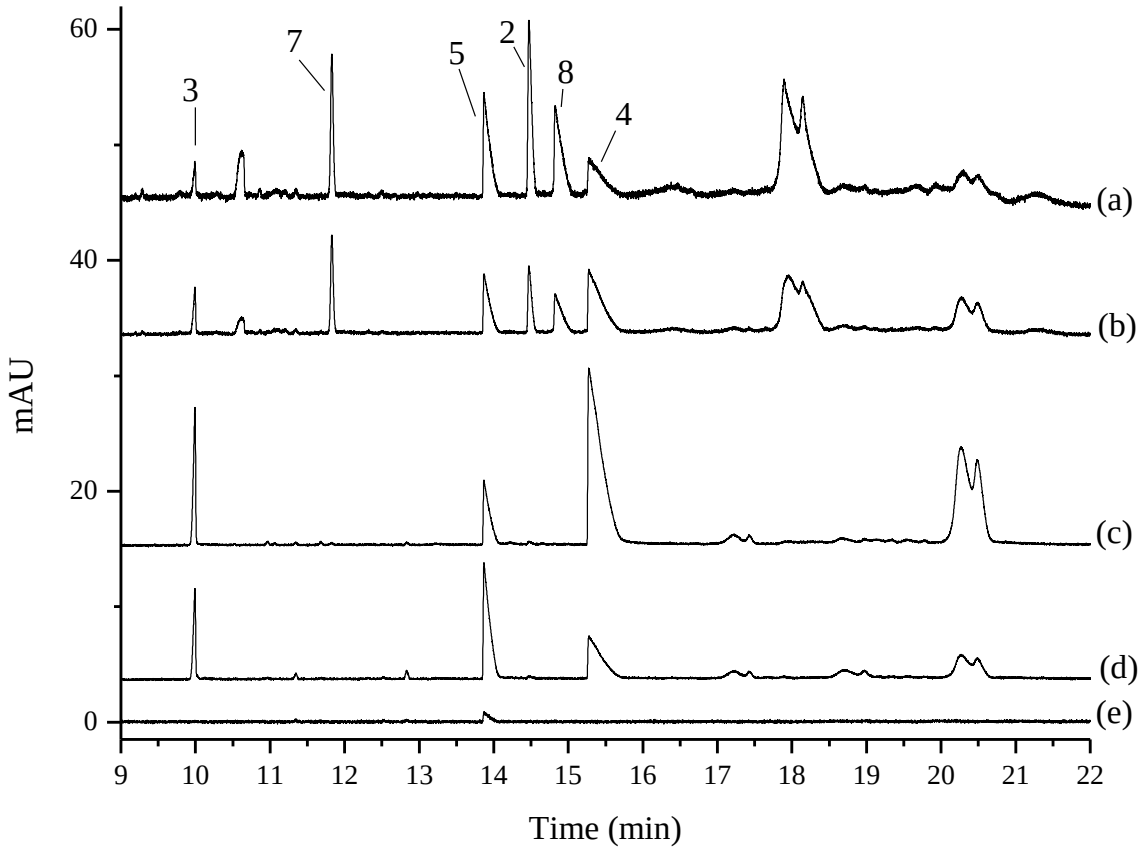

Figure 5-29 Electropherograms of a 0.1% v/v venetian turpentine in methanol, analysed in positive polarity, 20 kV, capillary 58 cm (49.5 cm to detector), 50 µm i.d., 25°C, 50 mbar 4 s injection times, 15% MeOH 5 mM HPγCD 10 mM SBCD 20 mM tris buffer at pH 9. Wavelengths are (a) 200 nm, (b) 214, (c) 240 nm, (d) 265 nm and (e) 310 nm. Numbers indicate (2) DHA, (3) NEO, (4) ABA, (5) PAL, (7) SAN and (8) ISO.

Figure 5-29 shows the venetian turpentine when analysed by the acid method. NEO, SAN, PAL, DHA, ISO and ABA were detected, and their concentrations shown in Table 5-12. Unlike the gum rosin samples, DHA was the acid present in the lowest concentration. The PAL concentration is over four times higher than the highest concentration found in a gum rosin sample. The ISO and NEO concentrations are comparable to that of the rosin samples while the ABA concentration is comparable to that of the crystallising gum rosins. It is likely that the unidentified peaks at 18.2 and 20.4 min correspond to larixol and larixyl acetate which are known to be present in venetian turpentine [55, 59, 172].

In the analysis of old painting and varnish samples, DHA and 7OXO are frequently used as markers for venetian turpentine and little ABA is present as it has been converted to DHA and 7OXO [165]. However, little DHA and no 7OXO were expected here as a fresh sample of venetian turpentine was analysed.

Table 5-12 Average concentrations and standard deviations for acids present in venetian turpentine, n=3

	Venetian turpentine			Balsam resin		
	Concentration (mg L^{-1})	SD	RSD (%)	Concentration (mg L^{-1})	SD	RSD (%)
NEO	38.2	1.5	3.9			
SAN	40.5	1.5	3.8			
PAL	174.6	8.7	4.9			
DHA	19.5	1.2	6.1	53.5	0.2	0.4
ISO	77.1	2.9	3.8	43.8	6.1	13
ABA	225.3	13.7	6.1	6.1	0.5	7.5
PIM				27.4	0.9	3.6
7OXO				14.6	0.9	6.8

The reproducibility of the method when applied to the venetian turpentine sample is shown by the RSD values in Table 5-12 which are <5.2%.

The resin acids present in various resins used in artwork have been analysed by GC-MS. While the analysis time for the GC-MS method was shorter than this CE method (13 min compared to 22 min), it required the derivatisation of both carboxylic groups to ethyl esters and the hydroxyl groups to trimethylsilyl ethers. In addition, the LVO and PAL ethyl esters could not be separated [53].

5.3.3.2.2 Terpene method

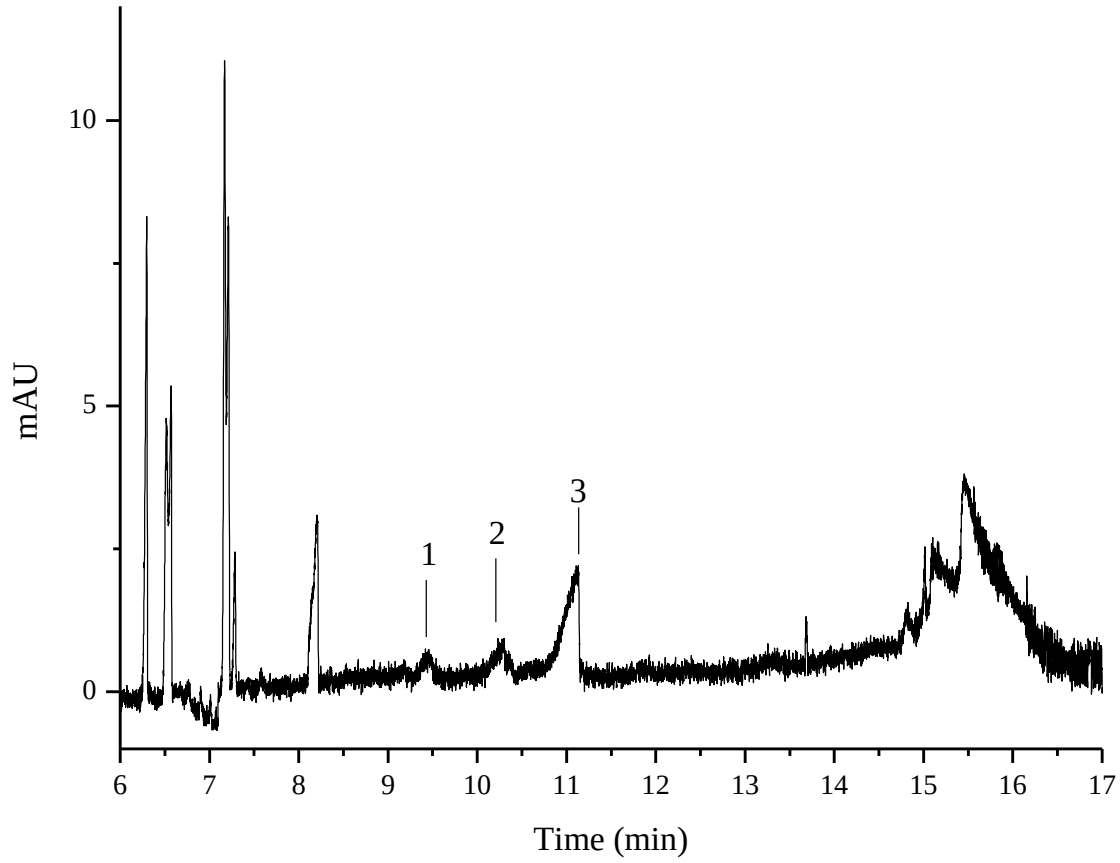

Figure 5-30 Electropherogram of a 0.1% v/v venetian turpentine in 1:5 MeOH:buffer, analysed in positive polarity, 20 kV, capillary 58 cm (49.5 cm to detector), 50 µm i.d., 25°C, 5 mbar 20 s injection times, 5 mM β-CD 10 mM SDS 50 mM tris pH 8, detection at 200 nm. Numbers indicate (1) camphene, (2) β-pinene and (3) 3-carene.

As seen in Figure 5-30, the electropherogram of venetian turpentine is very different when analysed by the terpene method. The acid peaks now elute in the 6-8.5 min range. Camphene, β-pinene and 3-carene were identified and again the mass of peaks at 15-16 min is likely to include larixol and larixyl acetate [55, 59, 172]. The concentration of 3-carene was found to be 406.9 mg L^{-1}, higher than the amounts of acids present. The peaks at 18.2 and 20.4 min in Figure 5-29 may also correspond to 3-carene. Camphene and β-pinene were found to be present in smaller amounts, 153.1 and 181.7 mg L^{-1}.

5.3.3.3 Balsam resin

A sample of balsam resin, an amber solid, was analysed using both the acid and terpene CE separation methods from chapters 2 and 3.

5.3.3.3.1 Acid method

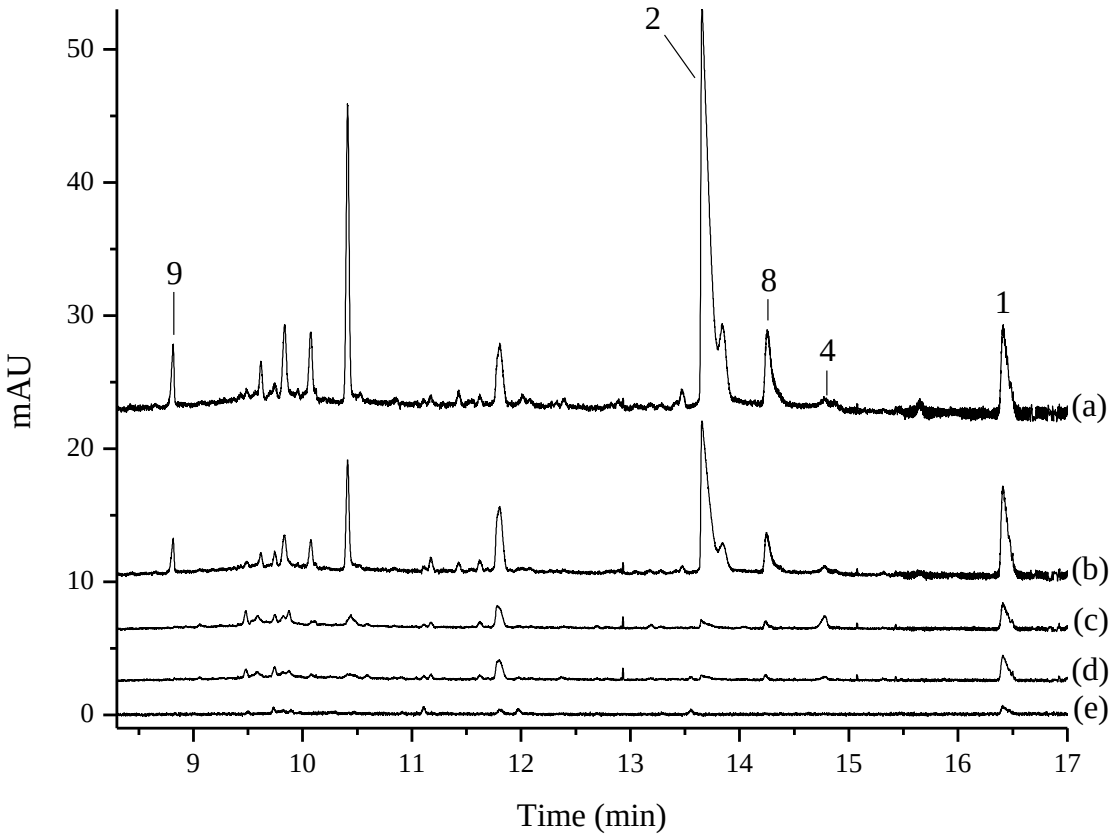

Figure 5-31 Electropherograms of a 0.1% v/v balsam resin in methanol, analysed in positive polarity, 20 kV, capillary 58 cm (49.5 cm to detector), 50 µm i.d., 25°C, 50 mbar 4 s injection times, 15% MeOH 5 mM HPγCD 10 mM SBCD 20 mM tris buffer at pH 9. Wavelengths are (a) 200 nm, (b) 214, (c) 240 nm, (d) 265 nm and (e) 310 nm. Numbers indicate (1) 7OXO, (2) DHA, (4) ABA, (8) ISO and (9) PIM.

The electropherogram in Figure 5-31 shows the balsam resin analysed by the acid method. PIM, DHA, ISO, ABA and 7OXO were found to be present, while there are many other peaks not seen in the rosin electropherograms. As shown in Table 5-12, the balsam resin sample was found to have higher a DHA concentration than the venetian turpentine sample, and contained PIM and 7OXO where none was found in the other resin sample. A lower ISO concentration and only 6.1 mg L^{-1} of ABA were found in balsam resin.

5.3.3.3.2 Terpene method

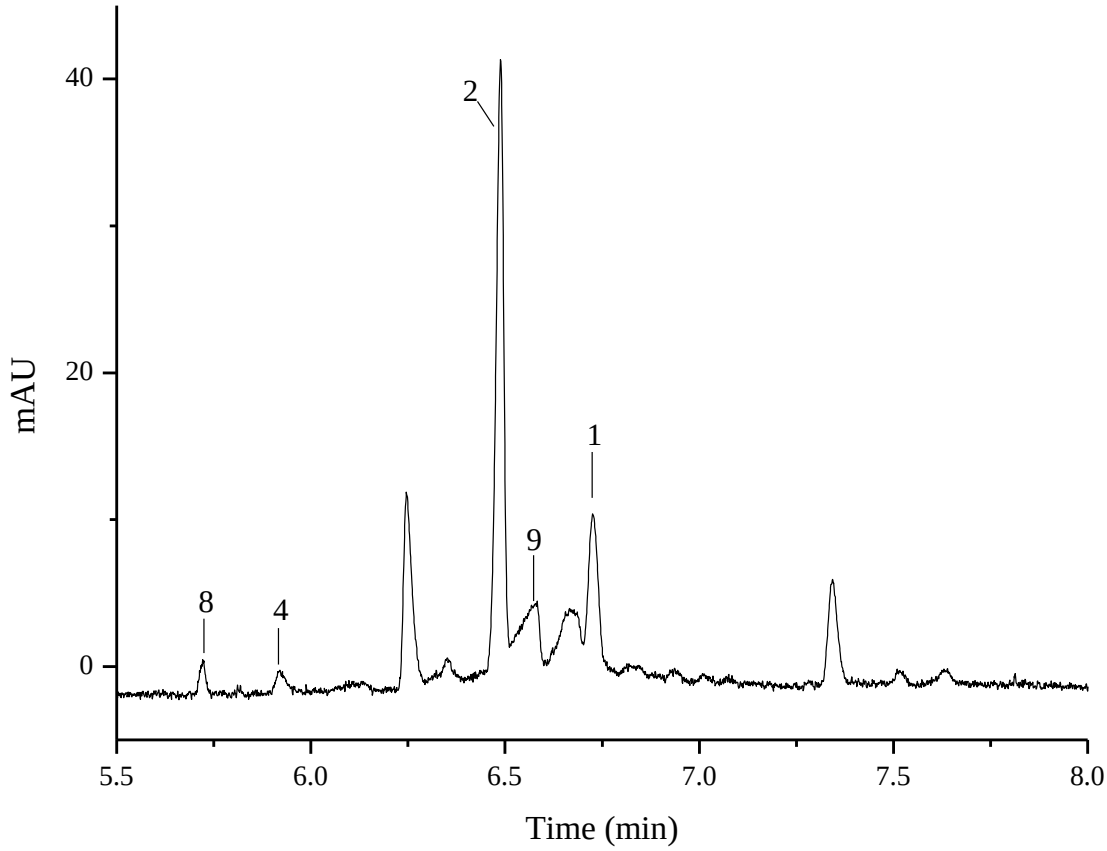

Figure 5-32 Electropherogram of 0.1% v/v balsam resin in 1:5 MeOH:buffer in positive polarity, 20 kV, capillary 58 cm (49.5 cm to detector), 50 µm i.d., 25°C, 5 mbar 20 s injection times, 5 mM β-CD 10 mM SDS 50 mM tris pH 8, detection at 200 nm. Numbers indicate (1) 7OXO, (2) DHA, (4) ABA, (8) ISO and (9) PIM.

Figure 5-32 shows the balsam resin sample analysed by the terpene method. This confirms that many of the balsam resin peaks correspond to the resin acids.

The acid concentration ratios of venetian turpentine and balsam resin are shown in Table 5-13. The ABA:DHA ratio of venetian turpentine is higher than all of the rosin samples. It was found to contain 225.3 mg L^{-1} ABA, which is less than that found in sample RD but the ABA:DHA ratio for RD was 7.2:1. The DHA:ISO also showed a higher ratio of ISO than found in the rosin samples. Again the ISO concentration is close to that found in sample RD but the DHA concentration found in venetian turpentine was lower. The ABA:ISO ratio is similar to that of sample RD while the ABA:PAL and DHA:PAL are similar to that of RA despite the PAL concentration in venetian turpentine being more than double that of concentrations in all rosin

samples. The ABA:NEO and ISO:NEO ratios are similar to those of samples RC and RD. There are not a sufficient amount of similar acid concentration ratios to link the venetian turpentine to a particular rosin sample and possible source.

The low ABA concentration found in balsam resin is seen in its acid ratios. While the DHA:PIM ratio is similar to that of good rosin RA, as with the venetian turpentine sample there are no obvious links between the resin sample and any of the rosins.

Table 5-13 Acid concentration ratios of resin samples

	Venetian turpentine	Balsam resin		Venetian turpentine	Balsam resin
ABA:DHA	11.6:1	1:8.8	NEO:PAL	1:4.6	
DHA:ISO	1:4	1.2:1	ABA:NEO	5.9:1	
DHA:PIM		1.9:1	DHA:NEO	1:1.9	
ABA:ISO	2.9:1	1:7.2	NEO:ISO	1:2	
ABA:PIM		1:4.5	ABA:SAN	5.6:1	
ISO:PIM		1.6:1	NEO:SAN	1:1	
ABA:PAL	1.3:1		DHA:SAN	1:2.1	
DHA:PAL	1:9		ISO:SAN	1.9:1	
DHA:7OXO		3.7:1	SAN:PAL	1:4.3	
ISO:PAL	1:2.3		PIM:7OXO		1.9:1
ISO:7OXO		3:1			

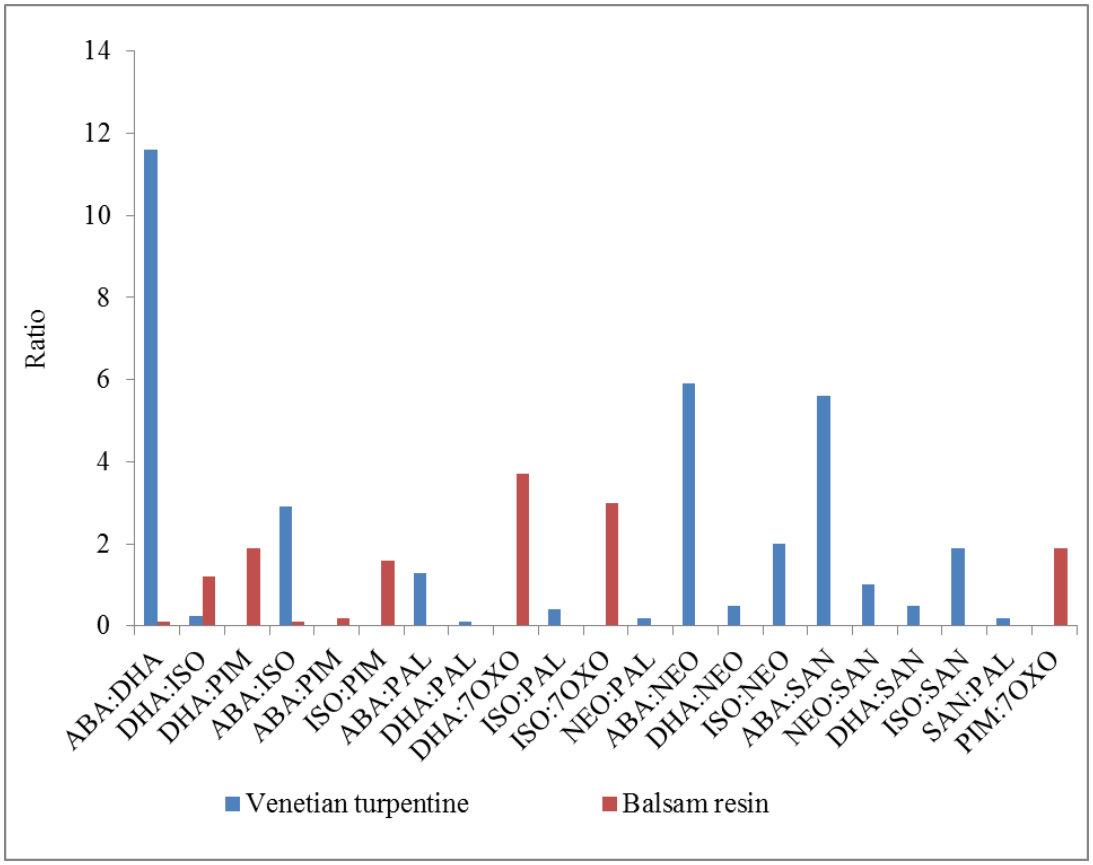

Figure 5-33 Bar chart for acid concentration ratios of resin samples

The acid concentration ratios from Table 5-13 are plotted in Figure 5-33. The venetian turpentine has a higher ABA:DHA ratio than all of the rosin samples. The DHA:7OXO ratio of balsam resin and the ISO:PAL, DHA:NEO, DHA:SAN, NEO:SAN, ABA:SAN and NEO:PAL ratios of the venetian turpentine are the smallest of all the rosin and resin samples. The ISO:7OXO ratio of balsam resin is close to the that of the polypale sample. The ABA:NEO ratio is similar to those of rosin samples RC and RD. The ISO:SAN ratio of the venetian turpentine is equal to that of the music rosin while the SAN:PAL ratio is equal to that of the cello rosin.

5.3.4 Rosin crystallisation

The acetone test was carried out on all of the modified and unmodified rosin samples to investigate which samples crystallised (see section 5.2.5 for the method). Non-crystallising rosin should give an amber-clear liquid that can be agitated without crystals forming in a time limit of 4 h. A rosin batch which forms crystals under the allotted time is deemed a fail and is not used in production. The speed and amount of crystals which form should be noted and are used to indicate the extent of the rosins tendency to crystallise. The resulting precipitates were also analysed by CE.

5.3.4.1 Natural gum rosins

The non-crystallising gum rosin samples RA and RB gave amber-clear liquids that formed no crystals within the 4 h test period. The samples were left in their containers and two months later there was still no evidence of crystal formation.

Both crystallising rosin samples also gave amber-clear liquids when dissolved in acetone. However, 15 min short of the 4 h test limit small crystals began to form in sample RD. Sample RC did not form any crystals in the 4 h test period. Over the next 24 h, crystals began to form in sample RC and continued to form in sample RD. 25% (by weight) of sample RC was crystallised while 14% (by weight) of sample RD. Technically, sample RC would have passed the acetone suitability test and been approved for use in products. This highlights a common issue for Henkel where unsuitable samples enter the production phase. This is significant as especially in this instance the sample which passed screening formed a greater percentage of crystals than the sample which failed. This test also confirmed that samples RA and RB were non-crystallising rosins and samples RC and RD were crystallising rosins. Over the following two months no change was observed.

5.3.4.2 Music and Cello rosins

The music rosin gave a dark green liquid when dissolved in acetone which was expected as the block itself was dark green. After the 4 h test period there were no crystals seen, however, the following day tiny crystals were observed on the walls of the jar container. Over the following 24 h more crystals formed until the liquid was 27% (by weight) crystallised. The cello rosin gave a dark orange liquid and tiny crystals were observed to form on the jar within the 4 h test period. Over the following 24 h the amount and size of the crystals in the cello rosin solution remained the same, however, within a week the cello rosin had formed more crystals than the music rosin solution. The cello crystals remained the same over the following two months while the music rosin crystals gradually increased until 90% of the solution was crystallised.

5.3.4.3 Modified rosins

The A-mod rosin gave a clear liquid while the polymerised and dimerised rosins gave amber solutions ranging from clear (dymerex) to dark amber (YT201 batches B and E). None of the modified rosins formed crystals within in the 4 h test period, and indeed the majority of modified samples showed no change two months later. This was expected as the purpose of modifying rosins is to prevent their crystallisation. However, after 5 months the A-mod rosin sample was observed to have formed crystals. On analysis it was found that the crystals composed mainly of DHA with the average concentration 214 mg L^{-1}. This is unexpected and emphasises the need for a screening method for rosin samples as simply modifying the gum rosin does not guarantee the avoidance of crystallisation.

5.3.4.4 Analysis of precipitate by CE

The precipitate was dissolved at 0.15% in MeOH and analysed using the acid CE method (Figure 5-34). In all cases it is clear from the electropherograms that the crystals consist mainly of acids, concentrations seen in Table 5-14. 7OXO and LVO were not found to be present in any of the crystal samples.

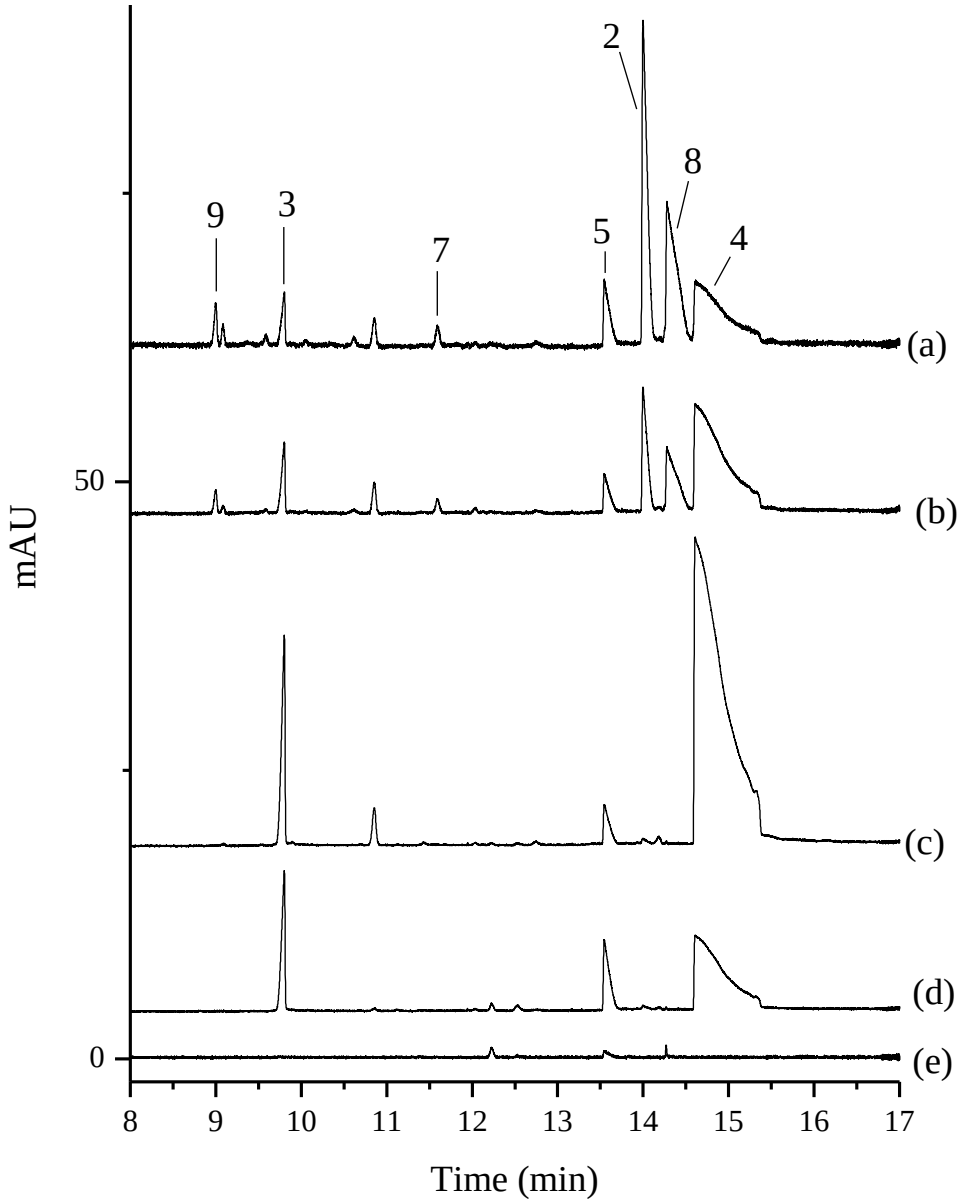

Figure 5-34 Electropherograms of a 0.15% v/v bad rosin crystals, analysed in positive polarity, 20 kV, capillary 58 cm (49.5 cm to detector), 50 µm i.d., 25°C, 50 mbar 4 s injection times, 15% MeOH 5 mM HPγCD 10 mM SBCD 20 mM tris buffer at pH 9. Wavelengths are (a) 200 nm, (b) 214, (c) 240 nm, (d) 265 nm and (e) 310 nm. Numbers indicate (2) DHA, (3) NEO, (4) ABA, (5) PAL, (7) SAN, (8) ISO and (9) PIM.

Table 5-14 Average concentrations and standard deviations for rosin crystals, n=3

	Sample RC crystals		Sample RD crystals		Music rosin crystals		Cello rosin crystals	
Acid	**Conc. (mg L^{-1})**	**SD**	**Conc. (mg L^{-1})**	**SD**	**Conc. (mg L^{-1})**	**SD**	**Conc. (mg L^{-1})**	**SD**
PIM	27	2.9	24.8	0.4	52.2	1.1	40.4	1.2
NEO	66.3	5.7	57.6	0.6	46.7	1.1	42.2	1.6
SAN	13.1	1.4	13.9	1.7				
PAL	86.5	9.5	84.9	2.2	66.7	1.1	69.9	6.5
DHA	38	4	45.1	1.2	60.8	0.9	46.9	2.9
ISO	144.3	14.9	163.4	7.4	44.2	2.8	29.7	1.7
ABA	749.1	91.6	767.3	11.5	585.1	7.9	265.3	18.3

The concentrations of the acids in the crystals formed by the two crystallising rosins are quite consistent. The biggest difference is the concentration of DHA and ISO which differ by 18.7% and 13.2% respectively between samples. The high ABA concentrations indicate that it is this acid with the highest tendency to crystallise. The lack of LVO indicates that it has isomerised to ABA.

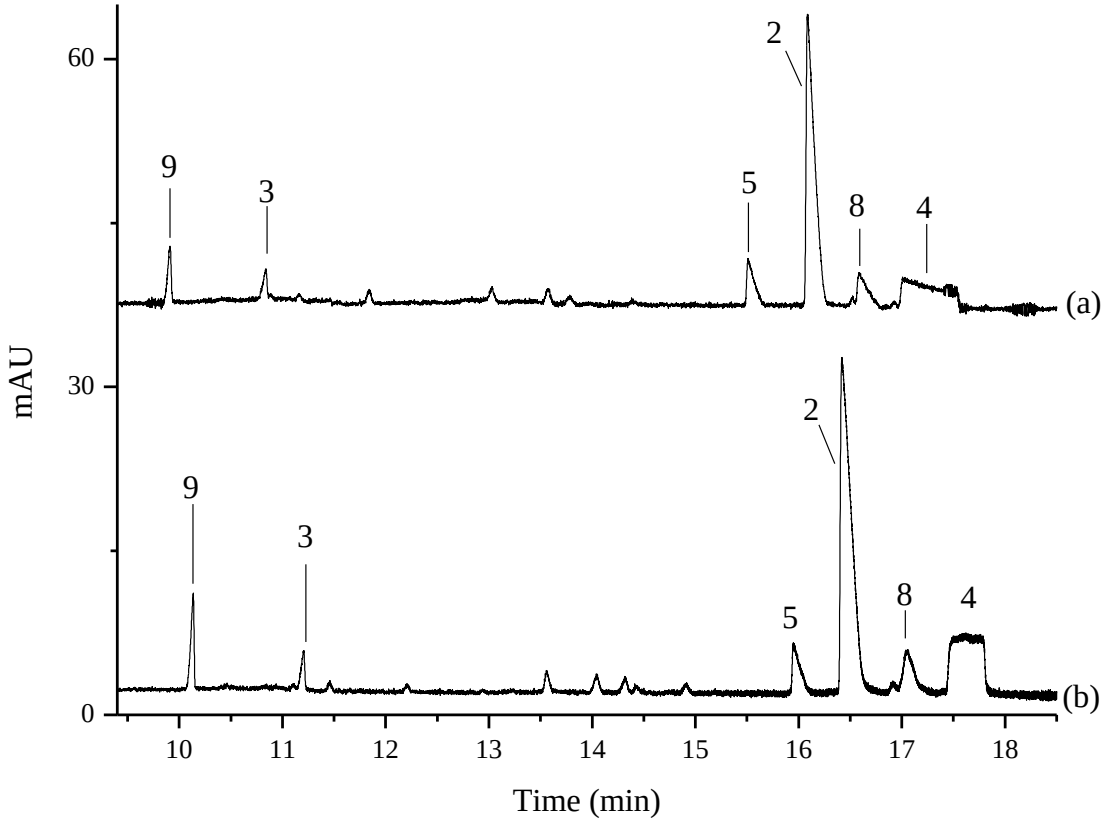

Figure 5-35 Electropherograms of a 0.15% v/v (a) cello rosin crystals and (b) music rosin crystals, analysed in positive polarity, 20 kV, capillary 58 cm (49.5 cm to detector), 50 µm i.d., 25°C, 50 mbar 4 s injection times, 15% MeOH 5 mM HPγCD 10 mM SBCD 20 mM tris buffer at pH 9. Detection at 200 nm. Numbers indicate (2) DHA, (3) NEO, (4) ABA, (5) PAL, (8) ISO and (9) PIM.

The crystals that precipitated from the music and cello rosins were analysed and the resultant electropherogram is in Figure 5-35. There are several differences in the crystal composition of these samples. As with samples RC and RD no LVO or 7OXO was found present. In addition, SAN was not detected in either sample. Compared to samples RC and RD, higher PIM and DHA concentrations were determined (see Table 5-14). Lower NEO and PAL concentrations were found in the music and cello rosin crystals. ISO and ABA showed the greatest decreases in concentration. All crystals showed ABA as the acid present in highest concentrations. The variation of DHA, ISO and ABA concentrations between cello and music is notable, with the music rosin crystals containing 55% more ABA. This suggests that either the cello and music rosins come from two different sources, or the supplier of rosin blocks for musical instruments modified it slightly, influencing its composition.

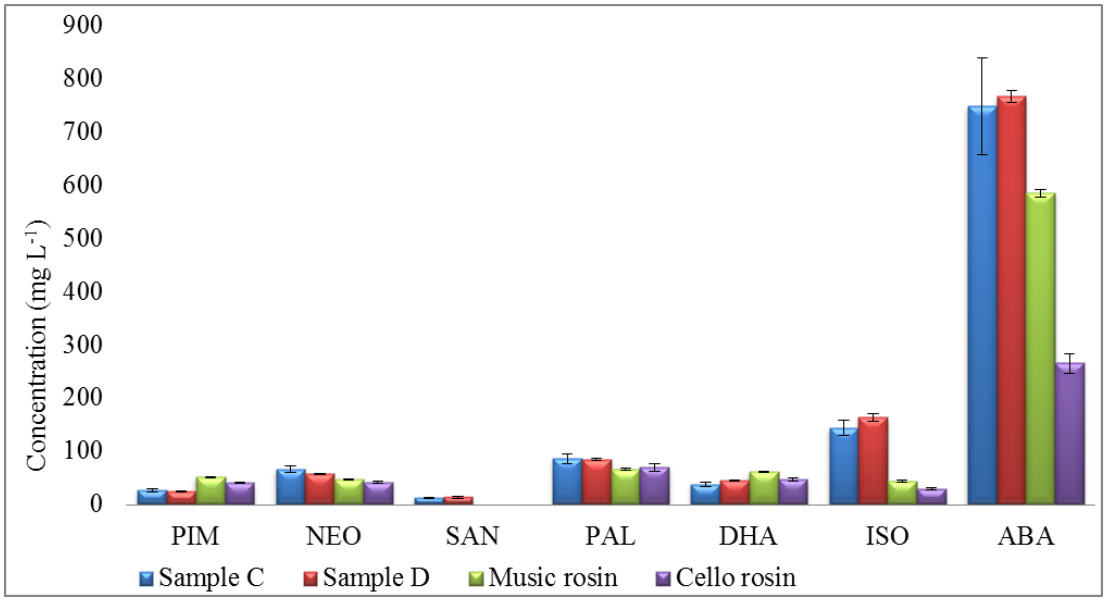

Figure 5-36 Acid plots of the precipitate from crystallising rosin samples

As illustrated in Figure 5-36, ABA is the majority of the precipitate formed when rosin samples crystallise. The music and cello rosin precipitates contain significantly less ABA and ISO than the gum rosin sample precipitates. No LVO or SAN was found in the music and cello rosin precipitates, while they contained higher concentrations of PIM and DHA.

5.4 Conclusions

A range of rosin and resin samples were analysed using the novel acid and terpene separation methods developed in chapters two, described in section 2.3.4.4 and chapter 3, described in section 3.3.4.5. The acids present were identified and quantified, and some differences and similarities of crystallising and non-crystallising rosin samples were noted.

Two crystallising and two non-crystallising rosin samples were analysed and several differences in their composition were noted. SAN and LVO were not detected in any of the gum rosin samples while NEO was only seen in the crystallising samples. In all gum rosins ISO and ABA were present in highest concentrations, with up to five times more ABA present in the crystallising samples. Some variation in acid concentration between similar samples was also observed. The crystallising samples contained slightly higher PIM and PAL concentrations, while the DHA concentration had decreased. The presence of NEO and elevated concentrations of ABA could be linked to a rosins tendency to crystallise.

Two commercial rosins sold for use with string instruments were analysed and found to be gum rosins. These rosins were found to contain small amounts of LVO and SAN. They also both contained NEO, indicating that they could be crystallising rosins. The ABA concentrations were also closer to those of the crystallising gum rosins.

Modified rosins including hydrogenated, disproportionated and polymerised rosin were also analysed using the acid separation method. In every case DHA was found to be the primary component as expected. The highest DHA concentrations were seen in the disproportionated rosin samples with smaller amounts of PIM present. LVO was also detected in the acid modified hydrogenated rosin. Varying concentrations of DHA and ABA were determined in different batches of one polymerised rosin. The difference in the composition of a partially-dimerised and a fully-dimerised rosin were highlighted by the presence of PIM, ISO and 7OXO, and higher DHA concentrations in a poly-pale rosin sample.

The acid concentration ratios of the music and cello rosin show many similarities to those of rosin samples RC and RD, the crystallising rosin samples. This suggests that they were sourced from a similar region, and may indicate a tendency of the music and cello rosins to crystallise. The acid concentration ratios of venetian turpentine do not indicate a common source with any of the gum rosin samples. Its ABA:DHA ratio was found to be higher than that off all the rosin samples. The high DHA concentration relative to the other acid in the modified rosin samples was highlighted in their acid concentration ratios. Some similarities between the ratios of the polypale sample and gum rosin samples RA and RB suggest it may have been sourced from the same region before modification.

No resin acids were detected in turpentine oil, while analysis using the terpene separation method showed that 3-carene and β-pinene were present. Venetian turpentine was analysed by both the acid and terpene method and both resin acids and terpenes detected. It was found to contain lower concentrations of DHA than the rosin samples while PAL and ABA were present in highest concentrations. A balsam resin sample was also analysed by both methods and found to contain resin acids.

The acetone crystallisation test was carried out on all natural and modified rosin samples. No crystals were formed by the non-crystallising rosin samples. Both crystallising gum samples resulted in crystals forming, however, one did so after the test period. This highlights that the test is a mere indicator and rosins which pass it can still go on to crystallise. The music and cello rosins both formed crystals, consistent with their acid composition which indicated they had a crystallisation tendency. Unexpectedly, the A-mod rosin sample was found to crystallise, highlighting that modifying the gum rosin does not guarantee the avoidance of crystallisation.

The CE methods developed allow for a rapid and simple screening of many rosin samples. With the application of this separation method to more samples of crystallising rosins, further links between variations in the composition of these and non-crystallising rosin can be deduced. The application of the acid and terpene method to resin samples highlights the versatility of the method to other natural samples.

Chapter 6

Conclusion

The aim of this work was to investigate the composition of rosin samples using capillary electrophoresis in order to provide an alternative separation technique to GC-MS, and to further investigate any links between the rosins composition and its tendency to crystallise. Figure 6-1 shows the general analytical protocol followed for the analysis of rosin composition.

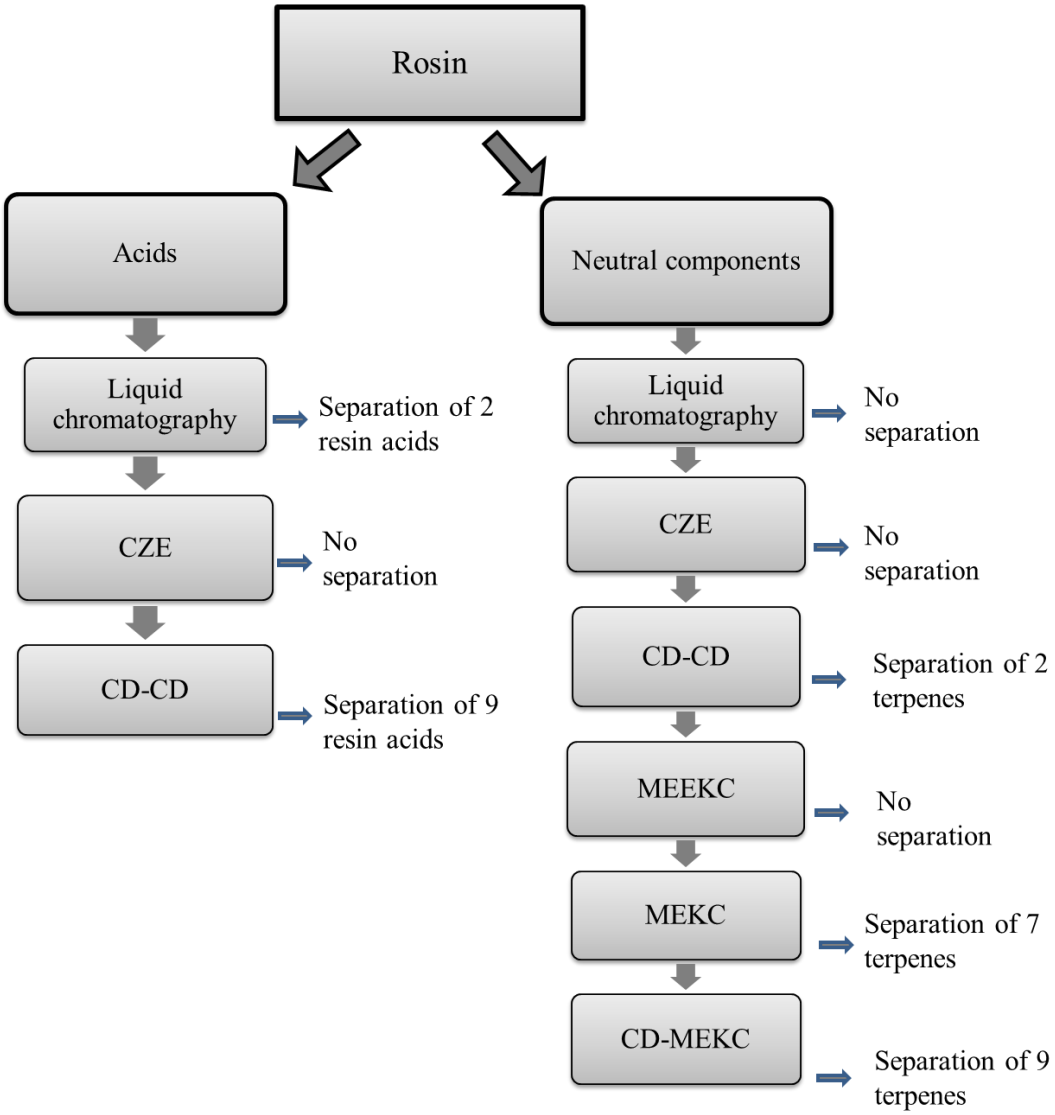

Figure 6-1 Flow chart of method development protocol

6.1 Acid separation method

A CE method was developed for the separation of nine resin acids; abietic-, dehydroabietic-, neoabietic-, pimaric-, isopimaric-, levopimaric-, sandaracopimaric-, palustric- and 7-oxo-dehydroabietic acid, three of which had not been successfully separated previously by CE. The optimum buffer was found to be 15% MeOH 5 mM HPγCD 10 mM SBCD in 20 mM tris buffer at pH 9. This was the first report of the use of CE for the quantification of resin acids in rosin samples. This method offers a rapid screening method for rosin samples that could be used in place of sometimes lengthy and often requiring a derivatisation step GC-MS methods. The quick screening method allows companies who intend on purchasing rosin which is usually sold in bulk to quickly analyse a sample from the batch and see if it suitable for its intended purpose.

6.2 Neutral separation method

The simultaneous determination of nine neutral compounds present in rosin samples including monoterpenes, sesquiterpenes and alcohols was shown. A cyclodextrin-modified MEKC method was used to separate α-pinene, β-pinene, camphene, 3-carene, terpineol, 4-allylanisole, longifolene, isolongifolene and aromadendrene for the first time. The optimum buffer was found to be 5 mM β-CD 10 mM SDS 50 mM tris pH 8 in the first application of CE to the analysis of the neutral fraction of rosin samples.

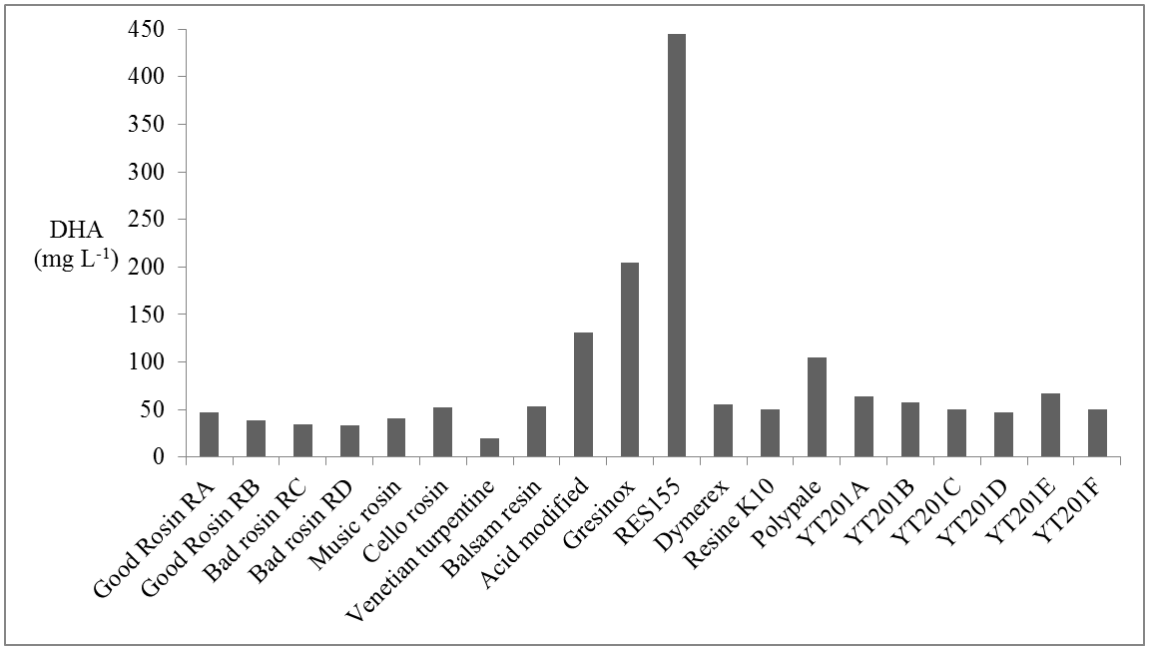

Figure 6-2 Bar chart showing the concentration of DHA in rosin and resin samples

6.3 Analysis of rosin and resin samples

Rosin and resin samples were analysed using the separation methods described in sections 6.1 and 6.2. The novel methods were applied to a range of modified and unmodified rosin samples and the resin acids in the rosins quantified. Differences in the composition of crystallising and non-crystallising rosins were observed. The separation methods were also applied to resin samples showing their usefulness in the analysis of other natural products. As seen in Table 6-1, DHA is the only acid present in every sample as illustrated in Figure 6-2.

Table 6-1 Rosin and resin samples analysed, X indicates the presence of the acids in the various samples

	ABA	DHA	ISO	NEO	PIM	LVO	PAL	SAN	7OXO
Good rosin	X	X	X		X		X		X
Bad rosin	X	X	X	X	X		X		X
Music	X	X	X	X	X	X	X	X	X
Cello	X	X	X	X	X	X	X	X	X
RES155		X			X				
Gresinox		X			X				
A-mod		X			X	X			
YT201 batches	X	X							
Dymerex	X	X							
Polypale	X	X	X		X				X
Resine K10	X	X							X
Venetian turpentine	X	X	X	X			X	X	
Balsam resin	X	X	X		X				X

Predictably, the modified rosin samples contained more DHA than the gum rosin samples as many modification techniques result in the formation of DHA. The highest concentrations were found in the disproportionated and hydrogenated rosin samples and the partially-dimerised polypale sample. The crystallising rosin samples RC and RC contained the lowest amounts of DHA of all the rosin samples while the venetian turpentine contained even less.

6.4 Rosin crystallisation

There were several differences in composition in crystallising and non-crystallising rosins noted. The concentration of ABA was found to be the main difference with crystallising rosin samples found to contain more than twice the amount of ABA compared to non-crystallising samples. The non-crystallising samples contained no NEO while it was present in both crystallising rosins. The non-crystallising samples also contained lower amounts of DHA. Both music rosins crystallised and were found to contain LVO and SAN which was not detected in any gum rosin samples.

This is another possible indicator of a tendency to crystallise. The A-mod sample was the only modified rosin sample to crystallise and the only one found to contain LVO which further supports this hypothesis. These methods can be used to analyse further rosin samples and build up a database of information on their compositions.

6.5 Association constants

The association constants of the inclusion complexes formed by cyclodextrins with some of the acids and neutral compounds found in rosin samples were investigated by affinity capillary electrophoresis. This method was found to be unsuitable for the determination of association constants of neutral compounds. The requirement of SDS in order to provide mobility to the neutral compounds resulted in SDS-CD interactions which meant that the change in complex mobility was not solely dependent on the CD concentration.

In conclusion the work presented in this thesis has led to a novel, rapid and robust screening method for rosin acids, a novel separation method for terpenes and has led to an improved understanding of the analyte:host separation mechanisms. These analytical methods can be used by the industry that has funded the research to improve their management of rosins used in their processes.

List of publications and presentations

Publications

L. Mckeon, F. Regan, B. Burns, R. Leonard, 2014. Determination of resin acid composition in rosin samples using cyclodextrin modified capillary electrophoresis, *Journal of Separation Science.*

Proposed publications

L. Mckeon, F. Regan, B. Burns, R. Leonard, Development of a Capillary Electrophoresis method for the separation of terpenes and other neutral compounds found in rosin samples, to be submitted to *Analytical Letters.*

L. Mckeon, F. Regan, B. Burns, R. Leonard, Determination of cyclodextrin association constants with terpenes and resin acids by affinity capillary electrophoresis using three linear plotting methods. To be submitted to *Electrophoresis.*

Conferences attended

9th Balaton Symposium on high-performance separation methods, Siófok, Hungary (September 2013).

Oral presentation: Determination of the Composition of Natural Rosins using Cyclodextrin-modified Capillary Electrophoresis.

Conference on Analytical Sciences Ireland (CASi), Cork, Ireland (July 2013).

Oral presentation: Determination of nine resin acids in natural gum rosins by cyclodextrin-modified capillary electrophoresis.

HPLC 2013, Amsterdam, Holland (June 2013).

Poster presented: HPLC and capillary electrophoresis for determination of acids, terpenes and aldehydes in natural rosins.

Analytical Research Forum (ARF) Durham, UK (June 2012).

Poster presented: Application of capillary electrophoresis to the determination of the composition of natural rosins.

The Irish Adhesion and Surface Coating Conference, Institute of Technology Tallaght, Dublin, Ireland (September 2011).

Poster presented: Characterisation and determination of rosin fingerprints using analytical chemistry.

Analytical Research Forum (ARF) University of Manchester, UK (June 2011).

Poster presented: Initial characterisation and determination of rosin fingerprints using analytical approaches.

Conference on Analytical Sciences Ireland (CASi), The Helix, Dublin City University (February 2011).

Poster presented: Ultrafiltration of anthracyclines and taxanes, and their simultaneous determination using Sweeping MEKC.

Chapter 7

References

[1] Zinkel, D. F.Russell, J. , Naval Stores; Production, Chemistry, Utilization, Pulp Chemicals Association, New York 1989.

[2] Botham, P. A., Lees, D., Illing, H. P. Malmfors, T. ,Regul. Toxicol. Pharmacol. 2008, 52, 257-263.

[3] Sadhra, S., Gray, C. N. Foulds, I. S. ,J. Chromatogr. B Biomed. Sci. Appl. 1997, 700, 101-110.

[4] Mandaogade, P. M., Satturwar, P. M., Fulzele, S. V., Gogte, B. B. Dorle, A. K. ,React. Funct. Polym. 2002, 50, 233-242.

[5] Watson, S. I., Cain, J. R., Cowie, H. Cherrie, J. W. ,Ann. Occup. Hyg. 2001, 45, 669-676.

[6] Joye, N. M.Lawrence, R. V. ,J. Chem. Eng. Data 1967, 12, 279-282.

[7] Olivares-Pérez, A., Ibarra-Torres, J. C., Ortiz-Gutiérrez, M., Pérez-Cortés, M. Fuentes-Tapia, I. ,Opt. Mater. 2005, 27, 1825-1831.

[8] Burge, P. S., Edge, G., Hawkins, R., White, V. Taylor, A. J. ,Thorax 1981, 36, 828-834.

[9] Smith, P. A., Son, P. S., Callaghan, P. M., Jederberg, W. W., Kuhlmann, K. Still, K. R. ,Toxicology 1996, 111, 225-238.

[10] Karlberg, A., Gäfvert, E. Lidén, C. ,J. Am. Acad. Dermatol. 1995, 33, 427-432.

[11] Illing, H. P. A., Malmfors, T. Rodenburg, L. ,Regul. Toxicol. Pharm. 2009, 54, 234-241.

[12] Burge, P. S. ,Clin. Immunol. Allergy 1984, 4, 55-81.

[13] Souto, J. C., Yustos, P., Ladero, M. Garcia-Ochoa, F. ,Bioresour. Technol. 2011, 102, 3504-3511.

[14] Shaw, D. N.Sebrell, L. B. ,Ind. Eng. Chem. Res. 1926, 18, 612-614.

[15] Atta, A. M., El-Saeed, S. M. Farag, R. K. ,React. Funct. Polym. 2006, 66, 1596-1608.

[16] Liu, X., Xin, W. Zhang, J. ,Bioresour. Technol. 2010, 101, 2520-2524.

[17] Luong, J. H. T., Rigby, T., Male, K. B. Bouvrette, P. ,Electrophoresis 1999, 20, 1546-1554.

[18] Kamaya, Y., Tokita, N. Suzuki, K. ,Ecotoxicol. Environ. Saf. 2005, 61, 83-88.

[19] Genge, C. A. ,Anal. Chem. 1959, 31, 1750-1753.

[20] Vianco, P. T. , Welding, Brazing, and Soldering, ASM International, USA 1993.

[21] Guenier, J. P., Simon, P., Delcourt, J., Didierjean, M. F., Lefevre, C. Muller, J. ,Chromatographia 1984, 18, 137-144.

[22] Smith, P. A., Bowerbank, C. R. Lee, M. L. ,Am. Ind. Hyg. Assoc. J. 2000, 61, 95-101.

[23] Pengelly, M., Foster, R. D., Groves, J. A., Ellwood, P. A., Turnbull, G. B. Wagg, R. M. ,Ann. Occup. Hyg. 1994, 38, 753-763.

[24] Wiyono, B., Tachibana, S. Tinambunan, D. ,Pak. J. Biol. Sci. 2006, 9, 7-14.

[25] A. Hadi. , 2010, Investigation of Natural Products in Rosins, and Related Supramolecular Complexes, Institute of Technology Tallaght, PhD thesis

[26] Palkin, S.Smith, W. C. ,J. Am. Oil Chem. Soc. 1938, 15, 120-122.

[27] R. Palmer. , 1930, US1787281 A, US 1787281, Process of treating rosin and product therefrom

[28] G. J. Kutsek. , 2005, EP20030817053, US 6939944 B2, Inhibition of rosin crystallization

[29] Stinson, J. S.Lawrence, R. V. ,Ind. Eng. Chem. Res. 1954, 46, 784-787.

[30] Fiebach, K.Grimm, D. , Ullman's Encyclopedia of Industrial Chemistry, Wiley-VCH, Berlin 2002.

[31] T. E. Thanos. , 1978, US 4105462, US 4105462, Non-crystallizing rosin

[32] Kumooka, Y. ,Forensic Sci. Int. 2008, 176, 111-120.

[33] Loeblich, V. M., Baldwin, D. E., O'Connor, R. T. Lawrence, R. V. ,J. Am. Chem. Soc. 1955, 77, 6311-6313.

[34] Loeblich, V. M., Baldwin, D. E. Lawrence, R. V. ,J. Am. Chem. Soc. 1955, 77, 2823-2825.

[35] Wang, L., Chen, X., Liang, J., Chen, Y., Pu, X. Tong, Z. ,Chem. Eng. J. 2009, 152, 242-250.

[36] Liu, S., Xie, C., Yu, S. Liu, F. ,Catal. Commun. 2008, 9, 2030-2034.

[37] Downs, A. M. R.Sansom, J. E. ,Contact Derm. 1999, 41, 305-310.

[38] Bailey, R. S. , Encyclopedia of Chemical Technology, Wiley, New York 1983.

[39] Wu, C. M. L., Yu, D. Q., Law, C. M. T. Wang, L. ,Mat. Sci. Eng. R. 2004, 44, 1-44.

[40] AWS Committee on Brazing and Soldering. , Soldering Manual, American Welding Society, Miami 1977.

[41] Barber, C. L. ,Ind. Eng. Chem. Res. 1937, 29, 1114-1117.

[42] Smith, B. A.Turbini, L. J. ,J. Electron. Mater. 1999, 28, 1299-1306.

[43] Galvan, J. C., Bastidas, J. M. Feliu, S. ,Weld. J. 1996, 75, S366-S371.

[44] Strauss, R. , SMT Soldering Handbook, Newnes, Oxford 1998.

[45] Institute for Interconnecting and Packaging Electronic Circuits (IPC). , J-STD-004, Requirements for soldering fluxes, 2011

[46] International Organization for Standardization. , ISO 9454-1, Soft Soldering Fluxes, 1990.

[47] Wei, X., Zhou, L., Huang, H. Xiao, H. ,Mater. Lett. 2005, 59, 1889-1892.

[48] Hudy, J. A. ,Anal. Chem. 1959, 31, 1754-1756.

[49] Norin, T.Westfelt, L. ,Acta Chem. Scand. 1963, 17, 1828-1830.

[50] Joye, N. M., Lawrence, R. V. Gough, L. J. ,J. Org. Chem. 1966, 31, 320-321.

[51] Joye, N. M.Lawrence, R. V. ,J. Chem. Eng. Data. 1967, 12, 279-282.

[52] Hasson, J. C.Kulkarni, M. V. ,Anal. Chem. 1972, 44, 1586-1589.

[53] Nestler, F. H. M.Zinkel, D. F. ,Anal. Chem. 1963, 35, 1747-1749.

[54] Osete-Cortina, L., Doménech-Carbó, M. T., Mateo-Castro, R., Gimeno-Adelantado, J. V. Bosch-Reig, F. ,J. Chromatogr. A. 2004, 1024, 187-194.

[55] Doménech-Carbó, M. T., Kuckova, S., de la Cruz-Cañizares, J. Osete-Cortina, L. ,J. Chromatogr. A. 2006, 1121, 248-258.

[56] Osete-Cortina, L.Doménech-Carbó, M. T. ,J. Chromatogr. A. 2005, 1065, 265-278.

[57] Doménech-Carbó, M. T., Osete-Cortina, L., De la, C. C., Bolívar-Galiano, F., Romero-Noguera, J., Fernández-Vivas, M. A. Martín-Sánchez, I. ,Anal. Bioanal. Chem. 2006, 385, 1265-1280.

[58] Dell`mour, M., Findeisen, A., Kaml, I., Baatz, W. Kenndler, E. ,Open Anal. Chem. J. 2008, 2, 67-73.

[59] Kaml, I.Kenndler, E. ,Curr. Anal. Chem. 2007, 3, 33-40.

[60] Findeisen, A., Kolivoska, V., Kaml, I., Baatz, W. Kenndler, E. ,J. Chromatogr. A. 2007, 1157, 454-461.

[61] Brooks, T. W., Fisher, G. S. Joye, N. M. ,Anal. Chem. 1965, 37, 1063-1064.

[62] Latorre, A., Rigol, A., Lacorte, S. Barceló, D. ,J. Chromatogr. A. 2003, 991, 205-215.

[63] Vandenabeele, P., Wehling, B., Moens, L., Edwards, H., De Reu, M. Van Hooydonk, G. ,Anal. Chim. Acta 2000, 407, 261-274.

[64] Kersten, P.J.: Kopper, B. J., Raffa, K. F. Illman, B. L. ,J. Chem. Ecol. 2006, 32, 2679-2685.

[65] McMartin, D. W., Peru, K. M., Headley, J. V., Winkler, M. Gillies, J. A. ,J. Chromatogr. A. 2002, 952, 289-293.

[66] Nilsson, U., Berglund, N., Lindahl, F., Axelsson, S., Redeby, T., Lassen, P. Karlberg, A. ,J. Sep. Sci. 2008, 31, 2784-2790.

[67] Landers, J. P. , Handbook of Capillary Electrophoresis, CRC Press LLC, USA 1997.

[68] Agilent Technologies. , Understanding Your ChemStation, Agilent Technologies, Germany 2001.

[69] Brown, P. R.Weston, A. , HPLC and CE, Principles and Practise, Academic Press, San Diego, California 1997.

[70] Tubaon, R. M. S., Rabanes, H., Haddad, P. R. Quirino, J. P. ,Electrophoresis 2014, 35, 190-204.

[71] Piergiovanni, A. ,Anal. Bioanal. Chem. 2013, 405, 481-491.

[72] Rabanes, H. R., Guidote Jr., A. M. Quirino, J. P. ,Electrophoresis 2012, 33, 180-195.

[73] Weinberger, R. , Practical Capillary Electrophoresis, Academic Press, San Diego, California 2000.

[74] Altria, K. D. , Capillary Electrophoresis Guidebook: Principles, Operation, and Applications, Humana Press Inc., New Jersey 1996.

[75] Terabe, S. ,Procedia Chemistry 2010, 2, 2-8.

[76] Silva, M. ,Electrophoresis 2013, 34, 141-158.

[77] Terabe, S., Otsuka, K., Ichikawa, K., Tsuchiya, A. Ando, T. ,Anal. Chem. 1984, 56, 111-113.

[78] Watari, H., Ogawa, K., Abe, M., Monta, T. Takahashi, L. ,Anal. Sci. 1991, 7 (supplement), 245-248.

[79] Yang, H., Ding, Y., Cao, J. Li, P. ,Electrophoresis 2013, 34, 1273-1294.

[80] Altria, K. D. ,J. Chromatogr. A. 2000, 892, 171-186.

[81] Atwood, J., Davies, J., Macnicol, D.Vögtle, F. , Comprehensive Supramolecular Chemistry: Cyclodextrins, Elsevier Science Ltd, New York 1996.

[82] Kurkov, S. V.Loftsson, T. ,Int. J. Pharm. 2013, 453, 167-180.

[83] Del Valle, E. M. M. ,Process Biochem. 2004, 39, 1033-1046.

[84] Yamada, A., Ezaki, Y., Matsuo, K., Yarita, T. Nomura, A. ,J. Chromatogr. A. 1995, 709, 345-349.

[85] Ye, Y. K.Stringham, R. W. ,J. Chromatogr. A. 2001, 927, 47-52.

[86] Lee, B. L., Ong, H. Y., Koh, D. Ong, C. N. ,J. Chromatogr. A. 1994, 685, 263-269.

[87] Kumooka, Y. ,Forensic Sci. Int. 2008, 176, 111-120.

[88] Vieweg, F.Verlagsgesellschaf, S. ,Chromatographia Supplement 2001, 54, 59-77.

[89] Sotthivirat, S., Haslam, J. L. Stella, V. J. ,Int. J. Pharm. 2007, 330, 73-81.

[90] Gahm, K., Chang, L. W. Armstrong, D. W. ,J. Chromatogr. A. 1997, 759, 149-155.

[91] Pereira, E. A., Carrilho, E. Tavares, M. F. M. ,J. Chromatogr. A. 2002, 979, 409-416.

[92] Panda, H. , The Complete Technology Book on Natural Products (Forest Based), National Institute Of Industrial Research, Dehli 2002.

[93] Lee, B. L., Koh, D., Ong, H. Y. Ong, C. N. ,J. Chromatogr. A. 1997, 763, 221-226.

[94] Boyce, M. ,J. Chem. Educ. 1999, 76, 815-819.

[95] Beckers, J. L.Bocek, P. ,Electrophoresis 2000, 21, 2747-2767.

[96] Orabi, A. S.Azab, H. A. ,J. Chem. Eng. Data 1997, 42, 1219-1223.

[97] Yeniceli, D., Deng, X., Adams, E., Dogrukol-Ak, D. Schepdael, A. V. ,Electrophoresis 2013, 34, 463-470.

[98] Axelsson, S., Eriksson, K. Nilsson, U. ,J. Environ. Monit. 2011, 13, 2940-2945.

[99] Kubesová, A., Horká, M., Růžička, F., Šlais, K. Glatz, Z. ,J. Chromatogr. A. 2010, 1217, 7288-7292.

[100] Joye Jr., N. M., Proveaux, A. T. Lawrence, R. V. ,J. Am. Oil Chem. Soc. 1973, 50, 104-107.

[101] Gotti, R. ,J. Pharm. Biomed. Anal. 2011, 55, 775-801.

[102] Asztemborska, M., Sybilska, D., Nowakowski, R. Perez, G. ,J. Chromatogr. A. 2003, 1010, 233-242.

[103] Diagone, C., Ogawa, C. Lanças, F. ,J. Liq. Chromatogr. Rel. Technol. 2003, 26, 505-516.

[104] Moeder, C., O'Brien, T., Thompson, R. Bicker, G. ,J. Chromatogr. A. 1996, 736, 1-9.

[105] Rodrigues, M. R. A., Caramão, E. B., Arce, L., Ríos, A. Valcárcel, M. ,J. Agric. Food Chem. 2002, 50, 4215-4220.

[106] Cao, J., Chen, J., Yi, L., Li, P. Qi, L. ,Electrophoresis 2008, 29, 2310-2320.

[107] Musenga, A., Mandrioli, R., Ferranti, A., D'Orazio, G., Fanali, S. Raggi, M. A. ,J. Sep. Sci. 2007, 30, 612-619.

[108] Pavia, D. L., Lampman, G. M., Kriz, G. S.Vyvyan, J. R. , Introduction to Spectroscopy, Brooks/Cole, Cengage Learning, USA 2009.

[109] Sherma, J. W.,M. , High Performance Liquid Chromatography in Phytochemical Analysis, CRC Press, USA 2011.

[110] Stapf, F. I., Oehme, M., Kiessig, S., Schwarz, M. A. Kálmán, F. ,Electrophoresis 2007, 28, 3625-3638.

[111] Ràfols, C., Poza, A., Fuguet, E., Rosés, M. Bosch, E. ,Electrophoresis 2002, 23, 2408-2416.

[112] Cao, Y.Sheng, J. ,Electrophoresis 2010, 31, 672-678.

[113] Sirén, H.Karttunen, A. ,J. Chromatogr. B. 2003, 783, 113-124.

[114] Honoré Hansen, S., Gabel-Jensen, C. Pedersen-Bjergaard, S. ,J. Sep. Sci. 2001, 24, 643-650.

[115] Oledzka, I., Kowalski, P., Baluch, A., Baczek, T., Paradziej-Lukowicz, J., Taciak, M. Pastuszewska, B. ,J. Sci. Food Agric. 2014, 94, 544-551.

[116] Yang, F., Yang, J., Zhang, X., Xu, P. Xia, Z. ,J. Chromatogr. Sci. 2013, 51, 155-160.

[117] Pomponio, R., Gotti, R., Luppi, B. Cavrini, V. ,Electrophoresis 2003, 24, 1658-1667.

[118] Cifuentes, A., Bernal, J. L. Diez-Masa, J. ,Anal. Chem. 1997, 69, 4271-4274.

[119] Fuguet, E., Ràfols, C., Rosés, M. Bosch, E. ,Anal. Chim. Acta 2005, 548, 95-100.

[120] Benito, I., García, M. A., Monge, C., Saz, J. M. Marina, M. L. ,Colloids Surf., A 1997, 125, 221-224.

[121] Gahm, K., Chang, L. W. Armstrong, D. W. ,J. Chromatogr. A. 1997, 759, 149-155.

[122] Rodrigues, M. R. A., Caramão, E. B., Arce, L., Rios, A. Valcárcel, M. ,J. Microcolumn Sep. 2001, 13, 293-299.

[123] Ceborska, M., Asztemborska, M., Luboradzki, R. Lipkowski, J. ,Carbohydr. Polym. 2013, 91, 110-114.

[124] Chatjigakis, A., Clarot, I., Cardot, P., Nowakowski, R. Coleman, A. ,J. Liq. Chromatogr. Rel. Technol. 1999, 22, 1267-1284.

[125] Bao-Hui Li, Li-Ping Yu Xiu-Ping Yan. ,Anal. Lett. 2005, 38, 1975-1985.

[126] Szejtli, J. ,Chem.Rev. 1998, 98, 1743-1754.

[127] Benes, M., Zusková, I., Svobodová, J. Gas, B. ,Electrophoresis 2012, 33, 1032-1039.

[128] Larsen, K. L.Zimmermann, W. ,J. Chromatogr. A. 1999, 836, 3-14.

[129] Valente, A. J. M.Söderman, O. ,Adv. Colloid Interface Sci. 2013, 205, 156-176.

[130] Dvorák, M., Svobodová, J., Benes, M. Gas, B. ,Electrophoresis 2013, 34, 761-767.

[131] Steed, J. W.Atwood, J. L. , Supramolecular Chemistry, Wiley, USA 2009.

[132] Bellini, M. S., Deyl, Z., Manetto, G. Kohlíčková, M. ,J. Chromatogr. A. 2001, 924, 483-491.

[133] Jiang, C.Armstrong, D. W. ,Electrophoresis 2010, 31, 17-27.

[134] Cirri, M., Maestrelli, F., Orlandini, S., Furlanetto, S., Pinzauti, S. Mura, P. ,J. Pharm. Biomed. Anal. 2005, 37, 995-1002.

[135] Flaherty, R. J., Nshime, B., DeLaMarre, M., DeJong, S., Scott, P. Lantz, A. W. ,Chemosphere 2013, 91, 912-920.

[136] Shakalisava, Y.Regan, F. ,Electrophoresis 2006, 27, 3048-3056.

[137] Rundlett, K. L.Armstrong, D. W. ,J. Chromatogr. A. 1996, 721, 173-186.

[138] François, Y., Varenne, A., Sirieix-Plenet, J. Gareil, P. ,J. Sep. Sci. 2007, 30, 751-760.

[139] Karakasyan, C., Taverna, M. Millot, M. ,J. Chromatogr. A. 2004, 1032, 159-164.

[140] Phuong, N., Lee, K., Kim, K., Choi, J., Kim, J. Kang, J. ,Arch. Pharm. Res. 2004, 27, 1290-1294.

[141] Al Azzam, K. M., Saad, B. Aboul-Enein, H. Y. ,Electrophoresis 2010, 31, 2957-2963.

[142] Li-Wei Zhang, Ding, L. Xin-Xiang Zhang. ,Anal. Bioanal. Chem. 2007, 387, 2833-2841.

[143] Lin, C., Huang, H. Chen, H. ,J. Chromatogr. A. 2001, 917, 297-310.

[144] Palepu, R.Reinsborough, V. C. ,Can. J. Chem. 1988, 66, 325-328.

[145] Cserhati, T., Forgacs, E.Smith, R. M. , Cyclodextrins in Chromatography, The Royal Society of Chemistry, UK 2003.

[146] Brocos, P., Banquy, X., Díaz-Vergara, N., Pérez-Casas, S., Pineiro, Ã Costas, M. ,J. Phys. Chem. B 2011, 115, 14381-14396.

[147] Asztemborska, M., Nowakowski, R. Sybilska, D. ,J. Chromatogr. A. 2000, 902, 381-387.

[148] Rekharsky, M. V.Inoue, Y. ,Chem. Rev. 1998, 98, 1875-1918.

[149] Connors, K. A. ,Chem. Rev. 1997, 97, 1325-1358.

[150] Ciobanu, A., Landy, D. Fourmentin, S. ,Food Res. Int. 2013, 53, 110-114.

[151] Micke, G. A., Moraes, E. P., Farah, J. P. S. Tavares, M. F. M. ,J. Chromatogr. A. 2003, 1004, 131-143.

[152] Tanaka, Y.Terabe, S. ,J. Chromatogr. B. 2002, 768, 81-92.

[153] Uselová-Vceláková, K., Zusková, I. Gas, B. ,Electrophoresis 2007, 28, 2145-2152.

[154] Li, Z., Wei, C., Zhang, Y., Wang, D. Liu, Y. ,J. Chromatogr. B. 2011, 879, 1934-1938.

[155] Rekharsky, M. V., Goldberg, R. N., Schwarz, F. P., Tewari, Y. B., Ross, P. D., Yamashoji, Y. Inoue, Y. ,J. Am. Chem. Soc. 1995, 117, 8830-8840.

[156] Schneiderman, E.Stalcup, A. M. ,J. Chromatogr. B. 2000, 745, 83-102.

[157] Nishi, H., Fukuyama, T. Terabe, S. ,J. Chromatogr. A. 1991, 553, 503-516.

[158] Kalogeropoulos, N., Konteles, S., Mourtzinos, I., Troullidou, E., Chiou, A. Karathanos, V. T. ,J. Microencapsul. 2009, 26, 603-613.

[159] Cepeda, M., Daviña, R., García-Río, L. Parajó, M. ,Chem. Phys. Lett. 2010, 499, 70-74.

[160] Paul, B. K., Ray, D., Ganguly, A. Guchhait, N. ,J.Colloid Interface Sci. 2013, 411, 230-239.

[161] Astray, G., Cid, A., García-Río, L., Lodeiro, C., Mejuto, J. C., Moldes, O. Morales, J. ,Prog. React. Kinet. Mec. 2010, 35, 105-129.

[162] Yan, Y., Jiang, L. Huang, J. ,Phys. Chem. Chem. Phys. 2011, 13, 9074-9082.

[163] Bendazzoli, C., Mileo, E., Lucarini, M., Olmo, S., Cavrini, V. Gotti, R. ,Microchim. Acta 2010, 171, 23-31.

[164] Prati, S., Sciutto, G., Mazzeo, R., Torri, C. Fabbri, D. ,Anal. Bioanal. Chem. 2011, 399, 3081-3091.

[165] Vincenzo Russo, M.Avino, P. ,Chem. Cent. J. 2012, 6, 59-68.

[166] Mannino, M. R., Orecchio, S. Gennaro, G. ,Microchem. J. 2013, 110, 407-416.

[167] Portugal, I., Vital, J. Lobo, L. S. ,Chem. Eng. Sci. 1996, 51, 2577-2582.

[168] Satturwar, P. M., Fulzele, S. V. Dorle, A. K. ,AAPS PharmSciTech 2005, 6, E649-E654.

[169] Fulzele, S. V., Satturwar, P. M. Dorle, A. K. ,Int. J. Pharm. 2002, 249, 175-184.

[170] Fuse, T., Kusu, F. Takamura, K. ,J. Pharm. Biomed. Anal. 1997, 15, 1515-1519.

[171] Scalarone, D., Lazzari, M. Chiantore, O. ,J. Anal. Appl. Pyrolysis 2002, 64, 345-361.

[172] Romero-Noguera, J., Bolívar-Galiano, F. C., Ramos-López, J. M., Fernández-Vivas, M. A. Martín-Sánchez, I. ,Int. Biodeterior. Biodegrad. 2008, 62, 427-433.